

Issue 1

2021 | Volume 17

The Journal on Advanced Studies in Theoretical and Experimental Physics,
including Related Themes from Mathematics

PROGRESS IN PHYSICS



“All scientists shall have the right to present their scientific research results, in whole or in part, at relevant scientific conferences, and to publish the same in printed scientific journals, electronic archives, and any other media.” — Declaration of Academic Freedom, Article 8

ISSN 1555-5534

PROGRESS IN PHYSICS

A quarterly issue scientific journal, registered with the Library of Congress (DC, USA). This journal is peer reviewed and included in the abstracting and indexing coverage of: Mathematical Reviews and MathSciNet (AMS, USA), DOAJ of Lund University (Sweden), Scientific Commons of the University of St. Gallen (Switzerland), Open-J-Gate (India), Referativnyi Zhurnal VINITI (Russia), etc.

Electronic version of this journal:
<http://www.ptep-online.com>

Advisory Board

Dmitri Rabounski,
Editor-in-Chief, Founder
Florentin Smarandache,
Associate Editor, Founder
Larissa Borissova,
Associate Editor, Founder

Editorial Board

Pierre Millette
millette@ptep-online.com
Andreas Ries
ries@ptep-online.com
Gunn Quznetsov
gunn@mail.ru
Ebenezer Chifu
chifu@ptep-online.com

Postal Address

Department of Mathematics and Science,
University of New Mexico,
705 Gurley Ave., Gallup, NM 87301, USA

Copyright © *Progress in Physics*, 2021

All rights reserved. The authors of the articles do hereby grant *Progress in Physics* non-exclusive, worldwide, royalty-free license to publish and distribute the articles in accordance with the Budapest Open Initiative: this means that electronic copying, distribution and printing of both full-size version of the journal and the individual papers published therein for non-commercial, academic or individual use can be made by any user without permission or charge. The authors of the articles published in *Progress in Physics* retain their rights to use this journal as a whole or any part of it in any other publications and in any way they see fit. Any part of *Progress in Physics* howsoever used in other publications must include an appropriate citation of this journal.

This journal is powered by \LaTeX

A variety of books can be downloaded free from the Digital Library of Science:
<http://fs.gallup.unm.edu/ScienceLibrary.htm>

ISSN: 1555-5534 (print)

ISSN: 1555-5615 (online)

Standard Address Number: 297-5092

Printed in the United States of America

April 2021

Vol. 17, Issue 1

CONTENTS

Johns O. D. Relativistically Correct Electromagnetic Energy Flow	3
Msindo S., Nyambuya G. G., Nyamhere C. Plausible Fundamental Origins of Emis- sivity (I)	10
Kritov A. Remark to Approach to the Schwarzschild Metric with $SL(2, R)$ Group De- composition	14
Belyakov A. V. The Substantive Model of the Proton According to J. Wheeler's Geo- metrodynamic Concept	15
Dvoeglazov V. V. Algebra of Discrete Symmetries in the Extended Poincaré Group	20
Weng S. Theoretical Study on Polarized Photon	23
Dvoeglazov V. V. A Note on the Barut Second-Order Equation	30
Dorda G. The Unification of the Basic Units Meter, Kilogram and Second and the Essence of the Phenomenon Time	32
Dumitru S. A Survey on Uncertainty Relations and Quantum Measurements: Arguments for Lucrative Parsimony in Approaches of Matters	38
Millette P. A. Laser Action in the Stellar Atmospheres of Wolf-Rayet Stars and Quasi-Stellar Objects (QSOs)	71
Müller H. Physics of Transcendental Numbers Meets Gravitation	83
Zhang T. X. The Role Played by Plasma Waves in Stabilizing Solar Nuclear Fusion	93
Potter F. Antarctic Circumpolar Current: Driven by Gravitational Forces?	99
Millette P. A. Stellar Evolution of High Mass-Loss Stars	104
Müller H., Angeli R., Baccara R., Hofmann R. L., Muratori S., Nastasi O., Papa G., Santoni F., Venegoni C., Zanellati F., Khosravi L. Physics of Numbers as Model of Telepathic Entanglement	116
Nyambuya G. G. Dirac 4×1 Wavefunction Recast into a 4×4 Type Wavefunction	124

Information for Authors

Progress in Physics has been created for rapid publications on advanced studies in theoretical and experimental physics, including related themes from mathematics and astronomy. All submitted papers should be professional, in good English, containing a brief review of a problem and obtained results.

All submissions should be designed in L^AT_EX format using *Progress in Physics* template. This template can be downloaded from *Progress in Physics* home page <http://www.ptep-online.com>

Preliminary, authors may submit papers in PDF format. If the paper is accepted, authors can manage L^AT_EX typing. Do not send MS Word documents, please: we do not use this software, so unable to read this file format. Incorrectly formatted papers (i.e. not L^AT_EX with the template) will not be accepted for publication. Those authors who are unable to prepare their submissions in L^AT_EX format can apply to a third-party payable service for LaTeX typing. Our personnel work voluntarily. Authors must assist by conforming to this policy, to make the publication process as easy and fast as possible.

Abstract and the necessary information about author(s) should be included into the papers. To submit a paper, mail the file(s) to the Editor-in-Chief.

All submitted papers should be as brief as possible. Short articles are preferable. Large papers can also be considered. Letters related to the publications in the journal or to the events among the science community can be applied to the section *Letters to Progress in Physics*.

All that has been accepted for the online issue of *Progress in Physics* is printed in the paper version of the journal. To order printed issues, contact the Editors.

Authors retain their rights to use their papers published in *Progress in Physics* as a whole or any part of it in any other publications and in any way they see fit. This copyright agreement shall remain valid even if the authors transfer copyright of their published papers to another party.

Electronic copies of all papers published in *Progress in Physics* are available for free download, copying, and re-distribution, according to the copyright agreement printed on the titlepage of each issue of the journal. This copyright agreement follows the *Budapest Open Initiative* and the *Creative Commons Attribution-Noncommercial-No Derivative Works 2.5 License* declaring that electronic copies of such books and journals should always be accessed for reading, download, and copying for any person, and free of charge.

Consideration and review process does not require any payment from the side of the submitters. Nevertheless the authors of accepted papers are requested to pay the page charges. *Progress in Physics* is a non-profit/academic journal: money collected from the authors cover the cost of printing and distribution of the annual volumes of the journal along the major academic/university libraries of the world. (Look for the current author fee in the online version of *Progress in Physics*.)

Relativistically Correct Electromagnetic Energy Flow

Oliver Davis Johns

San Francisco State University, Department of Physics and Astronomy, Thornton Hall, 1600 Holloway Avenue, San Francisco, CA 94132 USA.
Email: ojohns@metacosmos.org

Detailed study of the energy and momentum carried by the electromagnetic field can be a source of clues to possible new physics underlying the Maxwell equations. But such study has been impeded by expressions for the parameters of the electromagnetic energy flow that are inconsistent with the transformation rules of special relativity. This paper begins by correcting a basic parameter, the local velocity of electromagnetic energy flow. This correction is derived by the direct application of the transformation rules of special relativity. After this correction, the electromagnetic energy-momentum tensor can then be expressed in a reference system comoving with the energy flow. This tensor can be made diagonal in the comoving system, and brought into a canonical form depending only on the energy density and one other parameter. The corrected energy flow and its energy-momentum tensor are illustrated by a simple example using static electric and magnetic fields. The proposal that electromagnetic momentum results from the motion of a relativistic mass contained in the fields is examined in the context of the corrected flow velocity. It is found that electromagnetic field momentum, though real, cannot be explained as due only to the motion of relativistic mass. The paper concludes that introducing the requirement of consistency with special relativity opens the study of electromagnetic energy and momentum to new possibilities.

1 Introduction

The Feynman example of a rotating disk with a magnet at its center and charged spheres on its perimeter provides a convincing argument that, to preserve the principle of angular momentum conservation, the field momentum of even a static electromagnetic field must be considered physically real.*

Since the energy density and momentum density of the electromagnetic field are real, it is important to investigate the details of the energy flow that they represent. Since special relativity is the symmetry theory of electrodynamics, it is essential that such investigations respect the transformation laws of special relativity.

In Section 2 a previously proposed candidate expression for a basic parameter, the velocity of energy flow at a given point in the electromagnetic field, is shown to be inconsistent with the transformation rules of special relativity and therefore incorrect. A corrected velocity expression is derived by explicit use of these rules.

Section 3 derives the electromagnetic energy-momentum tensor in a reference system comoving with this corrected velocity, and shows that it can be made diagonal and reduced to a canonical form that depends on two parameters derived from the values of the electric and magnetic fields.

Section 4 illustrates the results of the previous sections with an example using static electric and magnetic fields.

Section 5 considers the question of a relativistic mass density derived from the energy density of the electromagnetic

field. It is found that this mass density does not correctly relate the momentum density to the flow velocity. Electromagnetic field momentum, although real, is not due only to the motion of relativistic mass.

Section 6 concludes that introducing the requirement of special relativistic covariance into the study of the flow of energy in electromagnetic fields opens up new possibilities for investigation of such flows.

Electromagnetic formulas in this paper are taken from Griffiths [6] and Jackson [7] with translation to Heaviside-Lorentz units. I denote four-vectors as $\mathbf{A} = A^0 \mathbf{e}_0 + \mathbf{A}$ where \mathbf{e}_0 is the time unit vector and the three-vector part is understood to be $\mathbf{A} = A^1 \mathbf{e}_1 + A^2 \mathbf{e}_2 + A^3 \mathbf{e}_3$. In the Einstein summation convention, Greek indices range from 0 to 3, Roman indices from 1 to 3. The Minkowski metric tensor is $\eta_{\alpha\beta} = \eta^{\alpha\beta} = \text{diag}(-1, +1, +1, +1)$. Three-vectors are written with bold type \mathbf{A} , and their magnitudes as A . Thus $|\mathbf{A}| = A$.

2 Velocity of energy flow

We begin with a basic parameter of the electromagnetic field. The flow velocity of the energy contained in the field at a given event can be defined as the velocity of a comoving observer who measures a zero energy flux there. Expressed in the precise language of Lorentz boosts:[†]

The laboratory system coordinate velocity of the flow of electromagnetic field energy at a given event is the velocity \mathbf{V} of a Lorentz boost that transforms the laboratory reference system into a reference system in which the Poynting energy

*Feynman et al [4], Section 17-4, Section 27-6, and Figure 17-5. Quantitative matches of field to mechanical angular momentum are found, for example, in Romer [12] and Boos [2].

[†]The Lorentz boost formalism used here is defined in Appendix A.

flux vector is null at that event. An observer at that event and at rest in this system, which we call the comoving system and denote by primes, therefore measures a zero energy flux. The zero flux measurement indicates that this observer is comoving with the flow of energy. Such an observer has coordinate velocity \mathbf{V} relative to the laboratory*, and therefore \mathbf{V} is the laboratory system coordinate velocity of the energy flow at the given event.

A previously proposed† candidate for the laboratory system coordinate velocity of the electromagnetic energy flow is the momentum density divided by the relativistic mass (defined as energy density divided by the square of the speed of light). Denoting this velocity as \mathbf{u}_e gives

$$\frac{\mathbf{u}_e}{c} = \frac{\mathbf{G}}{(\mathcal{E}/c)} = \frac{2(\mathbf{E} \times \mathbf{B})}{(E^2 + B^2)} \quad (1)$$

where $\mathbf{G} = \mathbf{S}/c^2 = (\mathbf{E} \times \mathbf{B})/c$ is the linear momentum density of an electromagnetic field with electric and magnetic field vectors \mathbf{E} and \mathbf{B} and Poynting energy flux vector \mathbf{S} . The $\mathcal{E} = (E^2 + B^2)/2$ is the electromagnetic energy density, and c is the vacuum velocity of light.

If \mathcal{E}/c and \mathbf{G} were the time and space parts of a four-vector, then a Lorentz boost from the laboratory system using boost velocity $\mathbf{V} = \mathbf{u}_e$ would produce a comoving reference system (denoted by primes) in which the space part of that four-vector, that is \mathbf{G}' and hence the Poynting vector $\mathbf{S}' = c^2 \mathbf{G}'$, would vanish, indicating a system comoving with the energy flow.‡ Thus \mathbf{u}_e would be the comoving velocity of the energy flow.

However, \mathcal{E}/c and \mathbf{G} are *not* components of a four-vector. There is no four-vector momentum density of the form $\mathbf{G} = (\mathcal{E}/c) \mathbf{e}_0 + \mathbf{G}$.

Rather, \mathcal{E} and $c\mathbf{G}$ are the T^{00} and T^{0i} components of the second-rank electromagnetic energy-momentum tensor

$$T^{\alpha\beta} = \begin{pmatrix} \mathcal{E} & cG_1 & cG_2 & cG_3 \\ cG_1 & M_{11} & M_{12} & M_{13} \\ cG_2 & M_{21} & M_{22} & M_{23} \\ cG_3 & M_{31} & M_{32} & M_{33} \end{pmatrix} \quad (2)$$

where $M_{ij} = -(E_i E_j + B_i B_j) + \frac{1}{2} \delta_{ij} (E^2 + B^2)$.

*See Appendix A for a demonstration that any point at rest in the primed system moves with laboratory system coordinate velocity \mathbf{V} .

†In a discussion of the Poynting theorem in material media, but with no special attention to Lorentz covariance, Born and Wolf [3] Section 14.2, Eq. (8) identify \mathbf{u}_e as the *velocity of energy transport* or *ray velocity*. Section B.2 of Smith [15] echoes Born and Wolf but provides no new derivation. (The first edition of Born and Wolf's text appeared in 1959.) Geppert [5] writes a non-covariant equation with the same identification. More recently, Sebens [13, 14] relies on these and other sources to identify \mathbf{u}_e as the electromagnetic mass flow velocity. (Following Sebens, expand $(E - B)^2 \geq 0$ and use the definitions of \mathcal{E} and \mathbf{G} to prove that $|\mathbf{u}_e| \leq c$.)

‡See Appendix A for a demonstration that \mathbf{G}' would be zero.

A related point is made by Rohrlich [11], using the so-called von Laue theorem to argue that *integrals* of \mathcal{E}/c and \mathbf{G} over hyperplanes may in some cases transform as four-vectors. But we are treating these quantities locally, at a particular event. Von Laue's theorem does not imply that the local field functions \mathcal{E}/c and \mathbf{G} themselves transform as components of a four-vector. They do not. Rather than attempting to derive a four-vector from \mathcal{E}/c and \mathbf{G} , we show how to use them in a relativistically correct manner as they are. See also Section 6.3 of [10].

Since \mathcal{E} and $c\mathbf{G}$ are components of $T^{\alpha\beta}$, contributions to the boost transformation from the other components of $T^{\alpha\beta}$ would produce a comoving system in which \mathbf{G}' and the Poynting vector would not vanish. *The electromagnetic energy flow velocity is not \mathbf{u}_e .*

The failure of \mathbf{u}_e to be the correct flow velocity can be contrasted with the well-understood theory of the flow of electric charge. The charge density ρ and the current density vector \mathbf{J} are shown by the divergence of the Maxwell field tensor to form a four-vector of the form $\mathbf{J} = c\rho \mathbf{e}_0 + \mathbf{J}$. In general, \mathbf{J} can be timelike, spacelike, or null. If spacelike, there is no velocity \mathbf{v}_q less than the speed of light with $\mathbf{J} = \rho \mathbf{v}_q$. But if we consider, for example, a system in which all the moving charges have the same sign, it can be shown that \mathbf{J} is timelike and hence the definition $\mathbf{u}_q = \mathbf{J}/\rho$ does produce a vector of magnitude less than the speed of light. Then a Lorentz boost with boost velocity $\mathbf{V} = \mathbf{u}_q$ indeed leads to a comoving primed reference system in which the current flux density \mathbf{J}' vanishes§, and \mathbf{u}_q is therefore the correct flow velocity of the moving charge.

But the fact that \mathbf{J} transforms as a four-vector is crucial to this argument. If it were not a four-vector transforming as in Appendix A, the system reached by boost $\mathbf{V} = \mathbf{u}_q$ would have a residual current flow $\mathbf{J}' \neq 0$, and \mathbf{u}_q would therefore not be the correct flow velocity. The equation $\mathbf{J} = \rho \mathbf{u}_q$ would still follow from the definition of \mathbf{u}_q , but that formula would not imply that \mathbf{u}_q is the correct velocity of the flowing charge.

The failure of \mathbf{u}_e as a candidate for the flow velocity of electromagnetic energy is precisely because, unlike \mathbf{J} , the expression written here in four-vector form $\mathbf{G} = (\mathcal{E}/c) \mathbf{e}_0 + \mathbf{G}$ actually does *not* transform as a four-vector. The equation $\mathbf{G} = (\mathcal{E}/c^2) \mathbf{u}_e$ (or equivalently $\mathbf{S} = \mathcal{E} \mathbf{u}_e$) still follows from the definition of \mathbf{u}_e , but that formula does not imply that \mathbf{u}_e is the correct velocity of the flowing energy.

However, the correct boost velocity \mathbf{V} can be found by starting from \mathbf{u}_e and applying a scalar correction factor. The corrected velocity \mathbf{V} will have the same *direction* as \mathbf{u}_e but not the same *magnitude*. To find this corrected velocity \mathbf{V} it is best to turn to a direct method, using the transformation rules for the fields \mathbf{E} and \mathbf{B} .

§Substitute $c\rho = J^0$ and \mathbf{J} for G^0 and \mathbf{G} in Appendix A to see that \mathbf{J}' vanishes.

The rules for transformation of electric and magnetic fields by a boost with velocity \mathbf{V} can be written in a special relativistically correct but not manifestly covariant form as*

$$\begin{aligned}\mathbf{E}' &\doteq \gamma \left(\mathbf{E} + \frac{\mathbf{V}}{c} \times \mathbf{B} \right) + (1 - \gamma) \frac{\mathbf{V}(\mathbf{V} \cdot \mathbf{E})}{V^2} \\ \mathbf{B}' &\doteq \gamma \left(\mathbf{B} - \frac{\mathbf{V}}{c} \times \mathbf{E} \right) + (1 - \gamma) \frac{\mathbf{V}(\mathbf{V} \cdot \mathbf{B})}{V^2}\end{aligned}\quad (3)$$

where the Lorentz factor is $\gamma = (1 - V^2/c^2)^{-1/2}$. The \doteq symbol means that the components of the three-vector on the left side of this symbol expressed in the primed coordinate system are numerically equal to the components of the three-vector on the right side of this symbol expressed in the original unprimed system. If $\mathbf{a}' \doteq \mathbf{c}$ and $\mathbf{b}' \doteq \mathbf{d}$, it is easily proved that: (a) $\mathbf{a}' \times \mathbf{b}' \doteq \mathbf{c} \times \mathbf{d}$ and (b) $(\mathbf{a}' \cdot \mathbf{b}') = (\mathbf{c} \cdot \mathbf{d})$.

Define the boost velocity \mathbf{V} to be an unknown but rotationally scalar quantity λ times \mathbf{u}_e

$$\mathbf{V} = \lambda \mathbf{u}_e. \quad (4)$$

Since \mathbf{u}_e and \mathbf{V} are perpendicular to both the electric and magnetic fields, it follows that $(\mathbf{V} \cdot \mathbf{E}) = (\mathbf{V} \cdot \mathbf{B}) = 0$. Thus, (3) reduces to[†]

$$\begin{aligned}\mathbf{E}' &\doteq \gamma \left(\mathbf{E} + \frac{\mathbf{V}}{c} \times \mathbf{B} \right) \\ \mathbf{B}' &\doteq \gamma \left(\mathbf{B} - \frac{\mathbf{V}}{c} \times \mathbf{E} \right).\end{aligned}\quad (5)$$

Insert (5) into the definition $\mathbf{S}' = c\mathbf{E}' \times \mathbf{B}'$. Using (4) and then (1) leads to[‡]

$$\mathbf{S}' = c\mathbf{E}' \times \mathbf{B}' \doteq \gamma^2 c (\mathbf{E} \times \mathbf{B}) \left((u_e^2/c^2) \lambda^2 - 2\lambda + 1 \right). \quad (6)$$

Notice that (6) verifies the statement above that \mathbf{u}_e is not the comoving velocity of the energy flow. Setting $\lambda = 1$ in (4) makes $\mathbf{V} = \mathbf{u}_e$. But setting $\lambda = 1$ in (6) makes

$$\mathbf{S}' \doteq \gamma^2 c (\mathbf{E} \times \mathbf{B}) (u_e^2/c^2 - 1) \quad \text{when } \lambda = 1 \quad (7)$$

which is not zero, except in the unphysical limit $u_e = V = c$.

For a second and more important use of (6), choose λ to solve the quadratic equation $((u_e^2/c^2)\lambda^2 - 2\lambda + 1) = 0$. Then (6) makes $\mathbf{S}' = 0$. The solution is

$$\lambda = \frac{1}{(u_e/c)^2} \left\{ 1 - \sqrt{1 - (u_e/c)^2} \right\}. \quad (8)$$

From (4), the correct velocity of the energy flow is therefore

$$\mathbf{V} = \lambda \mathbf{u}_e = \frac{1}{(u_e/c)^2} \left\{ 1 - \sqrt{1 - (u_e/c)^2} \right\} \mathbf{u}_e \quad (9)$$

*See Section 11.10 of Jackson [7], eqn (11.149).

[†]Note that $\mathbf{V}' \doteq \mathbf{V}$ as defined in Appendix A, together with (5) and property (b) of the symbol \doteq noted above, imply that $(\mathbf{V}' \cdot \mathbf{E}') = \mathbf{V} \cdot \gamma [\mathbf{E} + (\mathbf{V}/c) \times \mathbf{B}] = \gamma(\mathbf{V} \cdot \mathbf{E}) = 0$. Similarly, $(\mathbf{V}' \cdot \mathbf{B}') = 0$.

[‡]See a detailed derivation of (6) in Appendix B.

where \mathbf{u}_e is defined in (1).

This \mathbf{V} is the relativistically correct boost velocity from the laboratory frame to the comoving reference frame in which $\mathbf{S}' = 0$, and is therefore the laboratory system coordinate velocity of the electromagnetic energy flow[§].

Since both \mathbf{V} and \mathbf{u}_e are parallel to the energy flux vector \mathbf{S} , the energy flow velocity can also be written as $\mathbf{V} = V(\mathbf{S}/S)$ where the magnitude V is given by[¶]

$$(V/c) = \frac{1}{(u_e/c)} \left\{ 1 - \sqrt{1 - (u_e/c)^2} \right\}. \quad (10)$$

This equation can be inverted to give

$$(u_e/c) = \frac{2(V/c)}{1 + (V/c)^2} \quad (11)$$

which can be used to write the correction factor λ in (8) as a function of the corrected velocity

$$\lambda = \frac{1 + (V/c)^2}{2}. \quad (12)$$

3 Comoving energy-momentum tensor

The derivation of a reference system comoving with the flow of energy allows the electromagnetic energy-momentum tensor to be examined in more detail. The energy-momentum tensor in (2) can be transformed into the comoving (primed) coordinate system that was produced by the Lorentz boost \mathbf{V} . In this system, the electromagnetic energy-momentum tensor is represented by the tensor components $T'^{\alpha\beta}$ in which the cG'_i elements are zero.

$$T'^{\alpha\beta} = \begin{pmatrix} \mathcal{E}' & 0 & 0 & 0 \\ 0 & M'_{11} & M'_{12} & M'_{13} \\ 0 & M'_{21} & M'_{22} & M'_{23} \\ 0 & M'_{31} & M'_{32} & M'_{33} \end{pmatrix} \quad (13)$$

where

$$\mathcal{E}' = \frac{1}{2} (E'^2 + B'^2) = \mathcal{E} \frac{1 - (V/c)^2}{1 + (V/c)^2} \quad (14)$$

$$\text{and } M'_{ij} = - (E'_i E'_j + B'_i B'_j) + \delta_{ij} \mathcal{E}'.$$

We can now make another Lorentz transformation, an orthogonal spatial rotation at fixed time, to diagonalize the real, symmetric sub-matrix M'_{ij} in (13).

The required spatial rotation can be defined as the product of two proper rotations. First rotate the coordinate system to bring the \mathbf{e}'_3 axis into the $\mathbf{V}' \doteq \mathbf{V}$ direction. Denote

[§]Appendix C gives details of the comoving system for possible values of $(\mathbf{E} \cdot \mathbf{B})$ at a given event.

[¶]Footnote [†] on page 4 proves that $0 \leq u_e \leq c$. As u_e/c increases from 0 to 1, (10) shows that V/c increases monotonically from 0 to 1, with $V \leq u_e$ at every point. It follows that $0 \leq V \leq c$ also.

this rotated system by tildes. Rotations do not change three-vectors, which are invariant objects under rotations. However, rotations do change the *components* of three-vectors. Thus $\tilde{\mathbf{V}} = \mathbf{V}'$, $\tilde{\mathbf{E}} = \mathbf{E}'$, and $\tilde{\mathbf{B}} = \mathbf{B}'$, but in the tilde system $\tilde{\mathbf{V}}$ now has components $\tilde{V}_1 = \tilde{V}_2 = 0$ and $\tilde{V}_3 = V$. Then using Footnote † on page 5, we have $0 = (\mathbf{E}' \cdot \mathbf{V}') = (\tilde{\mathbf{E}} \cdot \tilde{\mathbf{V}}) = V\tilde{E}_3$. Since the magnitude $V \neq 0$, it follows that $\tilde{E}_3 = 0$. A similar argument proves that $\tilde{B}_3 = 0$. Thus the {33} component of the energy-momentum tensor when expressed in the tilde system is $\tilde{T}^{33} = -(\tilde{E}_3^2 + \tilde{B}_3^2) + \tilde{\mathcal{E}} = \tilde{\mathcal{E}}$. The tensor from (13), when expressed in the tilde system, becomes

$$\tilde{T}^{\alpha\beta} = \begin{pmatrix} \tilde{\mathcal{E}} & 0 & 0 & 0 \\ 0 & \tilde{M}_{11} & \tilde{M}_{12} & 0 \\ 0 & \tilde{M}_{21} & \tilde{M}_{22} & 0 \\ 0 & 0 & 0 & \tilde{\mathcal{E}} \end{pmatrix} \quad (15)$$

where $\tilde{\mathcal{E}} = \mathcal{E}'$.

Since the invariant trace of the electrodynamic energy-momentum tensor vanishes*, it follows from (15) that

$$0 = \eta_{\alpha\beta} \tilde{T}^{\alpha\beta} = -\tilde{\mathcal{E}} + \tilde{M}_{11} + \tilde{M}_{22} + \tilde{\mathcal{E}} \quad (16)$$

and hence $\tilde{M}_{11} = -\tilde{M}_{22}$. Also, the symmetry of the energy-momentum tensor makes $\tilde{M}_{21} = \tilde{M}_{12}$. Thus

$$\tilde{T}^{\alpha\beta} = \begin{pmatrix} \tilde{\mathcal{E}} & 0 & 0 & 0 \\ 0 & -\tilde{\psi} & \tilde{\xi} & 0 \\ 0 & \tilde{\xi} & \tilde{\psi} & 0 \\ 0 & 0 & 0 & \tilde{\mathcal{E}} \end{pmatrix} \quad (17)$$

where $\tilde{\psi} = \tilde{M}_{22}$ and $\tilde{\xi} = \tilde{M}_{12}$.

A second proper rotation, this time about the $\tilde{\mathbf{e}}_3$ axis, produces the final coordinate system, denoted with double primes. After this rotation, $E_3'' = \tilde{E}_3 = 0$, $B_3'' = \tilde{B}_3 = 0$, and $\mathbf{V}'' = \tilde{\mathbf{V}}$ has components $V_1'' = V_2'' = 0$ and $V_3'' = V$. The only effect of this second rotation is to diagonalize the matrix $\begin{pmatrix} -\tilde{\psi} & \tilde{\xi} \\ \tilde{\xi} & \tilde{\psi} \end{pmatrix}$. The energy momentum tensor then has its final, diagonal form in the double-prime system

$$T''^{\alpha\beta} = \begin{pmatrix} \mathcal{E}'' & 0 & 0 & 0 \\ 0 & -a'' & 0 & 0 \\ 0 & 0 & a'' & 0 \\ 0 & 0 & 0 & \mathcal{E}'' \end{pmatrix} \quad (18)$$

where $\mathcal{E}'' = \tilde{\mathcal{E}} = \mathcal{E}'$. The parameter a'' has absolute value $|a''| = \{\tilde{\psi}^2 + \tilde{\xi}^2\}^{1/2}$ where $\pm\{\tilde{\psi}^2 + \tilde{\xi}^2\}^{1/2}$ are the two eigenvalues of the matrix $\begin{pmatrix} -\tilde{\psi} & \tilde{\xi} \\ \tilde{\xi} & \tilde{\psi} \end{pmatrix}$ that were calculated during the diagonalization process. The sign of a'' depends on the directions and relative magnitudes of the electric and magnetic fields.

*See Section 7.8 of Rindler [9].

The rotation that takes the system from the primed to the double-primed system is then the product of the first and second rotations. The various representations of the boost velocity are related by $\mathbf{V}'' = V\mathbf{e}_3'' = \tilde{\mathbf{V}} = V\tilde{\mathbf{e}}_3 = \mathbf{V}' \doteq \mathbf{V}$ where all of these vectors have the same original magnitude V .

The energy-momentum tensor in the double-prime system is diagonal and in a canonical form that depends only on the energy density \mathcal{E}'' in the comoving system and one other parameter a'' .

Section 4 shows that there are realistic electromagnetic cases in which $a'' \neq 0$ and hence the diagonal elements M''_{ii} for $i = 1, 2, 3$ are not all equal, unlike the analogous elements in the energy-momentum tensor of a perfect fluid†, all of which are equal by definition, a fact of relevance for future studies that might attempt a fluid-dynamic model of electrodynamic energy flow.

4 Example: crossed static fields

Consider an example with static, perpendicular electric and magnetic fields.‡ Choose the Cartesian axes of the laboratory system so that $\mathbf{E} = E\hat{\mathbf{x}}$ and $\mathbf{B} = B\hat{\mathbf{y}}$. Then (1) becomes

$$\frac{\mathbf{u}_e}{c} = \left(\frac{2EB}{E^2 + B^2} \right) \hat{\mathbf{z}}. \quad (19)$$

The energy flow velocity is thus $\mathbf{V} = V\hat{\mathbf{z}}$ where $V = \lambda u_e$ with λ from (8). Inserting this \mathbf{V} into (5) with the above values of the electric and magnetic fields gives

$$\mathbf{E}'' \doteq \gamma \left(E - \frac{VB}{c} \right) \hat{\mathbf{x}} \quad (20)$$

$$\mathbf{B}'' \doteq \gamma \left(B - \frac{VE}{c} \right) \hat{\mathbf{y}}.$$

Thus the definitions in (2) when applied in the double-prime system give $M''_{ij} = 0$ for $i \neq j$ and

$$\begin{aligned} M''_{11} &= -E_1''^2 + \mathcal{E}'' = -\frac{1}{2} (E_1''^2 - B_2''^2) \\ M''_{22} &= -B_2''^2 + \mathcal{E}'' = \frac{1}{2} (E_1''^2 - B_2''^2) \\ M''_{33} &= \mathcal{E}'' = \frac{1}{2} (E_1''^2 + B_2''^2). \end{aligned} \quad (21)$$

where E_1'' and B_2'' are the components of \mathbf{E}'' and \mathbf{B}'' , respectively, in (20).

The step of rotating from primed to double-primed reference systems that was necessary to move from (13) to (18) above was not necessary here due to a propitious choice of original laboratory reference system. The Lorentz boost with velocity $\mathbf{V} = V\hat{\mathbf{z}}$ produces an already diagonal energy momentum tensor with $M''_{ij} = 0$ for $i \neq j$.

†See Part I, Chapter 2, Section 10 of Weinberg [16].

‡The center of a parallel plate capacitor at the center of a long solenoid, for example.

Consider the case $E \neq B$. From (19), this inequality implies that $u_e < c$ and hence, from (10), that $V < c$, a physically possible value. Also $E \neq B$ implies, either from the invariance of $(E^2 - B^2)$ noted in Appendix C or directly from (20), that $2M''_{22} = (E_1''^2 - B_2''^2) = (E^2 - B^2) \neq 0$. Thus $E \neq B$ implies that $M''_{11} = -M''_{22} \neq 0$ and hence that $M''_{11} \neq M''_{22}$.

Comparing (21) to (14) and (18) shows that for the crossed-field example with $E \neq B$, the energy-momentum tensor in the double-prime system is (18) with

$$a'' = (E^2 - B^2)/2 \neq 0 \quad (22)$$

$$\text{and } \mathcal{E}'' = \mathcal{E} \left(1 - (V/c)^2\right) / \left(1 + (V/c)^2\right)$$

where $\mathcal{E} = (E^2 + B^2)/2$.

As asserted at the end of Section 3, the inequality $E \neq B$ in the crossed-field example shows a physically reasonable case for which $a'' \neq 0$ and the M''_{ii} for $i = 1, 2, 3$ are not all equal.*

There are questions about the interpretation of this example globally[†]. In our use of this example, however, we need not consider the question of so-called *hidden momentum* required to balance the total field momentum[‡]. Here, the only relevant use of this example is to illustrate the correct local definition of the energy flow velocity and comoving energy-momentum tensor in a vacuum region where the fields are well known — at the center of the parallel plate capacitor far from the edges.

5 Relativistic mass density

The energy density \mathcal{E} of either static or time-varying vacuum electromagnetic fields can be used to define a *relativistic* mass density[§]

$$\mathcal{M}_{\text{rel}} = \mathcal{E}/c^2. \quad (23)$$

The adjective *relativistic* indicates that this mass density is analogous to a single-particle relativistic mass $m_{\text{rel}} = \gamma m = e/c^2$ where e is the particle relativistic energy, m is the invariant or rest mass of the particle, and $\gamma = (1 - v^2/c^2)^{-1/2}$ is the Lorentz factor of its velocity \mathbf{v} .

It follows from (23) that the flow velocity of the energy \mathcal{E} , the velocity \mathbf{V} derived in Section 2 and summarized in (9), must also be the flow velocity of the relativistic mass \mathcal{M}_{rel} .

In the single-particle case, the same m_{rel} can be used to relate the momentum of the particle to its velocity, $\mathbf{p} = \gamma m \mathbf{v} =$

*Our use of this example is based on $E \neq B$. The case $E = B \neq 0$ would have to be approached as a limit, as discussed in Appendix C(c). With $E \neq 0$ and $B = E(1 + \delta)$, retaining leading order in the small quantity δ gives $(u_e/c) \approx (1 - \delta^2/2)$, $\lambda \approx (1 - |\delta|)$, $(V/c) \approx (1 - |\delta|)$, $(\mathcal{E}''/E^2) \approx |\delta|$, $(T''^{\alpha\beta}/E^2) \approx \text{diag}(|\delta|, \delta, -\delta, |\delta|)$, and $(a''/E^2) \approx -\delta$.

[†]See McDonald [8] for calculation of the total field momentum of a similar example.

[‡]See, for example, Babson et al [1].

[§]For example, see Section 3 of Sebens [13].

$m_{\text{rel}} \mathbf{v}$. However in the case of electromagnetic fields, the same mass density \mathcal{M}_{rel} cannot be used for both purposes.

Due to the correction of the flow velocity in Section 2, which was necessitated by adherence to the transformation rules of special relativity, the relation between momentum density \mathbf{G} and corrected flow velocity \mathbf{V} is

$$\mathbf{G} = \left(\frac{\mathcal{M}_{\text{rel}} \mathbf{V}}{\lambda} \right) \neq \mathcal{M}_{\text{rel}} \mathbf{V} \quad (24)$$

where λ is the correction factor in (12).

The inequality in (24) shows that the electromagnetic momentum density at an event is not equal to the electromagnetic mass density at that event times the relativistically correct mass flow velocity there.

The explicit expression for the correction factor λ from (12) quantifies the extent of the inequality. The effective mass for momentum calculation is the larger value $\mathcal{M}_{\text{rel}}/\lambda$ rather than \mathcal{M}_{rel} [¶].

The failure of $\mathcal{M}_{\text{rel}} \mathbf{V}$ to equal the momentum density \mathbf{G} in (24) suggests that vacuum electromagnetic field momentum cannot be explained only by the motion of relativistic mass. There must be another source of real electromagnetic field momentum.

6 Conclusion

The electromagnetic field contains energy and momentum. Calculation of the energy flow velocity and energy-momentum tensor in a relativistically correct manner opens the subject to new insights into that energy and momentum. For example, the energy-momentum tensor measured by an observer comoving with the flow velocity is obtained in diagonal, canonical form suggestive of possible fluid dynamical models. And the momentum density of the electromagnetic field is shown to require some source other than the flow of relativistic mass.

Appendix A: Lorentz boosts

Consider a Lorentz transformation from an *unprimed* coordinate system (which we also refer to as the *laboratory* system) with coordinates $x = (x^0, x^1, x^2, x^3)$ to a *primed* coordinate system with coordinates $x' = (x'^0, x'^1, x'^2, x'^3)$ where $x^0 = ct$ and $x'^0 = ct'$. The most general proper, homogeneous Lorentz transformation from the unprimed to the primed systems can be written as a Lorentz boost times a rotation.^{||}

Definition of Lorentz boost

A Lorentz boost transformation is parameterized by a boost velocity vector \mathbf{V} with components (V_1, V_2, V_3) and magnitude $V = (V_1^2 + V_2^2 + V_3^2)^{1/2}$. Using the Einstein summation

[¶]Note that (24) can be written as $\mathbf{G} = \mathcal{M}_{\text{eff}} \mathbf{V}$ where, using (12), (14), and (23), $\mathcal{M}_{\text{eff}} = \mathcal{M}_{\text{rel}}/\lambda = 2\gamma^2(\mathcal{E}'/c^2)$ where $\gamma = (1 - V^2/c^2)^{-1/2}$.

^{||}See Part I, Chapter 2, Section 1 of Weinberg [16].

convention, it is written as $x'^{\alpha} = \Lambda^{\alpha}_{\beta} x^{\beta}$ where $\Lambda^0_0 = \gamma$, $\Lambda^i_0 = \Lambda^i_j = -\gamma V_j/c$, and $\Lambda^i_j = \delta_{ij} + (\gamma - 1)V_i V_j/V^2$. The δ_{ij} is the Kronecker delta function. Also $\gamma = (1 - V^2/c^2)^{-1/2}$.

The inverse boost $\underline{\Lambda}^{\alpha}_{\beta}$ is the same except for the substitution $V_i \rightarrow -V_i$. Thus the inverse boost vector is $(-\mathbf{V}')$ where $\mathbf{V}' \doteq \mathbf{V}$.

Meaning of the boost velocity \mathbf{V}

The velocity \mathbf{V} that parameterizes the Lorentz boost is also the coordinate velocity, as measured from the unprimed laboratory system, of any point that is at rest in the primed system. In this sense, the entire primed system is moving with velocity \mathbf{V} as observed from the laboratory system.

To see this, apply the inverse Lorentz boost to the differentials of a point at rest in the primed system, $dx'^i = 0$ for $i = 1, 2, 3$, but $dx'^0 > 0$. The result is $dx^0 = \gamma dx'^0$ and $dx^i = \gamma(V_i/c) dx'^0$. Thus $dx^i/dt = V_i$, as was asserted.

Consequence of existence of a four-vector \mathbf{G}

The discussion surrounding (2) shows that $\mathbf{G} = (\mathcal{E}/c)\mathbf{e}_0 + \mathbf{G}$ is *not* a four-vector, despite being written in four-vector form here. Its components instead transform as components of the energy-momentum tensor. But suppose for a moment that it is a four-vector. If so, then a Lorentz boost with a boost velocity $(\mathbf{u}_e/c) = \mathbf{G}/(\mathcal{E}/c)$ would make the transformed space part of \mathbf{G} equal to zero.

As applied to a four-vector, the Lorentz boost transformation rule is $G'^{\alpha} = \Lambda^{\alpha}_{\beta} G^{\beta}$. Hence

$$\begin{aligned} G'^i &= \Lambda^i_0 G^0 + \Lambda^i_j G^j \\ &= -\gamma \frac{V_i}{c} G^0 + G^i + (\gamma - 1) \frac{V_i (V_j G^j)}{V^2}. \end{aligned} \quad (25)$$

Replacing V_i/c by $(u_e)_i/c = G^i/G^0$ in (25) makes $G'^i = 0$, as asserted.

Appendix B: Detailed derivation of Eq. (6) for \mathbf{S}'

We have (1), (4) and (5) and $(\mathbf{V} \cdot \mathbf{E}) = (\mathbf{V} \cdot \mathbf{B}) = 0$. Inserting (5) into $\mathbf{S}' = c(\mathbf{E}' \times \mathbf{B}')$ gives

$$\mathbf{S}' = c\mathbf{E}' \times \mathbf{B}' \doteq c\gamma^2 \{(\mathbf{E} \times \mathbf{B}) + \mathbf{f} + \mathbf{g}\} \quad (26)$$

where, omitting zero terms,

$$\begin{aligned} \mathbf{f} &= -\mathbf{E} \times \left(\frac{\mathbf{V}}{c} \times \mathbf{E} \right) + \left(\frac{\mathbf{V}}{c} \times \mathbf{B} \right) \times \mathbf{B} \\ &= -(E^2 + B^2) \frac{\mathbf{V}}{c} = -\lambda (E^2 + B^2) \frac{\mathbf{u}_e}{c} \\ &= -\lambda (E^2 + B^2) \frac{2(\mathbf{E} \times \mathbf{B})}{(E^2 + B^2)} = -2\lambda (\mathbf{E} \times \mathbf{B}) \end{aligned} \quad (27)$$

and, again omitting zero terms,

$$\begin{aligned} \mathbf{g} &= -\left(\frac{\mathbf{V}}{c} \times \mathbf{B} \right) \times \left(\frac{\mathbf{V}}{c} \times \mathbf{E} \right) \\ &= -\frac{\mathbf{V}}{c} \left\{ \left(\frac{\mathbf{V}}{c} \times \mathbf{B} \right) \cdot \mathbf{E} \right\} = \frac{\mathbf{V}}{c} \left\{ \frac{\mathbf{V}}{c} \cdot (\mathbf{E} \times \mathbf{B}) \right\} \\ &= \lambda^2 \left\{ \frac{2(\mathbf{E} \times \mathbf{B})}{(E^2 + B^2)} \right\} \left\{ \frac{\mathbf{u}_e}{c} \cdot \left(\frac{E^2 + B^2}{2} \right) \frac{\mathbf{u}_e}{c} \right\} \\ &= \lambda^2 \left(\frac{\mathbf{u}_e}{c} \cdot \frac{\mathbf{u}_e}{c} \right) (\mathbf{E} \times \mathbf{B}) = \lambda^2 \left(\frac{u_e}{c} \right)^2 (\mathbf{E} \times \mathbf{B}). \end{aligned} \quad (28)$$

Collect terms and factor out $\mathbf{E} \times \mathbf{B}$ to get

$$\mathbf{S}' = c\mathbf{E}' \times \mathbf{B}' \doteq \gamma^2 c (\mathbf{E} \times \mathbf{B}) \left\{ \left(\frac{u_e}{c} \right)^2 \lambda^2 - 2\lambda + 1 \right\} \quad (29)$$

which is (6).

Appendix C: Detail of the comoving system

The comoving system is defined by $\mathbf{S}' = c(\mathbf{E}' \times \mathbf{B}') = 0$. Thus $|\mathbf{E}' \times \mathbf{B}'| = E'B' \sin \theta' = 0$ where θ' is the angle between \mathbf{E}' and \mathbf{B}' in the comoving system.

From Eqs (7.62) and (7.63) of Rindler [9], we have $(E'^2 - B'^2) = (E^2 - B^2)$ and $(\mathbf{E}' \cdot \mathbf{B}') = (\mathbf{E} \cdot \mathbf{B})$. It follows that:

(a) An event with $\mathbf{E} \cdot \mathbf{B} \neq 0$ has $E'B' \neq 0$ and therefore \mathbf{E}' and \mathbf{B}' must be either parallel or anti-parallel, $\theta' = 0$ or $\theta' = \pi$, at this event;

(b) An event with $0 = (\mathbf{E} \cdot \mathbf{B}) = (\mathbf{E}' \cdot \mathbf{B}') = E'B' \cos \theta'$ cannot have $E'B' \neq 0$ in the comoving system because that would require both $\cos \theta' = 0$ and $\sin \theta' = 0$. Thus $E'B' = 0$ and one of E' and B' must be zero. If $E > B$ then $E' > B'$ and hence $B' = 0$. If $E < B$ then $E' < B'$ and hence $E' = 0$;

(c) If both $0 = \mathbf{E} \cdot \mathbf{B}$ and $E = B \neq 0$ at an event, then both $E'B' = 0$ and $E' = B'$, and therefore $E' = B' = 0$. But (1) and (10) show that such an event also has $u_e/c = 1$ and hence $V/c = 1$. The case $E = B \neq 0$ and $0 = \mathbf{E} \cdot \mathbf{B}$ therefore must be approached as a limit.

Received on Sept. 23, 2020

References

1. Babson D., Reynolds S. P., Bjorkquist R., Griffiths D. J. Hidden momentum, field momentum, and electromagnetic impulse. *American Journal of Physics*, 2009, v. 77, 826–833.
2. Boos F. L. More on the Feynman's disk paradox. *American Journal of Physics*, 1984, v. 52 (8), 756.
3. Born M., Wolf E. Principles of Optics, 6th edn. Pergamon Press, Oxford, 1980.
4. Feynman R., Leighton R., Sands M. The Feynman Lectures on Physics, vol II. Addison-Wesley Pub. Co., Reading, MA, 1964.
5. Geppert D. V. Energy-transport velocity in electromagnetic waves. *Proceedings of the IEEE (correspondence)*, 1965, v. 53, 1790.
6. Griffiths D. J. Introduction to Electrodynamics, 3rd edn. Prentice Hall, Upper Saddle River, NJ, 1999.

7. Jackson J.D. Classical Electrodynamics, 2nd edn. John Wiley and Sons, New York, 1975.
 8. McDonald K. T. Electromagnetic momentum of a capacitor in a uniform magnetic field. 2015. https://www.hep.princeton.edu/~mcdonald/examples/cap_momentum.pdf
 9. Rindler W. Relativity Special, General, and Cosmological, 2nd edn. Oxford University Press, Oxford, 2006.
 10. Rohrlich F. Classical Charged Particles. Addison-Wesley Pub. Co., Reading, MA, 1965.
 11. Rohrlich F. Answer to question 26 “Electromagnetic field momentum” *American Journal of Physics*, 1996, v, 64, 16.
 12. Romer R.H. Angular momentum of static electromagnetic fields. *American Journal of Physics*, 1966, v. 34, 772.
 13. Sebens C. T. Forces on fields. *Studies in the History and Philosophy of Modern Physics*, 2018, v. 63, 1–11.
 14. Sebens C. T. The mass of the gravitational field. *British Journal for the Philosophy of Science*, forthcoming. arXiv: abs/1811.10602v2.
 15. Smith R. L. The velocities of light. *American Journal of Physics*, 1970, v. 38,(8), 978–984.
 16. Weinberg S. Gravitation and Cosmology. John Wiley and Sons, New York, 1972.
-

Plausible Fundamental Origins of Emissivity (I)

S. Msindo^{†*}, G. G. Nyambuya[‡], and C. Nyamhere[†]

[‡]National University of Science and Technology, Faculty of Applied Sciences – Department of Applied Physics, Fundamental Theoretical and Astrophysics Group, P. O. Box 939, Ascot, Bulawayo, Zimbabwe.

[†]Midlands State University – Faculty of Science and Technology, Department of Applied Physics and Telecommunications, P. Bag 9055, Gweru, Zimbabwe.

*E-mail: simbarashemsindo@gmail.com

Emissivity is a fundamental property of matter that measures the ratio of the thermal radiation emanating from a thermodynamic surface to the radiation from an ideal black-body surface at the same temperature and it takes values from 0 to 1. This property is not a theoretically derived thermodynamic property of matter, but a *posteriori justified* property that is derived from experiments after its need was found necessary in order to balance up the theoretically expected radiation of a black-body at the same temperature to that actually measured in the laboratory for a material body at the same temperature. From a fundamental theoretical stand-point, we argue herein that emissivity may arise due perhaps to the *existence of non-zero finite lower and upper cut-off frequencies* in the thermal radiation of matter, thus leading to material bodies emitting not all the radiation expected from them when compared to equivalent black-body surfaces. We demonstrate that a non-zero lower limiting frequency is implied by the refractive index of materials, while an upper limit frequency is adopted from Debye's (1912) ingenious idea of an upper limiting cut-off frequency which arises from the fact that the number of modes of vibrations of a finite number of oscillators must be finite.

1 Introduction

Emissivity is a fundamental, intrinsic and inherent property of all known materials. Commonly, one talks of the emissivity of solid materials and as such, emissivity is a property typically associated with solids. In reality, all forms (solid, liquid, gas) of matter exhibit this property. In general, the emissivity of a given material is defined as the ratio of the thermal radiation from a surface to the radiation of an ideal black surface at the same temperature. As presently obtaining, this important property of matter – *emissivity* – has no fundamental theoretical justification – it is an experimentally derived property of matter. This article seeks to lay down a theoretical framework and basis that not only justifies the existence of this property of matter, but to investigate this from a purely theoretical standpoint.

To that end, in the present article, we conduct an *initial forensic analysis* of the modern derivation of the Planck Radiation Law (PRL) [1–3]. In this analysis, we identify two *loopholes* in the derivation of the PRL, and these are:

1. **Dispersion Relation Problem:** The dispersion relation assumed in the PRL is that of a photon in a *vacuo*, i.e.:

$$E = pc_0, \quad (1)$$

where: (E, p) are the (kinetic) energy and momentum of the photon in question, and: $c_0 = 2.99792458 \times 10^8 \text{ m s}^{-1}$ is the speed of light in *vacuo* (2018 CODATA*). This Eq.(1), is what is used in the derivation of the PRL in relation to the energy and momentum of the photon in the interior of material bodies. Without an iota of doubt, the interior of material

bodies is certainly not a *vacuo*. This means that the dispersion relation (1) is not the appropriate dispersion relation to describe these photons generated therein material bodies. We need to use the correct equation – i.e. by replacing (1) with:

$$E = pc, \quad (2)$$

where: $c = c_0/n$; and here: c , is the speed of light in the material (medium) whose refractive index is n and $n: 0 < n < 1$. This is the first correction to the PRL that we shall conduct.

2. **Limits Problem:** The second correction has to do with the lower and upper limits in the integral leading to the PRL. As one will notice (and most probably ignore) is that the derivation leading to the PRL does not have a finite upper limit (i.e. $\nu_H = \infty$) and at the same time, this same integral has a lower bound limit of zero (i.e. $\nu_L = 0$). What this means is that the photons emitted by material bodies have wavelengths in the range – zero ($\nu_L = 0$) to infinity ($\nu_H = \infty$). A zero frequency photon implies zero kinetic energy and an infinite frequency photon implies an infinite kinetic energy of the photon. The lower bound frequency ($\nu_L = 0$) has serious problems with Heisenberg's uncertainty principle [4], while the upper infinite frequency ($\nu_H = \infty$) has obvious *topological defects* with physical and natural reality as we know it.

Using the above *two points of critique* in the derivation of the PRL, we shall advance a thesis which seeks to demonstrate that, it is possible *in principle* to justify from a physical and fundamental theoretical level the existence and the need of the emissivity function of a material. There is no such effort in the present literature where such an endeavour has been attempted – this, at least is our view point derived from the wider literature that we have managed to lay our hands on.

*<https://physics.nist.gov/cgi-bin/cuu/Value?c>

Now, in closing this introductory section, we shall give a synopsis of the remainder of this article. In §2 and §3, for self-containment, instructive and completeness purposes, we present an exposition of the Planck radiation theory and the derivation of the Stefan-Boltzmann Law respectively, where emphasis is made on the two points of critique to the Planck theory that we made above. In §4, we present our derivation. In §5, a general discussion is presented. Lastly, in §6, in a rather succinct manner, the conclusion drawn from the present work is laid down.

2 Planck radiation theory

As was presented in the first article of this series [5], we shall make the derivation of the PRL our point of departure. We know that the number of quantum states dN in the momentum volume space d^3p and physical volume space V , is given by:

$$dN = \frac{2Vd^3p}{h^3}, \quad (3)$$

where: $h = 6.62607015 \times 10^{-34}$ J s is Planck's constant (2018 CODATA*). The factor 2 in (3) comes in because of the number of degrees of freedom of the photon: one for traverse and the other for longitudinal polarisation – i.e. the photon has two polarization states. Now, given that: $d^3p = 4p^2dp$, it follows that:

$$dN = \frac{8\pi Vp^2dp}{h^3}, \quad (4)$$

and further, given that for a photon of momentum p_γ , energy E_γ and frequency ν , its energy-momentum is such that: $p_\gamma = E_\gamma/c_0 = h\nu/c_0$, it follows from this, that the number of modes in the frequency interval: ν to $\nu + d\nu$ is:

$$dN = \left(\frac{8\pi V}{c_0^3} \right) \nu^2 d\nu. \quad (5)$$

The actual number of occupied states dn is such that $dn = f_{BE}(\nu, \mathcal{T}) dN$ where:

$$f_{BE}(\nu, \mathcal{T}) = \frac{1}{e^{h\nu/k_B T} - 1}, \quad (6)$$

is the Bose-Einstein probability function which for a temperature \mathcal{T} , gives the probability of occupation of a quantum state whose energy is $E_\gamma = h\nu$ and: $k_B = 1.38064852(79) \times 10^{-23}$ J K⁻¹ is the Boltzmann constant (2018 CODATA†). From the foregoing:

$$dn_* = \frac{8\pi V}{c_0^3} \frac{\nu^2 d\nu}{e^{h\nu/c_0 h_B T} - 1}, \quad (7)$$

leading to the energy density: $B_\nu(\nu, T)d\nu = E_\gamma dn_*/V$, now being given by:

$$B_\nu(\nu, T)d\nu = \frac{8\pi h}{c_0^3} \frac{\nu^3 d\nu}{e^{h\nu/k_B T} - 1}, \quad (8)$$

where: $B_\nu(\nu, T)$ is the spectral irradiance given in terms of ν : (8) is our sought-for PRL.

3 Stephan-Boltzmann law

Now, to derive the Stefan-Boltzmann Law (SBL) from (8), we start by setting: $x = h\nu/k_B T$. This setting implies that: $d\nu = k_B T dx/h$, thus substituting this into (8), we then have:

$$B_\nu(\nu, T)d\nu = \frac{8\pi k_B^4 \mathcal{T}^4}{h^3 c_0^3} \frac{x^3 dx}{e^x - 1}. \quad (9)$$

From the foregoing theory, the total energy density $\mathcal{E}_{\text{theo}}$ radiated per unit time by a radiating body is such that:

$$\begin{aligned} \mathcal{E}_{\text{theo}} &= \frac{c_0}{4} \int_{\nu_L=0}^{\nu_H=\infty} B_\nu(\nu, T) d\nu, \\ &= \frac{2\pi k_B^4 \mathcal{T}^4}{h^3 c_0^3} \int_0^\infty \frac{x^3 dx}{e^x - 1}, \end{aligned} \quad (10)$$

and given that: $\int_0^\infty \frac{x^2 dx}{(e^x - 1)} = \pi^4/15$, it follows that the SBL will thus be given by:

$$\mathcal{E}_{\text{theo}} = \sigma_0 \mathcal{T}^4, \quad (11)$$

where one can most easily deduce that the fundamental and universal constant – the *Stefan-Boltzmann constant*: $\sigma_0 = 2\pi^2 k_B^4 / 15h^3 c_0^2$. In terms of its actually experimentally measured value: $\sigma_0 = 5.670374419 \times 10^{-8}$ W m⁻² K⁻⁴ (2018 CODATA‡).

Written as it appears in (11), the SBL is not compatible with physical and natural reality as it needs to be supplemented with a new term – namely the emissivity ϵ , i.e.:

$$\mathcal{E}_{\text{exp}} = \epsilon \sigma_0 \mathcal{T}^4. \quad (12)$$

The above result is what one gets from experiments. We shall derive the emissivity function: $\epsilon = \epsilon(\nu, \mathcal{T})$ from the fundamental soils of theory.

4 Derivation

In this section, we shall in two parts, i.e. §4.1 and §4.2, derive a relation that connects the emissivity function with the refractive index of the given material and both the upper and lower limits in the energy of the photon.

4.1 Dispersion relation problem

In the derivation of the PRL, i.e. (8), and as well as the SBL, i.e. (11), we have used the *vacuo* dispersion relation (1) for the photon. As stated in the introductory section, this is *not correct* as one is supposed to use the correct non-*vacuo* photon dispersion relation (2). If we do the *correct* thing and

*<https://physics.nist.gov/cgi-bin/cuu/Value?h>

†<https://physics.nist.gov/cgi-bin/cuu/Value?k>

‡<https://physics.nist.gov/cgi-bin/cuu/Value?sigma>

instead use (2) in the derivation of the PRL, instead of the PRL given in (8), we will obtain the new revised PRL:

$$\begin{aligned} B_v(\nu, T)d\nu &= \frac{8\pi h}{c^3} \frac{\nu^3 d\nu}{e^{h\nu/k_B T} - 1}, \\ &= \frac{8\pi h}{c_0^3} \frac{n^3 \nu^3 d\nu}{e^{h\nu/k_B T} - 1}. \end{aligned} \quad (13)$$

The difference between (13) and (8), is the introduction of the refractive index, n .

Now, from this new PRL (13) together with the correct non-*vacuo* photon dispersion relation (2), one obtains the following refractive index modified SBL:

$$\mathcal{E}_{\text{exp}} = \frac{c_0}{4} \int_{\nu_L}^{\nu_H} \frac{c B_v(\nu, T) d\nu}{c_0} = \frac{c_0}{4} \int_{\nu_L}^{\nu_H} \frac{B_v(\nu, T) d\nu}{n}, \quad (14)$$

where in (14), we have not set the limits ($\nu_H = \infty; \nu_L = 0$), but have left this as a task to be dealt with in §4.2.

Now – proceeding to institute in (14) the substitution: $x = h\nu/k_B T$, and remembering that the refractive index n is a function of ν and possibly \mathcal{T} as well (i.e. $n = n(\nu, \mathcal{T}) = n(x)$), it follows that (14) will reduce to:

$$\mathcal{E}_{\text{exp}} = \sigma_0 \mathcal{T}^4 \int_{x_L}^{x_H} \frac{15}{\pi^4} \frac{x^3 n^2(x) dx}{e^x - 1}. \quad (15)$$

With \mathcal{E}_{exp} now written as it has been written in (15), one can reasonably identify the emissivity function as:

$$\epsilon = \frac{15}{\pi^4} \int_{x_L}^{x_H} \frac{x^3 n^2(x) dx}{e^x - 1} = \epsilon(x) = \epsilon(\nu, \mathcal{T}). \quad (16)$$

In this way, the emissivity has not been introduced as a result of an experimental requirement, but foisted by subtle theoretical requirements to do with the (obvious *but* neglected) shortcomings stated in the introduction section.

Our intention in the present article is not to investigate this newly-derived emissivity function (16), but merely to make a statement to the effect that the emissivity function can be derived from the fundamental soils of theoretical physics. We shall slate for the next installation, the task to test the emissivity function (16) against real data. In the subsequent subsection, we will now deal with the issue of the limits in the integral (16).

4.2 Limits problem

As stated previously, a photon frequency of zero (i.e. photon with zero energy) does not make sense especially in the face of Heisenberg's [4] uncertainty limit. To obtain a reasonable estimate of this, one can appeal to logical reasoning by simply asking the question: *What is the largest wavelength of a photon that can travel in a medium with a mean inter-molecular spacing: $\ell = \ell(T)$?* We know that the speed of our photon is c and that this speed is such that it is equal to: $\lambda\nu$, where λ is the

wavelength of our photon. In order for the smooth passage of the photon in such a medium, it is reasonable to assume that the wavelength of the photon be at most equal to one half of the mean spacing of the given medium, i.e. $\lambda_{\text{max}} = \ell/2$. Given that: $c = \lambda\nu$, it follows that we must have: $\nu_L = 2c_0/n\ell$.

Now, in establishing the upper limiting frequency that must enter the integral leading to the PRL, we will use the reasoning already laid down by Debye [9]. As is well known, in November of 1907, Einstein [10] proposed the first reasonably good model of the *Heat Capacity of a Solid* that employed the then nascent concept of quantization of energy. Einstein's [10] motivation was really not to propose a rigorous working model of a solid but to promote the then strange *Quanta Hypothesis* that had been promulgated earlier by Planck [1–3] and had been *given breath to* by him in his landmark and 1921 *Nobel Prize* winning 1905 explanation of the *Photoelectric Effect* [11].

In his model of a solid, Einstein [10] made three fundamental assumptions: (1) Each atom in the lattice is an independent 3D quantum harmonic oscillator and the energy of this oscillator is quantized, (2) All atoms oscillate with the same fundamental frequency of vibration and (3) The probability of occupation of any given microstate is given by the Boltzmann thermodynamic probability. In summing up (integrating) all the energies of these oscillators, Einstein's oscillators have a minimum of zero frequency and an infinity frequency for a maximum frequency. While Einstein's [10] model gave a reasonably good fit to data, Debye [9] realized that Einstein's limits of integration were non-physical, especially the upper limiting frequency: $\nu_H = \infty$. So, in constructing a revised (modified) version of Einstein's [10] model, Debye [9] had to correct this by limiting the upper frequency ν_H .

Debye [9] required that for the N oscillators – each with three degrees of freedom – the sum total of the modes of vibration must equal $3N$. That is to say, if $g(\nu)$ is the density of states, then:

$$\int_{\nu_L}^{\nu_H} g(\nu) d\nu = 3N. \quad (17)$$

Debye [9] set: $\nu_L = 0$ because in reality: $\nu_L \simeq 0$ and keeping ν_L as non-zero in his model did not bring in any significant improvement to the model, so he simply set this equal zero. Thus from (17), Debye [9] could calculate ν_H , and this maximum frequency one obtains from this calculation is known as the *Debye frequency* and symbolized ν_D .

For the photons under probe (in the present article), the density of states: $g(\nu) = dN/d\nu$ can be calculated from (5)*, and so doing one obtains: $g(\nu) = 8\pi V\nu^2/c^3$. Since a photon has two degrees of freedom, accordingly, N photons will have

*The reader must remember to substitute c in place of c_0 because in the foregoing calculation, we have disposed of the *vacuo* dispersion relation (1), and adopted the non-*vacuo* dispersion relation (2).

$2N$ degrees of freedom, hence:

$$\int_{\nu_L}^{\nu_H} \frac{8\pi V \nu^2 d\nu}{c^3} = \frac{8\pi V}{c_0^3} \int_{\nu_L}^{\nu_H} n^3(\nu, \mathcal{T}) \nu^2 d\nu = 2N. \quad (18)$$

Since ν_L is known, ν_H can be known if $n(\nu, \mathcal{T})$ is known. In the present article, we have no intention of evaluating the model, i.e. (16) and (18), that we have just set because we are yet to make further modifications where we shall include possible *non-zero photon mass effects*. For now, all we want to do is to show that one can demonstrate from a most fundamental level, that the emissivity function ϵ can be furnished with solid theoretical foundations rather than have this function as an experimental construct with no solid fundamental theoretical basis.

5 Discussion

The main aim of this paper has been to seek a fundamental and foundational basis and justification for the existence of the emissivity property of matter from the soils of fundamental theoretical physics. We are of the view that the grounds for such an endeavour have herein been set. Our final theoretically derived expression for the emissivity is given in (16). This expression we arrived at by revising the traditional derivation of the PRL as articulated in the introduction section. This emissivity function, i.e. (16), here derived has three free parameters associated with it and these parameters are:

1. The lower cut-off frequency: ν_L . The meaning of which is that there exists in this material medium in question, a *Lower Cutoff Frequency* (ν_L) below which frequency the body does not emit.
2. The upper frequency: ν_H . The meaning of which is that there exists in this material medium in question, an *Upper Cutoff Frequency* (ν_H) above which frequency the body does not emit.
3. The refractive index: n of the given material.

Of these three free adjustable parameters, the refractive index is less free as an adjustable parameter as there are already experimentally verified models of this quantity (see e.g. [12–14]). However, the lower (ν_L) and upper (ν_H) frequencies can be fixed to suit the given material, thus one can *in principle* fit the emissivity function (16) to the experimentally measured emissivity of a given material medium. When we say *one can in principle fit the emissivity function (16) to the experimentally measured emissivity of a given material medium*, we do not mean in an arbitrary manner, but that one will have to work out a realistic model that leads to a theory that fits to the data. In closing, allow us to say that in our next instalment, an attempt to fit the herein derived emissivity function, i.e. (16), to real data will be made.

6 Conclusion

Without the dictation of experience, it is possible in principle to justify by way of solid physical arguments and from a *bona*

fide fundamental theoretic level, the existence and the need of the emissivity function for natural material.

Acknowledgements

We are grateful to the *Editorial Board* of the *Progress in Physics Journal* for the publication waiver on this article.

Received on August 6, 2020

References

1. Planck M. K. E. L. Entropie und Temperatur Strahlender Wärme. *Annalen der Physik*, 1900, v. 306 (4), 719–737.
2. Planck M. K. E. L. Ueber Irreversible Strahlungsvorgänge. *Annalen der Physik*, 1900, v. 306 (1), 69–122.
3. Planck M. K. E. L. Ueber das Gesetz der Energieverteilung im Normalspectrum. *Annalen der Physik*, 1901, v. 309 (3), 553–563.
4. Heisenberg W. K. Ueber den anschaulichen Inhalt der Quantentheoretischen Kinematik und Mechanik. *Zeitschrift für Physik*, 1927, v. 43 (3), 172–198. In English: Wheeler J. A. and Zurek W. H., eds. *Quantum Theory and Measurement*. Princeton University Press, Princeton, NJ, 1983, pp. 62–84.
5. Nyambuya G. G. Planck Radiation Formula for Massive Photons. *Prespacetime Journal*, 2017, v. 8 (5), 663–674.
6. Crisóstomo C. and Pitarma R. The Importance of Emissivity on Monitoring and Conservation of Wooden Structures Using Infrared Thermography. In: *Advances in Structural Health Monitoring*, IntechOpen, 2019, 16 pp. doi:10.5772/intechopen.82847.
7. Minissale M., Pardanaud C., Bisson R., and Gallais L. The Temperature Dependence of Optical Properties of Tungsten in the Visible and Near-Infrared Domains: An Experimental and Theoretical Study. *Journal of Physics D: Applied Physics*, 2017, v. 50 (45), 455601.
8. Sadiq H., Wong M. B., Tashan J., Al-Mahaidi R., and Zhao X.-L. Determination of Steel Emissivity for the Temperature Prediction of Structural Steel Members in Fire. *Journal of Materials in Civil Engineering*, 2013, v. 25 (2), 167–173.
9. Debye P. Zur Theorie der Spezifischen Wärmen. *Annalen der Physik*, 1912, v. 344 (14), 789–839.
10. Einstein A. Die Plancksche Theorie der Strahlung und die Theorie der spezifischen Wärme. *Annalen der Physik*, 1907, v. 327 (1), 180–190.
11. Einstein A. Über einen die Erzeugung und Verwandlung des Lichtes betreffenden heuristischen Gesichtspunkt. *Annalen der Physik*, 1905, v. 322 (6), 132–148.
12. Tang J., Sun M., Huang Y., Gou J., Zhang Y., Li G., Li Y., Man Y., and Yang J. Study on Optical Properties and Upconversion Luminescence of $\text{Er}^{3+}/\text{Yb}^{3+}$ co-Doped Tellurite Glass for Highly Sensitive Temperature Measuring. *Optical Materials Express*, 2017, v. 7 (9), 3238.
13. Tan C. Z. and Arndt J. Temperature Dependence of Refractive Index of Glassy SiO_2 in the Infrared Wavelength Range. *Journal of Physics and Chemistry of Solids*, 2000, v. 61 (8), 1315–1320.
14. Sellmeier W. Ueber die durch die Aetherschwingungen erregten Mitschwingungen der Körpertheilchen und deren Rückwirkung auf die ersteren, besonders zur Erklärung der Dispersion und ihrer Anomalien. *Annalen der Physik und Chemie*, 1872, v. 223 (11), 386–403.

Remark to Approach to the Schwarzschild Metric with $SL(2, \mathbb{R})$ Group Decomposition

Alexander Kritov

E-mail: alex@kritov.ru

1 Remark to Section 5

1. The $SL(2, \mathbb{C})^*$ group definition. Let the group $SL(2, \mathbb{C})^*$ be a subgroup of $SL(2, \mathbb{C})$ with an element $Z' \in SL(2, \mathbb{C})^*$ such as

$$Z' = \left\{ \begin{bmatrix} a_1 & a_2 \\ a_3 & a_4 \end{bmatrix} : a_1, a_4 \in Re, a_2, a_3 \in Im, \det(Z') = 1 \right\}.$$

The definition reflects the general Jacobian matrix form as given by (12) in [1].

2. The proof of the isomorphism of $SL(2, \mathbb{C})^*$ to $SL(2, \mathbb{R})$. The mapping (13) in [1] can be equivalently defined by the function that sends element of $Z' \in SL(2, \mathbb{C})^*$ to $Z \in SL(2, \mathbb{R})$

$$Z = T \cdot Z' \cdot T^{-1}$$

where

$$T = \begin{bmatrix} \sqrt{-i} & 0 \\ 0 & \sqrt{i} \end{bmatrix} \quad T^{-1} = \begin{bmatrix} \sqrt{i} & 0 \\ 0 & \sqrt{-i} \end{bmatrix} \quad \det(T) = 1.$$

The function is clearly a group homomorphism since

$$T \cdot Z'_1 \cdot Z'_2 \cdot T^{-1} = T \cdot Z'_1 \cdot T^{-1} \cdot T \cdot Z'_2 \cdot T^{-1} = Z_1 \cdot Z_2$$

for all $Z_1, Z_2 \in SL(2, \mathbb{R})$. It is obviously surjective. At last, as the inverse mapping

$$Z' = T^{-1} \cdot Z \cdot T$$

that sends any element of $SL(2, \mathbb{R})$ to $SL(2, \mathbb{C})^*$ is well defined it proves the injectivity. Hence, as a bijective homomorphism is shown, it finalizes the proof of $SL(2, \mathbb{C})^* \cong SL(2, \mathbb{R})$ mentioned in Section 5.

2 Corrections

The typo in the expression (10). The expression should evidently read with $\cosh^2(\beta)$ as follows

$$g_{\mu\nu} = \begin{bmatrix} -(1-v^2) & 0 \\ 0 & (1-v^2)^{-1} \end{bmatrix} = \begin{bmatrix} -\cosh^{-2}(\beta) & 0 \\ 0 & \cosh^2(\beta) \end{bmatrix}. \tag{10}$$

Section 5. A more appropriate notation for the Lorentz/Minkowski basis for $SL(2, \mathbb{R})$ is $\mathbb{R}^{1(2)}$ as the group consists of the real numbers.

Received on Oct 11, 2020

References

1. Kritov A. Approach to the Schwarzschild Metric with $SL(2, \mathbb{R})$ Group Decomposition. *Progress in Physics*, 2020, v. 16 (2), 139–142.

The Substantive Model of the Proton According to J. Wheeler's Geometrodynamical Concept

Anatoly V. Belyakov

E-mail: belyakov.lih@gmail.com

The review article presents the proton structure in accordance with the model based on a mechanistic interpretation of Wheeler's geometrodynamics. It is shown that this model gives a physically justified interpretation of the concepts introduced in quantum chromodynamics, such as "quark", "color", and also excludes the problem of confinement and others. The main parameters of the proton are calculated, namely: its mass, magnetic moment, lifetime, the proton-neutron mass difference, and also an analytical formula for its radius is derived. Typical lifetimes for various classes of elementary particles have been determined. Successful usage of the model gives reason to assume the model can be used for development a more rational theory of strong interactions instead of QCD.

1 Introduction

The internal structure of elementary particles, in particular of the proton, and their interactions with each other are considered in the theory of strong interactions (quantum chromodynamics). In QCD, there are no complete substantive models of the physical systems under consideration; instead, idealized virtual particles and quasiparticles (quarks, gluons) are introduced, as well as the concepts of an abstract image ("color") are appealed. QCD is based only on the observed properties of hadrons. It is assumed, that in hadrons interaction processes the numerous laws of conservation and redistribution (the amount of matter, energy, momentum, angular momentum, electric charge, magnetic flux and others) must simultaneously be fulfilled and various conditions must be observed.

In the absence of essential real models of elementary particles, the standard theory uses the approach of quantum mechanics: the properties of quarks and hadrons are simply described using wave functions and unitary symmetry combinatorics. The combination rules has formally been derived using the mathematical apparatus of quantum field theory and confirmed by experiments (there are 17 parameters that cannot be derived from the theory). However, it is not known why their physical nature is exactly this. In particular, it is not known why quarks can exist only in a bound state ("confinement"), which is recognized as one of the seven problems of the millennium.

This article shows the possibility of replacing the abstract QCD concepts applied to elementary particles with the particles real physical parameters. In contrast to the quantum theory, which states that micro-phenomena cannot be understood in any way from the point of view of our world scale, the mechanistic interpretation of Wheeler's idea first of all presupposes the presence of uniform or similar natural laws that are reproduced at different scale levels of matter. These laws, or at least their macroanalogues, are revealed in the structure

of elementary particles. Therefore, there is reason to believe that the model based on Wheeler's idea can be used to construct a more rational theory of strong interactions instead of QCD.

2 On the macroanalogues

According to Wheeler's concept charges are considered as singular points on a three-dimensional surface, connected by a "wormhole" or vortex current tubes of the drain-source type, forming a generally closed contour, which a physical vacuum or some medium circulates along. From a purely mechanistic viewpoint the charge is proportional to the momentum of this medium in its motion along the vortex current tube contour, the spin, respectively, is proportional to the angular momentum of this medium relative to the contour longitudinal axis, while the magnetic interaction of the conductors is analogous to the forces acting between the current tubes.

The work [1] shows the possibility and expediency of introducing the "Coulombless" system of units and replacing the Coulomb with momentum. This approach allows using of well-known physical macroanalogues. The space and medium unit elements in the model are: an element with an electron mass m_e and size r_e and a vortex tube with a linear density $\varepsilon_0 = m_e/r_e$.

Microparticles are likened to vortex formations in an ideal liquid, where a vortex funnel (conditionally it is a surface X) is a *fermion analogue* with mass m_x , and a vortex thread in depth below the surface (conditionally it is a region Y) is a *boson analogue* with mass m_y , length l_y , radius r , and peripheral speed v . The vortex thread, in turn, is capable of twisting into a spiral forming subsequent structures (current tubes). In a real medium, these structures oscillate, transforming into each other (oscillation of oscillators); it is assumed that this is accompanied by the "packing" of the bosonic thread into a fermionic form. Apparently, fermion particles retain the bosonic part with half spin, which determines their magnetic

and spin properties, and in the bosonic form the spin is restored to an integer value.

By the well-known physical analogy, the vortex tube of a contour, crossing over the surface of a liquid, creates ring waves or *contours of the next order*. Thus, interconnected contours are formed. Therefore, any particle seems to have two quantum numbers, depending on how one consider it: as a fermion (the analog of the proton being part of the greater contour of the subsequent family of particles) or as a boson (the mass of the contour of the previous family of particles). Thus, three generations of elementary particles as shown in [2] to form and there cannot be more. The microparticle itself is no longer considered as a point object and is characterized by the parameters of its own contour with a quantum number n .

The parameters of a bosonic vortex thread (or a contour with mass M) are determined in dimensionless units: in the fractions of the electron mass m_e , its classical radius r_e , and the speed of light c :

$$m_y = l_y = (an)^2, \quad (1)$$

$$v = \frac{c_0^{1/3}}{(an)^2}, \quad (2)$$

$$r = \frac{c_0^{2/3}}{(an)^4}, \quad (3)$$

where a is the inverse fine structure constant, c_0 is the dimensionless light velocity $c/[m/sec]$.

In [3] a closed proton-electron contour is considered. From the condition of equality of the medium motion energy along the contour Mv^2 and the ultimate electron energy $m_e c^2$ the charge numerical value as the vortex current tube momentum and the projection angle value are determined. The projection angle value turned out to be complementary to the Weinberg angle $q_w \approx 28.7^\circ$. Such a contour is "standard" and has parameters: the main quantum number $n = c_0^{1/3}/a = 4.884$, mass $M = c_0^{2/3} = 4.48 \times 10^5$, and the charge value (momentum)

$$e_0 = m_e c_0^{4/3} \cos q_w \times [m/sec] = 1.602 \times 10^{-19} \text{ kg} \times m/sec. \quad (4)$$

One can state therefore that the vortex current tube is formed by three vortex threads rotating around the common longitudinal axis. These threads are finite structures. They possess, by necessity, the right and left rotation; the last thread (it is evidently double one) possesses summary null rotation. These threads can be associated with vector bosons W^+ , W^- , Z^0 .

For the rotating unidirectional currents vortex threads with the condition of the magnetic and inertial (centrifugal) forces equilibrium their peripheral velocity v_0 is derived. If there are unit parameters, then it is true [2]:

$$v_0 = \frac{r_e}{(2\pi)^{1/2} \times [sec]} = 1.124 \times 10^{-15} \text{ m/sec}. \quad (5)$$

This speed does not depend on the vortex threads length and on the distance between them. Thus, having some definite mass and length, bosonic vortex tubes *do not have a certain configuration and shape*. The latter indicates the difference between bosonic vortex tubes and their physical analogue; this is also the physical reason for their difference from fermions in that bosons do not obey the Pauli exclusion principle.

3 The proton and its parameters

With the extremely dense packing of a bosonic thread into a fermionic form, as shown in [2], the proton and electron own quantum numbers have the following values:

$$n_p = \left(\frac{2c_0}{a^5}\right)^{1/4} = 0.3338, \quad (6)$$

$$n_e = \left(\frac{2c_0}{a^5}\right)^{1/8} = 0.5777. \quad (7)$$

It was found that the relative mass of any fermion m_x with an arbitrary quantum number n_x is determined by the ratio:

$$m_x = \left(\frac{n_e}{n_x}\right)^{14}. \quad (8)$$

For a proton, as it turned out (with slight simplifications), its fermionic and boson masses are equal, $m_x = m_y = 2090$, which is the reason for its minimum baryon mass and its stability. When corrected by the Weinberg angle cosine, the proton relative mass is determined quite accurately, i.e. $m_p = 2090 \times \cos q_w = 1836$.

The charged particle included in a circulation contour is the place where a medium flow intersects the boundary between X - and Y -regions; there occurs a phase transformation. In this case, the fermionic and boson densities become equal, and the parameters of the medium acquire density and velocity *critical values*. The values of these critical parameters can be attributed to some quasiparticle — a *quark* that exists only in the phase transition region, which in fact is the part of the proton mass obtaining critical parameters. Moreover, in order to comply with the critical parameters at the standard contour energy $m_e c^2$, it is necessary to split the general contour current in the proton region into three parts (calculated value is 3.2). Under these conditions, the total quark mass m_k is 12.9. At the same time, as shown in [2] and [4], this mass depends on the interaction conditions and can take a minimum value equal to the electron mass.

In addition, the conditions for the flow continuity and charge constancy in any cross section of the contour (there must be three current lines) require the *reverse circulation currents* in the proton region to arise, which can be interpreted as the presence of zones with different charge signs in the proton. Using the minimal number of non-recurrent force current lines, one can schematically express current lines in a

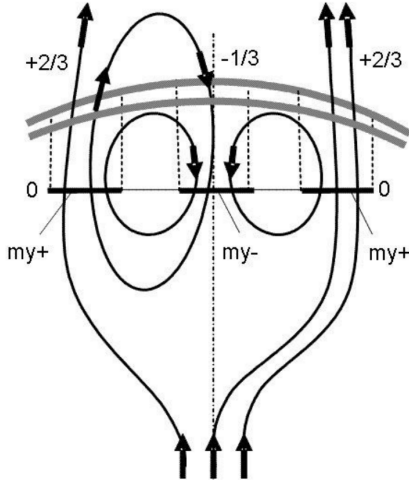


Fig. 1: A scheme of the proton: distribution of the current lines inside the proton.

proton in a unique way, as shown in Fig. 1. As seen, there exist two critical sections with a conditionally plus current (on the scheme up) and one section with a conditionally minus current (on the scheme down), where three current lines correspond to a general current in the scheme. Consequently, the proton fermionic surface for an external observer is as follows: the regions where force lines intersect the critical sections on the line 0-0 inside a proton will be projected onto the proton surface in the form of +2/3, +2/3, -1/3 of the total charge in accordance with the number and direction of the force lines crossing this surface. It would be more correct to associate quarks not with critical sections, but with stable ring currents containing, as follows from the diagram, one or two closed unit contours intersecting the critical sections.

Obviously, the proton parts in the critical sections have the velocity c and radius r_e , and they must have the bosonic vortex tubes of such length l_y that their own momentum would be equal to the momentum (charge) of an electron e_0 . Assuming that the vortex tube linear density for critical conditions is proportional to the average quark mass $\frac{1}{3} m_k$, we can write:

$$\frac{1}{3} m_k \frac{m_e}{r_e} l_y r_e c = e_0. \quad (9)$$

Bearing in mind that in a “Coulombless” system the charge has the dimension of momentum and substituting the known parameter values, we find $l_y = 136.4$. Thus, the relative bosonic part length is actually equal to a , its unexcited mass is am_e , respectively, the vortex tube angular momentum (spin) is equal to $am_e cr_e = h/2\pi = \hbar$. Thus, the structures inside the proton are found with the relative length l_y and boson mass m_y , numerically equal to a , and the spin, equal to \hbar . Apparently, there are pairs of such boson tubes with the mass equal to that of a pion and with the counter-directional rotation that compensates for the spin. Depending on the cur-

rents impulse direction, they can form the pions family or be part of other mesons, which are supposed to exist in the close environment of protons in the form of a virtual meson “coat”.

The magnetic moment of the proton μ_p in this model is calculated in accordance with its definition, where μ_p is the product (charge \times velocity \times path) and is determined by the bosonic configuration of the proton. The peripheral speed of the vortex threads relative to the Y-axis is v , the path is πr . Revealing v and r through (2) and (3), we finally get:

$$\mu_p = \frac{\pi c_0 e_0 c r_e}{(a n_p)^6} = 1.39 \times 10^{-26} \text{ Am}^2. \quad (10)$$

For an electron, the path is the Bohr radius, and (10) takes the form:

$$\mu_e = \frac{\pi c_0 e_0 c R_B}{(a n_e)^6} = 9.30 \times 10^{-24} \text{ Am}^2. \quad (11)$$

Only closed current lines remain in the neutron. The magnetic moment of the neutron equals two thirds of the proton’s magnetic moment, i.e. proportional to the number of intersections of the critical sections by current lines (six instead of nine, existing in a proton, see Fig. 1) and is equal to $-0.92 \times 10^{-26} \text{ Am}^2$. Naturally, the magnetic moment sign changes in addition, because three positive open current lines are removed. The obtained values differ slightly from the actual ones, since the parameters n_p and n_e are determined with some simplifications.

The neutron-proton mass difference arises due to the acquisition of additional mass-energy by the neutron when the proton absorbs the electron. In [2] it was assumed that in the proton-neutron transition state one of the quark contours is located at the intersection of X-Y regions, and, becoming axisymmetric, increases itself to the maximum value m_{max} . In this case, keeping in mind (1) and (3), its parameters are $l_y = r = c_0^{2/9} = m_{max} = 76.5$. The difference between the kinetic energies of rotation of the excited contour and the initial quark contour with an average mass $\frac{1}{2} m_k$ should correspond (when corrected by the cosine of the Weinberg angle) to the proton-neutron mass difference Δm :

$$\left(m_{max} v_{max}^2 - \frac{1}{2} m_k v_k^2 \right) \cos q_w = \Delta m. \quad (12)$$

Indeed, proceeding from their relative masses 76.5 and 12.9/2 and calculating their quantum numbers and velocities by (8) and (2), as a result, after substituting all quantities in (12), we find $\Delta m = 2.51$, which coincides with the actual value (2.53).

The exact size of the proton was determined in recent experiments [5]. It is significant that within the framework of this model, which does not use a complex mathematical apparatus and, in fact, is not a physical and mathematical model, but rather is a physical and logical one, it was possible to obtain an analytical formula for the proton size, proceeding from general laws only.

So, in [6] it was found that a single contour or a vortex tube having the momentum equivalent to the electron charge contains $n_i = 3$ single vortex threads, and the formula is obtained:

$$n_i = \frac{\{(m_e c_0^{2/3} r_e) / ((2\pi)^{1/2} \times [\text{sec}^2])\}^{1/3}}{\{(2\pi)^{1/2} \gamma m_e^2 / r_e^2\}^{1/3}} = 2.973 \approx 3. \quad (13)$$

The formula is the cubic root of the ratio of the inertial forces, arising during the acceleration of the standard boson contour mass and acting towards the periphery (the value $r_e / ((2\pi)^{1/2} \times [\text{sec}])$ is the rotation speed of the vortex threads relative to the contour longitudinal axis), to the gravity forces acting between masses of the size m_e at the distance r_e . The numerator is a constant value, so the formula depends only on the gravity forces, that is, on the interacting masses and the distance between them. It was shown in [4] that this ratio (or its modification for arbitrary m and r) can serve as a *coupling constant* equivalent, since it indicates the strength of bonds between the proton structure elements (quarks).

Moreover, it is the equality of these forces that determines the proton radius r_p and makes it possible to obtain an exact analytical formula under the condition $m_k = m_e$. Let us specify formula (13) under the assumption that the quarks are located at the corners of a regular triangle and that each of them is affected by the sum of two projections of forces, and also take into account that r_p is the size of the circumscribed circle. Then the formula is written in the form of equality of the dynamic and gravitational forces:

$$\frac{m_e c_0^{2/3} r_e}{2\pi \times [\text{sec}^2]} = \frac{2 \sin 60^\circ \gamma m_e^2}{(r_p \sin 60^\circ)^2}, \quad (14)$$

whence we get:

$$r_p = \frac{(8\pi\gamma\epsilon_0)^{1/2} \times [\text{sec}]}{3^{1/4} c_0^{1/3}} = 0.836 \times 10^{-15} \text{ m}, \quad (15)$$

which exactly coincides with the proton charge radius value obtained in the recent experiments (0.833 femtometers, with an uncertainty of ± 0.010 femtometers [5]). Thus, the boson mass of the standard contour, which is in the Y region and is, as it were, hidden, having the value $m_e c_0^{2/3}$, determines not only the proton charge and spin, but also its radius. Note that this radius is determined for the proton in the hydrogen composition, but not for a single proton, where it can have a greater value. It is important that the formula (15) contains the gravitational constant; in papers [2, 7, 8] the necessity of introducing gravity into the microcosm is shown, in particular, to determine the neutrino mass.

Thus, there is a sufficient set of parameters for the proton internal structure to describe the strong interaction. The concepts of fractional charge, quarks and color find here their physical representation. Indeed, there are two different ring

currents or circuits (quarks u and d), the force lines of which are projected onto the proton outer surface in the form of fractional charges, and three different critical sections (“colored” quarks). Moreover, as the contour currents can be directed in the opposite direction, forming antiquarks, so the vortex tubes in the critical sections can have the opposite direction of rotation, creating an “anticolor”. It is obvious that the proposed proton structure in the form of a field lines unique configuration no longer requires the confinement existence and, consequently, the filling of the proton region with the “sea” of virtual quarks and gluons.

In fact, the concept originating from the hydrodynamics of a continuous inviscid media is proposed here and this analogy turned out to be correct. Moreover, it has been established that the light velocity can be calculated by the equation describing the wave propagation on a liquid surface [9].

4 On the elementary particles lifetime

The microparticles decay probability and their lifetimes depend on many factors. The most important of them is the type of interaction (electromagnetic, weak, strong), which is responsible for the decay that occurs. The lifetimes of elementary particles differ extremely strongly: $10^{-6} \dots 10^{-25}$ seconds, at that most of them are grouped according to their lifetimes in rather narrow intervals. This model has objective parameters that allow one to estimate the microparticle various classes lifetime. Further there are calculated values, in general, corresponding to the average lifetimes for these classes.

The *microparticle lifetime* t (except for resonances and W , Z bosons) can be estimated as the time it takes to run around with a velocity v over the entire “stretched” contour length [7]:

$$t = \frac{a^8 n^8 r_e}{c_0 c}. \quad (16)$$

But W , Z bosons and resonances decay even before the final spiral structure is formed, i.e. they are, as it were, not completely particles. W , Z bosons have the shortest decay time, and it is determined by the time it takes to run with the speed of light around the electron vortex tube with the radius r . Bearing in mind (3),

$$t_{min} = \pi \frac{r_e}{c} \frac{c_0^{2/3}}{(an_e)^4} = 3.4 \times 10^{-25} \text{ sec}. \quad (17)$$

For numerous resonances the lifetime correlates well with the run time with the light velocity of the contour radius $l_y/2\pi$. Since $l_y = m_y$, then

$$t = \frac{m_y r_e}{2\pi c}. \quad (18)$$

For example, for Y , J/Ψ , η -particles with masses $m_y = 19700, 6056, 1074$ values $t = 2.95 \times 10^{-20}, 0.91 \times 10^{-20}, 0.30 \times 10^{-20}$ seconds.

In the group of heavy hadrons, particles contain unstable heavy quarks, and they decay through rapid weak decays. Then, in formula (16) for a weak decay n must be minimal, i.e. equal to 1.643 [7], and $t = 2.1 \times 10^{-13}$ seconds.

Light and “strange” hadrons are more stable, and in formula (16) the parameter n should have the value of its own Y -contour [4]. For a group, on average, $n \approx 3.5$, and $t \approx 10^{-10}$ seconds.

Particles that decay due to strong interaction, for example η and π^0 -particles, live only within the proton or electron own contours. Therefore, for them, when substituting the values of n_p and n_e in (16), the values of t is about 6×10^{-19} and 5×10^{-17} seconds.

Finally, during the electromagnetic decay of light charged particles (pions, kaons) the contour with large n and, accordingly, with the largest value of t manages to form.

As for the *neutron lifetime*, it is assumed [2] that the neutron loses the acquired mass-energy Δmc^2 gradually with fractions of $m_e v^2 c^2$ for a time per each fraction equal to the vortex threads rotation period inside the current tube r_e/v_0 . Bearing in mind (2) and (5), we obtain the duration of the total energy dissipation by the neutron:

$$t = (2\pi)^{1/2} \frac{\Delta m}{\cos q_w} \frac{a^4 n_e^4}{c_0^{2/3}} \times [\text{sec}] = 629 \text{ sec.} \quad (19)$$

The same duration is determined by the time constant - the return duration of the excited axisymmetric contour with the total length $\pi c_0^{2/9}$ to its initial state due to its constituent current lines rotation with the speed v_0 :

$$t = \frac{\pi c_0^{2/9} r_e}{v_0} = 604 \text{ sec.} \quad (20)$$

The neutron half-life is about 609 seconds. Thus, the consistency of formulas (12), (19), (20) with each other and their results with the actual values of the neutron lifetime and the neutron-proton mass difference confirm the accepted model of proton-neutron transitions.

5 Conclusion

In the articles concerning the microworld and, in particular, the proton properties, it has been established that there are only three generations of elementary particles. The parameters of the proton (mass, magnetic moment, charge radius, proton lifetime, neutron-proton mass difference) are determined. A physical explanation is proposed for such abstract images as quarks and their confinement, “color”, pions “coat”, etc. The results were obtained within the framework of the elementary model based on the mechanistic interpretation of Wheeler’s geometrodynamics. Wherein the balances between the main interactions and general patterns were only used, moreover, without adding any empirical coefficients.

The model can be used as a basis for constructing the theory of strong interactions, which can be an alternative for

QCD. In a possible new theory, the interpretation of the concepts and results obtained, which form the model basis, can be performed in some terms of electrodynamics (or some other) on the basis of a suitable mathematical apparatus.

Submitted on November 4, 2020

References

1. Belyakov A.V. On the uniform dimension system. Is there the necessity for Coulomb? *Progress in Physics*, 2013, v.9, issue 3, 142–143.
2. Belyakov A.V. Macro-analogies and gravitation in the micro-world: further elaboration of Wheeler’s model of geometrodynamics. *Progress in Physics*, 2012, v.8, issue 2, 47–57.
3. Belyakov A.V. Charge of the electron, and the constants of radiation according to J. A. Wheeler’s geometrodynamics model. *Progress in Physics*, 2010, v.6, issue 4, 90–94.
4. Belyakov A.V. Nuclear power and the structure of a nucleus according to J. Wheeler’s geometrodynamics concept. *Progress in Physics*, 2015, v.11, issue 1, 89–98.
5. Bezginov N., Valdez T., Horbatsch M., Marsman A., Vutha A.C., Hesses E.A. A measurement of the atomic hydrogen Lamb shift and the proton charge radius. *Science*, 06 Sep. 2019, v.365, issue 6457, 1007–1012.
6. Belyakov A.V. On materiality and dimensionality of the space. Is there some unit of the field? *Progress in Physics*, 2014, v.10, issue 4, 203–206.
7. Belyakov A.V. Gravity in the microworld. *Progress in Physics*, 2020, v.16, issue 1, 58–61.
8. Belyakov A.V. Determination of the neutrino mass. *Progress in Physics*, 2016, v.12, issue 1, 34–38.
9. Belyakov A.V. On the speed of light and the continuity of physical vacuum. *Progress in Physics*, 2018, v.14, issue 4, 211–212.

Algebra of Discrete Symmetries in the Extended Poincaré Group

Valeriy V. Dvoeglazov

UAF, Universidad Autónoma de Zacatecas, Apartado Postal 636, Zacatecas 98061 Zac., México
E-mail: valeri@fisica.uaz.edu.mx

We begin with the comprehensive review of the basics of the Lorentz, (extended) Poincaré Groups and $O(3,2)$ and $O(4,1)$. On the basis of the Gelfand-Tsetlin-Sokolik-Silagadze research [1-3], we investigate the definitions of the discrete symmetry operators both on the classical level, and in the secondary-quantization scheme. We study physical content within several bases: light-front form formulation, helicity basis, angular momentum basis, on several practical examples. The conclusion is that we have ambiguities in the definitions of the corresponding operators $P, C; T$, which lead to different physical consequences.

Talk presented at the LXII Congreso Nacional de Física. 6–11/10/2019. Villahermosa, Tab., México.

1 The standard definitions

The Lorentz Group conserves the interval $ds^2 = dx^\mu dx_\mu$ in the 4-space with respect to (pseudo) Euclidean rotations. The Poincaré Group includes translations in the Minkowski space. The extended Poincaré Group includes discrete transformations, the unitary C, P , and the antiunitary T in quantum field theory (QFT). The P is the space inversion: $x^0 \rightarrow x^0, \mathbf{x} \rightarrow -\mathbf{x}$. The T is the time reversal: $x^0 \rightarrow -x^0, \mathbf{x} \rightarrow \mathbf{x}$. The C is the electric charge conjugation. It is related to the PT operation: $x^0 \rightarrow -x^0, \mathbf{x} \rightarrow -\mathbf{x}$. The interval is also conserved under these operations. In QFT, the eigenvalues of the combined CPT are also invariants.

While [4] presented the derivation method to obtain the field operator *ab initio*, we define the field operator [5, 6] in the pseudo-Euclidean metrics as follows:

$$\Psi(x) = \sum_h \int \frac{d^3\mathbf{p}}{(2\pi)^3 2E_p} [u_h(\mathbf{p})a_h(\mathbf{p})e^{-ip \cdot x} + v_h(\mathbf{p})b_h^\dagger(\mathbf{p})e^{+ip \cdot x}]. \quad (1)$$

Hence, the Dirac equation is:

$$[i\gamma^\mu \partial_\mu - m]\Psi(x) = 0. \quad (2)$$

At least, 3 methods of its derivation exist [7–9]:

- the Dirac method (the Hamiltonian should be linear in $\partial/\partial x^i$, and be compatible with $E_p^2 - \mathbf{p}^2 c^2 = m^2 c^4$);
- the Sakurai one (based on the equation $(E_p - \sigma \cdot \mathbf{p})(E_p + \sigma \cdot \mathbf{p})\phi = m^2 \phi$);
- the Ryder one (the relation between 2-spinors at rest is $\phi_R(\mathbf{0}) = \pm \phi_L(\mathbf{0})$ and boosts).

It has solutions of positive energies and negative energies. The latter are reinterpreted as the antiparticles.

$$E_p = \sqrt{\mathbf{p}^2 + m^2}, \quad c = \hbar = 1, \quad g^{\mu\nu} = \text{diag}\{1, -1, -1, -1\}.$$

The solutions in the momentum representation are: $u_h(\mathbf{p}) = \text{column}(\phi_R^h(\mathbf{p}), \phi_L^h(\mathbf{p}))$. Next,

$$u_h = \begin{pmatrix} \exp(+\sigma \cdot \varphi) \phi_R^h(\mathbf{0}) \\ \exp(-\sigma \cdot \varphi) \phi_L^h(\mathbf{0}) \end{pmatrix}, \quad v_h(\mathbf{p}) = \gamma^5 u_h(\mathbf{p}), \quad (3)$$

where $\cosh(\varphi) = E_p/m, \sinh(\varphi) = |\mathbf{p}|/m, \hat{\varphi} = \mathbf{p}/|\mathbf{p}|$, and h is the polarization index. It is shown that the parity operator can be chosen as

$$P = e^{i\alpha_s} \gamma^0 R, \quad \gamma^0 = \begin{pmatrix} 0 & 1 \\ 1 & 0 \end{pmatrix}, \quad (4)$$

because

$$[i\gamma^\mu \partial'_\mu - m]\Psi(x^{\mu'}) = 0, \quad (\text{change of variables}), \quad (5)$$

where

$$\Psi(x^{\mu'}) = \mathcal{A}\Psi(x^\mu), \quad (\text{linearity}). \quad (6)$$

These conditions can be satisfied by the γ^0 matrix in the Weyl basis. R can be chosen

$$R \equiv (\theta \rightarrow \pi - \theta, \phi \rightarrow \pi + \phi, r \rightarrow r).$$

For fermions, it is well known that a particle and an antiparticle have opposite eigenvalues of the parity operator in this $(1/2, 0) \oplus (0, 1/2)$ representation of the Lorentz Group. In QFT we should have:

$$U_P \psi(x) U_P^\dagger = e^{i\alpha_s} \gamma^0 \psi(x'). \quad (7)$$

So,

$$U_P a_h(\mathbf{p}) U_P^\dagger = e^{+i\alpha_s} a_h(\mathbf{p}'), \quad (8)$$

$$U_P b_h(\mathbf{p}) U_P^\dagger = -e^{-i\alpha_s} b_h(\mathbf{p}').$$

The operator U_P can be constructed in the usual way, see [5] and [6]. The charge operator interchanges the particle and the antiparticle. For example, in the Dirac case on the classical level:

$$u_\uparrow \rightarrow -v_\downarrow, \quad u_\downarrow \rightarrow +v_\uparrow, \quad v_\uparrow \rightarrow +u_\downarrow, \quad v_\downarrow \rightarrow -u_\uparrow. \quad (9)$$

Thus, we can write, thanks to E. Wigner:

$$C_{1/2} = e^{i\alpha_c} \begin{pmatrix} 0 & i\Theta \\ -i\Theta & 0 \end{pmatrix} \mathcal{K}, \quad \Theta = \begin{pmatrix} 0 & -1 \\ 1 & 0 \end{pmatrix} = -i\sigma_2. \quad (10)$$

In QFT, we should have:

$$U_C \psi(x) U_C^\dagger = e^{i\alpha_c} C \psi^\dagger(x). \quad (11)$$

So [5],

$$U_C a_h(\mathbf{p}) U_C^\dagger = e^{+i\alpha_c} b_h(\mathbf{p}), \quad U_C b_h(\mathbf{p}) U_C^\dagger = e^{-i\alpha_c} a_h(\mathbf{p}). \quad (12)$$

See however [11], where two possibilities for the charge conjugation operator have been proposed.

The time reversal operator is antiunitary (see Wigner and [4]). Let us remind that the operator of hermitian conjugation does not act on c -numbers on the left side of (13) below. This fact is connected with the properties of an antiunitary operator: $[V^T \lambda A (V^T)^{-1}]^\dagger = [\lambda^* V^T A (V^T)^{-1}]^\dagger = \lambda [V^T A^\dagger (V^T)^{-1}]$.

$$[V_{[1/2]}^T \Psi(x^\mu) (V_{[1/2]}^T)^{-1}]^\dagger = S(T) \Psi^\dagger(x'^{\mu}). \quad (13)$$

We can see that C and P anticommute in the Dirac case:

$$\{C, P\}_+ = 0, \quad P^2 = 1, \quad C^2 = 1, \quad (14)$$

and $(CPT) = \pm 1$. However, we present the opposite case later, where $(CPT) = \pm i$, which is related to the commutation (anticommutation) of the C and P operators.

The table on p. 157 of [5] gives us the properties of the scalar, 4-vector, tensor, axial-vector and pseudoscalar under these transformations in the case of the ‘‘Dirac-like parity’’ definitions. However, see the next Section.

2 Anomalous representations of the inversion group

The previous Section perfectly describes the CPT properties of the charged fermions. Nevertheless, the authors of [1,2,10] proposed another class of representations of the full Lorentz Group long ago. As it was shown recently, it may be applied to the (anti)bosons of the opposite parities, and to the (anti)fermions of undefined parities. The latter are not the eigenstates of the parity operator, but they are the eigenstates of the charge-conjugate operator. Gelfand, Tsetlin and Sokolik noted that there exist representations of the full Lorentz Group of the anomalous parity. Originally, this concept was intended to be applied to explain the decay of K -mesons.

The examples are: one can note that in the $(1/2, 1/2)$ representation (or for x^μ) the operators of the space inversion (t_{01}), the time reversal (t_{10}) and the combined space-time inversion (t_{11}) are commutative. They form the inversion group together with the unit element. Let us search the projective representations of the Lorentz group combined with the discrete group. As opposed to the usual case, $t_{01}t_{10} = t_{11}$,

$t_{10}t_{11} = t_{01}$, $t_{01}t_{11} = t_{10}$, for instance, one can drop the condition of commutativity, and one can form the projective representation with $T_{10}T_{01} = -T_{11}$, or $T_{11}T_{11} = -1$, see the full table in [1]. They noted that there are *two* normal-parity (in their notation) and *two* anomalous parity representations for (bi)spinors. Then, they extended the concept of the anomalous parity to any representation of the proper Lorentz Group characterized by the numbers (k_0, k_1) and $(-k_0, k_1)^*$. When

$$[T_{i'k'}, T_{i''k''}]_+ = 0, \quad (15)$$

this is the case of the anomalous parity (later, this was confirmed by Nigam and Foldy [12]). G. Sokolik noted that this concept is related to the concept of the 5-D representations of the proper orthogonal group with pseudo-Euclidean metrics. For example,

$$\begin{aligned} T_{10} &\sim H_{54} = \exp(i\pi I_{54}/2), \\ T_{11} &\sim H_{43} H_{21} = \exp(i\pi I_{43}) \exp(i\pi I_{21}), \\ T_{01} &= T_{11} T_{10}. \end{aligned} \quad (16)$$

T_{10}, T_{01}, T_{11} leave invariant the extended 8-component Dirac equation only (compare with [13] and [14]):

$$\Gamma_\mu \partial^\mu \psi + m\psi = 0, \quad \Gamma_\mu = \begin{pmatrix} \gamma_\mu & 0 \\ 0 & -\gamma_\mu \end{pmatrix}. \quad (17)$$

They claimed relations to the concepts (known in that time):

- istopic spin;
- fusion theory;
- the non-linear Heisenberg theory

were mentioned. The corresponding matrix representations of the anomalous-parity representations have been presented:

$$T_{01} = \begin{pmatrix} 0 & I \\ I & 0 \end{pmatrix}, \quad T_{10} = \begin{pmatrix} 0 & -I \\ I & 0 \end{pmatrix}, \quad T_{11} = \begin{pmatrix} I & 0 \\ 0 & -I \end{pmatrix}, \quad (18)$$

and

$$T_{01} = \begin{pmatrix} 0 & -iI \\ iI & 0 \end{pmatrix}, \quad T_{10} = \begin{pmatrix} 0 & iI \\ iI & 0 \end{pmatrix}, \quad T_{11} = \begin{pmatrix} I & 0 \\ 0 & -I \end{pmatrix}. \quad (19)$$

Later Wigner [10] repeated their results in the Istanbul School lectures (1962), and Silagadze [3] rediscovered and applied this possibility in 1992. The conclusion of these papers is: we noted that both new versions of the representations of the full Lorentz Group (commuting spinor and anticommuting boson representations) lead to the doubling of the dimensionality of the ψ -function.

3 The self/anti-self charge conjugate states

The content of this Section contains the material of [11]. The conclusions are: we have constructed another explicit example of the BWW-GTS theory. The matter of physical dynamics connected with this mathematical construct should be

solved in the future, dependent on what gauge interactions with potential fields we introduce [14] and what experimental setup we choose.

Received on Nov. 6, 2020

References

1. Gelfand I. M. and Tsetlin M. L. *Sov. Phys. JETP*, 1957, v. 4, 947.
2. Sokolik G. A. *Sov. Phys. JETP*, 1958, v. 6, 1170; *ibid.*, 1959, v. 9, 781; *Dokl. Akad. Nauk SSSR*, 1957, v. 114, 1206.
3. Silagadze Z. K. *Sov. J. Nucl. Phys.*, 1992, v. 55, 392.
4. Bogoliubov N. N. and Shirkov D. V. *Introduction to the Theory of Quantized Fields*. John Wiley & Sons, NY, 1980.
5. Itzykson C. and Zuber J.-B. *Quantum Field Theory*. McGraw-Hill International Book Co., NY, 1980.
6. Greiner W. *Field Quantization*. Springer, Berlin-Heidelberg, 1996.
7. Dirac P. A. M. *Proc. Roy. Soc. Lond.*, 1929, v. A117, 610.
8. Sakurai J. J. *Advanced Quantum Mechanics*. Addison-Wesley, Reading, 1967, §3.2.
9. Ryder L. H. *Quantum Field Theory*. Cambridge University Press, Cambridge, 1985.
10. Wigner E. P. in: Gursev F., ed., *Group Theoretical Concepts and Methods in Elementary Particle Physics*. Gordon and Breach, NY, 1964.
11. Dvoeglazov V. V. *Mod. Phys. Lett.*, 1997, v. A12, 2741. arXiv: hep-th/9609142.
12. Nigam B. P. and Foldy L. L. *Phys. Rev.*, 1956, v. 102, 1410.
13. Markov M. A. *ZhETF*, 1937, v. 7, 579; *ibid.*, 1937, v. 7, 603.
14. Dvoeglazov V. V. *Nuovo Cim.*, 1995, v. 108A, 1467.

Theoretical Study on Polarized Photon

Shixing Weng

E-mail: wengs2015@gmail.com, Brampton, Canada

A solution of electromagnetic four-potential for polarized photon is obtained by solving its wave equations in elliptic cylindrical coordinates. An explicit energy wave function for the photon is presented in the form of a linear combination of the electric field and magnetic field from the solution. This wave function is used to calculate the angular momentum value of the photon. The elliptic coordinate parameter, a , for the photon is considered to be equal to a quarter of its wavelength.

1 Introduction

Photon as a quantum of light has attracted many researchers to develop explanations on its behaviors and to experiment to determine its properties. The photon as a fundamental wave-particle which moves at the speed of light serves like a messenger traveling from one place to another, which is necessary for the physical world to work properly. The classical view on light is provided by Maxwell's theory of electromagnetism [1], hence light is considered as a bundle of electromagnetic transverse waves. The particle view of light in modern physics may be provided by Einstein [2], so a photon has not only energy but also momentum. Work has been done to unify these two views. An expression for photon wave function is introduced by using the Riemann-Silberstein vector which is a linear combination of the electric field and magnetic field of the photon. An overview of the work on photon wave function is available in [3].

A photon has wave-particle duality which may be explained by a single entity as a joint wave-particle [4]. A more specific view on the electromagnetic structure for the photon is presented in [5], which is for circularly polarized photons. Hence the photon in circular polarization may be viewed as a charged moving electric capacitor with electric charge distributed circularly on its cylindrical surface of radius $\lambda/2\pi$, where λ is the wavelength of the photon.

In this article, we present our theoretical study on polarized photons. It is well known that polarized light has the property of certain orientation which may be generated by an optical polarizer. Recent experiment [6] shows that the transmission intensity of polarized light strongly correlates to the orientation of elliptically-shaped holes on the transmission plate. This as an example indicates that the transverse field strength of photons in the polarized light is not circularly distributed evenly as different from that of circularly polarized photons. The novelty of this article is on: the wave equation for the photon is solved within the elliptic cylindrical coordinates; an explicit photon energy wave function is presented based on the expression of Riemann-Silberstein vector wave function (in the next section); quantum expressions of the energy density, energy current density and the angular momentum or spin density for the photon are derived from the wave

function. We are not aware of such work in the literature.

This article is divided into the following sections: Introduction, Method, Results and Discussions, and Conclusion. The Introduction section provides a brief overview on our current understanding of the photon.

In the Method section, we will use similar method as in [5]. First we obtain a solution for the electromagnetic four-potential by solving the wave equations in elliptic cylindrical coordinates. The electromagnetic four-potential generally includes a scalar potential, which is an electric potential divided by the speed of light, and a vector potential. Then show to get the electric field and magnetic field from the solution of the four-potential; an explicit energy wave function for the photon is presented as a linear combination of the electric field and magnetic field; other expressions such as photon energy density, energy current density and angular momentum density are derived based on quantum mechanics.

In the Results and Discussions section we show the results for the photon expressions developed in the previous section, such as the four-potential, electromagnetic fields, the wave function, energy and energy current densities, and angular momentum for the photon; fairly detailed work is presented in evaluating the angular momentum value for the photon; some particularities are discussed. The Conclusion section provides a brief summary of the work presented in this article. We use MKS units in this work.

2 Method

In the space region where there are no other free electric charge and electric current, the electric potential ψ and the vector potential \mathbf{A} satisfy the following wave equations, respectively,

$$\frac{1}{c^2} \frac{\partial^2 \psi}{\partial t^2} - \nabla^2 \psi = 0, \quad (1)$$

$$\frac{1}{c^2} \frac{\partial^2 \mathbf{A}}{\partial t^2} - \nabla^2 \mathbf{A} = 0, \quad (2)$$

where c is the speed of light, t is time, ∇^2 is the Laplacian operator, and $\frac{1}{c^2} \frac{\partial^2}{\partial t^2} - \nabla^2$ is D'Alembert's operator which is also written as \square . In obtaining these equations the set of Maxwell equations with Lorenz gauge is employed. The Lorenz gauge

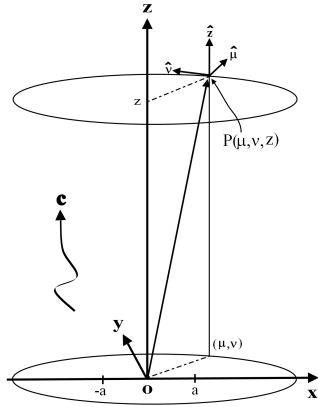


Fig. 1: A drawing of the elliptic cylindrical coordinate system together with the cartesian coordinates, where $\hat{\mu}$, $\hat{\nu}$, and \hat{z} are unit vectors for the coordinate system and a is a length parameter that marks the focal points on x of the ellipse. The major axis of the ellipse is x . The wave symbol represents a photon moving in the direction of the positive z axis at the speed of light c .

is given by

$$\nabla \cdot \mathbf{A} + \frac{1}{c^2} \frac{\partial \psi}{\partial t} = 0. \tag{3}$$

Eqs. (1) and (2) are satisfied with solutions for traveling waves.

For the polarized photon, we solve (1) and (2) in elliptic cylindrical coordinates as shown in Fig. 1. Where the relationships between the cartesian and elliptic cylindrical coordinates are

$$\begin{aligned} x &= a \cosh \mu \cos \nu, \\ y &= a \sinh \mu \sin \nu, \\ z &= z, \end{aligned} \tag{4}$$

where x, y, z are cartesian coordinate values and μ, ν, z are elliptic cylindrical coordinate values, a is a length parameter which specifies the focal points of the ellipse, $\mu \in (0, \infty)$ and $\nu \in (0, 2\pi)$. The value of a will be considered later to be proportional to the wavelength of the photon. The scale factors are

$$\begin{aligned} h_\mu &= h_\nu = a\gamma, \\ h_z &= 1, \end{aligned} \tag{5}$$

where $\gamma = \sqrt{\sinh^2 \mu + \sin^2 \nu}$.

We find for this particular case that the vector potential \mathbf{A} has a z component only so $\mathbf{A} = \hat{z}A_z$ and $\nabla^2 \mathbf{A} = \hat{z}\nabla^2 A_z$, where \hat{z} is the unit vector for the z axis. The Laplacian operator ∇^2

for the elliptic cylindrical coordinates is expressed as

$$\nabla^2 = \frac{1}{a^2\gamma^2} \left(\frac{\partial^2}{\partial \mu^2} + \frac{\partial^2}{\partial \nu^2} \right) + \frac{\partial^2}{\partial z^2}. \tag{6}$$

Hence (1) and (2) in the elliptic cylindrical coordinates are satisfied with the following general solution:

$$f = f_0 e^{-\mu} \sin(\phi), \tag{7}$$

where f is a general quantity that may represent either ψ or A_z here, f_0 is the corresponding constant, $\phi = kz + \nu - \omega t$, and $k = \omega/c$, and ω is the angular frequency of the photon. We choose the “-” sign in the exponential function to make the solution to be limited in space. Here we let the photon travel in the z direction. And we arbitrarily choose the sine function here, one may choose cosine function as well but the results should be similar. By using the Lorenz gauge we have the following relationship for the electric potential constant, ψ_0 , and the vector potential constant, A_0 , as

$$A_0 = \psi_0/c. \tag{8}$$

Once we have the solution of the four-potential we can calculate [7] the electric field \mathbf{E} and magnetic field \mathbf{B} using the following equations,

$$\mathbf{E} = -\nabla\psi - \frac{\partial \mathbf{A}}{\partial t} = -\frac{1}{a\gamma} \left(\hat{\mu} \frac{\partial}{\partial \mu} + \hat{\nu} \frac{\partial}{\partial \nu} \right) \psi, \tag{9}$$

$$\mathbf{B} = \nabla \times \mathbf{A} = \frac{1}{a\gamma} \left(\hat{\mu} \frac{\partial}{\partial \nu} - \hat{\nu} \frac{\partial}{\partial \mu} \right) A_z, \tag{10}$$

where $\hat{\mu}, \hat{\nu}$ are unit vectors for μ and ν , respectively, and “ \times ” represents the vector cross operator. In deriving (9) for the electric field, we used this case relationship:

$$\frac{\partial \psi}{\partial z} + \frac{\partial A_z}{\partial t} = 0.$$

Both the electric field \mathbf{E} and magnetic field \mathbf{B} are vectors with μ and ν components, which are perpendicular to the direction of the wave propagation. They represent transverse waves.

As we know, a photon is a packet of energy in electromagnetic field form and moves at the speed of light. This means that the electric field \mathbf{E} or the magnetic field \mathbf{B} of the photon can not exist alone and they are both like two faces of one body. We have the following expression of the electromagnetic field \mathbf{F} suit for the photon

$$\mathbf{F} = \frac{1}{\sqrt{2}} \left(\sqrt{\epsilon} \mathbf{E} + i \frac{\mathbf{B}}{\sqrt{u}} \right), \tag{11}$$

where ϵ is the permittivity and u is the permeability in the space region where photon absorption is negligible, and i is

the imaginary unit. This expression is known as the Riemann-Silberstein vector and was introduced as a photon wave function in [8]. Here the choice of “+” sign for the imaginary part is arbitrary, one may choose “-” for similar results. Like \mathbf{E} or \mathbf{B} , \mathbf{F} is also a vector which satisfies the wave equation and also represents a transverse traveling wave. The field \mathbf{F} is a complex vector in general and is characterized as a quantum vector wave function. Hence methods developed in quantum mechanics may be employed here [9]. By the dimensional analysis we know that \mathbf{F} represents an energy density wave function. In the following we use \mathbf{F} to derive expressions for energy and current densities and then the angular momentum for the photon. For clarity, the cartesian coordinates are used in the following work. We start from the wave equations:

$$\frac{1}{c^2} \frac{\partial^2 \mathbf{F}}{\partial t^2} - \nabla^2 \mathbf{F} = 0, \quad (12)$$

and

$$\frac{1}{c^2} \frac{\partial^2 \mathbf{F}^*}{\partial t^2} - \nabla^2 \mathbf{F}^* = 0, \quad (13)$$

where \mathbf{F}^* is the conjugate of \mathbf{F} . And

$$\mathbf{F} = \hat{\mathbf{x}}F_x + \hat{\mathbf{y}}F_y, \quad (14)$$

where $\hat{\mathbf{x}}$ and $\hat{\mathbf{y}}$ are unit vectors and F_x, F_y are the field components for x and y axes, respectively. As a transverse wave, \mathbf{F} has x and y components only and the z component, F_z is zero. Since our original solution for \mathbf{F} is in elliptic coordinates with components of μ and ν , we may convert those to x and y components using the following matrix multiplication,

$$\begin{bmatrix} \hat{\mu} \\ \hat{\nu} \end{bmatrix} = \frac{1}{\gamma} \begin{bmatrix} \sinh \mu \cos \nu & \cosh \mu \sin \nu \\ -\cosh \mu \sin \nu & \sinh \mu \cos \nu \end{bmatrix} \begin{bmatrix} \hat{\mathbf{x}} \\ \hat{\mathbf{y}} \end{bmatrix}. \quad (15)$$

Since F_x and F_y are explicit functions of μ and ν , in order to do their derivatives with respect to x and y we need partial derivatives of μ and ν to x and y by using the following matrix form:

$$\begin{bmatrix} \delta \mu \\ \delta \nu \end{bmatrix} = \frac{1}{a\gamma^2} \begin{bmatrix} \sinh \mu \cos \nu & \cosh \mu \sin \nu \\ -\cosh \mu \sin \nu & \sinh \mu \cos \nu \end{bmatrix} \begin{bmatrix} \delta x \\ \delta y \end{bmatrix}, \quad (16)$$

where δ is a tiny increment. In obtaining (16), we first do the tiny variations of (4) for x and y to μ and ν to get a conversion matrix between the two coordinate systems. And then find the inverse matrix as in (16). Eq. (15) is equivalent to (16) if we replace each variation together with its scale factor such as $a\gamma$ in the latter equation by the corresponding unit vector.

As is common in quantum mechanics to find the energy density and the energy current density for the photon, we do this operation:

$$\mathbf{F}^* \cdot (12) - \mathbf{F} \cdot (13), \quad (17)$$

where “ \cdot ” represents the dot product operator and “ $*$ ” is the complex conjugate symbol, and

$$\mathbf{F}^* \cdot \nabla^2 \mathbf{F} = \sum_i^{x,y,z} F_i^* \nabla^2 F_i, \quad (18)$$

where the summation is over the three cartesian components. By a few mathematical operations, we have the following form of energy current and density continuity equation:

$$\nabla \cdot \mathbf{j} + \frac{\partial \rho}{\partial t} = 0 \quad (19)$$

with

$$\mathbf{j} = \frac{c^2}{2i\omega} \sum_i^{x,y,z} (F_i \nabla F_i^* - F_i^* \nabla F_i) \quad (20)$$

and

$$\rho = \frac{1}{2i\omega} \left(\mathbf{F}^* \cdot \frac{\partial \mathbf{F}}{\partial t} - \mathbf{F} \cdot \frac{\partial \mathbf{F}^*}{\partial t} \right) = \mathbf{F} \cdot \mathbf{F}^*, \quad (21)$$

where \mathbf{j} is the energy current density and ρ is the energy density for the photon, $\nabla = \hat{\mathbf{x}} \frac{\partial}{\partial x} + \hat{\mathbf{y}} \frac{\partial}{\partial y} + \hat{\mathbf{z}} \frac{\partial}{\partial z}$. The photon propagation phase factor is $e^{-i\phi}$ in this case (see next section) and $\frac{\partial \mathbf{F}}{\partial t} = i\omega \mathbf{F}$. The energy density ρ is positive.

Now the angular momentum increment for the photon is

$$d\mathbf{S} = \hat{\mathbf{z}} (xj_y - yj_x) \frac{dV}{c^2}, \quad (22)$$

where \mathbf{S} is the angular momentum vector or spin for the photon, j_x/c^2 and j_y/c^2 are the momentum densities in the x and y directions, respectively, and dV is the tiny volume in space. Notice that \mathbf{j} needs to be divided by c^2 to be converted to the momentum density. The angular momentum for the photon in the present case has only the z component and zero x and y components. Eq. (22) may be rewritten in the form of spin momentum density as

$$\frac{d\mathbf{S}}{dV} = \frac{1}{c^2} (xj_y - yj_x). \quad (23)$$

In the next section we present results using relationships developed here and also provide discussions on the results.

3 Results and Discussions

To start this section we first present the mathematical solution of the four-potential for the polarized photon, which are two traveling wave functions, one for the electric potential ψ , which is a scalar, and the other for the vector potential \mathbf{A} . These functions are desirable since they are limited in space and show wave-particle duality with a limited length. These basic representations are important since, from which we may derive other physical quantities for the photon, such as electromagnetic fields and the spin angular momentum.

Now the solution for the four-potential in elliptic cylindrical coordinates is

$$\psi = \psi_0 e^{-\mu} \sin(\phi) \quad (24)$$

and

$$\mathbf{A} = \hat{\mathbf{z}}A_0 e^{-\mu} \sin(\phi), \quad (25)$$

where we assume that the photon travels in the z direction.

The vector potential in this case has only a z component. The choice of the sine function here is arbitrary, one may use the cosine function but the result should be similar since they only have a phase difference of $\pi/2$. Notice that (24) and (25) are in the same form with corresponding magnitude, and with the same phase change in both space and time. Since the physical meaning of the electric potential ψ is clear, $c^2\mathbf{A}$ may be interpreted as an electric potential current or the total-electric-potential current density flowing in the same direction as the photon, which satisfy the continuity equation given by the Lorenz gauge condition (3). Hence the Lorenz gauge may be considered as the conservation of the total-electric-potential, a physical quantity of the integration of electric potential in the whole space. With the Lorenz gauge, we can get the relationship between the two constants as in (8)

Comparing with that of circularly polarized photons [5], the strength of the four-potential for the elliptically polarized photon decreases exponentially with μ in the single space region, while the other is divided into two regions by a parameter r_0 and decreases with $1/r$ for $r > r_0$, where r is the radial value in polar cylindrical coordinates. As a result, the potential strength for the polarized photon with certain energy decreases quicker with distance from its center than that for circularly polarized photon, and hence the polarized photon may occupy less space.

Now we present expressions for the electric and magnetic fields using (9) and (10):

$$\mathbf{E} = \frac{\psi_0 e^{-\mu}}{a\gamma} [\hat{\mu} \sin(\phi) - \hat{\nu} \cos(\phi)], \quad (26)$$

and

$$\mathbf{B} = \frac{A_0 e^{-\mu}}{a\gamma} [\hat{\mu} \cos(\phi) + \hat{\nu} \sin(\phi)]. \quad (27)$$

These results of \mathbf{E} and \mathbf{B} show that they are transverse waves and are perpendicular to each other. The energy density in classical theory for the photon is

$$\rho = \frac{1}{2} \left(\epsilon \mathbf{E}^2 + \frac{\mathbf{B}^2}{u} \right) = \frac{\epsilon \psi_0^2}{a^2 \gamma^2} e^{-2\mu} \quad (28)$$

and the Poynting vector is

$$\mathbf{P} = \frac{\mathbf{E} \times \mathbf{B}}{u} = \hat{\mathbf{z}} \frac{c\epsilon\psi_0^2}{a^2\gamma^2} e^{-2\mu}, \quad (29)$$

where, in converting A_0 , we used (8). These quantities are finite in space and are physically meaningful. The magnitudes of these quantities decrease exponentially with 2μ . Since the factor $a^2\gamma^2$ is equal to the combination of scale factors for both μ and ν , it can be canceled in each space integration by the same volume factor as shown later. With the Poynting

vector, the photon may be viewed as a packet of energy moving at the speed of light along its propagation direction.

Since a photon is actually a quantum entity in modern physics view, we need an integral expression as (11). This is a linear combination of both the electric field and magnetic field for the elliptically polarized photon. Therefore we have a photon wave function. There are at least two advantages to have the wave function. First it can be used to calculate the value of the angular momentum for the photon; secondly it may be used to calculate the penetration probability for the photon in a sub-wavelength hole since in the view of quantum mechanics it represents the photon probability distribution. But in this article, we aim at the angular momentum value for the photon with the wave function.

In the following, we first obtain an explicit wave function using the developed expression in last section, (11), secondly derive the component expressions for energy current densities, and finally calculate the angular momentum value for the photon. This procedure has been first applied successfully to the circularly polarized photon. In this article, we report results on elliptically polarized photon.

By inserting results from (26) and (27) into (11), we have a photon wave function:

$$\mathbf{F} = \frac{\sqrt{\epsilon}\psi_0 e^{-i\phi}}{\sqrt{2}a\gamma} e^{-\mu}(i\hat{\mu} - \hat{\nu}). \quad (30)$$

Using the unit vector conversion (15), we have the cartesian components of \mathbf{F} as

$$F_x = \frac{\sqrt{\epsilon}\psi_0 e^{-i\phi}}{\sqrt{2}a\gamma^2} e^{-\mu}(i \sinh \mu \cos \nu + \cosh \mu \sin \nu), \quad (31)$$

$$F_x^* = \frac{\sqrt{\epsilon}\psi_0 e^{i\phi}}{\sqrt{2}a\gamma^2} e^{-\mu}(-i \sinh \mu \cos \nu + \cosh \mu \sin \nu), \quad (32)$$

$$F_y = iF_x, \quad (33)$$

and F_z is zero.

Due to the simple relationship between F_y and F_x , we have

$$F_y^* \nabla F_y = F_x^* \nabla F_x \quad (34)$$

and

$$F_y \nabla F_y^* = F_x \nabla F_x^*. \quad (35)$$

Hence in this case, (20) becomes

$$\mathbf{j} = \frac{c^2}{i\omega} (F_x \nabla F_x^* - F_x^* \nabla F_x) \quad (36)$$

and the work is reduced to one component. Furthermore since

$$F_x \nabla F_x^* = (F_x^* \nabla F_x)^*, \quad (37)$$

we have

$$\mathbf{j} = -\frac{2c^2}{\omega} \text{Im}(F_x^* \nabla F_x), \quad (38)$$

where “Im” means taking the real value of the imaginary part. And similarly, (21) becomes

$$\rho = \mathbf{F} \cdot \mathbf{F}^* = 2F_x \cdot F_x^* \tag{39}$$

Now inserting (31) and (32) into (39), we have

$$\rho = \frac{\epsilon\psi_0^2}{a^2\gamma^2} e^{-2\mu}, \tag{40}$$

which is the same as that of (28) for photon energy density. Now we do integration of (40) in space with the tiny volume, $dV = a^2\gamma^2 d\mu dv dz$. Assuming the photon length is $n\lambda$, where λ is the wavelength of the photon and n may be a positive integer, but is not exactly determined in the present work. The result should be equal to the photon energy $\hbar\omega$, where \hbar is the reduced Planck constant. By doing that, we determine the electric potential constant to be

$$\psi_0 = \sqrt{\frac{2\hbar c}{\epsilon n}} \frac{1}{\lambda}. \tag{41}$$

Now we evaluate the energy current densities for the photon. F_x contains z explicitly in ϕ of the exponential function, therefore the derivative with z is simple. We have $\frac{\partial F_x}{\partial z} = -ikF_x$ and

$$j_z = \frac{c\epsilon\psi_0^2}{a^2\gamma^2} e^{-2\mu}, \tag{42}$$

which is consistent with the Poynting vector (29).

And from (38), we have

$$j_x = -\frac{2c^2}{\omega} \text{Im} \left(F_x^* \frac{\partial F_x}{\partial x} \right) \tag{43}$$

and

$$j_y = -\frac{2c^2}{\omega} \text{Im} \left(F_x^* \frac{\partial F_x}{\partial y} \right). \tag{44}$$

The work is now turned to calculate $\frac{\partial F_x}{\partial x}$ and $\frac{\partial F_x}{\partial y}$. Because F_x contains explicit variables of μ and ν , we need the following equations to calculate the cartesian derivatives,

$$\frac{\partial F_x}{\partial x} = \frac{\partial F_x}{\partial \mu} \frac{\partial \mu}{\partial x} + \frac{\partial F_x}{\partial \nu} \frac{\partial \nu}{\partial x} \tag{45}$$

and

$$\frac{\partial F_x}{\partial y} = \frac{\partial F_x}{\partial \mu} \frac{\partial \mu}{\partial y} + \frac{\partial F_x}{\partial \nu} \frac{\partial \nu}{\partial y}, \tag{46}$$

where $\frac{\partial \mu}{\partial x}, \frac{\partial \nu}{\partial x}, \frac{\partial \mu}{\partial y}, \frac{\partial \nu}{\partial y}$ may be obtained from (16). We find that

$$\frac{\partial F_x}{\partial \mu} = \beta \left[i \left(\cosh \mu - \sinh \mu - 2 \frac{\sinh^2 \mu \cosh \mu}{\gamma^2} \right) \cos \nu + \left(\sinh \mu - \cosh \mu - 2 \frac{\sinh \mu \cosh^2 \mu}{\gamma^2} \right) \sin \nu \right], \tag{47}$$

$$\frac{\partial F_x}{\partial \nu} = \beta \left[-i \left(\cosh \mu + \sinh \mu + 2 \frac{\sinh \mu \cos^2 \nu}{\gamma^2} \right) \sin \nu + \left(\cosh \mu + \sinh \mu - 2 \frac{\cosh \mu \sin^2 \nu}{\gamma^2} \right) \cos \nu \right], \tag{48}$$

where $\beta = \sqrt{\epsilon}\psi_0 e^{-\mu} e^{-i\phi} / \sqrt{2}a\gamma^2$.

Now the cartesian derivatives are

$$\begin{aligned} \frac{\partial F_x}{\partial x} = \beta' & \left[i \left(\cosh^2 \mu \sin^2 \nu - \sinh^2 \mu \cos^2 \nu + \sinh \mu \cosh \mu - \right. \right. \\ & \left. \left. - 2 \sinh \mu \cosh \mu \cos^2 \nu \frac{\sinh^2 \mu - \sin^2 \nu}{\gamma^2} \right) - \right. \\ & \left. - \sin \nu \cos \nu \left(1 + 2 \sinh \mu \cosh \mu + \right. \right. \\ & \left. \left. + 2 \cosh^2 \mu \frac{\sinh^2 \mu - \sin^2 \nu}{\gamma^2} \right) \right], \end{aligned} \tag{49}$$

$$\begin{aligned} \frac{\partial F_x}{\partial y} = \beta' & \left[i \sin \nu \cos \nu \left(1 - 2 \sinh \mu \cosh \mu - \right. \right. \\ & \left. \left. - 2 \sinh^2 \mu \frac{\cosh^2 \mu + \cos^2 \nu}{\gamma^2} \right) + \right. \\ & \left. + \sinh^2 \mu \cos^2 \nu - \cosh^2 \mu \sin^2 \nu + \sinh \mu \cosh \mu - \right. \\ & \left. - 2 \sinh \mu \cosh \mu \sin^2 \nu \frac{\cosh^2 \mu + \cos^2 \nu}{\gamma^2} \right], \end{aligned} \tag{50}$$

where $\beta' = \sqrt{\epsilon}\psi_0 e^{-\mu} e^{-i\phi} / \sqrt{2}a^2\gamma^4$. These expressions are a little bit long but manageable. The purpose here is to serve as check points to guide the reader to the final correct results.

Using (43) and (44), we have

$$j_x = -\beta'' \sin \nu \left(\cosh \mu + \sinh \mu \frac{\cosh^2 \mu + \cos^2 \nu}{\gamma^2} \right), \tag{51}$$

$$j_y = \beta'' \cos \nu \left(\sinh \mu + \cosh \mu \frac{\sinh^2 \mu - \sin^2 \nu}{\gamma^2} \right), \tag{52}$$

where $\beta'' = c^2\epsilon\psi_0^2 e^{-2\mu} / \omega a^3 \gamma^4$.

Now using (23), we have

$$\begin{aligned} \frac{dS}{dV} = \alpha e^{-2\mu} & \left(\frac{\sinh \mu \cosh \mu}{\gamma^2} + \right. \\ & \left. + \frac{\sinh^2 \mu \cosh^2 \mu - \sin^2 \nu \cos^2 \nu}{\gamma^4} \right), \end{aligned} \tag{53}$$

where $\alpha = \epsilon\psi_0^2 / \omega a^2 \gamma^2$.

To calculate the spin value, we integrate (53) in the whole space. There are two parts to be integrated on the right hand side of the equation. This integration is a bit challenging since each integration part is divergent at $\mu = 0$ and $\nu = 0, \pi$. To avoid this problem we work around by first doing the integration of the second part which fortunately produces an exact

term to cancel the first part and the remaining is finite and manageable. We now show the integration of the second part:

$$\begin{aligned}
 I &= \int_0^{n\lambda} \int_0^\infty \int_0^{2\pi} dz d\mu dv \\
 &\quad e^{-2\mu} \frac{\sinh^2 \mu \cosh^2 \mu - \sin^2 \nu \cos^2 \nu}{\gamma^4} \\
 &= n\lambda \int_0^\infty \int_0^{2\pi} d\mu dv \\
 &\quad e^{-2\mu} \frac{\sinh^2 \mu \cosh^2 \mu - \sin^2 \nu \cos^2 \nu}{\gamma^4},
 \end{aligned} \tag{54}$$

where the scale factors in the integration volume are canceled within the α factor and we omit the rest of the constants here for simplicity. This integration may be further separated into sub-integration as

$$I_1 = \int_0^\infty \int_0^{2\pi} e^{-2\mu} \frac{\sinh^2 \mu \cosh^2 \mu}{(\sinh^2 \mu + \sin^2 \nu)^2} d\mu dv \tag{55}$$

and

$$I_2 = \int_0^\infty \int_0^{2\pi} e^{-2\mu} \frac{\sin^2 \nu \cos^2 \nu}{(\sinh^2 \mu + \sin^2 \nu)^2} d\mu dv. \tag{56}$$

These may be done by the partial integration method: for (55) first integrate with μ and for (56) first integrate with ν . Hence we have

$$\begin{aligned}
 I_1 &= - \int_0^\infty \int_0^{2\pi} e^{-2\mu} \frac{\sinh \mu \cosh \mu}{\sinh^2 \mu + \sin^2 \nu} d\mu dv + \\
 &+ \frac{1}{2} \int_0^\infty \int_0^{2\pi} e^{-2\mu} \frac{\sinh^2 \mu + \cosh^2 \mu}{\sinh^2 \mu + \sin^2 \nu} d\mu dv - \\
 &- \frac{1}{2} \left[e^{-2\mu} \sinh \mu \cosh \mu \int_0^{2\pi} \frac{d\nu}{\sinh^2 \mu + \sin^2 \nu} \right]_0^\infty
 \end{aligned} \tag{57}$$

and

$$I_2 = \frac{1}{2} \int_0^\infty \int_0^{2\pi} e^{-2\mu} \frac{\cos^2 \nu - \sin^2 \nu}{\sinh^2 \mu + \sin^2 \nu} d\mu dv. \tag{58}$$

Now the last integration term in (57) is zero at both $\mu = 0$ and $\mu \rightarrow \infty$. Hence (54) becomes

$$\begin{aligned}
 I &= -n\lambda \int_0^\infty \int_0^{2\pi} e^{-2\mu} \frac{\sinh \mu \cosh \mu}{\sinh^2 \mu + \sin^2 \nu} d\mu dv + \\
 &+ n\lambda \int_0^\infty \int_0^{2\pi} e^{-2\mu} d\mu dv,
 \end{aligned} \tag{59}$$

where the second integration term is the second integration term of (57) minus that of (58). And finally by finishing the second integration we have

$$I = - \int_0^{n\lambda} \int_0^\infty \int_0^{2\pi} e^{-2\mu} \frac{\sinh \mu \cosh \mu}{\gamma^2} dz d\mu dv + n\lambda\pi. \tag{60}$$

The first integration term in (60) cancels exactly the integration of the first part in (53) so the angular momentum for the photon is

$$S = \frac{\epsilon\psi_0^2}{\omega} n\lambda\pi = \hbar, \tag{61}$$

where we used (41). The value of spin or the angular momentum calculated here for the elliptically polarized photon is indeed \hbar .

Before concluding this section we consider the elliptic coordinate parameter a for the photon. The divergence of the electric field (26) is zero everywhere except at the two focal points ($x = \pm a$). This leads us to believe that electricity may only exist in these two focal points formed traveling lines. To further consider the value of a we take a look at that for circularly polarized photon [5]. In that case the electromagnetic field occupies two space regions divided by r_0 with the center core region carrying zero angular momentum for spin one. The elliptically polarized photon may be understood as transformed from the circularly polarized photon with its core region collapsed by its energy popped out without change in its length of circumference. If that is the case then $a = \lambda/4$.

4 Conclusion

To conclude this article we summarize what has been presented here. First, we have solved the wave equations for the electromagnetic four-potential in the elliptic cylindrical coordinates for the polarized photon. The solution for each potential is an electromagnetic traveling wave and its transverse strength decreases exponentially with μ . These expressions for the four-potential are simple but essential representations since they may be used to obtain other physical quantities for the polarized photon.

We first obtained the electric field and magnetic field for the photon from the four-potential solution. Then we have presented the energy wave function explicitly, which is a linear combination of the electric field and magnetic field. Using concepts from quantum mechanics, we first derived expressions then evaluated for photon energy, energy current, and angular momentum densities. Work is shown particularly in calculating the value of the angular momentum or spin for the photon. Considerations are given about the value of the elliptic coordinate parameter a which may be equal to a quarter of the photon wavelength.

Received on October 28, 2020

References

1. Jackson J.D. Classical Electrodynamics, 3rd ed. John Wiley & Sons Inc., New York, 1999.
2. Einstein A. *Annalen der Physik* (in German), 1905, v. 17 (6), 132. Einstein A. On a Heuristic Point of View Concerning the Production and Translation of Light. The Swiss Years: Writings, 1900–1909, v. 2, 86.
3. Millette P.A. Wave-Particle Duality in the Elastodynamics of the Spacetime Continuum (STCED). *Progress in Physics*, 2014, v. 10 (4), 255–258.

4. Lehnert B. Joint Wave-Particle Properties of the Individual Photon. *Progress in Physics*, 2007, v. 4, 104–108.
 5. Weng S. A Classical Model of the Photon. *Progress in Physics*, 2016, v. 12(1), 49–55.
 6. Gordon R., Brolo A. G., McKinnon A., Rajora A., Leathem B., and Kavanagh B. L. Strong Polarization in the Optical Transmission through Elliptical Nanohole Arrays. *Physical Review Letters*, 2004, v. 92(3), 037401(4).
 7. Arfken G., *Mathematical Methods for Physicists*, 3rd ed. Academic Press, Inc., New York, 1985
 8. Bialynicki-Birula I. Photon Wave Function. In Wolf E., ed. *Progress in Optics XXXVI*. Elsevier, Amsterdam, 1996, 245–294. arXiv: quantph/0508202v1.
 9. Davydov A. S. *Quantum Mechanics*, 2nd ed. Translated by Ter Haar D., Pergamon Press, New York, 1988
-

A Note on the Barut Second-Order Equation

Valeriy V. Dvoeglazov

UAF, Universidad Autónoma de Zacatecas, Apartado Postal 636, Zacatecas 98061 Zac., México
E-mail: valeri@fisica.uaz.edu.mx

The second-order equation in the $(1/2, 0) \oplus (0, 1/2)$ representation of the Lorentz group has been proposed by A. Barut in the 70s [1]. It permits to explain the mass splitting of leptons (e, μ, τ). The interest is growing in this model (see, for instance, the papers by S. Kruglov [2] and J. P. Vigié *et al.* [3, 4]). We note some additional points of this model.

The Barut main equation is

$$\left[i\gamma^\mu \partial_\mu + \alpha_2 \partial^\mu \partial_\mu - \kappa \right] \Psi = 0, \quad (1)$$

where α_2 and κ are the constants later related to the anomalous magnetic moment and mass, respectively. The matrices γ^μ are defined by the anticommutation relation:

$$\gamma^\mu \gamma^\nu + \gamma^\nu \gamma^\mu = 2g^{\mu\nu}, \quad (2)$$

$g^{\mu\nu}$ is the metrics of the Minkowski space, $\mu, \nu = 0, 1, 2, 3$. The equation represents a theory with the conserved current that is linear in 15 generators of the 4-dimensional representation of the $O(4, 2)$ group, $N_{ab} = \frac{1}{2} \gamma_a \gamma_b$, $\gamma_a = \{\gamma_\mu, \gamma_5, i\}$. Instead of 4 solutions, (1) has 8 solutions with the correct relativistic relation $E = \pm \sqrt{\mathbf{p}^2 + m_i^2}$. In fact, it describes states of different masses (the second one is $m_2 = 1/\alpha_2 - m_1 = m_e(1 + 3/2\alpha)$, α is the fine structure constant), provided that the certain physical condition is imposed on $\alpha_2 = (1/m_1)(2\alpha/3)/(1 + 4\alpha/3)$, the parameter (the anomalous magnetic moment should be equal to $4\alpha/3$). One can also generalize the formalism to include the third state, the τ -lepton [1b]. Barut has indicated the possibility of including γ_5 terms (e.g. $\sim \gamma_5 \kappa'$).

The most general form of spinor relations in the $(1/2, 0) \oplus (0, 1/2)$ representation has been given by Dvoeglazov [5]. It was possible to derive the Barut equation from first principles [6]. Let us reveal the connections with other models. For instance, in [3, 7] the following equation has been studied:

$$\begin{aligned} & \left[(i\hat{\partial} - e\hat{A})(i\hat{\partial} - e\hat{A}) - m^2 \right] \Psi = \\ & \left[(i\partial_\mu - eA_\mu)(i\partial^\mu - eA^\mu) - \frac{1}{2} e\sigma^{\mu\nu} F_{\mu\nu} - m^2 \right] \Psi = 0 \end{aligned} \quad (3)$$

for the 4-component spinor Ψ . $\hat{A} = \gamma^\mu A_\mu$; A_μ is the 4-vector potential; e is electric charge; $F_{\mu\nu}$ is the electromagnetic tensor. $\sigma^{\mu\nu} = \frac{i}{2} [\gamma^\mu, \gamma^\nu]$. This is the Feynman-Gell-Mann equation. In the free case we have the Lagrangian (see Eq. (9) of [3c]):

$$\mathcal{L}_0 = \overline{(i\hat{\partial}\Psi)}(i\hat{\partial}\Psi) - m^2 \overline{\Psi}\Psi. \quad (4)$$

Let us re-write (1) into the form:*

$$\left[i\gamma^\mu \partial_\mu + a\partial^\mu \partial_\mu + b \right] \Psi = 0. \quad (5)$$

*Of course, one could admit p^4, p^6 etc. in the Dirac equation too. The dispersion relations will be more complicated [6].

So, one should calculate ($p^2 = p_0^2 - \mathbf{p}^2$)

$$\text{Det} \begin{pmatrix} b - ap^2 & p_0 + \boldsymbol{\sigma} \cdot \mathbf{p} \\ p_0 - \boldsymbol{\sigma} \cdot \mathbf{p} & b - ap^2 \end{pmatrix} = 0 \quad (6)$$

in order to find energy-momentum-mass relations. Thus, $[(b - ap^2)^2 - p^2]^2 = 0$ and if $a = 0$, $b = \pm m$ we come to the well-known relation $p^2 = p_0^2 - \mathbf{p}^2 = m^2$ with four Dirac solutions. However, in the general case $a \neq 0$ we have

$$p^2 = \frac{(2ab + 1) \pm \sqrt{4ab + 1}}{2a^2} > 0, \quad (7)$$

that signifies that we do not have tachyons. However, the above result implies that we cannot just put $a = 0$ in the solutions, while it was formally possible in (5). When $a \rightarrow 0$ then $p^2 \rightarrow \infty$; when $a \rightarrow \pm\infty$ then $p^2 \rightarrow 0$. It should be stressed that *the limit in the equation does not always coincide with the limit in the solutions*. So, the questions arise when we consider limits, such as Dirac \rightarrow Weyl, and Proca \rightarrow Maxwell. The similar method has also been presented by S. Kruglov for bosons [8]. Other fact should be mentioned: when $4ab = -1$ we have only the solutions with $p^2 = 4b^2$. For instance, $b = m/2$, $a = -1/2m$, $p^2 = m^2$. Next, I just want to mention one Barut omission. While we can write

$$\frac{\sqrt{4ab + 1}}{a^2} = m_2^2 - m_1^2, \text{ and } \frac{2ab + 1}{a^2} = m_2^2 + m_1^2, \quad (8)$$

but m_2 and m_1 should not necessarily be associated with $m_{\mu, e}$ (or $m_{\tau, \mu}$). They may be associated with their superpositions, and applied to neutrino mixing, or quark mixing.

The lepton mass splitting has also been studied by Markov [9] on using the concept of both positive and negative masses in the Dirac equation. Next, obviously we can calculate anomalous magnetic moments in this scheme (on using, for instance, methods of [10, 11]).

We previously noted:

- The Barut equation is a sum of the Dirac equation and the Feynman-Gell-Mann equation.
- Recently, it was suggested to associate an analogue of (4) with dark matter, provided that Ψ is composed of

[†] a has dimensionality [1/m], b has dimensionality [m].

the self/anti-self charge conjugate spinors, and it has the dimension [energy]¹ in the unit system $c = \hbar = 1$. The interaction Lagrangian is $\mathcal{L}^H \sim g\bar{\Psi}\Psi\phi^2$, ϕ is a scalar field.

- The term $\sim \bar{\Psi}\sigma^{\mu\nu}\Psi F_{\mu\nu}$ will affect the photon propagation, and non-local terms will appear in higher orders.
- However, it was shown in [3b,c] that a) the Mott cross-section formula (which represents the Coulomb scattering up to the order $\sim e^2$) is still valid; b) the hydrogen spectrum is not much disturbed; if the electromagnetic field is weak the corrections are small.
- The solutions are the eigenstates of the γ^5 operator.
- In general, the current J_0 is not the positive-defined quantity, since the general solution $\Psi = c_1\Psi_+ + c_2\Psi_-$, where $[i\gamma^\mu\partial_\mu \pm m]\Psi_\pm = 0$, see also [9].
- We obtained the Barut-like equations of the 2nd order and 3rd order in derivatives.
- We obtained dynamical invariants for the free Barut field on the classical and quantum level.
- We found relations with other models (such as the Feynman-Gell-Mann equation).
- As a result of analysis of dynamical invariants, we can state that at the free level, the term $\sim \partial_\mu\bar{\Psi}\sigma_{\mu\nu}\partial_\nu\Psi$ in the Lagrangian does not contribute.
- However, the interaction terms $\sim \bar{\Psi}\sigma_{\mu\nu}\partial_\nu\Psi A_\mu$ will contribute when we construct the Feynman diagrams and the S -matrix. In the curved space (the 4-momentum Lobachevsky space), the influence of such terms has been investigated in the Skachkov work [10,11]. Briefly, the contribution will be such as if the 4-potential were to interact with some “renormalized” spin. Perhaps, this explains why Barut used the classical anomalous magnetic moment $g \sim 4\alpha/3$ instead of $\alpha/2\pi$.

Acknowledgements

The author acknowledges discussions with participants of recent conferences.

Received on November 17, 2020

References

1. Barut A. O. *Phys. Lett.*, 1978, v. B73, 310; *Phys. Rev. Lett.*, 1979, v. 42, 1251; Wilson R. *Nucl. Phys.*, 1974, v. B68, 157.
2. Kruglov S. I. *Ann. Fond. Broglie*, 2004, v. 29 (H2), 1005. In: Dvoeglazov V. V. et al., eds. The special issue dedicated to Yang and Mills. arXiv: quant-ph/0408056.
3. Petroni N. C., Vigier J. P. et al. *Nuovo Cim.*, 1984, v. B81, 243; *Phys. Rev.*, 1984, v. D30, 495; *ibid.*, 1985, v. D31, 3157.
4. Dvoeglazov V. V. *J. Phys. Conf. Ser.*, 2005, v. 24, 236–240; *Adv. Appl. Clifford Algebras*, 2008, v. 18, 579–585.
5. Dvoeglazov V. V. *Hadronic J. Suppl.*, 1995, v. 10, 349; *Int. J. Theor. Phys.*, 1998, v. 37, 1909.
6. Dvoeglazov V. V. *Ann. Fond. Broglie*, 2000, v. 25, 81–92.
7. Feynman R. and Gell-Mann M. *Phys. Rev.*, 1958, v. 109, 193.
8. Kruglov S. I. *Int. J. Mod. Phys.*, 2001, v. A16, 4925–4938. arXiv: hep-th/0110083.
9. Markov M. *ZhETF*, 1937, v. 7, 579; *ibid.*, 1937, v. 7, 603; *Nucl. Phys.*, 1964, v. 55, 130.
10. Skachkov N. B. *Theor. Math. Phys.*, 1975, v. 22, 149; *ibid.*, 1976, v. 25, 1154.
11. Dvoeglazov V. V. and Skachkov N. B. *Sov. J. Nucl. Phys.*, 1988, v. 48, 1065.

The Unification of the Basic Units Meter, Kilogram and Second and the Essence of the Phenomenon Time

Gerhard Dorda

Institute of Physics, University of Armed Forces Muenchen, Werner-Heisenberg-Weg 39, 85577 Neubiberg, Germany.
E-mail: physik@unibw.de

It is shown by experimental data that a causal connection between the categories mass and time, as well as between the categories electric current and time is given. The equation of the mass–time relation, valuated together with the constant of the velocity of light c and the length–mass relation of Planck L_E/M_E , results in a specific, single number related equation of the units mass, length and time without any dimension, thus representing unreality. It is made evident that the unified equation of the basic units, which reflects the not explicable experimental findings of the Quantum-Hall-Effect (QHE, i.e. KE), the findings of the physical description of vision and sound and also the third law of Kepler, yields the possibility to describe the essence of time. It is shown that the Hubble time $T_{U,E}$ and the Earth-related time t_E should be considered to be the fundamental factor of realization of masses between unreality and reality. Based on the presented description of the essence of the phenomenon time, the difference between time and frequency is disclosed.

1 Introduction

The MOS transistors as an amplifier of electric signals was developed after the second world war in the USA by W. Shockley, W. H. Brattain and J. Bardeen. Its economic importance is given by its extraordinary ability of miniaturization. This fact was the start of a world-wide rapid technical development at all areas of economy. The extensive studies of the specific properties of these MOS transistors led to the observation of the Quantum-Hall-Effect (QHE) in 1980 by K. von Klitzing, thus named Klitzing-Effect (KE) [1]. This effect, observed at low temperatures, disclosed on the one hand the existence of a macroscopic quantization at discrete states, given by the quantization of resistivity of the MOS module in form of $R_{xx} = h/ie^2$ (here, h is the Planck-constant, e the charge of electron, and i the quantum-number), and on the other hand the existence of a simultaneous, i.e. contemporaneous condition of an unresistance $R_{xx} = 0$ ohm. Both these effects, especially the contemporaneity of $R_{xx} = h/ie^2$ and $R_{xx} = 0$ ohm, was at that time not foreseen by the given theory, i.e. also quantum mechanical theory.

The exceptional importance of the QHE is given not only by the observation of a macroscopical quantization, described by the $R_{xx} = h/ie^2$, but also by the unexpected finding of the simultaneously given independence $R_{xx} = 0$ ohm at any integral and fractional quantum number. Evidently, the observed $R_{xx} = h/ie^2$ effect yields the possibility to find a connection to the state of physics before the year 1980, the year of the observation of the QHE by K. von Klitzing (KE) [1], but the $R_{xx} = 0$ ohm effect is a quite new observation within the whole scientific field of being, showing the existence of a state of space–mass–time independence. This finding has been observed after a world-wide extensive experimental investigation of the QHE. This spectacular observation allows

to postulate that due to the independence of the $R_{xx} = 0$ ohm effect on the integral as well as fractional quantum number that especially this $R_{xx} = 0$ ohm effect represents the fundamental background of the QHE. This assumption will be confirmed in the following by the description of the essence of time, especially by the unforeseen formulation of an equation of space–mass–time independence.

The surprising observation of the existence of a state without length, mass and time suggests a reform of the *International System of Units* (SI). It should be pointed out that a reform of the SI was recently highly recommended by F. W. Hehl and C. Lämmerzahl [2] with reference to physical results observed in the last centuries, and thus also to the experimentally observed dependence of the value of the velocity of light c on gravity. In [2] it was not borne in mind that the value of c is given by a free choice [3], i.e. the numerical value of c was determined by man, and “not by nature”. Thus the free choice of the numerical value of c determines in the last consequence the numerical value of the fundamental physical constants. Moreover, when describing the effect of gravitation on the number of velocity of light c we have to assume that in agreement with the physical interpretation of vision and sound [4, 5] the light-related distance refers to the localized wavy 2D-state, thus including no gravity effects, whereas the length-, i.e. mass-related distance, according to the third law of Kepler, i.e. due to the three-dimensionality, includes also the gravitational effects: Thus the different background of the light-related distance and the gravity, i.e. mass-related distance shows that the variability of the number of the velocity of light c , caused by gravity, cannot influence the numerical values of basic units. Furthermore, as will be demonstrated in sections 4 and 5, these discoveries result in the general validity of the following discussed equations and shows

that this finding reveals the applicability of all explored fundamental constants at any place of the cosmos.

Unfortunately, also the weighty problem of the phenomenon time was not incorporated in the extensive analysis of [2], though Lee Smolin [6] has shown in *The Trouble with Physics* that the main open question of the existing physics refers to not knowing of the essence of the phenomenon time. Therefore, in the presented analysis of the curious experimental effect of an existence of a state, being independent of a mass, space and time, as well as of the lack of a basic interpretation of the phenomenon time, it will be demonstrated that both these problems of physics can be solved only together. It will be shown in the next sections that the description of these phenomena does not become possible before the demonstration of the unexpectedly given causal connection between the category mass and frequency, as well as also between the category electric current and frequency.

2 The background for the basic interpretation of time

To find a physical answer to the fundamental problems of physics, we start with the analysis of the phenomenon time. It will be shown that the physical description of the process of vision and sound [4, 5], which demonstrates the existence of a differentiation of the three-dimensional space DSS into the two-dimensionality 2D, i.e. electromagnetism, and the one-dimensionality 1D, i.e. length, i.e. gravitation, is extremely helpful for the analysis of the phenomenon time. It has become aware that the description of time is not dependent on the wavelength of the used light, but solely on the frequency, reflecting the electromagnetism. Based on the DSS-model, in fact the source of the phenomenon time must refer to dynamics, i.e. to the electromagnetism, which is an effect of the 2D-state. The unit time is always noticeable merely in connection with the category length [6]. This finding suggests that the perception of the phenomenon time must be a result of the connection of the wave related 2D-state with the real, i.e. 1D-state, which represents the state of observable facts. The analysis of the process of vision has shown [4] that the 1D-state, representing the gravity and thus also the category length, relates to the effect of the gravitational constant $G_E = c^2(L_E/M_E)$, where L_E is the Planck-length and M_E the Planck-mass and c the velocity of light. It is generally assumed that the gravitational constant G_E is valid at the whole cosmos. From this decisive supposition follows that the relation L_E/M_E , i.e. the fundamental connection between the three-dimensionally related mass and the category length, is describable in an extended form, given by

$$\frac{L_E}{M_E} = \frac{\lambda_C}{M_{0,E}} = \frac{\lambda_{G,E}}{M_{G,E}} = \frac{L_{U,E}}{M_{U,E}}. \quad (1)$$

Here λ_C is the Compton wave-length and $M_{0,E}$ the corresponding to this length related mass, $\lambda_{G,E}$ is the so-called reference length of the earth and $M_{G,E}$ the corresponding mass

of the earth, and finally $L_{U,E}$ the length of the cosmos and $M_{U,E}$ its mass. The index E indicates that the explorations are performed from an earth-related place.

It should be emphasized that (1) and thus also the relation $\lambda_C/M_{0,E}$ represent the particular state of identity of the observable electromagnetism with gravitation. Considering the model of the differentiated structure of space DSS [4, 5], this state is given by the non-possibility to distinguish between the 2D-state and the 1D-state. But this specific condition does not exist at the surface of the earth. The third law of Kepler [4], which is related to the spatial three-dimensionality of the cosmos, shows that the relation between the square velocity of light c^2 and the square of the orbital speed at the surface of the earth v_E^2 (which reflects the difference between the electromagnetism and gravitation) is given by $c^2/v_E^2 = a_{G,E}$. This number $a_{G,E}$, related to the surface of the earth, in [4] described by (8) and (9) and formulated in agreement with (1), is given by

$$a_{G,E} = \frac{M_E R_{G,E}}{L_E M_{G,E}} = \frac{M_{0,E} R_{G,E}}{\lambda_C M_{G,E}} = \frac{R_{G,E}}{\lambda_{G,E}}, \quad (2)$$

where $R_{G,E}$ is the radius of the earth and $M_{G,E}$ its mass.

It should be pointed out that according to the DSS-model we have to proceed from the 1D, i.e. from the noticeable, i.e. real state. In the next sections, it is demonstrated that, according to the spatial three-dimensionality, the 2D-state is valued in a "square" relation to the 1D-state. Thus the frequency f_C , being related to the 2D-state, must be modified on the surface of earth by $(a_{G,E})^{1/2}$, resulting in a real value, given by $f_E = f_C (a_{G,E})^{-1/2}$. When we take the value $f_C = 1.235589964 \times 10^{20}$ Hz for the velocity of light related frequency, the value $M_{G,E} = 5.974 \times 10^{24}$ kg for the mass of the earth and the approximate value $R_{G,E} = 6.36 \times 10^6$ m [7] for its radius $R_{G,E}$, then, according to (2), we obtain for f_E the real value

$$f_E = f_C (a_{G,E})^{-1/2} = 3.26321(64) \times 10^{15} \text{ Hz}. \quad (3a)$$

It is of great importance for our further analysis to compare this experimentally established numerical value of f_E with the numerical value $M_{0,E} = \lambda_C(M_E/L_E)$, which refers to (1). As known, the Compton-wavelength is given by

$$\lambda_C = 2.4263102389 \times 10^{-12} \text{ m},$$

and for the relation L_E/M_E we have the value

$$L_E/M_E = 7.42565(74) \times 10^{-28} \text{ m kg}^{-1}.$$

This value of L_E/M_E was determined from the analysis of the cosmos generally used, experimentally observed gravitation constant $G_E = c^2(L_E/M_E) = 6.67384(80) \times 10^{-11} \text{ m}^3/(\text{kg s}^2)$ [7]. Based on (1) and using these values, we obtain for $M_{0,E}$ a 1D related value, given by

$$M_{0,E} = \lambda_C (M_E/L_E) = 3.26746(86) \times 10^{15} \text{ kg}. \quad (3b)$$

The comparison of the “numerical” value f_E , given by (3a), with the “numerical” value $M_{0,E}$, given by (3b), “astonishingly” reveals a near identity of their numbers. This exceptional finding leads us to the dared assumption that a causal connection between mass and frequency, i.e. time, seems to be possible in being. This exceptional assumption can be formulated by means of the spectacular equation

$$M_{0,E} = f_E . \quad (4)$$

The comparison of the values of $M_{0,E}$ with f_E shows that the experimental value of f_E is a little higher, but only about 0.13 %. This relatively small deviation is necessarily a consequence of the fact that according to vision and sound the effect of $M_{G,E}$ on the value of $a_{G,E}$ is a little lower, caused by the reduced earth density at the surface. Therefore, indeed, it is physically allowed to postulate that on the surface of the earth an absolute numerical identity of $M_{0,E}$ with f_E is given, as proposed by (4).

It should be pointed out that the careful analysis of (4), given in sections 3–5, shows that the proposed identity of the limits of mass with frequency has to be valid not only on the surface of the earth, but generally valid at the whole cosmos. Thus, it should be considered that beside the physical constants c and L_E/M_E , a third important, generally valid constant should be effective, representing a connection of mass with frequency. Due to the importance of this exceptional postulate, experimental findings will be presented in the next section to substantiate the validity of the extraordinary (4).

3 Experimental verifications of the identity of the mass–time connection

3.1 The analysis of the limiting current of the Quantum-Hall-Effect (QHE)

The limiting current of the QHE, obtained by the experimental investigation of W. Wittmann [8], is presented in Fig. 2.1 of [9], page 37. Assessing these data with respect to the process of seeing and hearing, we have to conclude that the investigated electric current of the sample, the so-called source-drain current I_{SD} , being a real effect, must be related to the 1D-state, i.e. to frequency being in the real form of time, and not to the 2D wave state. Therefore it must be concluded that the factor of modification $(a_{G,E})^{1/2}$ has to be in relation solely to the source-drain frequency f_{SD} and not also to the charge of the electron e of the electric current, as former assumed in [9]. This shows, formulated in a general form, that the limiting frequency on the surface of the earth f_E must be given by (3a) and thus the limiting current $I_{0,E}$ by

$$I_{0,E} = e f_E = 5.23510(29) \times 10^{-4} \text{ A} . \quad (5)$$

This theoretical value of the limiting current really agrees on the whole with the experimental data of the QHE, as shown and discussed on pages 39–40 of [9], together with the results

of the extension of the time-analysis, given in [10], part II, pages 37–50. This particular finding demonstrates that the basic unit ampere of the MKSA- or SI-system of basic units must be considered to be a fix relation to the basic unit time, and that by means of the electron charge e . From this follows that the limit voltage of the QHE $V_{0,QHE}$ is at the limit resistivity $R_{0,QHE} = 2.581281 \times 10^4$ ohm given by $V_{0,QHE} = 13.51316(38) \text{ V}$ and that the relation between the mass and the charge of the electron results in $m_e/e = (a_{G,E})^{1/2} V_{0,QHE}/c^2$, which agrees with the experimental experience. These experimental results suggest the striking conclusions that, on the one side, the equation of the frequency indeed should be given by $f_E = f_C (a_{G,E})^{-1/2}$, as proposed in section 2 and thus supporting the assumption of (4), and, on the other side, only a reduced MKS basic system of units, i.e. without the category “electric current”, should be taken into account in the physical science, being a far-reaching conclusion of the QHE.

3.2 The comparison of the mass–time relation effect with the Hubble time $T_{U,E}$

An indirect experimental confirmation of (4) can be obtained when we interpret the connection between the mass $M_{0,E}$ and the frequency f_E as a fundamental coupling number, and that seen in similarity to the speed of light c , and when we consider the relation L_E/M_E also as a fundamental coupling number. The numerical value of the relation L_E/M_E is given by the constant of gravity G_E [7], where the factor c^2 is based on the value $c = 2.99792458 \times 10^8 \text{ m s}^{-1}$ [9]. The fundamentality of the numerical value of L_E/M_E was demonstrated by the equation of the Hubble-effect [4]. Therefore, describing the velocity of light as a fundamental coupling number between the categories length and time, given by the number 2.99792458×10^8 , and the relation L_E/M_E as a fundamental coupling number between categories length and mass, given by the number $7.42565(74) \times 10^{-28}$, thus the connection between the mass $M_{0,E}$ and the frequency f_E , i.e. time, given by (3a), (3b) and (4), has according to our analysis to be assessed as a general valid fundamental coupling number between the relation of the categories mass and time, describable by the number 1.

Summarizing these propositions, a general valid fundamental connection between the categories length, time and mass can be achieved by

$$\begin{aligned} 1 \text{ m} &= 1/c = (1/2.99792458 \times 10^8) \text{ s} \\ &= 3.335640952 \times 10^{-9} \text{ s} , \end{aligned} \quad (6a)$$

$$\begin{aligned} 1 \text{ m} &= 1/(L_E/M_E) \\ &= (1/7.42565(74) \times 10^{-28}) \text{ kg} \\ &= 1.346682(11) \times 10^{27} \text{ kg} \end{aligned} \quad (6b)$$

$$\text{and } 1 \text{ kg} = 1/(1 \text{ s})^* , \quad (6c)$$

where we introduce a fundamental time $(1\text{ s})^*$ in (6c), a consequence of the assumption of the existence of a general valid fundamental connection between the categories length, mass and time. Thus (6a)–(6c) yield

$$(1\text{ s}^2)^* = (M_E/L_E)c = 4.03725(14) \times 10^{35} \text{ s}^2, \quad (7)$$

being a square of the fundamental time. Thus the unit of time, representing the fundamental coupling number, therefore must be given by

$$(1\text{ s})^* = 6.35393(69) \times 10^{17} \text{ s}, \quad (8)$$

which must be considered to be a result, related to the freely chosen value of c .

To get a further possibility to confirm the correctness of our analysis and thus of (4), we start from the idea that this specific time of (8), deduced from the numerical values c , L_E/M_E and (4), correspond with the Hubble time $T_{U,E}$. Throughout the scientific literature, the Hubble time $T_{U,E}$ is determined by means of the Hubble constant H_0 , determined by telescopes. The value of the time of (8) corresponds with the Hubble-value $H_0 = 48.564 \text{ km s}^{-1} \text{ Mpc}^{-1}$. Thus it is interesting that the experimentally detected H_0 values show the Hubble constant, found in the last decades, to be between $H_0 = 40 \text{ km s}^{-1} \text{ Mpc}^{-1}$ and $H_0 = 100 \text{ km s}^{-1} \text{ Mpc}^{-1}$ [11], and the recently determined value shows to be [4]

$$H_0 = 72.1 \text{ km s}^{-1} \text{ Mpc}^{-1}.$$

It is now clear that the values of the experimental findings of H_0 , according to the size, are identical with the size of the theoretical value given by (8). Thus we can state that the size-related agreement of the telescopes given $T_{U,E}$ values with the theoretical value, given by (8), additionally proves that the postulated identity of the category mass with the category time, expressed by (4), indeed can be considered to be experimentally verified.

4 The formulation of an equation of transformed basic units without dimensions

As has been manifested in subsection 3.2, it is very interesting that the generally valid limit values c and L_E/M_E yield in (7) the square of the category time. As will be discussed in detail in section 5, this odd finding can be solved when we take into consideration both the experimental data of the QHE [1] and the physical description of vision and sound [4, 5].

The KE shows the $R_{xx} = 0$ ohm effect, which manifests the existence of an extraordinary state without any difference between mass, length and time. To reflect this mysterious experimental finding, a transformation of (6a)–(6c) is necessary to achieve the basic units given simply by numbers. This

spectacular goal is attained by

$$1\text{ m}^* = 2.11944(52) \times 10^9, \quad (9a)$$

$$1\text{ kg}^* = 1.573827(44) \times 10^{-18}, \quad (9b)$$

$$1\text{ s}^* = 6.35393(69) \times 10^{17}. \quad (9c)$$

The numbers of (9a)–(9c) are obtained, when we use $1/c$ and $1/(L_E/M_E)$ as fundamental coupling numbers and when we suppose that the time of (8) is identical with the limit time of the cosmos $T_{U,E}$. Thus the numbers of (9a)–(9c) are given by

$$1\text{ m}^* = \frac{1}{c} (1\text{ s})^*, \quad (10a)$$

$$1\text{ kg}^* = \frac{L}{Mc} (1\text{ s})^*, \quad (10b)$$

$$1\text{ kg}^* = \frac{1}{(1\text{ s})^*}. \quad (10c)$$

When starting from the cosmic length, given by $L_{U,E} = c T_{U,E} = 1.90486(24) \times 10^{26} \text{ m}$ and from the cosmic mass, given according to (1) by

$$\begin{aligned} M_{U,E} &= (M_E/L_E) L_{U,E} = (M_E/L_E) c T_{U,E} \\ &= 2.56524(41) \times 10^{53} \text{ kg}, \end{aligned}$$

and multiplying these values with the transformed basic units 1 m^* and 1 kg^* of (9a) and (9b), evidently we obtain the transformed values of length $L_{U,E}^*$ and of mass $M_{U,E}^*$. Moreover, when the square of the time of (8) is taken as the expression of the transformed cosmic time $T_{U,E}^{*2}$, then we obtain –*fully unexpected*– for $M_{U,E}^*$, $L_{U,E}^*$ and $T_{U,E}^{*2}$ one and the same number. This extremely spectacular observation results in the possibility to connect the transformed expressions of mass $M_{U,E}^*$, length $L_{U,E}^*$ and time $T_{U,E}^{*2}$ simply into one equation, given by

$$M_{U,E}^* = L_{U,E}^* = T_{U,E}^{*2} = 4.03725(14) \times 10^{35}. \quad (11)$$

It is evident that the spectacular non-dimensionality of (11) represents a particular state of unreality, which indicates the existence of an extraordinary state, seen in comparison to the in reality given basic units mass, length and time. It should be emphasized that this peculiar observation indeed reflects the experimental finding of the Klitzing-Effect (KE). The unexpected observation of the same number, resulting in (11), suggests the general validity of unification of basic units for the whole cosmos.

Besides, it should be emphasized that the disclosed possibility in this section 4 to describe each basic unit only by the same number can hardly be substantiated by the given physical argumentation in our times. Evidently, (11) is based on

the proposed identity in section 2 of the category mass with frequency, i.e. with the category time. But, in an extensive manner valued, the reasoning of (11) can be indirectly supported by both the cosmological principle as well as by the mathematically unsolvable three-body-problem, which supports the DSS-model [4, 5], and which are generally valid. Moreover, a comprehensive analysis of (4) and (11) shows that the used constancy of the velocity of light c in the whole cosmos (reflecting the independence on the place of investigation) is only possible, when a universal validity of unification of the basic units is given. This statement is discussed in the next section.

5 The far-reaching findings about the category time

Based on all the data, shown in the preceding section 4, a comprehensive interpretation of the category time is possible by further analyzing the substance of (11). In fact, (8) together with (6a)–(6c), (9a)–(9c) and (11) yields a noticeable, far-reaching expression, given by

$$M_{U,E} = T_{U,E} T_{U,E}^{*2} = T_{U,E} M_{U,E}^* . \quad (12)$$

Considering (8), (9c) and (10a)–(10c), then (11) and (12), as well as the discussion of the results of the Hubble time $T_{U,E}$ become more understandable for the interpretation of the essence of time, when we further postulate that the cosmic time $T_{U,E}$ complies the remarkable “numerical” identity

$$T_{U,E} = T_{U,E}^* . \quad (13)$$

The identity of the limit numbers of the real and unreal cosmic times, given by $T_{U,E}$ and $T_{U,E}^*$, can be confirmed, when analyzing (7) and (8) with respect to the results of vision and sound. According to (11) and (12), and especially to (13), the Hubble time $T_{U,E}$ should be considered to be a particular magnitude, being numerically quite different to both $M_{U,E}$ and $L_{U,E}$ (the values of them are given in section 4) as well as to $M_{U,E}^*$ and $L_{U,E}^*$. Moreover, it must be pointed out that this specific exclusiveness of the cosmic time is also given in (11), where the real time $T_{U,E}$, being in unreal state, appears in a “square”. This important fact is a consequence of the specific circumstance that $T_{U,E}$, in contrast to $M_{U,E}^*$ and $L_{U,E}^*$, is in this state used as a “real” magnitude, and that in form of $(1\text{ s})^*$. Thus, when we consider (12), it becomes evident that the circumstance of $T_{U,E}$ can be in agreement with the DSS-model about the square relation of the 2D-state to the 1D-state “only”, when the in (13) proposed numerical identity of the real and unreal cosmic time is given for the whole cosmos. It is obvious that this disclosure is confirmed by the existence of the Hubble effect [4].

Moreover, it should be pointed out that (11) and its general validity is based solely on the proposition of the validity of (4). It is given by the possibility to express the connection of the mass with the frequency, given in the reality related

form by $f_c(a_{G,E})^{-1/2}$. The used rooty form of the gravitational value $a_{G,E}$ is in full agreement with both the physical description of vision and sound [4, 5], and also the third law of Kepler, showing that the relation between the 2D-state and the 1D-state is given inevitably in squared form. This observation demonstrates the generally validity of the difference between the essence of frequency and time in the real state, which in the last consequence approves the correctness of (4) and (11).

All these discussed observations are important also for the confirmation of the general validity of (12), which can be obtained by comparison of this equation with the third law of Kepler. Due to the third law of Kepler, the orbital time of earth $t_{G,E}$ is given by [4]

$$t_{G,E} = (a_{G,E})^{3/2} t_E , \quad (14)$$

where the specific time of earth t_E with respect to (1) is defined by

$$t_E = \lambda_{G,E}/c = 1.4797 \times 10^{-11} \text{ s} . \quad (15)$$

Starting from (12), the application of it to the particular conditions of the earth yields the equation

$$M_{G,E} = t_E M_{U,E}^* . \quad (16)$$

Eqs. (12) and (16) demonstrate that the category time represents a connection of the real values of the masses $M_{U,E}$ and $M_{G,E}$ with the unreal value $M_{U,E}^*$. Therefore, finally, we can draw the striking and for our investigation of the essence of time important conclusion that according to the effect of KE [1] and the DSS-model [4, 5], the category time suggests to be a magnitude to connect the 2D-state with the 1D-state, thus to be a factor of realization between reality and unreality.

As has been shown, this description of the essence of time is based on the proposed identity of the limit of mass with the limit of frequency, formulated by (4) and experimentally confirmed by many, quite different observations:

1. By the mysterious Klitzing-Effect (KE), which discloses the existence of an unresistance $R_{xx} = 0$ ohm at the Quantum-Hall-Effect (QHE),
2. by the physical description of the process of seeing and hearing [4, 5], resulting in the discovery of the DSS structure of space,
3. by the value of the gravitational number of the surface of the earth $a_{G,E}$, determined from the mass and the radius of the earth, which modifies the limits of mass and frequency in (4),
4. by the results of the limiting current of the QHE [8, 9],
5. by the found approximate identity of the value of the Hubble time $T_{U,E}$, experimentally determined by telescopes [4, 11], with the theoretically deduced limit time given by (8), which certifies the validity of the statements of (4) and (11),

6. by the coherence of the summarized result of the here listed experimental observations with the third law of Kepler [4], demonstrating that indeed the finding of the DSS-state and the possibility of unification of the basic units are in a perfect agreement with the assumed general validity of the third law of Kepler.

Considering all these experimental findings, the presented model of the essence of time should be viewed as physically confirmed.

6 Summarized conclusions

The physical description of vision and sound in form of the DSS-model [4,5], reflecting the experimental data of the Klitzing-Effect (KE) [1], reveals that the phenomenon time is given as a consequence of the interaction of the wave-related 2D-state with the 1D-state, i.e. the particular state, which shows exclusively real circumstances. This finding is the physical reasoning for the fact that the phenomenon time as well as the frequency in real form are always observable solely in connection with the category length [6] [9, pp. 9–10].

The analysis of the experimental data of basic units shows that surprisingly a generally valid identity of mass and frequency can be supposed, theoretically described by (4) and confirmed by different experimental data. These findings result in the possibility to formulate an equation, given by (11), in which, astonishingly, the transformed categories mass, length and time are given only by the same, single number, referring in the last consequence to the existence of an unreality in being. This observation has to be considered to be the physical description of the mysterious experimental effect of the $R_{xx} = 0$ ohm related Klitzing-Effect (KE), discovered in the Quantum-Hall-Effect (QHE) [1].

The third law of Kepler proves that the phenomenon time is observable only in the given state of the spatial three-dimensionality. This circumstance points out that – with respect to the DSS-model – the category time must be effective as a mediator for the coupling of the 2D-state with the 1D-state, thus being an important background of the realization of the category mass.

Summarizing all the presented experimental findings, it is allowed to conclude that the “unification” of the basic units length, mass, time and electric current appears to be a physical fact. Based on this important discovery, we can state that the phenomenon time is a dualistic factor, which is related on the one side to the localized, i.e. real 1D-state, noticeable as time, on the other side in the wavy, i.e. unreal 2D-state, in realistic form known as frequency. Evidently, this finding shows the existence of a substantial difference between time and frequency, and that to be a physical legitimate circumstance.

Acknowledgements

The author is indebted to *Prof. Walter Hansch*, University of Armed Forces, Muenchen, for the support of this subject and

for his significant comments to some statements of this paper. He would also like to express special thanks to *Alexander Hirler* for his co-operation within the scope of critical reading of the paper and for its extensive completion for printable publication. Finally, the author expresses many thanks to *Klara Kirschner* for proof-reading of the English text.

Received on November 4, 2020

References

1. von Klitzing K., Dorda G. and Pepper M. New method for high-accuracy determination of fine-structure constant based on quantized Hall resistance. *Phys. Rev. Lett.*, 1980, v. 45, 494–497.
2. Hehl F.W. and Lämmerzahl C. Physical Dimensions/Units and Universal Constants: Their Invariance in Special and General Relativity. *Ann. Phys. (Berlin)*, 2019, 1800407.
3. Kose V. and Wöger W. Neuere empfohlene Werte von Fundamentalkonstanten. *Phys. Bl.*, 1987, v. 43, 397–399.
4. Dorda G. The Interpretation of the Hubble-Effect and of Human Vision Based on the Differentiated Structure of Space. *Prog. Phys.*, 2020, v. 16 (1), 3–9.
5. Dorda G. The Interpretation of Sound on the Basis of the Differentiated Structure of Three-Dimensional Space. *Prog. Phys.*, 2020, v. 16 (1), 15–19.
6. Smolin L. *The Trouble with Physics*. Houghton Mifflin Company, New York, 2006. In German: *Die Zukunft der Physik*. Deutsche Verlags-Anstalt, Muenchen, 2009, pp. 344–346.
7. Mende D. and Simon G. *Physik. Gleichungen und Tabellen*. Carl Hanser Verlag, Fachbuchverlag Leipzig, Muenchen, 2013.
8. Wittmann F. *Magnetotransport am zweidimensionalen Elektronensystem von Silizium-MOS-Inversionsschichten*. Dissertation, University of Armed Forces, Muenchen, Institute of Physics, Abb. 4–5.3, S. 143, 1992.
9. Dorda G. *Quantisierte Zeit und die Vereinheitlichung von Gravitation und Elektromagnetismus*. Cuvillier Verlag, Goettingen, ISBN 978-3-86955-240-8, 2010. In particular: pp 34–42, Fig. 2.1 and 2.2, and (2.14).
10. Dorda G. *Die Struktur von Raum und Zeit und die Interpretation der Wärme*. Cuvillier Verlag, Goettingen, ISBN 978-3-7369-9388-4, eISBN 978-3-7369-8388-5, 2016.
11. Bernhard H., Lindner K. and Schukowski M. *Wissenspeicher Astronomie*. Volk und Wissen Verlag, Berlin, ISBN 3-06-081705-7, 1995.

A Survey on Uncertainty Relations and Quantum Measurements: Arguments for Lucrative Parsimony in Approaches of Matters

Spiridon Dumitru

(Retired) ex-Department of Physics, "Transilvania" University,
B-dul Eroilor 29, R-2200 Braşov, Romania,
E-mail: s.dumitru42@yahoo.com

This survey tries to investigate the truths and deficiencies of prevalent philosophy about Uncertainty Relations (UR) and Quantum Measurements (QMS). The respective philosophy, known as being eclipsed by unfinished controversies, is revealed to be grounded on six basic precepts. But one finds that all the respective precepts are discredited by insurmountable deficiencies. So, in regard to UR, the alluded philosophy discloses oneself to be an unjustified mythology. Then UR appear either as short-lived historical conventions or as simple and limited mathematical formulas, without any essential significance for physics. Such a finding reinforces the Dirac's prediction that UR "*in their present form will not survive in the physics of future*". The noted facets of UR motivate reconsiderations of associated debates on QMS. Mainly one reveals that, properly, UR have not any essential connection with genuine descriptions of QMS. For such descriptions, it is necessary that, mathematically, the quantum observables to be considered as random variables. The measuring scenarios with a single sampling, such are wave function collapse or Schrödinger's cat thought experiment, are revealed as being useless inventions. We propose to describe QMS as transmission processes for stochastic data. Note that, for existing quantum debates, the above UR–QMS revaluations, offer a few arguments for lucrative parsimony in approaches of matters. The unlucrative aspects of those debates have to be reconsidered too, probably in more or less speculative visions.

Motto 1: "I think one can make a safe guess that uncertainty relations in their present form will not survive in the physics of future."

P. A. M. Dirac, 1963

Motto 2: "The word 'measurement' has had such a damaging effect on the discussions that ... it should be banned altogether in quantum mechanics."

J. S. Bell, 1990

Foreword

A. The present review-study germinates from some of our preceding more modest investigations some of them already published in this journal, Progress in Physics. Also, it was influenced by a number of opinions published by other scientists (opinions which, usually, are ignored in mainstream literature).

In the main, the study was stimulated by the known existence of numerous debates (unfinished controversies on unelucidated questions) regarding the foundations and interpretation of Quantum Mechanics (QM). The considered debates refer mainly to the significance of Uncertainty Relations (UR) and to the associated descriptions of Quantum Measurements (QMS). By their obstinate persistence, the mentioned debates delay and obstruct the desired (and expected) clarifications about some basic aspects of QM.

Within the here emerged text, we try to gather, systematize, improve, consolidate and mainly to present more

argued our non-conventional viewpoints about the existing prevalent debates on UR, QMS and QM.

B. The here proposed article approaches step-by-step the following main items:

- i.1 A consistent Introduction which points out:
 - (a) The nowadays existence of unfinished debates (disputes and controversies) about the meaning of UR and description of QMS;
 - (b) The today necessity for search the truth about own philosophy of UR and description of QMS, regarded as relevant pieces for foundations/interpretation of QM;
- i.2 An inventory section which identifies the Basic Precepts of the prevalent philosophy regarding UR and QMS;
- i.3 A large section about most important deficiencies of the mentioned precepts. Within the respective section we concern on:
 - (a) Detailed examinations of deficiencies specific to the respective precepts;
 - (b) Elucidation, piece by piece, of the real value/meaning for each of the pointed out deficiencies;
- i.4 A first concluding section about the true significance of UR. In that section the current prevalent interpretation of UR is proved to be nothing but a veritable myth without any special or extraordinary value for physics. But such a proof reinforces the Dirac's prediction that UR

“in their present form will not survive in the physics of future”;

- i.5 A section containing considerations on description of QMS. The respective considerations are done in the light of the debates about deficiencies of dominant philosophy about UR. Also the measuring scenarios with a single sampling, such are wave function collapse or Schrödinger’s cat thought experiment, are revealed as being superfluous fictions. We argue that the QMS descriptions should be approached additionally comparatively with the description and interpretation of UR. They must be discussed in new insights by regarding the measurements as transmission processes for stochastic data. (see our examples from Subsections 5.2 and 5.4 or from Appendices F and G);
- i.6 A final section with some concluding remarks;
- i.7 A supplementary section of Appendices containing:
- Technical/computational details — in seven cases, respectively;
 - A copy of “A private letter from the late scientist J. S. Bell to the author”.

C. Notes:

- I. Through the elucidations referred to in item i.3 we offer genuine solutions for some controversial theoretical problems such are:
- The adequate form of UR for the supposed rebellious pairs of observables: $L_z-\varphi$ (angular momentum — azimuthal angle), $N-\phi$ (number-phase) and $E-t$ (energy-time);
 - The case of macroscopic operators;
 - The uniqueness (individuality) of Planck’s constant;
- II. In its essence, the suggested revaluation of UR and QMS philosophy does not disturb in any way the basic lucrative framework of usual QM (which keeps its known specific concepts, principles, theoretical models, computing rules and studied systems); Moreover, I try to give arguments for lucrative parsimony in approaches of QM matters; I believe that, to some extent, such a revaluation of UR-QMS prevalent philosophy can be beneficent for interpretation and understanding of QM. Potentially that revaluation can bring at least a modest contribution to non-conventional investigations of some open questions regarding views about UR, QMS, and QM.
- III. My article tries to clarify certain past misunderstandings, of historical, philosophical, and cultural essence, which still persists in activities (of publishing and mainly of teaching nature), connected with QM;
- IV. As a significant aspect, in my paper, the discussions are presented and detailed in forms accessible to readers with knowledge of QM at a not-advanced level. That is why in the version proposed here the article was con-

ceived (especially through a number of detailed Appendices) as an accessible teaching material for those interested in QM education at undergraduate/graduate levels.

D. I think that, by its theme, style and writing level, my paper ensures the following desiderata:

- It approaches representative methodological and philosophical topics concerning the structure and the growth (interpretation and foundations) of QM investigated as a significant constituent of natural sciences;
- It can give a starting forum for the exchange of views and ideas among readers interested, in foundations of QM regarded as an important constituent of modern sciences;
- It identifies and highlights foundational issues, suggesting constructive and genuine solutions for approached problems;
- It offers a number of original opinions concerning some controversial theoretical/philosophical scientific problems;
- It initiates and develops discussions on the philosophy and epistemology of physics, at a level accessible to a wide class of readers (scientists, teachers and even students in physics, mathematics, chemistry or philosophy);
- It provides an argued appeal toward an increasing research field, namely to the one regarding the non-conventional approach of QM interpretation and foundations.

Given the above-mentioned aspects, I think that my article can offer a modest contribution to newly rising investigations on non-conventional views in quantum physics.

Braşov, November 26, 2020

Spiridon Dumitru

1 Introduction

Nearly a century until nowadays, in the publications regarding Quantum Mechanics (QM) and even other areas, have persisted discussions (debates and controversies) about the meaning of Uncertainty Relations (UR). Moreover UR in their entirety were ranked to a status of fundamental concept named Uncertainty Principle (UP) (for a bibliography of the better known specific publications see [1–12]). Mostly the respective discussions have credited UR/UP with considerable popularity and crucial importance, both in physics and in other domains. The mentioned importance was highlighted by compliments such as:

- UR are “*expression of the most important principle of the twentieth century Physics*” [13],
- UP is “*one of the cornerstones of quantum theory*” [9];

- UP “*epitomizes quantum physics, even in the eyes of the scientifically informed public*” [7].

But, as a fact, in spite of such compliments, in scientific literature of our days the essential aspects regarding UR/UP remain as unsolved and misleading questions. Today keeps their topicality many critiques reported during last decades, like the next ones:

- UR “*are probably the most controverted formula in the whole of the theoretical physics*” [14];
- “*Still now, 80 years after its inception, there is no general consensus over the scope and validity of this principle (‘UP’)*” [7];
- “*Overcoming the early misunderstanding and confusion, the concept (notion of uncertainty — i.e. of UR/UP) “grew continuously and still remains an active and fertile research field”* [8].

Note that the above reminded appreciations (compliments and critiques) regard mainly the own essence (intrinsic meaning) of UR/UP. But, within many texts about QM fundamentals, one finds also an adjacent topic which, historically, is a direct sub-sequence of the debates about the mentioned essence. The respective topic refers to the significance and description of Quantum Measurements (QMS).

Marked by the previously noted points, during the decades, the discussions about UR and QMS meaning and implications have generated a true prevalent philosophy (i.e. “*a group of theories and ideas related to the understanding of a particular subject*” [15]). For almost a century, the respective philosophy dominates in mainstream physics publications and thinking. It obstructs (delays) the expected progresses in clarifying some of main aspects regarding the fundamentals/interpretation of QM respectively the essentials of QMS problem. Add here the more alarming observation [16] that: “*there is still no consensus on ... interpretation and limitations of QM*”. Then it becomes of immediate interest to continue searches for finding the truth about own essence and consecutive topics of the UR/UP and QMS matters.

A search of the alluded type can be done (or facilitated at least) by a pertinent survey on deficiencies of the mentioned philosophy. Such a survey (of modest extent) we intend to present in this article. Our survey tries firstly to identify the basic elements of nowadays prevalent views within UR and QMS philosophy. Afterward we will investigate truth and value of the respective elements. Within the investigation we promote a number of re-considerations regarding the conventional (and now dominant) views about UR and QMS matters. Mainly we reveal the fact that the alluded views are discredited (and denied) by a whole class of insurmountable deficiencies, overlooked in the mainstream literature. So our survey aims to represent an unconventional analysis of the actual dominant philosophy about UR and QMS. The above-announced analysis germinated from some of our preceding

investigations (see [17–21] and references). **Also, it was stimulated by a number of opinions due to other scientists (usually the respective opinions are ignored in dominant literature, but here they are highlighted by specifying the proper bibliographic sources).** Through the present survey, we try to gather, extend, systematize, improve and consolidate the results of our mentioned investigations in order to present a more argued viewpoints about the approached topics.

In our survey, when it is usefully, we will appeal to the so called ‘parsimony principle’ (or ‘law ’). The respective principle (known also as Ockham’s razor) will be applied as a heuristic method of simplicity which can be summarized [22] by the next two desiderata:

- “*Of two competing theories, the simpler explanation of an entity is to be preferred*”.
- “*Entities are not to be multiplied beyond necessity*”.

The mentioned principle will be accounted for in order that the text to be easy understood for readers (including students) not highly specialized.

By the present article-survey, through adequate arguments and details, we try to elucidate what is in fact the true meaning of UR, respectively to evaluate the genuine scientific aspects regarding QMS.

From the conclusions resulting from this survey the most important one is that, in its entirety, the actual prevalent philosophy about UR must be regarded as a veritable myth without any special or extraordinary status/significance for physics. This because, in reality, the UR reveal themselves to be nothing but short-lived historical conventions (in empirical, thought-experimental version) or simple and restricted formulas (in theoretical approach). But such a conclusion come in consonance, from another perspective, with the Dirac’s guess [23] that: “*uncertainty relations in their present form will not survive in the physics of future*”.

Add here the fact that, essentially, the above mentioned re-evaluation of UR and QMS philosophy does not disturb in any way the basic framework (principles, concepts, models and working rules) of usual QM. Furthermore, the QMS description remains as a distinct and additional subject comparatively with the elements of QM in itself. Add here the observation that, for existing quantum debates, the above UR–QMS revaluations give a few arguments for lucrative parsimony in approaches of matters. The unlucrative aspects of those debates have to be reconsidered, probably in more or less speculative visions.

The mentioned description of QMS requires to regard quantum observables* as true random variables. Also it must

***Drafting specifications:** (i) In the next parts of this article, for naming a physical quantity, we shall use the term “*observable*” (promoted by the UR and QMS philosophy literature), (ii) Also, according to the mainstream publications, we adopt the titles “*commuting*” or “*non-commuting*” observables for the QM quantities described by operators which “*commute*” respec-

be dissociated of some fictive QMS scenarios with a unique sampling (such scenarios are schema with wave function collapse and Schrödinger's cat thought experiment). We recommend to describe QMS as transmission processes of stochastic data.

2 Basic precepts of UR–QMS prevalent philosophy

Firstly it must be pointed out the fact that, in spite of its prevalence inside of nowadays scientific debates, the actually dominant philosophy about UR and QMS germinates mainly from an old doctrine which can be called Conventional Interpretation of UR (CIUR). The mentioned doctrine (or dogma) was initiated by the Copenhagen School founders and, subsequently, during nine decades, it was promoted (or even extrapolated) by the direct as well indirect partisans (conformists) of the respective school. Currently CIUR enjoys of a considerable acceptance, primarily in QM studies but also in other thinking areas. Moreover, today, within the normative (mainstream/authoritarian) physics publications, CIUR dominates the leading debates about foundations and interpretation of QM.

But as a notable fact, in publications, CIUR doctrine, as well as most aspects of UR and QMS philosophy, are presented rather through independent or disparate assertions but not through a complete and systematized set of clearly defined “precepts” (considered as “beliefs ... accepted as authoritative by some group or school” [24]). That is why, for a fruitful survey of the UR–QMS philosophy, it is of direct interest to identify such an set of **Basic Precepts (BP)** from which the mentioned assertions turn out to be derived or extrapolated. Note that the aforesaid set of precepts (i.e. the true core of CIUR doctrine along with prevalent philosophy of UR and QMS) can be collected by means of a careful examination of the today known publications. In its essence the respective collection can be presented as follows.

The history regarding Conventional Interpretation of UR (CIUR) began with two main generative elements which were the following ones:

(i) Heisenberg's “Thought-Experimental” (TE) relation:

$$\Delta_{TEA} \cdot \Delta_{TEB} \cong \hbar \quad \text{or} \quad \Delta_{TEA} \cdot \Delta_{TEB} \geq \hbar; \quad (1)$$

(ii) Robertson-Schrödinger relation of theoretical origin:

$$\Delta_{\Psi A} \cdot \Delta_{\Psi B} \geq \frac{1}{2} \left| \langle [\hat{A}, \hat{B}] \rangle_{\Psi} \right|. \quad (2)$$

For introducing relation (1) in [25, 26] were imagined some “Thought Experiments” (TE) (or “gedanken” experiments). The respective TE referred on simultaneous measurements of two (canonically) conjugate observables A and B regarding a same quantum micro-particle. As such pairs of two

tively “do not commute”, (iii) For improving fluency of our text some of the corresponding mathematical notations, formulas and proofs are summarized briefly and unitary in few Appendices located in the final of the article.

observables were considered coordinate q and momentum p respectively time t and energy E . Then the quantities Δ_{TEA} and Δ_{TEB} were indicated as corresponding “uncertainties” of the imagined measurements, while \hbar denotes the Planck's constant.

Relation (2) was introduced in [27, 28] and it is depicted as above in terms of traditional QM notations [29, 30]. The main features of the respective notations are reminded briefly below in Appendices A and B while some aspects regarding the Dirac's bracket QM notations [29–32] are discussed in Appendix B.

Note here the fact that the right-hand side term from (2) is dependent on Planck's constant \hbar , e.g. $|\langle [\hat{A}, \hat{B}] \rangle_{\Psi}| = \hbar$ when A and B are (canonically) conjugate.

Starting from the generative elements (1) and (2), CIUR doctrine jointly with UR and QMS philosophy have been evolved around the following **Basic Precepts (BP)**:

- **BP₁**: Quantities Δ_{TEA} and $\Delta_{\Psi A}$ from relations (1) and (2), have similar significances of measuring uncertainties for the observable A . Consequently, the respective relations should be regarded as having a same meaning of Uncertainty Relations (UR) concerning the simultaneous measurements of observables A and B . Such a regard is fortified much more by the fact that

$$\left| \langle [\hat{A}, \hat{B}] \rangle_{\Psi} \right| = \hbar$$

when A and B are (canonically) conjugate.

- **BP₂**: In case of a solitary observable A , for a micro-particle, the quantities Δ_{TEA} or $\Delta_{\Psi A}$ can have always an unbounded small value. Therefore such an observable should be considered as measurable without any uncertainty in all cases of micro-particles (systems) and states.
- **BP₃**: For two commuting observables A and B (whose operators \hat{A} and \hat{B} commute, i.e. $[\hat{A}, \hat{B}] = 0$) relation (2) allows for the product $\Delta_{\Psi A} \cdot \Delta_{\Psi B}$ to be no matter how small. Consequently the quantities $\Delta_{\Psi A}$ and $\Delta_{\Psi B}$ can be unlimited small at the same time. Such observables have to be regarded as being compatible, i.e. measurable simultaneously and without interconnected uncertainties, for any micro-particle (system) or state.
- **BP₄**: In case of two non-commuting observables A and B (described by operators \hat{A} and \hat{B} which do not commute, i.e. $[\hat{A}, \hat{B}] \neq 0$) the relation (2) shows that the product $\Delta_{\Psi A} \cdot \Delta_{\Psi B}$ has as lower bound a non-null and \hbar -dependent quantity. Then the quantities $\Delta_{\Psi A}$ and $\Delta_{\Psi B}$ can be never reduced concomitantly to null values. For that reason the respective observables must be accounted as measurable simultaneously only with non-null and interconnected uncertainties, for any situation (particle/state). Viewed in a pair such observables are proclaimed as being incompatible, respectively complementary when they are (canonically) conjugate.

- **BP₅**: The main elements of CIUR doctrine and UR philosophy show quantum particularities of uniqueness comparatively with other non-quantum areas of physics. Such elements are the very existence of relations (1) and (2), the above asserted measuring features and the discriminating presence of the Planck's constant \hbar .
- **BP₆**: For glorifying the precepts **BP₁–BP₅** and adopting the usages of dominant literature, UR philosophy in its entirety should be ranked to a status of fundamental concept named Uncertainty Principle (UP).

Add here the observation that, in their wholeness, CIUR doctrine conjointly with UR and QMS prevalent philosophy emerge completely from the assertions embedded in basic precepts “**BP₁–BP₆**”.

3 Deficiencies (D) of the mentioned precepts

The above mentioned emergence conceals a less popularized fact namely that each of the precepts **BP₁–BP₆** is discredited (and denied) by insurmountable deficiencies. Such a fact can be revealed through a deep analysis of the respective precepts, an analysis which is of major importance for an authentic and fruitful survey of UR and QMS prevalent philosophy. That is why here below we aim to reveal the most significant ones of the mentioned deficiencies. They will be presented in a meaningful ensemble, able to give an edifying global appreciation regarding the mentioned philosophy. The referred ensemble includes as distinct pieces the following *Deficiencies (D)*:

3.1 *D*₁: Provisional character of relation (1)

Now it must be noted firstly the aspect that, through an analysis of its origins, relation (1) shows only a provisional (transient) character. This because it was founded [25, 26] on old resolution criterion from optics (introduced by Abe and Rayleigh — see [33]). But the respective criterion was surpassed through the so-called super-resolution techniques worked out in modern experimental physics (see [34–38] and references). Then by means of of the mentioned techniques can be imagined some interesting “*Super-Resolution-Thought-Experiments*” (*SRTE*). Through such *SRTE* for two (canonically) conjugate observables *A* and *B*, instead of *TE*-uncertainties $\Delta_{TE}A$ and $\Delta_{TE}B$ from (1), it becomes possible to discuss situations with some *SRTE*-uncertainties denoted as $\Delta_{SRTE}A$ and $\Delta_{SRTE}B$. For the respective *SRTE*-uncertainties, instead of Heisenberg's restrictive formula (1) (first version), can be suggested some CIUR-discordant relations like as

$$\Delta_{SRTE}A \cdot \Delta_{SRTE}B < \hbar. \quad (3)$$

Note that an experimental example of discordant relation of (3)-type was mentioned in [39] (where the UR (1) “*would be violated by close to two orders of magnitude*”).

Now one observes that, from the our days scientific perspective, *SRTE* relations like (3) are suitable to replace the

old Heisenberg's formula (1) (second version). But such suitability invalidates a good part of the precept **BP₁** and, additionally, it incriminates the CIUR doctrine and UR–QMS philosophy in connection with one of their main (generative) element.

It is surprising that, after invention of the super-resolution techniques, the mainstream (normative /authoritarian) publications connected with UR–QMS philosophy avoided a just and detailed evaluation of the respective techniques. Particularly, even after eight year after the result reported in [39], almost all of the dominant publications omit to discuss the respective result. The surprise is evidenced to a great extent by the fact that parsimony desiderata noted in Section 1 offer a viable argumentation for completing the evaluations and discussions off the mentioned kind.

Another infringement (violation) of Heisenberg's relation (1) was reported in [40] as an experimental result. That report is criticized vehemently by CIUR partisans [12]. The respective criticism is done in terms of a few un-argued (and un-explained) accusatory-sentences. But it is expected that, if they are justifiable, such kind of critiques should be grounded on precise technical details and arguments. This in order that they to be credible.

Curiously is also the fact that, over the past decades within the UR philosophy, the debates have neglected the older criticisms of the relation (1) due to K. Popper [41].

Taking into account the above revealed aspects one can say that the precept **BP₁** proves oneself to be a misleading (even harmful) basic element for CIUR doctrine and UR–QMS philosophy. But such a proof is a first argument for reporting that the respective doctrine and philosophy cannot be accepted as solid (and credible) scientific constructions.

3.2 *D*₂: Significance of quantities from relation (2)

The term “*uncertainty*” used within CIUR doctrine for quantities $\Delta_{\Psi}A$ and $\Delta_{\Psi}B$ from (2) is groundlessly because of the following considerations. According the theoretical framework of QM, by their definitions, the respective quantities signify genuinely the standard deviations of the observables *A* and *B* regarded as random variables (see below Appendix A). With such significances the alluded quantities refer to intrinsic (own) properties (known as fluctuations) of the considered particle but not to characteristics of the measurements performed on respective particle. In fact, on a one hand, for a measured particle in a given state (described by certain wave function Ψ) the quantities $\Delta_{\Psi}A$ and $\Delta_{\Psi}B$ have unique and well definite values. On the other hand for the same particle/state the measuring uncertainties regarding the observables *A* and *B* can be changed through the improvements or deterioration of experimental devices/techniques.

The above revealed QM significances for quantities $\Delta_{\Psi}A$ and $\Delta_{\Psi}B$ are genuinely preferable comparatively with the assertions from the precepts **BP₁–BP₄** promoted by CIUR doc-

trine and UR–QMS philosophy. But such a preference is completely congruent with the previously mentioned desiderata of parsimony principle.

3.3 D_3 : Limitations of relation (2)

Relation (2) has only limited validity within the complete theoretical framework of QM. This because, as it is detailed below in Appendix A, for observables A and B , relation (2) is only a restricted consequence of the generally valid Cauchy-Schwarz formula, given in (A.2). From such a general formula the relation (2) results iff (if and only if) in circumstances when the conditions (A.3) are satisfied. In the respective circumstances in addition to relation (2)/ (A.7) from (A.2) arises also the formula (A.6). It is worthy to note that the mentioned particularities regarding the validity of the relation (2) discredit indirectly the precept BP_1 of CIUR doctrine and UR–QMS philosophy. In their essence the specifications recorded here are nothing but concretizations of parsimony desiderata regarding the respective doctrine and philosophy.

3.4 D_4 : On solitary observables

It is surprising to find that, within UR–QMS philosophy debates, the problem of solitary observables is not discussed carefully. Particularly, were neglected discussions regarding the measurements of such observables. This although the respective discussions can be sub-summed to the question of simultaneous measurements of two observables. Such a sub-summation can be imagined by means of the Thought Experiments (TE) which motivated the conventional relation (1). Namely, for example, if in the respective TE it is of interest only the quantity $\Delta_{TE}A$, by ignoring completely the quantity $\Delta_{TE}B$, one can say that $\Delta_{TE}A$ can be unlimited small. Therefore the observable A , regarded as a solitary variable, appears as measurable without any uncertainty in all cases. But, on the other hand, if the same solitary observable A is analyzed in terms of relation (2), it cannot be associated with an unlimited small value for the quantity $\Delta_{\Psi}A$. This because, from a QM perspective, $\Delta_{\Psi}A$ has a unique and well definite value, evaluated through the corresponding wave function Ψ . Consequently, even in the cases of solitary observables, the CIUR doctrine and the UR–QMS philosophy cannot provide a clear and unequivocal approach as it is suggested by precept BP_2 .

3.5 D_5 : About commutable observables

According to the precept BP_3 for two observables A and B , whose associated operators \hat{A} and \hat{B} are commutable, relation (2), allows for the product $\Delta_{\Psi}A \cdot \Delta_{\Psi}B$ to be however small. Then the quantities $\Delta_{\Psi}A$ and $\Delta_{\Psi}B$ can be unlimited small at the same time. Such observables are supposed compatible, they being measurable simultaneously and without interconnected uncertainties for any micro-particle (system) or state.

But, as it was shown above in deficiency D_2 , the mentioned assertions from BP_3 , conflict with the genuine signifi-

cance of the quantities $\Delta_{\Psi}A$ and $\Delta_{\Psi}B$. This because both $\Delta_{\Psi}A$ and $\Delta_{\Psi}B$ have unique values, determined theoretically by the wave function Ψ which describe the considered state of particle. Or it is possible to have some “rebellious situations” in which the respective values of $\Delta_{\Psi}A$ and $\Delta_{\Psi}B$ to be simultaneously non-zero but finite entities, even the corresponding observables are commutable.

Such a “rebellious situation” can be found [20] for the observables P_x and P_y (Cartesian moments) regarding a micro-particle situated in a potential well of a rectangular 2D configuration. If the well walls are inclined towards the X and Y axes, the both the quantities $\Delta_{\Psi}P_x$ and $\Delta_{\Psi}P_y$ have non-zero but finite values. In that situation for P_x and P_y , besides the relation (2), it is satisfied however the formula (A.2) with $|(\delta_{\Psi}\hat{P}_x\Psi, \delta_{\Psi}\hat{P}_y\Psi)|$ as a non-null quantity.

The above remarks show that, in fact, the cases of commutable observables require to repudiate firmly the precept BP_3 . Additionally we think that the same cases should be regarded in the spirit of parsimony principle desiderata, by their consideration in QM terms reminded briefly in Appendices A and B.

3.6 D_6 : Cases of angular observables L_z and φ

The precept BP_4 stipulates that, as a principle, two non-commutable observables A and B cannot be measured simultaneously because the product $\Delta_{\Psi}A \cdot \Delta_{\Psi}B$ has a non-null lower bound. But the respective stipulation is contradicted by some rebellious pairs of observables. Such a pair, widely discussed, is L_z – φ (angular momentum — azimuthal angle), regarded in certain particular situations. The respective contradiction was probably the most inciting subject of debates during the history of CIUR doctrine and UR–QMS philosophy (see [5, 17–20, 42–55]). The mentioned debates regarded mainly the quantum rotations which can be called “ L_z -non-degenerate — circular — rotations” (L_z -ndcr). But, besides of that situations, in QM framework can be discussed also other kinds of rotations, of direct significance for L_z – φ pair. Such kinds are the ones regarding the rotational eigenstates of a Quantum Torsion Pendulum (QTP) and respectively the “ L_z -degenerate — spatial — rotations” (L_z -dsr). The true situations of the L_z – φ pair in relation with all kinds of the mentioned rotations will be discussed below in more details.

3.6.1 D_{6a} : About non-degenerate circular rotations

Let us discuss now the cases of L_z -non-degenerate — circular — rotations (L_z -ndcr). As systems of with L_z -ndcr can be quoted the following ones: (i) a particle (bead) on a circle, (ii) an 1D rotator and (iii) non-degenerate spatial rotations of a particle on a sphere or of an electron in a hydrogen atom respectively. The mentioned spatial rotations are considered as L_z -non-degenerate if the magnetic quantum number m (associated with L_z) has a unique value (while, of course, all other specific (orbital) quantum numbers have well-defined values).

The rotations of respective systems are described through the wave functions given by

$$\Psi(\varphi) = \Psi_m(\varphi) = (2\pi)^{-\frac{1}{2}} \cdot \exp(im\varphi). \tag{4}$$

Here φ is an ordinary polar coordinate (angle) with the corresponding mathematical characteristics [56] i.e. $\varphi \in [0, 2\pi)$ and number m gets only one value from the set $m = 0, \pm 1, \pm 2, \dots$. Also in (4) the wave function $\Psi(\varphi) = \Psi_m(\varphi)$ has the property $\Psi(0) = \Psi_m(2\pi - 0) := \lim_{\varphi \rightarrow 2\pi-0} \Psi_m(\varphi)$.

In the same context, according to the known QM framework [29], L_z and φ should be regarded as polar observables, described by the conjugated operators and commutator represented as follows

$$\hat{L}_z = -i\hbar \frac{\partial}{\partial \varphi}, \quad \hat{\varphi} = \varphi, \quad [\hat{L}_z, \hat{\varphi}] = -i\hbar. \tag{5}$$

Therefore the conventional relation (2) motivates as a direct consequence the next formula

$$\Delta_\Psi L_z \cdot \Delta_\Psi \varphi \geq \frac{\hbar}{2}. \tag{6}$$

Now it is easy to observe that this last formula is explicitly inapplicable in cases described by wave functions (4). This because in such cases, for the quantities $\Delta_\Psi L_z$ and $\Delta_\Psi \varphi$ associated with the pair $L_z-\varphi$, one obtains the following values

$$\Delta_\Psi L_z = 0, \quad \Delta_\Psi \varphi = \pi \cdot (3)^{-\frac{1}{2}}. \tag{7}$$

But such values for $\Delta_\Psi L_z$ and $\Delta_\Psi \varphi$ are evidently incompatible with the conventional relation (2)/(6).

In order to avoid the above revealed incompatibility in many mainstream publications the CIUR partisans promoted some unusual ideas such are:

- For L_z and φ operators and commutator, instead of current expressions (5), it is conveniently to adopt other new denotations (definitions).
- The formula (6) must be abandoned/proscribed and replaced by one (or more) “*modified $L_z-\varphi$ UR*” able to mime the conventional relation (2) for the $L_z-\varphi$ pair.

The alluded ideas were promoted through the conception of “*impossibility of distinguishing ... between two states of angle differing by 2π* ”. But such a conception has not any realistic sense in cases of circular rotations. This because in such cases the angle φ has as physical range the interval $[0, 2\pi)$. Moreover in the respective cases the wave functions (4) are normalized on the same interval but not on other strange domains.

As regards the “*modified $L_z-\varphi$ UR*”, along the years, by means of some circumstantial (and more or less fictitious) considerations, were proposed a lot of such relations. In terms of usual QM notations (summarized below in Appendix A),

the alluded “*modified $L_z-\varphi$ UR*” can be written generically as follows

$$f(\Delta_\Psi L, \Delta_\Psi g(\varphi)) \geq \hbar \cdot \langle s(\varphi) \rangle_\Psi. \tag{8}$$

Here $f(\Delta_\Psi L, \Delta_\Psi g(\varphi))$, $g(\varphi)$ and $s(\varphi)$ denote some specially invented functions depending on the corresponding arguments. Note that some of the mostly known concrete examples of relations (8) can be found collected in [55].

Now it should be noted the fact that the “*modified $L_z-\varphi$ UR*” such are (8) show some troubling features like the following ones:

- Regarded comparatively, the mentioned “*modified $L_z-\varphi$ UR*” are not mutually equivalent. This despite of the fact that they were invented in order to substitute the same proscribed formula (6). Consequently, none of that modified relations, is agreed unanimously as a suitable model able to give such a substitution.
- Relations (8) are in fact ad hoc artifices without any source in mathematical framework of QM. Then, if one wants to preserve QM as a unitary theory, like it is accredited in our days, the relations (8) must be regarded as unconvincing and inconvenient (or even prejudicial) inventions.
- In fact in relations (8) the relevant angular quantities $\Delta_\Psi L_z$ and $\Delta_\Psi \varphi$ are substituted more or less factitious with the adjusting functions $f(\Delta_\Psi L_z, \Delta_\Psi g(\varphi))$, $g(\varphi)$ and $s(\varphi)$. But, from a genuine perspective, such substitutions, and consequently the corresponding relations, are only mathematical constructs but not elements with useful physical significance. Of course that such constructs overload (or even impede) the scientific discussions by additions of extraneous entities which are not associated with true information about the real world.

Then, for a correct evaluation of the facts, all the aspects regarding relations (8) versus (6) ought to be judged by taking into consideration the parsimony principle desideratum: “*Entities are not to be multiplied beyond necessity*”. Such an evaluation can be started by clarifying firstly the origin and validity conditions of the formula (6) regarded as descendant of conventional relation (2). For the respective clarification it is usefully to see some QM elements briefly summarized in Appendix A.

So it can be observed easy that, in its essence, the relations (2) follow from the generally valid formulas (A.2) pertaining to the mathematical framework of QM. But, attention, (2) results correctly from (A.2) iff (if and only if) when it is satisfied the condition (A.3). In other cases (2) are not valid at all. Such an invalidity is completely specific for the cases of $L_z-\varphi$ pair in relations with situations described by the wave functions (4). This because in respective cases instead of conditions (A.3) it is true the relation

$$(\hat{L}_z \Psi, \hat{\varphi} \Psi) = (\Psi, \hat{L}_z \hat{\varphi} \Psi) + i\hbar. \tag{9}$$

Therefore, for systems described by the wave functions (4), the formula (6) is invalid by its essence.

Now note that, even when the condition (A.3) is not satisfied, according to the QM general formula (A.2), for the discussed situations it is true the relation

$$\Delta_{\Psi} L_z \cdot \Delta_{\Psi} \varphi \geq \left| \left(\delta_{\Psi} \hat{L}_z \Psi, \delta_{\Psi} \hat{\varphi} \Psi \right) \right| \quad (10)$$

written in compliance with definitions (4) and (5). But, attention, in respective situations the last relation (10) degenerates into trivial equality “ $0=0$ ”. Add here the fact that relation (10) is completely equivalent with the formula (C.13) deductible within Fourier analysis.

The above presented details argue undoubtedly the view that in cases with L_z -ndcr the L_z - φ pair must to satisfy not the troublesome formula (6) but the QM justified relation (10) (which in fact reduces itself to banal equality “ $0=0$ ”). Such an argued view clarifies all disputes regarding the mentioned cases. Moreover the same view disproves the idea of some “entities ... multiplied beyond necessity” (such are the modified UR (8)) intended to replace the inoperative relation (6).

3.6.2 D_{6b} : Case of Quantum Torsion Pendulum (QTP)

The case of Quantum Torsion Pendulum (QTP) regards a quantum harmonic oscillator with torsional rotations [19, 20, 55]. Such an oscillator can be considered as the simplest theoretical model for molecular twisting motion (“change in the angle between the planes of two groups of atoms” [57]). For a QTP oscillating around the z-axis the Hamiltonian operator has the form

$$\hat{H} = \frac{1}{2I} \hat{L}_z^2 + \frac{1}{2} I \omega_0^2 \varphi^2. \quad (11)$$

Here φ denotes the twisting angle with domain $\varphi \in (-\infty, +\infty)$ while the operators \hat{L}_z and $\hat{\varphi}$ obey the rules (5). The other symbols from (11) are: I and ω_0 represent the momentum of inertia respectively the (undamped) resonant frequency ($\omega_0 = \sqrt{\kappa/I}$ while κ = torsion elastic modulus).

By means of Schrödinger equation $E\Psi = \hat{H}\Psi$ one finds that the QTP eigenstates are described by the wave functions

$$\Psi_n(\varphi) = \Psi_n(\xi) \propto \exp\left(-\frac{\xi^2}{2}\right) \cdot \mathcal{H}_n(\xi), \quad \xi = \varphi \sqrt{\frac{I\omega_0}{\hbar}}. \quad (12)$$

These wave functions correspond to the oscillation quantum numbers $n = 0, 1, 2, 3, \dots$ and energy eigenvalues $E_n = \hbar\omega_0\left(n + \frac{1}{2}\right)$. In (12) $\mathcal{H}_n(\xi)$ represent the Hermite polynomials of ξ .

For each of the states (12) for observables L_z and φ associated with the operators (5) one obtains the expressions

$$\begin{aligned} \Delta \varphi &= \sqrt{\frac{\hbar}{I\omega_0} \left(n + \frac{1}{2}\right)}, & \Delta L_z &= \sqrt{\hbar I \omega_0 \left(n + \frac{1}{2}\right)}, \\ \left| \left(\Psi, \left[\hat{L}_z, \hat{\varphi} \right] \right) \right| &= \hbar, \\ \Delta \varphi \cdot \Delta L_z &= \hbar \cdot \left(n + \frac{1}{2}\right). \end{aligned} \quad (13)$$

These expressions show the fact that, for each QTP eigenstate, the L_z - φ pair satisfies the relation (6)/(2). But note that the respective fact is due to the circumstance that in the mentioned case, in relation with the wave functions (12), the operators \hat{L}_z and $\hat{\varphi}$ satisfy a condition of (A.3) type, i.e. $(\hat{L}_z \Psi, \hat{\varphi} \Psi) = (\Psi, \hat{L}_z \hat{\varphi} \Psi)$.

3.6.3 D_{6c} : On degenerate spatial rotations

Let us now regard the cases of L_z -degenerate-spatial-rotations (L_z -dsr). Such kinds of rotations refer [20, 21, 55] to states of: (i) a particle on a sphere, (ii) a 2D rotator and (iii) an electron in a hydrogen atom. The respective rotations are L_z -degenerate in sense that the magnetic quantum number m (associated with L_z) has multiple values while the other quantum numbers have unique values. A particle on a sphere or a 2D rotator are in a L_z -dsr when the orbital number l has a unique value greater than zero while m can take all the values $m \in [-l, +l]$. Then the corresponding rotations are described through the global wave function

$$\Psi(\vartheta, \varphi) = \Psi_l(\vartheta, \varphi) = \sum_{m=-l}^{m=+l} c_m \cdot Y_{lm}(\vartheta, \varphi). \quad (14)$$

Here ϑ and φ denote polar respectively azimuthal angles with $\vartheta \in [0, \pi]$ and $\varphi \in [0, 2\pi)$. In (14) $Y_{lm}(\vartheta, \varphi)$ denote spherical functions while c_m are coefficients normalized through the condition $\sum_{m=-l}^{m=+l} |c_m|^2 = 1$. Also the wave functions $\Psi_l(\vartheta, \varphi)$ from (14) have the property $\Psi_l(\vartheta, 0) = \Psi_l(\vartheta, 2\pi - 0) := \lim_{\varphi \rightarrow 2\pi-0} \Psi_l(\vartheta, \varphi)$. In a direct connection with such a property the operators \hat{L}_z and $\hat{\varphi}$ obey the rules (5).

Now let us regard what are the peculiarities of the L_z -dsr cases in respect with the controversial relation (6). Principled, such a regard demands that, by using the formulas (5) and (14), to evaluate the corresponding expressions for the quantities $\Delta_{\Psi} L_z$, $\Delta_{\Psi} \varphi$ and $\left| \left(\Psi, \left[\hat{L}_z, \hat{\varphi} \right] \Psi \right) \right|$. With the respective expressions one finds possibilities that the relation (6) to be or not to be satisfied. Of course that such possibilities are conditioned by the concrete values of the coefficients c_m . But note that, if the relation (6) is not satisfied, the fact appears because essentially in such a situation the condition (A.3) is not fulfilled. Add here the important observation that, independently of validity for relation (6), in all cases of L_z -dsr the L_z - φ pair obeys the prime QM relation (A.2) through adequate values for the quantities $\Delta_{\Psi} L_z$, $\Delta_{\Psi} \varphi$ and $\left| \left(\delta_{\Psi} \hat{L}_z \Psi, \delta_{\Psi} \hat{\varphi} \Psi \right) \right|$. The previous considerations offer a clear evaluation of the situation for L_z -dsr cases relatively to the conventional relation (2) and precept BP_4 .

Summing up of deficiencies D_6 (including D_{6a} , D_{6b} and D_{6c}): The above discussion about the three kinds of rotations reveals the deficiencies of the conventional relation (2) and of the associated precept BP_4 in regard with the non-commutable observables L_z and φ . But such revealing is noth-

ing but a direct and irrefutable incrimination of CIUR doctrine and UR-QMS philosophy.

3.7 D₇: On number and phase observables

The pair N and ϕ (number and phase) is another couple of rebellious non-commutable observables which contradict the corresponding stipulation from the precept **BP₄** of UR-QMS philosophy. That contradiction emerged in connection with the associated operators \hat{N} and $\hat{\phi}$. The respective operators were introduced by means of the ladder (lowering and raising) operators \hat{a} and \hat{a}^+ , destined to convert some QM calculations procedures from an analytical version to an algebraic one. Through the respective connection, by taking as base the relation $[\hat{a}, \hat{a}^+] = 1$, it was inferred the commutation formula $[\hat{N}, \hat{\phi}] = i$.

The last noted formula motivated the idea that operators \hat{N} and $\hat{\phi}$ must satisfy the conventional relation (2) with both $\Delta_\Psi N$ and $\Delta_\Psi \phi$ as non-null quantities. But afterward it was found the fact that, in the case of a harmonic oscillator eigenstates, one obtains $\Delta_\Psi N = 0$ and $\Delta_\Psi \phi = \pi \cdot (3)^{-\frac{1}{2}}$ i.e. a violation of the relation (2). Of course that such a fact leads to a deadlock for harmonization of N - ϕ observables with the CIUR doctrine and UR-QMS philosophy. Note that this deadlock is completely analogous with the one regarding to L_z - φ observables in the above discussed case of L_z - $ndcr$ (L_z -non-degenerate — circular — rotations).

For avoiding the mentioned N - ϕ deadlock in many publications were promoted various adjustments (see [6, 43, 48, 58–61] and references therein). But it is easy to observe that the respective adjustments regarded the conventional relation (2) as an absolute mark and tried to adapt accordingly the pair N - ϕ for a description of a harmonic oscillator. So it was suggested to replace the original operators \hat{N} - $\hat{\phi}$ by some ad hoc “adjusted” (*adj*) operators \hat{N}_{adj} and $\hat{\phi}_{adj}$, able to generate formulas resembling (more or less) with the conventional relation (2) (examples of such adjusted operators can be found in the literature of recent decades). However it is very doubtfully that the corresponding “adjusted observables” N_{adj} and ϕ_{adj} can have natural (or even useful) physical significances. Moreover, until now, it not exist a unanimously agreed conception able to guarantee a true elucidation regarding the status of number-phase observables relatively to terms of CIUR doctrine and UR philosophy.

Our opinion is that a genuine clarification of the N - ϕ problem can be done similarly with the above discussed situation of L_z - φ observables in the cases of L_z - $ndcr$. More exactly we have to note that the disagreement of N - ϕ pair with the conventional relation (2) results from fact that in such a case the respective relation is mathematically incorrect. The aforesaid incorrectness is due mainly to the circumstance that, in cases of a linear oscillator eigenstates, the N - ϕ pair does not satisfy the essential condition (A.3). This because in that cases for the operators \hat{N} - $\hat{\phi}$ is true the for-

mula $(\hat{N}\Psi, \hat{\phi}\Psi) = (\Psi, \hat{N}\hat{\phi}\Psi) + i$ which evidently infringes the condition (A.3). But it should be pointed out that, even in the mentioned cases, the \hat{N} - $\hat{\phi}$ operators satisfy the primary relation (A.2) which degenerates into trivial equality “ $0 = 0$ ”.

We think that the above noted opinion gives a natural and incontestable solution for the problem regarding the N - ϕ pair versus the conventional relation (2). Accordingly the fictional operators \hat{N}_{adj} and $\hat{\phi}_{adj}$, of an ad hoc adjusted essence, proves themselves to be nothing but “*entities . . . multiplied beyond necessity*”.

So it can be said that the situation of observables N and ϕ contradict directly the precept **BP₄** in connection with non-commutable observables. Consequently, the respective situation invalidates completely one of basic elements of CIUR doctrine and UR-QMS philosophy.

3.8 D₈: Concerning the energy — time pair

Closely to the conventional views of CIUR doctrine and UR-QMS philosophy the pair of observables E - t (energy-time) was subject for a large number of controversial discussions (e.g. in works [5, 6, 62–64], in their references and, certainly, in many other publications). The alluded discussions were generated within following circumstances. On one hand, accordingly to the mentioned views, E and t are regarded as conjugated observables, having to be described by the next operators and commutator

$$\hat{E} = i\hbar \frac{\partial}{\partial t}, \quad \hat{t} = t, \quad [\hat{E}, \hat{t}] = i\hbar. \tag{15}$$

Then the operators \hat{E} and \hat{t} should satisfy the conventional relation (2) in a nontrivial version. On the other hand, because of the fact that, in terms of usual QM, the time t is a deterministic but not random variable, for any quantum situation one finds the following expressions $\Delta_\Psi E =$ “*a finite quantity*” respectively $\Delta_\Psi t \equiv 0$. But these expressions invalidate the relation (2) and consequently the E - t pair shows an anomaly in respect with the alluded conventional ideas, especially with the precept **BP₄**. For avoiding the noted anomaly, within the literature about E - t pair, it was substituted the unsuitable relation (2) by some adjusted formulas written generically as follows

$$\Xi E \cdot \Xi t \geq \frac{\hbar}{2}. \tag{16}$$

The so introduced quantities ΞE and Ξt have various significances such are: (i) line-breadth and half-life of a decaying excited state, (ii) frequency domain and temporal widths of a wave packet, (iii) $\Xi E = \Delta_\Psi E$ and $\Xi t = \Delta_\Psi A \cdot (d(A)/dt)^{-1}$, with A = an arbitrary observable.

As regards the adjusted formulas (16) note firstly the fact that various of their versions are not congruent with the original conception of relation (2). Also the respective versions are not mutually equivalent from a mathematical (theoretical) viewpoint. So they have no reasonable justification in

the true QM framework. Moreover in specific literature none of the formulas (16) is accepted unanimously as a correct (or natural) substitute for conventional relation (2).

Now it is the place to present the following clarifying remarks. Even if the $E-t$ pair is considered to be described by the operators (15), according to the true QM terms, one finds the relation

$$(\hat{E}\Psi, \hat{t}\Psi) = (\Psi, \hat{E} \hat{t}\Psi) - i\hbar. \quad (17)$$

By comparing this relation with condition (A.3) one sees directly that the $E-t$ pair cannot ever satisfy the respective condition. This is the essential reason because of which for the $E-t$ pair the conventional relation (2) is not applicable at all. Nevertheless, for the same pair described by the operators (15), the QM relation (A.2) is always true. But because in QM the time t is a deterministic (i.e. non-stochastic) variable in all cases the respective true relation degenerates into the trivial equality " $0 = 0$ ".

The above noted comments lead to the next findings:

- In case of the $E-t$ pair the conventional views (of CIUR doctrine and UR-QMS philosophy) are completely nonfunctional.
- Genuinely, within a true QM framework, the time t is in fact a pure deterministic (non-stochastic) quantity without any standard deviation (or fluctuation).

But, taken together, such findings about time-energy pair must be reported as a serious and insurmountable deficiency of CIUR doctrine and UR-QMS philosophy.

3.9 D_9 : Atypical analogues of UR (1) and (2)

By basic precept **BP**₅ the UR philosophy claims idea that relations (1) and (2) possess an essential typicality represented by their QM uniqueness related with the systems of atomic size. Consequently, the respective relations should not have analogues in other areas of physics or for systems of radically different sizes. But the respective idea is definitely denied by some example that we will present below.

3.9.1 D_{9a} : Classical Rayleigh formula

As a first example of an atypical analogue of the UR (1) can be quoted the formula

$$\sin \alpha \cong \frac{\lambda}{d} \quad (18)$$

which expresses [35, 39, 40, 65] the Rayleigh resolution criterion from classical optics. In (18) α denotes the "angular resolution", λ is the wavelength of light, and d represents the diameter of lens aperture. Note that criterion (18) was introduced in classical optics in 1879, i.e. by long time before the QM appeared. Later one relation (1) was introduced by taking in (18) $d \sim \Delta_{TE} \cdot q$ for coordinate uncertainty, respectively $\lambda = (\hbar/p)$ for momentum p (through wave-particle duality formula) and $p \cdot \sin \alpha \sim \Delta_{TE} \cdot p$ for momentum uncertainty.

3.9.2 D_{9b} : Classical "Gabor's uncertainty relation"

An example of an atypical analog of (2) can be found within the mathematical harmonic analysis in connection with a pair of random quantities regarded as Fourier conjugated variables (see [66, 67] and the Appendix C below). In non-quantum physics such an analogue is known [67] as "Gabor's uncertainty relation" which can be represented through the relation

$$\Delta t \cdot \Delta \nu \geq \frac{1}{4\pi}. \quad (19)$$

This last relation (19) shows the fact that for a classical signal, regarded as a wave packet (of acoustic or electromagnetic nature), the product of the "uncertainties" ("irresolutions") Δt and $\Delta \nu$ in the time and frequency domains cannot be smaller than a specific constant.

3.9.3 D_{9c} : A relation regarding thermodynamic observables

Another example of an atypical similar of UR (2) is given by the following classical formula

$$\Delta_W \mathbb{A} \cdot \Delta_W \mathbb{B} \geq |\langle \delta_W \mathbb{A} \cdot \delta_W \mathbb{B} \rangle_W| \quad (20)$$

showed as relation (D.3) in Appendix D of the present article. The elements (notations and physical significances) implied in (20) are those detailed in Appendix D. The respective elements are specific to the phenomenological theory, initiated by Einstein, about fluctuations of macroscopic thermodynamic observables (see [20, 68–72] and Appendix D below).

Note that, from the perspective of mathematics (more exactly of probability theory), the macroscopic formula (20) and UR (2) are analogue relations, both of them regard the fluctuations of the corresponding observables judged as random variables. Moreover they describe the intrinsic properties of considered systems (of macroscopic-thermodynamic respectively quantum nature) but not aspects of measurements performed on the respective systems. The corresponding measurements can be described through a distinct approaches modeled/depicted as transmission processes for stochastic data (see below Appendix E and Section 5 in present article).

As regards the formula (20), the following notifications should be done too. To a some extent the respective formula can be considered as being member to a family of so called "thermodynamic UR", discussed in a number of publications from the last century (see [78, 79] and references). Note that the alluded membership is true only in respect with the "regular" subset of respective family, derivable from the Einstein's phenomenological theory. But the mentioned family includes moreover a class of "irregular" relations. The most known such an "irregular" relation regards the conjugate variables energy U and temperature T of a thermodynamic system. It

has [78] the form

$$\Delta U \cdot \Delta \left(\frac{1}{T} \right) \geq k_B \quad (21)$$

where k_B denote the Boltzmann's constant.

It must be noted now the reality that fluctuation formula (20) and "irregular" relations like is (21) are completely dissimilar, first of all, due to the important distinction between reference frames of their definitions. The respective dissimilarity is pointed out by the following aspects. On the one hand, the quantities $\Delta_W \mathbb{A}$ and $\Delta_W \mathbb{B}$ from (20) are defined by referring to the same state of the considered system. On the other hand the quantities U and T which appear in (21) refer to different states of a system, namely states characterized by an energetic isolation respectively by a thermal contact. Due mainly to the above mentioned dissimilarity: "a derivation of the uncertainty relation (21) analogous to that of the usual Heisenberg relations (i.e. UR (2)) is impossible" [78].

Add here the fact that, within associate literature, it was reported a number of controversies about the aspects regarding the possible similarities between the "thermodynamic UR" (mainly from the same subset as (21)) and quantum UR (2) (see [78] and references). Among respective aspects can be quoted:

- compatibility of macroscopic observables,
- commutativity of thermodynamic variables and
- reconstruction of QM from hidden variables theories similarly with the rebuilding of thermodynamics through subjacent molecular considerations.

Note that the just mentioned aspects are not taken into account (as relevant elements) for our present survey on deficiencies of prevalent philosophy regarding UR and QMS.

3.9.4 D_{9d} : On the so called macroscopic operators

In the spirit of conventional precept BP_5 the uniqueness of UR (2) consists in its strict specificity for micro-particles (of atomic size), without analogues in cases of macroscopic systems. But, as it is pointed out through relation (D.12) from Appendix D, in case of macroscopic thermodynamic system studied in quantum statistical physics one finds the formula

$$\Delta_\rho \mathbb{A} \cdot \Delta_\rho \mathbb{B} \geq \frac{1}{2} \left| \left\langle \left[\hat{\mathbb{A}}, \hat{\mathbb{B}} \right] \right\rangle_\rho \right|. \quad (22)$$

This last formula is similar with the conventional UR (2) (more exactly, mathematically, with its primary versions (A.7) and (B.4)). Due to such a similarity, probably, some publications (e.g. [74] and references) have tried to regard (22) as a macroscopic UR. But the respective regard was found to be incompatible with the known UR-QMS philosophy, mainly with the precept BP_4 .

The alluded incompatibility is pointed out by the following facts. On the one hand, in spirit of UR philosophy (precepts BP_1 – BP_4), the quantities $\Delta_\rho \mathbb{A}$ and $\Delta_\rho \mathbb{B}$ from (22) should be considered as measuring uncertainties of macroscopic observables \mathbb{A} and \mathbb{B} . Additionally when the operators $\hat{\mathbb{A}}$ and $\hat{\mathbb{B}}$ and do not commute (i.e. $[\hat{\mathbb{A}}, \hat{\mathbb{B}}] \neq 0$), according to (22), the quantities $\Delta_\rho \mathbb{A}$ and $\Delta_\rho \mathbb{B}$ can be never reduced concomitantly to null values. Consequently, in terms of UR-QMS philosophy, for any situation, the non-commutable macroscopic observables \mathbb{A} and \mathbb{B} are allowed to be measurable simultaneously only with non-null and interconnected uncertainties. But, on the other hand, according to the classical physics any two macroscopic observables can be measured concurrently with unlimited accuracies and without any interrelated uncertainties.

For avoiding the above noted incompatibility some partisans of UR philosophy have suggested the following expedient. Abrogation of (22) by replacement of genuine macroscopic operators $\hat{\mathbb{A}}$ and $\hat{\mathbb{B}}$ with another quasi-diagonal operators $\hat{\mathbb{A}}$ and $\hat{\mathbb{B}}$ (i.e. with operators whose representations in any base are quasi-diagonal matrices). Such substituting operators should commute and so the right hand term in (22) to be (quasi) null (i.e. $\left| \left\langle \left[\hat{\mathbb{A}}, \hat{\mathbb{B}} \right] \right\rangle_\rho \right| \approx 0$). Through the mentioned substitution the inconvenient relation (22) could be changed with the more convenient formula

$$\Delta_\rho \mathbb{A} \cdot \Delta_\rho \mathbb{B} \geq \frac{1}{2} \left| \left\langle \left[\hat{\mathbb{A}}, \hat{\mathbb{B}} \right] \right\rangle_\rho \right| \approx 0. \quad (23)$$

Then it seems to be possible that the substituted macroscopic uncertainties $\Delta_\rho \mathbb{A}$ and $\Delta_\rho \mathbb{B}$ to be reduced simultaneously to arbitrarily small (even zero) values. Apparently, such a possibility should to harmonize the interpretation of the relation (23) with the concepts of classical physics.

However, in fact, the above mentioned harmonization is not possible and the suggested expedient is useless. This, at least, due to the following reasons:

- Firstly, the relations (22) cannot be abrogated/substituted if the entire mathematical framework of quantum statistical physics is not abrogated/substituted too.
- Secondly, in common practice of studies of quantum statistical systems (e.g. such are the ones investigated in [80, 81]) are used the genuine operators $\hat{\mathbb{A}}$ and $\hat{\mathbb{B}}$ but not the quasi-diagonal ones $\hat{\mathbb{A}}$ and $\hat{\mathbb{B}}$.
- As a third reason, the following fact can be also noted. Even in certain situations when the original operators $\hat{\mathbb{A}}$ and $\hat{\mathbb{B}}$ are quasi-diagonal in the sense of the mentioned expedient, the relation (23) does not turn into a form having a null term in the right hand side. Such a situation can be found [20] in case regarding a macroscopic paramagnetic system made of a huge number of independent 1/2-spins. In such a case as macroscopic operators appear the Cartesian components \hat{M}_α ($\alpha = x, y, z$) of the system magnetization. Note that the

operators \hat{M}_α are quasi-diagonal in the sense required by the aforesaid expedient/substitution. But, for all that, the respective operators do not commute because $[\hat{M}_\alpha, \hat{M}_\beta] = i\hbar\gamma \cdot \epsilon_{\alpha\beta\mu} \cdot \hat{M}_\mu$ (γ = magneto-mechanical factor and $\epsilon_{\alpha\beta\mu}$ denotes the Levi-Civita tensor).

By taking into account the above pointed out deficiencies D_9 (including D_{9a} , D_{9b} , D_{9c} and D_{9d}) one may record the following conclusion. The relations (D.12)/(22) are relations regarding macroscopic areas of physics but not pieces which should be adapted to the requirements of prevalent philosophy about UR and QMS.

3.10 D_{10} : On the uniqueness of quantum measurements

Let us refer now to the uniqueness character of conventional relations (1) and (2) with regard to the measurements peculiarities at quantum level. The aforesaid character was largely debated in literature and it has generated the still open questions about the main characteristics (conceptual relevance and description procedures) of Quantum Measurements (QMS). By promoting all the assertions from percepts BP_1 – BP_4 the UR–QMS philosophy tried to enforce the opinion that relations (1) and (2) are closely linked with the measuring particularities that are unique in quantum context, without any correspondence (analogy) in non-quantum domains of physics. The mentioned opinion, often promoted as a true dogma, dominates the mainstream of existing publications.

On the other hand, as we have argued above through the deficiencies D_1 – D_9 , the alluded opinion is completely unfounded because, genuinely, the respective relations are:

- either an old-fashioned (and removable) empirical convention (in case of (1)),
- or simple (non-magistral) theoretical formula (in case of (2)).

Within UR–QMS prevalent philosophy, as a widespread belief, the uniqueness peculiarities of QMS are motivated through the so called “observer effect”. The respective effect is presented as a perturbing influence of observer (by experimental devices) on investigated systems and on measuring results. It is presumed to differentiate radically the QMS from classical measurements (of macroscopic physics). Such effects are absolutely unavoidable and affected by notable uncertainties in quantum contexts but entirely preventable and with negligible inaccuracies in classical situations.

The above mentioned belief is categorically disproved by the following observations. The “observer effect” appear not only in QMS but also in some classical measurements (e.g. [82] in electronics or in thermodynamics). Of course that in classical cases the measuring inaccuracies can be made negligible (by adequate improvements of experimental devices and/or procedures). It should be noted, that, in principle, quantum uncertainties can be also diminished (for example, with the super-resolution techniques discussed above in D_1).

Then the idea of uniqueness quantum measuring character for conventional relations (1) and (2), promoted by UR philosophy through BP_5 , proves oneself as being a groundless fiction which should be disregarded. But such a disregard come to fortify the J. Bell’s thinking [83, 84] that: “*the word ‘measurement’ should be avoided (or even . . . banned) altogether in quantum mechanics*”. Some annotations about the respective thinking are given below in Section 5 where we will present briefly a non-conventional approach of QMS problems.

3.11 D_{11} : On the uniqueness of Planck’s constant

Another aspect of quantum uniqueness invoked in precept BP_5 regards the presence of Planck’s constant \hbar as a specific symbol in conventional quantum relations (1) and (2), comparatively with a total absence of some similar symbols in all classical (non-quantum) formulas. We shall examine the alluded aspect in regard with the relation (2). Then of prime importance is to notify the fact that, mathematically, quantum observables from the relation (2) have a stochastic (non-deterministic) character. But a completely similar character one finds in cases of macroscopic observables implied in formula (20) regarding fluctuations specific to macroscopic thermodynamic systems.

Both kinds of mentioned stochastic observables describe fluctuations (at quantum respectively macroscopic scale). The mentioned fluctuations are characterized quantitatively by the corresponding standard deviations such are $\Delta_\Psi A$ or $\Delta_W A$. But, mathematically, the standard deviation indicates quantitatively the stochasticity (randomness) degree of an observable. This in the sense that the alluded deviation has a positive or null value as the corresponding observable is a random or, alternatively, a deterministic (non-stochastic) variable. Consequently the quantities $\Delta_\Psi A$ and $\Delta_W A$ can be regarded as similar indicators of stochasticity for quantum respectively macroscopic observables.

In principle for macroscopic thermal fluctuations the standard deviations like is $\Delta_W A$ can have various expressions (depending on system, state and observable). Apparently, it would seem that the respective expressions do not contain any common element. Nevertheless such an element can be found as being materialized by the Boltzmann’s constant k_B (see relation (D.4) in Appendix D below and articles [71, 73]). So, for any macroscopic fluctuating observable A , the quantity $(\Delta_W A)^2$ (i.e. dispersion = square of the standard deviation) appears as a product of Boltzmann’s constant k_B with factors which are independent of k_B .

This means that the quantity $(\Delta_W A)^2$, in its quality of quantitative indicator of thermal fluctuations, is directly proportional with k_B . Consequently $(\Delta_W A)^2$ has a non-null respectively null value as $k_B \neq 0$ or $k_B \rightarrow 0$ (Note that because k_B is a physical constant the limit $k_B \rightarrow 0$ means that the quantities directly proportional with k_B are negligible com-

paratively with other quantities of same dimensionality but independent of k_B). On the other hand, the standard deviation $\Delta_W \mathbb{A}$ is a particular indicator for macroscopic stochasticity revealed through thermal fluctuations.

Bringing together the above noted aspects it can be said that k_B has the qualities of an authentic generic indicator for thermal stochasticity which is specific for classical macroscopic fluctuating systems.

Now let us discuss about the quantum stochasticity whose particular indicators are the standard deviations $\Delta_\Psi A$. Based on the relations (13) one can say that in many situations the expressions for dispersions $(\Delta_\Psi A)^2$ consist in products of Planck constant \hbar with factors which are independent of \hbar . Then, by analogy with the above discussed macroscopic situations, \hbar places itself in the posture of generic indicator for quantum stochasticity.

The mentioned roles as generic indicators for k_B and \hbar (in direct connections with the quantities $\Delta_W \mathbb{A}$ and $\Delta_\Psi A$) regard the one-fold (simple) stochasticity, of thermal and quantum nature respectively. But in physics is also known a twofold (double) stochasticity, of a combined thermal and quantum nature. Such a kind of stochasticity one finds in cases of macroscopic thermodynamic systems composed of statistical assemblies of quantum micro-particles. The alluded twofold stochasticity can be evaluated in a way through the dispersions $(\Delta_{\rho \mathbb{A}_j})^2$ which estimate the level of fluctuations in the mentioned systems (see [20, 73, 76] and Appendix D below). As it is noted in relation (D.13) the dispersions $(\Delta_{\rho \mathbb{A}_j})^2$ can be given through of products containing the function $\mathfrak{f}(k_B, \hbar) = \hbar \cdot \coth(\frac{\hbar\omega}{2k_B T})$ and factors which are independent of both k_B and \hbar .

Then it results that k_B and \hbar considered together turn out to be a couple of generic indicators for the twofold (double) stochasticity of thermal and quantum nature. Such a kind of stochasticity is significant or negligible in situations when $k_B \neq 0$ and $\hbar \neq 0$ respectively if $k_B \rightarrow 0$ and $\hbar \rightarrow 0$.

Now we can note the indubitable remark that Planck's constant \hbar has an authentic classical analog represented by the Boltzmann's constant k_B , both \hbar and k_B having relevant significances as generic indicators of stochasticity. But such an analogy contradicts directly the basic precept **BP**₅ of CIUR doctrine and UR-QMS philosophy.

3.12 D_{12} : On the excessive ranking of UR

The ranking of UR to a position of principle, is widespread in the dominant literature, mainly through the authoritative and normative writings of many leading scientists. Surprisingly the respective ranking is argued merely in few occasions (e.g. in [10]) but only partially and not convincingly.

However, in [10], it was signaled the fact that “*over the years, some authors and foremost K. Popper, have contested this view, of such a ... ‘ranking’*”. The mentioned contestation seems to have been motivated by the assertion: “un-

certainty relations cannot be granted the status of a principle on the grounds that they are derivable from the theory (‘QM’), whereas one cannot obtain the theory from the uncertainty relations”. The aforesaid motivation was minimized and repudiated [10] through of the conventional (and prevalent) opinion that: “*there are many statements in physical theories which are called principles even though they are in fact derivable from other statements in the theory in question*”. Note that in spite of the mentioned repudiation, it was added in [10] the noteworthy observation that “*Serious attempts to build up quantum theory as a full-fledged Theory of Principle on the basis of the uncertainty principle have never been carried out*”.

As regards the above presented controversy our belief can be expressed as follows. The Popper's contestation of UR ranking (i.e., in fact, of the precept **BP**₆) has a genuine character while the opposing conventional opinion is nothing but a questionable (and unfounded) attempt to preserve a predominant traditionalist doctrine (dogma).

Now, from another perspective, we wish to point out a new important aspect. On the one hand a true scientific conception attests indubitably the idea that: “*A principle is statement which is taken to be true at all times and all places where it is applicable*” [85]. On the other hand all previously proved deficiencies **D**_{1–D}₁₁ show that usual philosophy of UR is not valid in a wide class of situations where they should to be applied. Therefore such a philosophy cannot provide (generate) a principle (fundamental concept) applicable in an unquestionable manner for a large area of situations. That is why it turns out to be totally unacceptable (and useless) the idea to raise the entire UR philosophy to a rank of fundamental principle for QM.

Consequently, the precept **BP**₆ shows oneself as being nothing but an unjustified thesis. At the same time, from a true scientific perspective, it is outside of acceptable usages to put in practice an idea such is [10]: “*we use the name “uncertainty principle” simply because it is the most common one in the literature*”.

4 Which is really the true significance of UR?

Summing all the discussions incorporated within deficiencies **D**_{1–D}₁₂ one can notify the following evident remarks:

- There are profound deficiencies regarding all the basic elements and precepts of the conventional conceptions (CIUR doctrine and UR-QMS philosophy).
- In their essence the respective deficiencies are unavoidable and insurmountable within own framework of respective conceptions.
- Consequently the mentioned conceptions prove themselves as being undoubtedly in a failure situation which impose their abandonment.

The above argued abandonment of conventional conceptions points out very clearly the indubitable ending of the ex-

isting prevalent philosophy about UR. But a fair evaluation of such an ending requires an adequate epilogue regarding the future scientific status of the respective philosophy and of its constitutive and associate concepts.

The alluded epilogue demands firstly, detailed re-evaluations of the generative relations (1) and (2) from which have been expanded themselves the mentioned philosophy and concepts. The respective re-evaluations have to be done and argued by taking into account all the aspects noted previously within the texts of deficiencies D_1 – D_{12} . Doing so one arrives to the following observations:

- Relation (1) is nothing but an old-fashioned (and removable) empirical convention. It persists as a piece of historical reminiscence, destitute of any wonderful status/significance for actual and future physics.
- Relation (2) proves to be only an ordinary QM formula, of well-defined (but not universal) validity. In such a posture it describes in a simple manner the connections between fluctuation characteristics of two quantum observables.
- In fact the relations (1) and (2) have not any crucial significance, for QM concretely and less so for physics in general.
- Relations (1) and (2) or their “adjustments” have not any connection with genuine descriptions of QMS.
- Particularly the respective relations do not depict in any way the so called “observer effect” (i.e. perturbing influence of “experimenter” on the investigated system).

5 Considerations on quantum measurements

Besides the main discussions about the meaning of early relations (1) and (2), the conventional UR philosophy generated also many collateral debates on Quantum Measurements (QMS) (see [1–12, 86–88] and references). The respective debates, still active in writings of many scientists, promoted an appreciable diversity of viewpoints about conceptual significance and practical importance of QMS. But in the same context, were recorded observations like is the following one

- “Despite long efforts, no progress has been made ... for ... the understanding of quantum mechanics, in particular its measurement process and interpretation” [89].

Nevertheless, beyond the mentioned debates, the respective subject of QMS involves also a matter of real interest for physics. That matter regards the natural interest in developing adequate theoretical description(s) for QMS, which should to be proved through viable arguments and which have to become of suitable utility for scientific and technical activities.

The above signaled situation have motivated interest for both conventional and non-conventional approaches of QMS problem. A modest non-conventional approach was put in work progressively in our investigations over many years (see

[17–20, 47, 55, 90–94]). Here, as well as in all sections of present article, we try to gather, extend, systematize and improve the results of mentioned investigations in order to present argued viewpoints about the main aspects of QMS matter.

5.1 D_{13} : The incorrect association of QMS with UR

As a first main aspect of the so much debated QMS problem is fact that it has a theoretical essence. Namely, it is focused around the idea of developing a general theoretical model for describing measurements on quantum systems. The respective model should have some similarity (a bit of reference) with the one centered on Schrödinger equation within QM.

From the perspective of the such supposed similarity most of publications promoted or accepted the opinion that QMS have a basic essentiality for QM in itself. During the years were recorded even assertions like the following one:

- ‘the description of QMS is “probably the most important part of the theory (QM)”’ [5].

But note that both the mentioned opinion and assertion are grounded on the belief that, mainly, the claimed essentiality/importance of QMS for QM is given by relations (1) and (2) in terms of precepts BP_1 – BP_6 .

On the other hand, it is easy to see that the respective belief is invalidated by the arguments from the entire collection of deficiencies D_1 – D_{12} notified by us above in Section 3.

Now, besides the aforesaid notifications, for starting our non-conventional approach of QMS subject, we take into account the following remarks of J. S. Bell:

- “I agree with what you say about the uncertainty principle: it has to do with the uncertainty in predictions rather the accuracy of ‘measurement’. **I think in fact that the word ‘measurement’ has been so abused in quantum mechanics that it would good to avoid it altogether**” (see [83] and Appendix I below).
- “... The word (‘measurement’) has had such a damaging effect on the discussions that ... it should be banned altogether in quantum mechanics” [84].

A similar account we give also to the next remark:

- “the procedures of measurement (comparison with standards) has a part which cannot be described inside the branch of physics where it is used”. [95]

The just noted remarks consolidate for us the following key view:

- The significance of UR is an intrinsic question of QM while the description of QMS constitutes an adjacent but distinct subject comparatively with QM in itself.

As another reference element for starting our approach we agree the following observation:

- “it seems essential to the notion of measurement that it answers a question about the given situation existing before the measurement. Whether the measurement leaves the measured system unchanged or brings about a new and different state of that system is a second and independent question” [96].

In sense of above observation for a measured physical system the “situation existing before the measurement” regards the intrinsic properties of that system. The characteristics of the respective properties play a role of input data (information) for measuring actions. On the other hand for the same system, the “answer (i.e. result) of measurement” is accumulated in “output data (information)” that are provided by measuring process. Correspondingly the whole measurement can be considered as a transmission process for information (stochastic data), while the measuring device appears as a communication channel (viewed as in [97]).

So the whole image of a measurement can be depicted through the scheme

$$\left| \begin{array}{c} \text{input} \\ \text{data} \end{array} \right\rangle \Rightarrow \left[\begin{array}{c} \text{communication} \\ \text{channel} \end{array} \right] \Rightarrow \left| \begin{array}{c} \text{output} \\ \text{data} \end{array} \right\rangle. \quad (24)$$

For giving concrete descriptions of the above scheme in cases of QMS (measurements on quantum systems) it should also take into view the next remark

- “To our best current knowledge the measurement process in quantum mechanics is non-deterministic” [89].

In such a view the mentioned input and output data as well the description of a QMS have to be presented by means of some non-deterministic (stochastic or random) entities. For a measured quantum system the totality of input data can be considered as being comprised in its specific (intrinsic) wave function Ψ_{in} , with known stochastic/probabilistic own significance. As regards the same system the output data should be represented by some quantities having also stochastic features. Formally, such quantities can be considered as being incorporated in an output wave function Ψ_{out} . Then the measuring process appear as communication channel which transposes the wave function from a Ψ_{in} reading into a Ψ_{out} image. So it can be suggested that, in case of a QMS, the scheme (24) can be represented through the following generic pattern:

$$\left| \begin{array}{c} \text{probabilistic} \\ \text{content of } \Psi_{in} \end{array} \right\rangle \Rightarrow [\widehat{SCC}] \Rightarrow \left| \begin{array}{c} \text{probabilistic} \\ \text{content of } \Psi_{out} \end{array} \right\rangle \quad (25)$$

where \widehat{SCC} , depicts the “Stochastic Communication Channel” regarded as an “operator” which describe the measuring process.

The above suggested pattern regarding QMS can be particularized for various concrete situations by using QM terminology. Two such particularization will be detailed below in the Subsections 5.2 and 5.4.

5.2 On an observable with discrete spectrum

Let us refer to the case of a QMS for a single quantum observable A endowed with a non-degenerate discrete spectrum of eigenvalues $\{a_j\}_{j=1}^n$. The respective observable is described by the operator \hat{A} which satisfy the equations $\hat{A}\varphi_j = a_j \cdot \varphi_j$, where $\{\varphi_j\}_{j=1}^n$ signify the corresponding eigenfunctions.

If the set of eigenfunctions $\{\varphi_j\}_{j=1}^n$ is regarded as an orthonormal basis the wave functions Ψ_{in} and Ψ_{out} can be represented as follows

$$\begin{aligned} \Psi_{in} &= \sum_{j=1}^n \alpha_j \varphi_j, & \sum_{j=1}^n |\alpha_j|^2 &= 1, \\ \Psi_{out} &= \sum_{k=1}^n \beta_k \varphi_k, & \sum_{k=1}^n |\beta_k|^2 &= 1. \end{aligned} \quad (26)$$

Then the the pattern (25) appears as a transformation of the corresponding probabilities from *in*-readings $\{|\alpha_j|^2\}_{j=1}^n$ into *out*-images $\{|\beta_k|^2\}_{k=1}^n$. According to mathematics (probability and information theories) the mentioned transformation (i.e.the operator \widehat{SCC}) can be depicted by means of a doubly stochastic matrix M_{kj} ($k, j = 1, 2, \dots, n$), interpreted as in [98]. Such a depiction has the form

$$|\beta_k|^2 = \sum_{j=1}^n M_{kj} \cdot |\alpha_j|^2 \quad (27)$$

where the matrix M_{jk} satisfies the conditions

$$\sum_{k=1}^n M_{kj} = \sum_{j=1}^n M_{kj} = 1.$$

As above described a QMS appear as being ideal respectively non-ideal, accordingly as $M_{kj} = \delta_{kj}$ or $M_{kj} \neq \delta_{kj}$, where δ_{kj} denotes a Kronecker delta.

By using (26) and (27) for the η -expected values $\langle A \rangle_\eta = (\Psi_\eta, \hat{A}\Psi_\eta)$, ($\eta = in, out$), of observable A one obtains

$$\langle A \rangle_{in} = \sum_{j=1}^n a_j \cdot |\alpha_j|^2, \quad (28)$$

$$\langle A \rangle_{out} = \sum_{k=1}^n a_k \cdot |\beta_k|^2 = \sum_{k=1}^n \sum_{j=1}^n a_k \cdot M_{kj} \cdot |\alpha_j|^2.$$

In terms of above notations the error for the expected value of A is:

$$\mathcal{E}\{\langle A \rangle\} = \langle A \rangle_{out} - \langle A \rangle_{in} = \sum_{k=1}^n \sum_{j=1}^n a_k \cdot (M_{kj} - \delta_{kj}) \cdot |\alpha_j|^2 \quad (29)$$

where δ_{jk} signifies a Kronecker delta.

Because, mathematically, the observable A is a random variable it is characterized also by the standard deviations

$\Delta_\eta A$ ($\eta = in, out$), defined as follows

$$\begin{aligned} (\Delta_{in}A)^2 &= \langle (A - \langle A \rangle_{in})^2 \rangle_{in} \\ &= \sum_{j=1}^n a_j^2 \cdot |\alpha_j|^2 - \left(\sum_{j=1}^n a_j \cdot |\alpha_j|^2 \right)^2 \\ (\Delta_{out}A)^2 &= \langle (A - \langle A \rangle_{out})^2 \rangle_{out} \\ &= \sum_{k=1}^n \sum_{j=1}^n a_k^2 \cdot M_{kj} \cdot |\alpha_j|^2 \\ &\quad - \left(\sum_{k=1}^n \sum_{j=1}^n a_k \cdot M_{kj} |\alpha_j|^2 \right)^2 \end{aligned} \tag{30}$$

So for error $\mathcal{E}\{\Delta A\}$ of standard deviation regarding the observable A one finds

$$\begin{aligned} \mathcal{E}\{\Delta A\} &= \Delta_{out}A - \Delta_{in}A \\ &= \sqrt{\sum_{k=1}^n \sum_{j=1}^n a_k^2 \cdot M_{kj} \cdot |\alpha_j|^2 - \left(\sum_{k=1}^n \sum_{j=1}^n a_k \cdot M_{kj} |\alpha_j|^2 \right)^2} - \\ &\quad \sqrt{\sum_{j=1}^n a_j^2 \cdot |\alpha_j|^2 - \left(\sum_{j=1}^n a_j \cdot |\alpha_j|^2 \right)^2}. \end{aligned} \tag{31}$$

Now note the fact that, to some extent, the above presented model of a QMS description has general features. This because, excepting the conditions of being doubly stochastic, the measuring matrix M_{kj} can consists of arbitrary components. The mentioned generality/arbitrariness should be reduced when one refers to the relatively accurate measurements. Such a reduction can be modeled if the measuring matrix elements M_{kj} are taken of the forms

$$\begin{aligned} M_{kj} &= \delta_{kj} + \tau_{kj}, \\ |\tau_{kj}| &\ll 1, \quad \sum_{k=1}^n \tau_{kj} = \sum_{j=1}^n \tau_{kj} = 0, \end{aligned} \tag{32}$$

where δ_{kj} signifies the a Kronecker delta and τ_{kj} are real and dimensionless quantities of (very) small values.

When the matrix elements M_{jk} are approximated as in (32) the errors $\mathcal{E}\{\langle A \rangle\}$ and $\mathcal{E}\{\Delta A\}$ from (29) and (31) can be estimated through a direct calculation, respectively by means of the first order term in Taylor series. Then one finds

$$\begin{aligned} \mathcal{E}\{\langle A \rangle\} &= \sum_{k=1}^n \sum_{j=1}^n a_k \cdot \tau_{kj} \cdot |\alpha_j|^2, \\ \mathcal{E}\{\Delta A\} &\approx \sum_{k=1}^n \sum_{j=1}^n \left[\frac{\partial \mathcal{E}(\tau_{kj})}{\partial \tau_{kj}} \right]_{\tau_{kj}=0} \cdot \tau_{kj}, \end{aligned} \tag{33}$$

where $\mathcal{E}(\tau_{kj})$ signifies the standard-deviation error $\mathcal{E}\{\Delta A\}$ from (31) in which one uses the approximations (32).

Relations (33) show that within mentioned approximations the parameters τ_{jk} appear as significant indexes regarding the measuring accuracies. So the discussed measurement

can be regarded as ideal when $\tau_{kj} = 0$ for all k and j , respectively as non-ideal when $\tau_{kj} \neq 0$ at least for some values of k or j .

5.3 D_{14} : On the measuring scenarios with a unique sampling

As it was pointed out in Subsection 5.1, a QMS is essentially a non-deterministic process. Due to the mentioned essentiality, the “result” of such a process must be represented in terms of some stochastic (probabilistic) output data. But, surprisingly, in conventional publications [99–106] a QMS is regarded as a scenario (i.e. an imagined sequence of possible events) conceived as a single sampling (i.e. as a unique-deterministic selection from a set of random data). So regarded, a QMS gives as its result (outcome) a single value in which falls (collapses) the whole physical content of the measured observable. The referred falling scenarios are illustrated by two widely debated themes regarding the Wave Function Collapse (WFC) [99–103] respectively the Schrödinger’s Cat Thought Experiment (SCTE) [104–106]. Historically, both the respective themes have occurred in a direct connection with the establishing of basic precepts BP_1 – BP_6 of CIUR doctrine and UR–QMS philosophy. Therefore, by taking into account the deficiencies of precepts BP_1 – BP_6 , revealed above in Section 3, it is here the place to investigate also the possible deficiencies of the aforesaid scenarios.

Let us begin the announced investigation by referring to the WFC-measuring-scenario. The respective scenarios germinated from the hypothesis that, due to unavoidable measuring perturbations, all QMS cause specific collapses (falls, jumps) in states of the measured quantum systems. It can be presented succinctly in usual terms of QM as follows.

Consider a measuring investigation focused on the system and observable A discussed in the previous Subsection 5.2. For the respective system in WFC-scenario the “situation existing before measurement” is inscribed in its intrinsic wave function Ψ_{in} . The probabilistic content of Ψ_{in} play the role of input data (information) for investigation actions. But, attention, within the WFC-scenario, the measuring actions are imagined as providing as result an **unique deterministic outcome (udo)** namely a_k .

Note that a_k is one of the eigenvalues $\{a_j\}_{j=1}^n$ from the spectrum of A . The eigenvalues $\{a_j\}_{j=1}^n$ are defined through the relations $\hat{A}\varphi_j = a_j \cdot \varphi_j$ ($j = 1, 2, \dots, n$), where $\{\varphi_j\}_{j=1}^n$ denote the eigenfunctions of operator \hat{A} associated to the observable A . Then, in terms detailed previously in Subsection 5.2, the whole WFC-scenario can be illustrated through the following two schemes

$$\left\{ \{a_j\}_{j=1}^n \cup \{|\alpha_j|^2\}_{j=1}^n \right\} \Rightarrow [\widehat{udo}] \Rightarrow a_k, \tag{34}$$

$$\left| \Psi_{in} = \sum_{j=1}^n \alpha_j \cdot \varphi_j \right\rangle \Rightarrow [\widehat{udo}] \Rightarrow \varphi_k, \quad (35)$$

where \widehat{udo} symbolize an operator which describe the measuring actions in WFC-scenario.

On the one hand, firstly, the schema (34) regards the measurement of observable A . It show a falling of the respective observable from a whole spectrum of values $\{a_j\}_{j=1}^n$, having probabilities $\{|\alpha_j|^2\}_{j=1}^n$ in measured state, to a unique value a_k as result of the scenario. Secondly, on the other hand, the schema (35) refers to the evolution of the considered system from a state “existing before the measurement” (at the beginning of scenario) in an “after measurement” state (in the end of scenario).

Specify here the fact that conventional publications (see [99–103] and references) regard relation (35) as being the essential symbol of WFC. That is why the mentioned publications tried to done analytical representations of the respective relation considered as image of a dynamical physical process. For such representations were promoted various inventions, e.g. nonlinear extensions of Schrödinger equation or even appeals to new kinds of fundamental physical constants.

The above mentioned WFC-scenario regarding QMS can be admonished through the following remarks.

Firstly note that quantum observables are stochastic variables. Consequently a true measurement of such an observable should be regarded as being provided not by an **udo** (unique deterministic outcome) but by an adequate probabilistic set of such outcomes. The data given by the respective set are expected to provide relevant (and as complete as possible) information about the considered observables.

Secondly, the idea of describing QMS through an analytical representation of the WFC schema (35) proves oneself as being an extravagance without solid arguments or credible hypotheses. Some main aspects of the respective extravagance can be revealed by taking into account the stochastic similitude between quantum and thermal (macroscopic) random observables. Such a reveal we point out here as follows.

Let us refer to a macroscopic thermodynamic system described in terms of phenomenological theory of fluctuations (see below the Appendix D). For simplicity the system will be considered to be characterized by a single macroscopic thermodynamic observable \mathbb{A} . Mathematically the macroscopic fluctuations of \mathbb{A} are accounted by a real random variable \mathcal{A} and described by the probability density $W = W(\mathcal{A})$. Through the before specified terms can be pointed out the analogy between measuring acts regarding the stochastic observables of quantum and macroscopic nature. An **udo**, specific to WFC-scenario, for a quantum observable was discussed succinctly above in connection with the relations (34) and(35). A completely similar **udo** regarding a macroscopic observable \mathbb{A} can be depicted as follows. By means of an **udo** for the variable \mathcal{A} one obtains a unique value say \mathcal{A}_0 .

Then for \mathbb{A} the respective **udo** can be illustrated through the following relations

$$|\mathcal{A} \in (-\infty, +\infty)\rangle \Rightarrow [\widehat{udo}] \Rightarrow \mathcal{A}_0, \quad (36)$$

$$|W(\mathcal{A})\rangle \Rightarrow [\widehat{udo}] \Rightarrow \delta(\mathcal{A} - \mathcal{A}_0), \quad (37)$$

where $\delta(X)$ denotes the Dirac’s δ -function of X .

In principle, the aspects of quantum and macroscopic observables, depicted by (34) and (35) respectively (36) and (37) are completely similar. Therefore the discussions regarding the two kinds of **udo** should be similarly too. But in the macroscopic case the relation (37) is not considered at all as illustrating a dynamic process. Moreover within the corresponding macroscopic studies there is no interest for giving an analytical representation (through some evolution equations) regarding a scenario of type (37). This even if for the investigation of macroscopic observables one can use in principle a subjacent description given by classical statistical mechanics. Then, by virtue of above noted similarity, it can be said that the quantum scenario (35) should be not considered as a dynamic process. Consequently the QM studies have to be not concerned about the analytical representation (by some evolution equations) of an **udo** as the one illustrated by (35). Such regards about the scenario (35) are required, with all the more, as QM is not complemented (until today) by any subjacent theory of sub-quantum essence. Furthermore, for a true physical approach, the result of the respective **udo** must be gathered together with the answers of a significant statistical group of many other akin **udo**. The respective answers should allow to find adequate probabilistic estimators of the investigated quantum observable.

Regarding the problem of QMS description, in the category of falling scenarios, along with the WFC idea one finds also the famous problem of SCTE (Schrödinger’s Cat Thought Experiment). The respective problem, known also as Schrödinger’s cat paradox, has retained the attention of many debates over the decades (see [104–106] and references). The essential element in SCTE is represented by a single decay of an individual radioactive atom (which, through some macroscopic machinery, kills an initially living cat). But the individual lifetime of a single decaying atom is a stochastic (random) variable. That is why the mentioned killing decay is in fact a twin analogue of the above mentioned **udo** taken into account by the WFC-scenario. So, the above considerations reveal the notifiable fact that, for a true evaluation of a stochastic observable (such is the mentioned decay lifetime), is worthlessly to operate with an **udo** which gives an unique result of measurement. Accordingly, the SCTE problem appears as a twin analogue of the IWFC-scenario, i.e. as a fiction (figment) without any real scientific value.

The aforesaid fictional character of the SCTE can be pointed out once more by observation [93, 94] that it is possible to imagine a macroscopic thought-experiment completely

analogous with the SCTE. Within the respective macroscopic analogue, a cousin of Schrödinger's cat can be killed through launching a single macroscopic ballistic projectile. More specifically, the killing machinery is activated by an uncontrollable (unobservable) sensor located within the "circular error probable" (CEP) [109] of a ballistic projectile trajectory. The hitting point of the projectile is expected to arrive within CEP with the probability 50%. That is why the murderous action of a single launched projectile is just as much unpredictable as that of the unique radioactive atom within original SCTE. Therefore, the mentioned macroscopic analogy makes clear once more the fictional character of the SCTE.

According to the above-noted remarks, it should be regarded as worthless statements some assertions such as: "*The Schrödinger's cat thought experiment remains a defining touchstone for modern interpretations of quantum mechanics*" [106]. Note that such or similar assertions can be found in many popular publications or in the texts disseminated via the Internet (e.g. [110]).

Therefore SCTE problem as well as its similar WFC idea, discussed previously, prove themselves to be not real scientific topics but rather useless exercises (fictive scenarios), without any conceptual or practical significance.

5.4 About observables with continuous spectra

As it was noted in the beginning of this Section 5, for physics, development of suitable models for QMS description present a natural necessity. Above, in Subsection 5.2 of this article, it is detailed such a model regarding the measurement of an observable endowed with a discrete non-degenerate spectra. Here below we try to propose a measuring model with similar purpose (QMS description) but regarding observables having continuous spectra of values.

As in case with discrete spectrum for here regarded measuring situation we adopt the same generic pattern depicted in (25). The probabilistic content of wave functions Ψ_{in} and Ψ_{out} incorporate information (data) about the intrinsic state of the measured system respectively concerning the results provided by measurement. We will restrict our considerations to the measurements of orbital characteristics for a quantum spin-less micro-particle, supposed in a unidirectional motion along the x -axis. Note that the announced considerations can be easily extended for measurements regarding systems with spatial orbital motions. Then the wave functions Ψ_η ($\eta = in, out$) will be taken of the form $\Psi_\eta = \Psi_\eta(x)$ (note that here we omit to specify the time t as visible variable because the considered state of system refers to a given ante-measurement instant).

Note now the fact that according QM rules the wave functions Ψ_η have only significance of probability amplitudes but not a direct probability meaning. Therefore, in the case of interest here, the picture (25) of QMS should be detailed not in terms of wave functions Ψ_η , but by means of some entities

with direct probabilistic meanings. This especially because the real measuring devices report the occurrence of some random values for investigated observables. In usual terms of QM entities with direct probabilistic significance are carriers of stochasticity: probability densities ρ_η and probability currents j_η ($\eta = in, out$). Let us write the wave functions Ψ_η as $\Psi_\eta(x) = |\Psi_\eta(x)| \cdot \exp\{i\Phi_\eta(x)\}$. Then, for a micro-particle with mass m considered as measured system, the alluded ρ_η and j_η are given by relations:

$$\begin{aligned}\rho_\eta &= \rho_\eta(x) = |\Psi_\eta(x)|^2, \\ j_\eta &= j_\eta(x) = \frac{\hbar}{m} |\Psi_\eta(x)|^2 \cdot \nabla_x \Phi_\eta(x),\end{aligned}\quad (38)$$

where $\nabla_x = \frac{\partial}{\partial x}$.

Now it must to specify that ρ_η and j_η refer to the positional and the motional kinds of probabilities respectively. Experimentally the two kinds can be regarded as measurable by distinct devices and procedures. The situation is similar with that of electricity studies where the aspects regarding position and mobility of electrical charges are evaluated through completely different devices and procedures. Due to the aforesaid specifications it results that in fact the generic pattern depicted in (25) has to be amended as follows

$$|\rho_{in}(x) \cup j_{in}(x)\rangle \Rightarrow [\widehat{SCC}] \Rightarrow [\rho_{out}(x) \cup j_{out}(x)]. \quad (39)$$

Mathematical considerations about the relations (25) and (E.1), (early referred also in [107]) can be applied by similarity for the pattern (39). So the respective pattern (i.e. the operator \widehat{SCC}) can be represented through the next two transformations:

$$\begin{aligned}\rho_{out}(x) &= \int_{-\infty}^{+\infty} \Gamma(x, x') \cdot \rho_{in}(x') \cdot dx', \\ j_{out}(x) &= \int_{-\infty}^{+\infty} \Lambda(x, x') \cdot j_{in}(x') \cdot dx' .\end{aligned}\quad (40)$$

Here $\Gamma(x, x')$ and $\Lambda(x, x')$ represent the corresponding doubly stochastic kernels (in sense defined in [108]). This means that the kernels $\mathfrak{K} = \{\Gamma, \Lambda\}$ satisfy the following relations $\int_{-\infty}^{+\infty} \mathfrak{K}(x, x') dx = \int_{-\infty}^{+\infty} \mathfrak{K}(x, x') dx' = 1$. The mentioned kernels incorporate some extra-QM elements regarding the characteristics of measuring devices and procedures. Such elements do not belong to the usual QM framework which refers to the intrinsic (own) characteristics of the measured micro-particle (system).

Through the above considerations can be evaluated the effects induced by QMS. The respective effects regards the probabilistic estimators for orbital observables A_j of considered quantum system. Such observables are described by the

operators \hat{A}_j ($j = 1, 2, \dots, n$). As in case of classical measuring model (see the Appendix E), without any loss of generality, here one can suppose that the quantum observables have identical spectra of values in both *in*-and *out*-situations. In terms of QM the mentioned supposition means that the operators \hat{A}_j have the same mathematical expressions in both *in*-and *out*-readings, i.e. that the respective expressions remain invariant under the transformations which describe QMS. In the here discussed case of a system with rectilinear orbital motion the mentioned expressions depend on x and ∇_x .

So one can say that in the situations associated with the wave functions $\Psi_\eta = \Psi_\eta(x)$ ($\eta = in, out$) the mentioned quantum observables A_j , can be characterized by the following lower order estimators (or numerical parameters): mean values $\langle A_j \rangle_\eta$, correlations $C_\eta(A_j, A_k)$ and standard deviations $\Delta_\eta A_j$. We use the common notation (f, g) for scalar product of functions f and g , i.e. $(f, g) = \int_{-\infty}^{+\infty} f^*(x) \cdot g(x) \cdot dx$. Then the mentioned estimators are defined by the relations

$$\begin{aligned} \langle A_j \rangle_\eta &= (\Psi_\eta, \hat{A}_j \Psi_\eta), & \delta_\eta \hat{A}_j &= \hat{A}_j - \langle A_j \rangle_\eta, \\ C_\eta(A_j, A_k) &= (\delta_\eta \hat{A}_j \Psi_\eta, \delta_\eta \hat{A}_k \Psi_\eta), & & \\ \Delta_\eta A_j &= \sqrt{C_\eta(A_j, A_j)}. \end{aligned} \tag{41}$$

Note here the fact that, on the one hand, the *in*-version of discussions the estimators (41) are calculated by means of the wave function Ψ_{in} . The respective function is supposed as being known from the considerations about the intrinsic properties of the investigated system (e.g. by solving the corresponding Schrödinger equation).

On the other hand, apparently, the evaluation of estimators (41) in $\eta = out$ -version requires to operate with the wave function Ψ_{out} . But the respective appearance can be surpassed [20] through operations which use the probability density ρ_{out} and current j_{out} . So if an operator \hat{A}_j does not depend on $\nabla_x = \frac{\partial}{\partial x}$, i.e. $\hat{A}_j = \hat{A}_j(x)$, in evaluating the scalar products from (41) can be used the evident equality $\Psi_{out}^* \hat{A}_j \Psi_{out} = \hat{A}_j \cdot \rho_{out}$. Additionally, when \hat{A}_j depends on $\nabla_x = \frac{\partial}{\partial x}$, i.e. $\hat{A}_j = \hat{A}_j(\nabla_x)$, in the same products the expressions of the type $\hat{A}_j(\nabla_x) \Psi_{out}(x)$ can be converted in terms of $\rho_{out}(x)$ and $j_{out}(x)$. Namely from (38) one finds directly:

$$\begin{aligned} \nabla_x |\Psi_{out}(x)| &= \nabla_x \sqrt{\rho_{out}(x)}, \\ \nabla_x \Phi_{out}(x) &= \frac{m}{\hbar} \frac{j_{out}(x)}{\rho_{out}(x)}. \end{aligned} \tag{42}$$

By a single or repeated application of these formulas, any expression of type $\hat{A}_j(\nabla_x) \Psi_{out}(x)$ can be transcribed in terms of ρ_{out} and j_{out} .

The aforesaid discussion should be supplemented by specifying some indicators able to characterize the errors (uncertainties) of considered QMS. For the above quoted observ-

ables A_j such indicators are the following ones:

$$\left. \begin{aligned} \mathcal{E}\{\langle A_j \rangle\} &= \langle A_j \rangle_{out} - \langle A_j \rangle_{in} \\ \mathcal{E}\{C(A_j, A_k)\} &= C_{out}(A_j, A_k) - C_{in}(A_j, A_k) \\ \mathcal{E}\{\Delta A_j\} &= \Delta_{out} A_j - \Delta_{in} A_j \end{aligned} \right\} \tag{43}$$

The above presented model regarding the description of QMS for observables with continuous spectra is illustrated on a simple example in the Appendix G below.

6 Some concluding remarks

The present paper was motivated by the existence of many unclearnesses (unfinished controversies and unelucidated questions) about the prevalent UR–QMS philosophy. It was built as a survey on deficiencies of respective philosophy. So were re-evaluated the main ideas claimed within the mentioned philosophy. The basic results of the respective re-evaluations can be summarized through the following **Concluding Remarks (CR)**:

- **CR₁**: Firstly, through multiple arguments, we have proved the observation that the UR (1) and (2) have not any essential significance for physics. Namely the respective UR are revealed as being either old-fashioned, short-lived (and removable) conventions (in empirical, thought-experimental justification) or simple (and limited) mathematical formulas (in theoretical vision). But such an observation comes to advocate and consolidate the Dirac’s intuitive prediction [23]: “*I think one can make a safe guess that uncertainty relations in their present form will not survive in the physics of future*”. Note that the respective prediction was founded not on some considerations about the UR essence but on an intuition about the future role in physics of Planck’s constant \hbar . Dirac predicted that \hbar will become a derived (secondary) quantity while c and e will remain as fundamental constants ($c =$ speed of light and $e =$ elementary electric charge). ■

- **CR₂**: A significant idea that emerges from previous discussions is the one that neither UR (1) and (2) nor various “generalizations” of them, have not any connection with genuine descriptions of Quantum measurements (QMS). All the respective descriptions should be considered as a distinct (and additional) subject which must be investigated separately but somewhat in association with QM. Examples of such description are presented briefly, in Subsection, 5.2 and 5.4, for observables having discrete respectively continuous spectra. ■

- **CR₃**: Note that, in all of their aspects, the discussions from Subsection 5.2 and 5.4 have a theoretical essence. This means that, the entities like wave function Ψ_{in} as well as the measuring indicators M_{jk} , $\Gamma(x, x')$ and $\Lambda(x, x')$, are nothing but abstract concepts which enable elaboration of theoretical models regarding the descriptions of QMS. On the one hand Ψ_{in} refers to the intrinsic data about the studied system. It is

evaluated by means of some known theoretic procedures (e.g. by means of the corresponding Schrödinger equation). On the other hand the indicators M_{jk} , $\Gamma(x, x')$ and $\Lambda(x, x')$ are introduced as theoretical entities for modeling the characteristics of the considered measuring devices/processes. ■

• **CR₄**: Correlated with the previous **CR₂** and **CR₃** it must be specified that, in relation with QMS, the inventions of Wave Function Collapse (WFC) and Schrödinger's Cat Thought Experiment (SCTE) are nothing but unnatural falling scenarios. Consequently, as we have argued above in Subsections 5.3, both idea of WFC and SCTE problem prove themselves as being not real scientific subjects but rather unnecessary figments. ■

• **CR₅**: It is interesting to note here the fact that the history of quantum mechanics was abounded by an impressive number of publications related to UR–QMS philosophy. So, for the years between 1935 and 1978, as regards EPR (Einstein-Podolsky-Rosen) paradox, associated [112] with the situation of non-commuting observables, some authors [113] noted that “ $\geq 10^6$ papers have been written” — i.e. ≥ 63 papers per day (!?). Also the same publishing abundance about QM matters (including UR–QMS philosophy) motivates remarks such as the following ones: “*A theory whose formalism can be written down on a napkin whilst attempts to interpret it fill entire libraries. A theory that has seen astonishing experimental conformation yet leaves us increasingly perplexed the more we think about it. How can we know so well how to apply this theory but disagree so vehemently about what it is telling us?*” [114]. Probably that, in some future, the alluded abundance will be investigated from historic and sociological perspectives.

• **CR₆**: Over the years original UR (1) and (2) were supplemented with many kinds of “generalizations” (see [115–120] and references). Until today, the respective “generalizations” appear as being de facto only extrapolation mathematical “constructs” (often of impressive inventiveness). As a rule, they are not pointed out as having significance for some concrete physical questions (of conceptual or experimental relevance). But the existence of such significance is absolutely necessary in order to associate the mentioned “generalizations” with matters of certain importance for physics. In the light of the discussions from the present paper one can say that the sole physical significance of some from the referred “generalizations” seems to be their meaning as quantitative indicators of fluctuations (i.e. of stochasticity). But from a practical perspective among the respective indicators of practical usage are only the ones of relative lower order. Therefore, for tangible interests of physics, all the discussed “generalizations” seem to be rather excessive pieces. They remain only as interesting mathematical “constructs”, which ignore the desideratum: “*Entities are not to be multiplied beyond necessity*”. ■

• **CR₇**: In discussions and revaluations proposed in this article, we have referred only to the prevalent philosophy of

UR and QMS regarding primarily the foundations and interpretation of QM. But, as it is known, the mentioned philosophy has been extrapolated in other “extra muros” domains, outside of QM. As aforesaid domains can be quoted the following ones: mathematical computations, biology and medical sciences, economy and finance, human behavior, social sciences and even politics. A relevant bibliography regarding the mentioned extramural extrapolations can be accessed easy via internet from Google sites. Note that our above reevaluations of UR–QMS philosophy do not contain analyzes referring to the mentioned extrapolations. Such analyzes remain as task for scientists working in the respective domains. Here we want to point out only one noticeable aspect that differentiates the extramural UR from the primary ones. On the one hand, according to their origin, the primary UR from QM are strongly associated with a cardinal marker represented by the Planck constant \hbar . On the other hand, as far as we know, for extramural extrapolations of UR, the existence of similar markers, represented by cardinal indicators of the corresponding scientific domains, were not reported. ■

• **CR₈**: In their essence, the above argued revaluations of UR and QMS, do not disturb in any way the basic framework of usual QM. This means that QM keeps its known specific elements: concepts (wave functions, operators) with their significances (of stochastic essence), principles and theoretical models (Schrödinger equation), computing rules (exact or approximate) and investigate systems (atoms, molecules, mesoscopic structures). Note here the observation that, for nowadays existing quantum debates, the above revaluations of UR–QMS, offer a few arguments for lucrative parsimony in approaches of matters. The unlucrative aspects of those debates have to be reconsidered too, probably in more or less speculative visions. We recall here that the basic framework of QM can be deduced [121] from direct physical considerations, without appeals to ambiguous discussions about UR or QMS. The alluded considerations start from real physical facts (particle-wave duality of atomic size systems). Subsequently they use the continuity equations for genuine probability density and current. After that one obtains the whole framework of QM (i.e. the Schrödinger equation, expressions of operators as descriptors of quantum observables and all the practical rules of QM regarded as a theoretical model for the corresponding investigated systems).

In the mentioned perspective, we dare to believe that, to some extent, the revaluations of UR and QMS promoted by us can give modest support for genuine reconsiderations regarding the interpretation and foundations of QM. ■

Appendices

A: A brief compendium of some QM elements

Here we remind briefly some significant elements, selected from the usual theoretical framework [5, 29, 30] of Quantum Mechanics (QM). In this appendix we use Traditional Nota-

tions (TN), taken over from mathematical algebra developed long before QM appeared. Few specifications about the more recent Dirac's bracket formalism are given in Appendix B.

So, in terms of TN, we consider a QM micro-particle whose state (of orbital nature) is described by the wave function Ψ . Two observables A_j ($j = 1, 2$) of the respective particle will be described by the operators \hat{A}_j . The notation (f, g) will be used for the scalar (inner) product of the functions f and g . Correspondingly, the quantities $\langle \hat{A}_j \rangle_\Psi = (\Psi, \hat{A}_j \Psi)$ and $\delta_\Psi \hat{A}_j = \hat{A} - \langle \hat{A}_j \rangle_\Psi$ will depict the mean (expected) value respectively the deviation-operator of the observable A_j regarded as a random variable. Then, by denoting two observables with $A_1 = A$ and $A_2 = B$, one can be written the following formula:

$$\begin{aligned} (\delta_\Psi \hat{A} \Psi, \delta_\Psi \hat{A} \Psi) \cdot (\delta_\Psi \hat{B} \Psi, \delta_\Psi \hat{B} \Psi) &\geq \\ &\geq \left| (\delta_\Psi \hat{A} \Psi, \delta_\Psi \hat{B} \Psi) \right|^2 \end{aligned} \quad (A.1)$$

which is nothing but a relation of Cauchy-Schwarz type from mathematics.

For an observable A_j considered as a random variable, in a mathematical sense, the quantity $\Delta_\Psi A_j = (\delta_\Psi \hat{A}_j \Psi, \delta_\Psi \hat{A}_j \Psi)^{1/2}$ signifies its standard deviation. From (A.1) it results directly that the standard deviations $\Delta_\Psi A$ and $\Delta_\Psi B$ of the mentioned observables satisfy the formula

$$\Delta_\Psi A \cdot \Delta_\Psi B \geq \left| (\delta_\Psi \hat{A} \Psi, \delta_\Psi \hat{B} \Psi) \right|. \quad (A.2)$$

This last formula, with quantities $\Delta_\Psi A$ and $\Delta_\Psi B$ regarded together, play an influential role in QM debates within UR and QMS philosophy. That is why the relation (A.2) can be called *Cauchy-Schwarz Quantum Formula* (CSQF). Note that formulas (A.1) and (A.2) are always valid, i.e. for all observables, particles and states. Therefore they must be considered as primary QM formulas.

For the discussions regarding the UR-QMS philosophy it is helpful to present the particular versions of formula (A.1) in the cases when the operators $\hat{A} = \hat{A}_1$ and $\hat{B} = \hat{A}_2$ satisfy the conditions

$$\text{iff} : (\hat{A}_j \Psi, \hat{A}_k \Psi) = (\Psi, \hat{A}_j \hat{A}_k \Psi), \quad (j, k = 1, 2) \quad (A.3)$$

(where iff \equiv if and only if). In the alluded cases it is true the next formula

$$\begin{aligned} (\delta_\Psi \hat{A} \Psi, \delta_\Psi \hat{B} \Psi) &= \frac{1}{2} (\Psi, \{ \delta_\Psi \hat{A}, \delta_\Psi \hat{B} \} \Psi) \\ &\quad - \frac{i}{2} (\Psi, i [\hat{A}, \hat{B}] \Psi). \end{aligned} \quad (A.4)$$

Here $\{ \hat{A}, \hat{B} \} = \hat{A} \hat{B} + \hat{B} \hat{A}$ and $[\hat{A}, \hat{B}] = \hat{A} \hat{B} - \hat{B} \hat{A}$ signify the anti-commutator respectively commutator of the operators \hat{A} and \hat{B} . Now note the fact that the two terms from the right hand side of (A.4) are purely real and strictly imaginary quantities respectively. Therefore in the mentioned cases from (A.2)

follows directly the enlarged inequality

$$\begin{aligned} (\Delta_\Psi A)^2 \cdot (\Delta_\Psi B)^2 &\geq \frac{1}{4} \left| \langle \{ \delta_\Psi \hat{A}, \delta_\Psi \hat{B} \} \rangle_\Psi \right|^2 \\ &\quad + \frac{1}{4} \left| \langle [\hat{A}, \hat{B}] \rangle_\Psi \right|^2. \end{aligned} \quad (A.5)$$

Sometimes this relation is referred to as the Schrödinger inequality. It imply subsequently the next two truncated inequalities

$$\Delta_\Psi A \cdot \Delta_\Psi B \geq \frac{1}{2} \left| \langle \{ \delta_\Psi \hat{A}, \delta_\Psi \hat{B} \} \rangle_\Psi \right|, \quad (A.6)$$

$$\Delta_\Psi A \cdot \Delta_\Psi B \geq \frac{1}{2} \left| \langle [\hat{A}, \hat{B}] \rangle_\Psi \right|. \quad (A.7)$$

One observes that (A.7) is nothing more than the conventional Robertson-Schrödinger relation (2), commonly quoted in the literature of CIUR doctrine and UR-QMS philosophy. Note that in the respective literature besides the relation (2)/(A.7) sometimes the formula (A.5) is also mentioned. But, as a fact, the respective mention is not accompanied with the important specification that formula (A.5) is valid iff (if and only if) the condition (A.3) is fulfilled.

In the end of this appendix we note the cases of more than two observables, i.e. for a set A_j ($j = 1, 2, \dots, n; n \geq 3$), when the quantities $\alpha_{jk} = (\delta_\Psi \hat{A}_j \Psi, \delta_\Psi \hat{A}_k \Psi)$ constitute the components of a positive semi definite matrix. In such cases, similarly with (A.1), are true the formulas

$$\det \left[(\delta_\Psi \hat{A}_j \Psi, \delta_\Psi \hat{A}_k \Psi) \right] \geq 0; \quad (j, k = 1, 2, \dots, n) \quad (A.8)$$

where $\det [\alpha_{jk}]$ is the determinant whose components are the quantities α_{jk} .

Note that within dominant publications promoted by the UR-QMS philosophy the interpretation of many-observable relations (A.8) is frequently omitted. The omission is due most probably to the fact that the idea of referring to simultaneous measurements for more than two observables is not supported convincingly by the current practice of experimental physics.

Addendum

Sometimes, in QM practice, a wave function Ψ is represented as a superposition of the form

$$\Psi = \sum_n \alpha_n \cdot \varphi_n, \quad \sum_n |\alpha_n|^2 = 1, \quad (A.9)$$

where $\{ \varphi_n \}$ denote a complete set of orthonormal basic functions for which $(\varphi_n, \varphi_m) = \delta_{nm} =$ a Kronecker delta.

Then, in a state described by Ψ , the mean value of an observable A is written as

$$\langle A \rangle_\Psi = \sum_{n,m} \alpha_n^* \cdot A_{nm} \cdot \alpha_m, \quad A_{nm} = (\varphi_n, \hat{A} \varphi_m), \quad (A.10)$$

with A_{nm} indicating the matrix elements of operator \hat{A} in representation given by $\{\varphi_n\}$.

When $\{\varphi_n\}$ are eigenfunctions of \hat{A} the following formulas can be written

$$\hat{A} \varphi_n = a_n \cdot \varphi_n, \quad \langle A \rangle_\Psi = \sum_n |\alpha_n|^2 \cdot a_n, \quad (\text{A.11})$$

where a_n signify the eigenvalue of \hat{A} in respect with the eigenfunction φ_n .

Note that the notations and formulas reminded in this Addendum can be used in connection with all quantities discussed above in present Appendix.

B: On the omission of conditions (A.3) within current literature

The mentioned omission is encountered in many generally agreed publications on QM (especially in textbooks, e.g. in [29]). It appears when the conventional Robertson-Schrödinger relation (A.7) is established by starting from the correct formula

$$\left\| \left((\delta_\Psi \hat{A} + i\lambda \delta_\Psi \hat{B}) \Psi \right) \right\| \geq 0 \quad (\text{B.1})$$

for the norm $\|f\|$ of function $f = (\delta_\Psi \hat{A} + i\lambda \delta_\Psi \hat{B}) \Psi$. In (B.1) are used the notations presented in the previous Appendix A and λ denote a real and arbitrary parameter. In order to go on from this last formula to the relation (A.5), it is presumed the equality

$$\begin{aligned} & \left((\delta_\Psi \hat{A} + i\lambda \delta_\Psi \hat{B}) \Psi, (\delta_\Psi \hat{A} + i\lambda \delta_\Psi \hat{B}) \Psi \right) = \\ & \left(\Psi, (\delta_\Psi \hat{A})^2 \Psi \right) + \lambda^2 \left(\Psi, (\delta_\Psi \hat{B})^2 \Psi \right) \\ & - i\lambda \left(\Psi, [\hat{A}, \hat{B}] \Psi \right). \end{aligned} \quad (\text{B.2})$$

Then, due to the fact that λ is a real and arbitrary quantity, from (B.1) it results the relation

$$\left\langle (\delta_\Psi \hat{A})^2 \right\rangle_\Psi \cdot \left\langle (\delta_\Psi \hat{B})^2 \right\rangle_\Psi \geq \frac{1}{4} \left| \left\langle [\hat{A}, \hat{B}] \right\rangle_\Psi \right|^2. \quad (\text{B.3})$$

In terms of notations from Appendix A this last relation gives directly the formula

$$\Delta_\Psi A \cdot \Delta_\Psi B \geq \frac{1}{2} \left| \left\langle [\hat{A}, \hat{B}] \right\rangle_\Psi \right| \quad (\text{B.4})$$

which is nothing but the relation (A.7) from the previous Appendix.

Observation: Note here the next two aspects: (i) Introduction of (B.4) demands with necessity the existence of equality (B.2), (ii) The respective equality is true only when the operators \hat{A} and \hat{B} satisfy the conditions (A.3). The noted aspects must be signalized as omissions of the current literature.

Another context in which appears the omission of conditions (A.3) is connected with the “braket notation” frequently used in QM literature. Within the respective notation, known

also as *Dirac’s Notation* (DN), the scalar (inner) product of two functions f and g is depicted as $\langle f | g \rangle$ (see [29–31]). Of course DN was used in many texts regarding UR–QMS philosophy. But it must be pointed out the fact that in those texts the condition (A.3), justified in the previous Appendix, is totally omitted and its implications are not analyzed at all. It is easy to notice that such an omission is due to the fact that, within the DN, both terms (from left-hand and right-hand sides) of the condition (A.3) have the same transcription, namely:

$$\begin{aligned} & \left(\hat{A}_j \Psi, \hat{A}_k \Psi \right) = \left\langle \Psi \left| \hat{A}_j \hat{A}_k \right| \Psi \right\rangle \\ & \text{and} \\ & \left(\Psi, \hat{A}_j \hat{A}_k \Psi \right) = \left\langle \Psi \left| \hat{A}_j \hat{A}_k \right| \Psi \right\rangle. \end{aligned} \quad (\text{B.5})$$

Obviously, such transcriptions create confusion and obstruct the just consideration of the condition (A.3) for cases where it is absolutely necessary in debates about UR–QMS philosophy. In order to avoid the above mentioned confusion in [32] we suggested that DN to be replaced by an Improved Dirac Notation (IDN). For such an IDN we proposed, that within scalar product of two functions f and g , to insert additionally the symbol “•” so that the respective product to be depicted as $\langle f | \bullet | g \rangle$. In such a way it becomes directly visible the separation of the entities implied in that product. Then, inside of IDN, the two terms from (A.3) are transcribed as

$$\begin{aligned} & \left(\hat{A}_j \Psi, \hat{A}_k \Psi \right) = \left\langle \Psi \left| \hat{A}_j \bullet \hat{A}_k \right| \Psi \right\rangle \\ & \text{and} \\ & \left(\Psi, \hat{A}_j \hat{A}_k \Psi \right) = \left\langle \Psi \left| \bullet \hat{A}_j \hat{A}_k \right| \Psi \right\rangle \end{aligned} \quad (\text{B.6})$$

Now one observes that in terms of IDN the condition (A.3) appears in the form

$$\text{iff} \quad \langle \Psi | \hat{A}_j \bullet \hat{A}_k | \Psi \rangle = \langle \Psi | \bullet \hat{A}_j \hat{A}_k | \Psi \rangle \quad (\text{B.7})$$

which no longer generates confusions in discussions about UR–QMS philosophy.

C: Classical “uncertainty relations” in Fourier analysis

In classical mathematical harmonic analysis it is known a relation (often named theorem) which, in terms of here used notations, is similar with the quantum UR depicted by relation (2). Through current mathematical representations the respective relation can be introduced as follows.

Let be a pair of variables x and ξ , with domains $x \in (-\infty, +\infty)$ and $\xi \in (-\infty, +\infty)$, regarded as arguments of a function $f(x)$ respectively of its Fourier transform

$$\tilde{f}(\xi) = \int_{-\infty}^{+\infty} \exp(-2i\pi\xi \cdot x) \cdot f(x) \cdot dx. \quad (\text{C.1})$$

If the norm $\|f\|$ of $f(x)$ has the property $\|f\| = 1$, both $|f(x)|^2$ and $|\tilde{f}(\xi)|^2$ are probability density functions for x and ξ regarded as real random (stochastic) variables. The variances

of such variables, evaluated through the corresponding probabilities, can be noted as $\langle(x - \langle x \rangle)^2\rangle$ and $\langle(\xi - \langle \xi \rangle)^2\rangle$. The respective variances express the effective widths of functions $f(x)$ and $\tilde{f}(\xi)$. Then [66] the aforesaid relation/theorem is given by the formula

$$\langle(x - \langle x \rangle)^2\rangle \cdot \langle(\xi - \langle \xi \rangle)^2\rangle \geq \frac{1}{16\pi^2}. \tag{C.2}$$

In mathematics this formula express the fact that: “A nonzero function and its Fourier transform cannot both be sharply localized” [66].

Often formula (C.2) is transcribed in a equivalent variant as follows

$$\Delta x \cdot \Delta \xi \geq \frac{1}{4\pi} \tag{C.3}$$

where Δx and $\Delta \xi$ denote the corresponding standard deviations of x and ξ , defined through conventions like $\Delta x = \sqrt{\langle(x - \langle x \rangle)^2\rangle}$. In non-quantum physics a version of relation (C.3) appears in studies of classical signals (waves of acoustic or electromagnetic nature) where $x = t = \text{time}$ and $\xi = \nu = \text{frequency}$. The respective version is written as

$$\Delta t \cdot \Delta \nu \geq \frac{1}{4\pi} \tag{C.4}$$

and it is known [67] as “Gabor’s uncertainty relation”. This last relation (C.4) means the fact that, for a classical signal (regarded as a wave packet), the product of the “uncertainties” (“irresolutions”) Δt and $\Delta \nu$ in time and frequency domains cannot be smaller than a specific constant.

Formally the classical relation (C.3) can be transposed to the case of “quantum wave packets” often discussed in introductory/intuitive texts about QM. Such a transposition focuses on the pairs of conjugated observables $q-p$ (coordinate-momentum) respectively $t-E$ (time-energy). The corresponding transpositions can be obtained by setting in (C.4) the substitutions $x = q$ and $\xi = p(2\pi\hbar)^{-1}$ respectively $x = t$ and $\xi = E(2\pi\hbar)^{-1}$. The substitutions of variable ξ are nothing but the so called duality relations (regarding the wave-particle connections). By means of the mentioned substitutions from (C.4) one finds the following two relations

$$\Delta q \cdot \Delta p \geq \frac{\hbar}{2} \quad \text{respectively} \quad \Delta t \cdot \Delta E \geq \frac{\hbar}{2}. \tag{C.5}$$

These last formulas are similar with the conventional UR (2) for the pairs of observables $q-p$ respectively $t-E$. Note that the mentioned similarity is admissible iff (if and only if) one accepts the conventions $|\langle[\hat{q}, \hat{p}]\rangle_\Psi| = \hbar$ and $|\langle[\hat{t}, \hat{E}]\rangle_\Psi| = \hbar$. But attention, the last convention has no more than a “metaphoric” value. This because in usual QM framework the time t is a deterministic but not random (stochastic) variable and, genuinely, for the respective framework a *time operator* \hat{t} is nothing but a senseless and fictitious concept (see also the discussions from the deficiency \mathbf{D}_8).

Note that the classical relation (C.3) can be transposed also in another quantum formula regarding the ground state of a Quantum Torsion Pendulum (QTP) (see Subsection 3.6.2). For respective transposition in (C.3) it should to take $f(x) = \Psi(\varphi)$, $x = \varphi$ and $\xi = L_z \cdot (2\pi\hbar)^{-1}$. So one obtains the formula

$$\Delta \varphi \cdot \Delta L_z \geq \frac{\hbar}{2} \tag{C.6}$$

which is nothing but the lowest level version of the last of formulas (13)

Addendum

It is worth to mention here the fact that, in the Fourier analysis, the x -unlimited relations (C.3) and (C.4) have correspondent formulas in x -limited cases (when the variable x has a finite domain of existence). The respective fact can be evidenced as follows.

Let be $x \in [0, b]$, with b a finite quantity and function $f(x)$ having the property $f(0) = f(b-0) := \lim_{x \rightarrow b-0} f(x)$. Then the quantities

$$c_n = \frac{1}{\sqrt{b}} \int_0^b \exp(-ik_n x) \cdot f(x) \cdot dx \tag{C.7}$$

represent the Fourier coefficients of $f(x)$, with $k_n = n \cdot \frac{2\pi}{b}$ and n denoting integers i.e. $n \in \mathbb{Z}$.

Moreover if the measure $|f(x)|^2 dx$ denotes the infinitesimal probability for $x \in (x, x+dx)$ the quantity $|c_n|^2$ signify the discrete probability associated to the value k_n . Then for functions $A = A(x)$ and $B = B(k_n)$, depending on x respectively on k_n , the mean (expected) values $\langle A \rangle$ and $\langle B \rangle$ are written as follows

$$\langle A \rangle = \int_0^b A(x) \cdot |f(x)|^2 dx, \tag{C.8}$$

$$\langle B \rangle = \sum_n B(k_n) \cdot |c_n|^2.$$

As the most used such mean (expected) values can be quoted the following ones: first order moments $\langle x \rangle$ and $\langle k_n \rangle = \langle k \rangle$, variances $\langle(x - \langle x \rangle)^2\rangle$ and $\langle(k_n - \langle k \rangle)^2\rangle$ respectively standard deviations $\Delta x = \sqrt{\langle(x - \langle x \rangle)^2\rangle}$ and $\Delta k = \sqrt{\langle(k_n - \langle k \rangle)^2\rangle}$.

In order to find the announced x -limited correspondents of x -unlimited relations (C.3) and (C.4) we take into account the following obvious formula

$$\int_0^b \left| \lambda(x - \langle x \rangle) \cdot f(x) + \left(\frac{d}{dx} - i \langle k \rangle \right) \cdot f(x) \right|^2 \cdot dx \geq 0 \tag{C.9}$$

where λ is a real, finite and arbitrary parameter. By using the above noted probabilistic properties of function $f(x)$ and coefficients c_n from (C.9) one obtains the relation

$$\lambda^2 \langle(x - \langle x \rangle)^2\rangle + \lambda (b |f(0)|^2 - 1) + \langle(k - \langle k \rangle)^2\rangle \geq 0. \tag{C.10}$$

Due to the mentioned characteristics of λ , from this last relation one finds the next formulas for variances of x and k_n

$$\langle (x - \langle x \rangle)^2 \rangle \cdot \langle (k_n - \langle k \rangle)^2 \rangle \geq \frac{1}{4} (b |f(0)|^2 - 1)^2 \quad (C.11)$$

respectively for standard deviations of x and k_n

$$\Delta x \cdot \Delta k \geq \frac{1}{2} \left| (b |f(0)|^2 - 1) \right|. \quad (C.12)$$

The formulas (C.11) and (C.12) are x -limited analogues of the x -unlimited relations (C.2) and (C.3).

In the end we note that formula (C.12) is applicable in cases of wave functions (4) regarding non-degenerate circular rotations. For such cases the application of (C.12) is obtained through the following substitutions: $x \rightarrow \varphi$, $b \rightarrow 2\pi$, $f(x) \rightarrow \Psi(\varphi)$ and $k_n \rightarrow \frac{L_z}{\hbar}$. So from (C.12) it results

$$\Delta \varphi \cdot \Delta L_z \geq \frac{\hbar}{2} \left| (2\pi |\Psi(0)|^2 - 1) \right|. \quad (C.13)$$

This last formula in case of wave functions (4) degenerates into trivial equality $0 = 0$

D: On the fluctuations of thermodynamic observables

Thermodynamic systems are macroscopic bodies composed by huge numbers of microscopic constituents (molecules and atoms). As whole bodies or through by their macroscopic parts such systems are described by so-called thermodynamic observables. The alluded observables are viewed as deterministic variables (in usual thermodynamics) respectively as stochastic quantities (in statistical physics). In the last view they are characterized by fluctuations (deviations from their deterministic values studied within usual thermodynamics). The mentioned fluctuations are investigated within the next conceptual frameworks: (a) phenomenological approach, (b) classical statistical mechanics, respectively (c) quantum statistical physics.

In phenomenological approach [68–72], proposed for the first time by Einstein, the respective fluctuations can be depicted briefly as follows. Let be a system of the mentioned kind, whose properties are described by a set of thermodynamic observables \mathbb{A}_j ($j = 1, 2, 3, \dots, n$). Each such observable \mathbb{A}_j is characterized by a global fixed value $\bar{\mathbb{A}}_j$, evaluable through the methods of deterministic usual thermodynamics. Then the fluctuations of observables \mathbb{A}_j should be discussed in terms of random variables $\mathcal{A}_j = \mathbb{A}_j - \bar{\mathbb{A}}_j$ ($j = 1, 2, \dots, n$), endowed with continuous spectra of values such as $\mathcal{A}_j \in (-\infty, +\infty)$. The random characteristics of variables \mathcal{A}_j , i.e. the fluctuations of observables \mathbb{A}_j , are depicted in phenomenological approach through the probability density $W = W(\vec{\mathcal{A}})$, where the vector $\vec{\mathcal{A}}$ signifies the set of all variables \mathcal{A}_j . Commonly for $W = W(\vec{\mathcal{A}})$ one uses distributions of Gaussian type. The mean value (expected) value $\langle \mathbb{A}_j \rangle_W$

and the random deviation $\delta_W \mathbb{A}_j$ of the observable \mathbb{A}_j are

$$\begin{aligned} \langle \mathbb{A}_j \rangle_W &= \int_{-\infty}^{+\infty} \mathbb{A}_j \cdot W(\vec{\mathcal{A}}) \cdot d\vec{\mathcal{A}}, \\ \delta_W \mathbb{A}_j &= \mathbb{A}_j - \langle \mathbb{A}_j \rangle_W = \mathcal{A}_j. \end{aligned} \quad (D.1)$$

Usually, the fluctuations of observables \mathbb{A}_j ($j = 1, 2, 3, \dots, n$) are characterized by a small number of numerical parameters evaluable through the random deviations $\delta_W \mathbb{A}_j$. Examples of such parameters are: dispersions $\langle (\delta_W \mathbb{A}_j)^2 \rangle_W = \langle (\mathcal{A}_j)^2 \rangle_W$ and their equivalents the standard deviations $\Delta_W \mathbb{A}_j = \sqrt{\langle (\delta_W \mathbb{A}_j)^2 \rangle_W}$, second order moments (correlations) $\langle \delta_W \mathbb{A}_j \cdot \delta_W \mathbb{A}_k \rangle_W$ ($j \neq k$) or even [72] higher order moments (correlations) $\langle (\delta_W \mathbb{A}_j)^r \cdot (\delta_W \mathbb{A}_k)^s \rangle_W$, ($r + s \geq 3$).

The correlations $\langle \delta_W \mathbb{A}_j \cdot \delta_W \mathbb{A}_k \rangle_W$ ($j, k = 1, 2, \dots, n$) constitute the components of a positive semi definite matrix. The respective components satisfy [70, 71] the following correlation formulas

$$\det \left[\langle \delta_W \mathbb{A}_j \cdot \delta_W \mathbb{A}_k \rangle_W \right] \geq 0, \quad (D.2)$$

where $\det [\alpha_{jk}]$ denote the determinant whose components are the quantities α_{jk} . Particularly for two thermodynamic observables $\mathbb{A}_1 = \mathbb{A}$ and $\mathbb{A}_2 = \mathbb{B}$ from (D.2) one obtains

$$\Delta_W \mathbb{A} \cdot \Delta_W \mathbb{B} \geq |\langle \delta_W \mathbb{A} \cdot \delta_W \mathbb{B} \rangle_W| \quad (D.3)$$

where $\Delta_W \mathbb{A} = \sqrt{\langle (\delta_W \mathbb{A})^2 \rangle_W}$ denotes the standard deviation of observable \mathbb{A} . Mathematically (in sense of probability theory) this last classical formula is completely analogous with the quantum UR (2).

Regarded in their detailed expressions the standard deviations like is $\Delta_W \mathbb{A}$ (introduced above) have an interesting generic property. Namely they appear as being in a direct and factorized dependence of Boltzmann's constant k_B . The respective dependence has the following physical significance. It is known the fact that, mathematically, for a given quantity the standard deviation indicates its randomness. This in the sense that the respective quantity is a random or, alternatively, a deterministic (non-random) variable according as the alluded deviation has a positive or null value. Therefore $\Delta_W \mathbb{A}$ can be regarded as an indicator of randomness for the thermodynamic observable \mathbb{A} . But, for diverse cases (of observables, systems and states), the deviation $\Delta_W \mathbb{A}$ has various expressions in which, apparently, no common element seems to be implied. Nevertheless such an element can be found out [20, 73] as being materialized by the Boltzmann's constant k_B . So, in Gaussian approximation within the framework of phenomenological theory of fluctuations one finds [20, 73]

$$(\Delta_W \mathbb{A})^2 = k_B \cdot \sum_{\alpha} \sum_{\beta} \frac{\partial \bar{\mathbb{A}}}{\partial \bar{\mathcal{X}}_{\alpha}} \cdot \frac{\partial \bar{\mathbb{A}}}{\partial \bar{\mathcal{X}}_{\beta}} \cdot \left(\frac{\partial^2 \bar{\mathcal{S}}}{\partial \bar{\mathcal{X}}_{\alpha} \partial \bar{\mathcal{X}}_{\beta}} \right)^{-1}. \quad (D.4)$$

Now note that, a kind of non-quantum formulas completely similar with (D.2) and (D.3), can be reported also

for the fluctuations of thermodynamic observables described in terms of classical statistical mechanics. In the respective terms the above phenomenological notations and relations can be transcribed formally as follows. Instead of random variables \mathcal{A}_j should to operate with the phase space ensemble denoted as μ of all coordinates and momenta of molecules/atoms which compose the thermodynamic system. Also instead of observables $\mathbb{A}_j = \overline{\mathbb{A}_j} + \mathcal{A}_j$ needs to be use the random functions of the form $\hat{\mathbb{A}}_j = \hat{\mathbb{A}}_j(\mu)$. Therewith the probability density $W = W(\vec{\mathcal{A}})$ should to be replaced with the statistical distribution function $w = w(\mu)$. Then, in terms of afore-said description of considered fluctuations, as example, can be written the relation

$$\Delta_w \mathbb{A} \cdot \Delta_w \mathbb{B} \geq |\langle \delta_w \mathbb{A} \cdot \delta_w \mathbb{B} \rangle_w| \quad (D.5)$$

which is completely similar with (D.3). Add here the observation that the standard deviations $\Delta_w \mathbb{A}$ and $\Delta_w \mathbb{B}$ from (D.5) have a factorization dependence on k_B of type (D.4), similarly with the case of quantities $\Delta_W \mathbb{A}$ and $\Delta_W \mathbb{B}$ from (D.3).

For describing the fluctuations of thermodynamic observables \mathbb{A}_j in framework of quantum statistical physics as probabilities carrier instead of phenomenological density $W = W(\vec{\mathcal{A}})$ should to use [73–76] the quantum density operator $\hat{\rho}$:

$$\hat{\rho} = \sum_k p_k |\psi_k\rangle \langle \psi_k|. \quad (D.6)$$

Here $|\psi_k\rangle$ ($k = 1, 2, \dots$) denote the wave functions of pure states of system and p_k are the corresponding probabilities of the respective states. In the same framework the above mentioned random variables \mathcal{A}_j are substituted with the thermo-quantum operators $\hat{\mathbb{A}}_j$ ($j = 1, 2, \dots, n$). In framework of quantum statistical physics the mean value $\langle \mathbb{A}_j \rangle_\rho$ and random deviation $\delta_\rho \hat{\mathbb{A}}_j$ of observable \mathbb{A}_j are

$$\begin{aligned} \langle \mathbb{A}_j \rangle_\rho &= \sum_k p_k \langle \psi_k | \hat{\mathbb{A}}_j | \psi_k \rangle \\ &= \text{tr} \left(\sum_k p_k |\psi_k\rangle \langle \psi_k| \hat{\mathbb{A}}_j \right) = \text{tr} (\hat{\rho} \cdot \hat{\mathbb{A}}_j), \quad (D.7) \\ \delta_\rho \hat{\mathbb{A}}_j &= \hat{\mathbb{A}}_j - \langle \mathbb{A}_j \rangle_\rho. \end{aligned}$$

The deviations $\delta_\rho \hat{\mathbb{A}}_j$ can be used in description of numerical parameters of fluctuations for observables \mathbb{A}_j in the mentioned framework. As such parameters can be quoted: dispersions $\langle (\delta_\rho \hat{\mathbb{A}}_j)^2 \rangle_\rho$ and their equivalents standard deviations $\Delta_\rho \mathbb{A}_j = \sqrt{\langle (\delta_\rho \hat{\mathbb{A}}_j)^2 \rangle_\rho}$, second order moments (correlations) $\langle \delta_\rho \hat{\mathbb{A}}_j \cdot \delta_\rho \hat{\mathbb{A}}_k \rangle_\rho$ (where $j \neq k$) or even higher order moments $\langle (\delta_\rho \hat{\mathbb{A}}_j)^r \cdot (\delta_\rho \hat{\mathbb{A}}_k)^s \rangle_\rho$ (where $r + s \geq 3$).

In case of two thermodynamic observables \mathbb{A} and \mathbb{B} , regarded in framework of quantum statistical physics, can be introduced also a correlation relation similar with (D.3) and (D.5). Such a relation can be introduced as follows. For the

corresponding thermo-quantum operators $\hat{\mathbb{A}}$ and $\hat{\mathbb{B}}$ it is evidently true the relation

$$\sum_k p_k \left\langle \left(\delta_\rho \hat{\mathbb{A}} + i\lambda \delta_\rho \hat{\mathbb{B}} \right) \psi_k \mid \left(\delta_\rho \hat{\mathbb{A}} + i\lambda \delta_\rho \hat{\mathbb{B}} \right) \psi_k \right\rangle \geq 0 \quad (D.8)$$

where λ is an arbitrary real parameter. If in respect with the functions ψ_k the operators $\hat{\mathbb{A}}$ and $\hat{\mathbb{B}}$ satisfy the conditions of type (A.3) one can write

$$\begin{aligned} &\sum_k p_k \left\langle \left(\delta_\rho \hat{\mathbb{A}} + i\lambda \delta_\rho \hat{\mathbb{B}} \right) \psi_k \mid \left(\delta_\rho \hat{\mathbb{A}} + i\lambda \delta_\rho \hat{\mathbb{B}} \right) \psi_k \right\rangle \\ &= \sum_k p_k \left\langle \psi_k \mid \left(\delta_\rho \hat{\mathbb{A}} \right)^2 \mid \psi_k \right\rangle \\ &\quad + \lambda^2 \sum_k p_k \left\langle \psi_k \mid \left(\delta_\rho \hat{\mathbb{B}} \right)^2 \mid \psi_k \right\rangle \\ &\quad + i\lambda \sum_k p_k \left\langle \psi_k \mid \left(\delta_\rho \hat{\mathbb{A}} \cdot \delta_\rho \hat{\mathbb{B}} - \delta_\rho \hat{\mathbb{B}} \cdot \delta_\rho \hat{\mathbb{A}} \right) \mid \psi_k \right\rangle. \end{aligned} \quad (D.9)$$

Then from (D.8) it results the relation

$$\left\langle \left(\delta_\rho \hat{\mathbb{A}} \right)^2 \right\rangle_\rho + \lambda^2 \left\langle \left(\delta_\rho \hat{\mathbb{B}} \right)^2 \right\rangle_\rho + \lambda \langle i [\hat{\mathbb{A}}, \hat{\mathbb{B}}] \rangle_\rho \geq 0 \quad (D.10)$$

where $[\hat{\mathbb{A}}, \hat{\mathbb{B}}]$ denotes the commutator of operators $\hat{\mathbb{A}}$ and $\hat{\mathbb{B}}$.

Because λ is an arbitrary real parameter from (D.10) one obtains the relation

$$\left\langle \left(\delta_\rho \hat{\mathbb{A}} \right)^2 \right\rangle_\rho \cdot \left\langle \left(\delta_\rho \hat{\mathbb{B}} \right)^2 \right\rangle_\rho \geq \frac{1}{4} \langle i [\hat{\mathbb{A}}, \hat{\mathbb{B}}] \rangle_\rho^2 \quad (D.11)$$

or the equivalent formula

$$\Delta_\rho \mathbb{A} \cdot \Delta_\rho \mathbb{B} \geq \frac{1}{2} \left| \langle i [\hat{\mathbb{A}}, \hat{\mathbb{B}}] \rangle_\rho \right|. \quad (D.12)$$

Now let us remind the fact that in quantum statistics the above discussed thermo-quantum quantities $\langle (\delta_\rho \hat{\mathbb{A}}_j)^2 \rangle_\rho$ and $\Delta_\rho \mathbb{A}$ are proved to be connected directly with a quantity from deterministic (simple thermodynamic) description of thermodynamic observables. The respective connection is due by the known fluctuation-dissipation theorem [76] which is expressed by the relation

$$\begin{aligned} \left\langle \left(\delta_\rho \hat{\mathbb{A}} \right)^2 \right\rangle_\rho &= (\Delta_\rho \mathbb{A})^2 \\ &= \frac{\hbar}{2\pi} \int_{-\infty}^{+\infty} \coth \left(\frac{\hbar\omega}{2k_B T} \right) \cdot \mathcal{X}''(\omega) \cdot d\omega. \end{aligned} \quad (D.13)$$

Here k_B = the Boltzmann's constant, \hbar = Planck's constant and T = temperature of the considered system. Also in (D.13) the quantity $\mathcal{X}''(\omega)$ denote the imaginary part of the susceptibility associated with the observable \mathbb{A} . Note that $\mathcal{X}''(\omega)$ is a deterministic quantity which is defined primarily in non-stochastic framework of macroscopic physics [77]. Due to the respective definition it is completely independent of both k_B and \hbar .

In the end of this Appendix the following conclusion may be recorded. All the relations (D.2), (D.3), (D.4), (D.10) and (D.11) are formulas regarding macroscopic fluctuations but not pieces which should be adapted to the UR–QMS philosophy requirements.

E: On the measurements of macroscopic fluctuations

The fluctuations parameters, defined above Appendix D, refer to the characteristics of intrinsic nature for the considered macroscopic systems. But in practical actions, for the same systems, one operates with global parameters, of double source (origin). A first source is given by the intrinsic properties of systems. A second source is provided by the actions of measuring devices. In such a vision a measurement can be regarded as an transmission process of information (referring to stochastic data). Consequently the data about the intrinsic properties of measured system appear as *input* (*in*) information while the global results of the corresponding measurement represent the *output* (*out*) information.

Here below we will appeal to the aforesaid vision for giving (as in [91, 107]) a theoretical model regarding the measurement of thermal fluctuations. The respective fluctuations will be considered in a phenomenological approach (see Appendix D). For simplicity let us consider a system characterized by a single macroscopic observable $\mathbb{A} = \bar{\mathbb{A}} - \mathcal{A}$, whose thermal fluctuations are impacted within the random variable \mathcal{A} having the spectrum $\mathcal{A} \in (-\infty, +\infty)$. The intrinsic fluctuations of \mathcal{A} is supposed to be described by the probability distribution $W_{in} = W_{in}(\mathcal{A})$ regarded as carrier of input-information. The results of measurements are depicted by the distribution $W_{out} = W_{out}(\mathcal{A})$ regarded as bearer of out-information. Then the measuring process may be symbolized as a transformation of the form $W_{in}(\mathcal{A}) \rightarrow W_{out}(\mathcal{A})$. If the measuring device is supposed to have stationary and linear characteristics, the mentioned transformation can be described as follows:

$$W_{out}(\mathcal{A}) = \int_{-\infty}^{+\infty} K(\mathcal{A}, \mathcal{A}') \cdot W_{in}(\mathcal{A}') \cdot d\mathcal{A}' \quad (\text{E.1})$$

where $K(\mathcal{A}, \mathcal{A}')$ appears as a doubly stochastic kernel (in sense defined in [108]). This means that $K(\mathcal{A}, \mathcal{A}')$ satisfy the relations $\int_{-\infty}^{+\infty} K(\mathcal{A}, \mathcal{A}') d\mathcal{A} = \int_{-\infty}^{+\infty} K(\mathcal{A}, \mathcal{A}') d\mathcal{A}' = 1$.

Add here the fact that, from a physical perspective, the kernel $K(\mathcal{A}, \mathcal{A}')$ incorporates the theoretical description of all the characteristics of the measuring device. Particularly, for an ideal device which ensure $W_{out}(\mathcal{A}) = W_{in}(\mathcal{A})$, it must to have the expression $K(\mathcal{A}, \mathcal{A}') = \delta(\mathcal{A} - \mathcal{A}')$, where $\delta(\mathcal{X})$ denote the Dirac's δ -function of argument \mathcal{X} .

By means of distributions $W_{\eta} = W_{\eta}(\mathcal{A})$ ($\eta = in; out$) can be introduced the corresponding η -numerical-characteristics of thermal fluctuations of observable $\mathbb{A} = \bar{\mathbb{A}} + \mathcal{A}$. Such are the η -mean (expected) value $\langle \mathbb{A} \rangle_{\eta}$ and η -standard deviation $\Delta_{\eta} \mathbb{A}$ defined through the relations

$$\begin{aligned} \langle \mathcal{A} \rangle_{\eta} &= \int_{-\infty}^{+\infty} \mathcal{A} \cdot W_{\eta}(\mathcal{A}) \cdot d\mathcal{A}, \\ (\Delta_{\eta} \mathcal{A})^2 &= \left\langle (\mathcal{A} - \langle \mathcal{A} \rangle_{\eta})^2 \right\rangle_{\eta}. \end{aligned} \quad (\text{E.2})$$

The above considerations allow to note some observations about the measuring uncertainties (errors) regarding the fluctuating macroscopic observable \mathbb{A} . Firstly the $\eta = in$ -versions of the parameters (E.2) describe only the "intrinsic" properties of the measured system. Secondly the $\eta = out$ -variants of the same parameters incorporate composite information about the respective system and considered measuring device. That is why one can say that, in terms of the above discussions, the measuring uncertainties of observable \mathbb{A} should be described by the following error indicators (characteristics)

$$\begin{aligned} \mathcal{E}\{\langle \mathbb{A} \rangle\} &= \langle \mathbb{A} \rangle_{out} - \langle \mathbb{A} \rangle_{in}, \\ \mathcal{E}\{\Delta \mathbb{A}\} &= \Delta_{out} \mathbb{A} - \Delta_{in} \mathbb{A}. \end{aligned} \quad (\text{E.3})$$

Observe here that because \mathbb{A} has stochastic characteristics for a relevant description of its measuring uncertainties it is completely insufficient the single indicator $\mathcal{E}\{\langle \mathbb{A} \rangle\}$. An adequate minimal such description requires at least the couple $\mathcal{E}\{\langle \mathbb{A} \rangle\}$ and $\mathcal{E}\{\Delta \mathbb{A}\}$. For further approximations of errors caused by measurements can be taken into account [111] the higher order moments like the next ones

$$\mathcal{E}\{\langle (\delta \mathbb{A})^n \rangle\} = \langle (\delta_{out} \mathbb{A})^n \rangle_{out} - \langle (\delta_{in} \mathbb{A})^n \rangle_{in} \quad (\text{E.4})$$

where $\delta_{\eta} \mathbb{A} = \mathbb{A} - \langle \mathbb{A} \rangle$, $\eta = in, out$ and $n \geq 3$.

F: An exemplification for subsection 5.2

For presenting the announced exemplification we will refer to QMS of the energy for a particle of mass m , located in an infinite square well potential of width L [29]. The intrinsic state of the microparticle will be considered as being described by the *in*-wave function $\Psi_{in}(x) = \sum_{j=1}^n \alpha_j \cdot \varphi_j(x)$. Here $\varphi_j(x)$ denote the eigenfunctions associated to the energetic eigenvalues $a_j = E_j = \mathfrak{J} \cdot j^2$ where $\mathfrak{J} = (\hbar^2 \pi^2 / 2mL^2)$ and $j = 1, 2, 3, \dots$. In the considered *in*-wave function the quantities α_j are probability amplitudes corresponding to the eigenvalues E_j .

We will restrict our exemplification by taking into account only the following circumstances. So we take $n = 3$ as the upper value of the inner energy of the particle while for the amplitudes α_j we will consider the values which give $(|\alpha_j|^2) = (0.5 \ 0.4 \ 0.1)$.

Then the intrinsic characteristics of the particle energy are described by the next mean value and the standard deviation

$$\langle E \rangle_{in} = 3 \cdot \mathfrak{J}, \quad \Delta_{in} E = 2.45 \cdot \mathfrak{J}. \quad (\text{F.1})$$

Accordingly with discussions from Subsection 5.2, for a particle in the mentioned intrinsic state, the measurement of energy can be described as follows. We need to define a model-expression for the matrix (M_{kj}) from (29). As a first example, we will consider a measurement done with a device endowed with flawed (FL) characteristics. Such devices, for

instance, can be associated with a matrix (M_{kj}) having the form

$$(M_{kj})_{FL} = \begin{pmatrix} 0.5 & 0.3 & 0.2 \\ 0.4 & 0.4 & 0.2 \\ 0.1 & 0.3 & 0.6 \end{pmatrix}. \quad (F.2)$$

Thus the outcomes of measurement will be characterized by probabilities $(|\beta_k|^2)_{FL} = (0.34 \ 0.38 \ 0.23)$. With such probabilities, the measurement outcomes for energy will be characterized by the next FL-expected-value and FL-standard-deviation

$$\langle E \rangle_{FL} = 3.98 \cdot \mathfrak{J}, \quad \Delta_{FL} E = 3.04 \cdot \mathfrak{J}. \quad (F.3)$$

Consequently, for the measurement described by (F.2), the error indicators (29) and (31) acquire the following FL-values

$$\mathcal{E}_{FL} \{ \langle E \rangle \} = 0.9 \cdot \mathfrak{J}, \quad \mathcal{E}_{FL} \{ \Delta E \} = 0.59 \cdot \mathfrak{J}. \quad (F.4)$$

If, for the above mentioned energy/particle, we want to describe a measurement done with a device having larger characteristics of accuracy (ACC) one can proceed as follows. In the spirit of the relations (31), for the matrix (M_{kj}) instead of the formula (F.2) we appeal, for example, to the following expression

$$(M_{kj})_{ACC} = \begin{pmatrix} 0.95 & 0.03 & 0.02 \\ -0.03 & 1.04 & -0.01 \\ 0.08 & -0.07 & 0.99 \end{pmatrix}. \quad (F.5)$$

So, for the probabilities associated to the outcomes of ACC-measurement, one obtains $(|\beta_k|^2)_{ACC} = (0.489 \ 0.4 \ 0.11)$. Associated to the respective probabilities, the considered ACC-measurement of energy is characterized by the next ACC-expected value and ACC-standard-deviation

$$\langle E \rangle_{ACC} = 3.088 \cdot \mathfrak{J}, \quad \Delta_{ACC} E = 2.52 \cdot \mathfrak{J}. \quad (F.6)$$

By comparing values from (F.6) with those from (F.1) one sees that the referred ACC-measurement is characterized by the following error indicators

$$\mathcal{E}_{ACC} \{ \langle E \rangle \} = 0.08 \cdot \mathfrak{J}, \quad \mathcal{E}_{ACC} \{ \Delta E \} = 0.07 \cdot \mathfrak{J}. \quad (F.7)$$

Finally, by comparing the results reported in relations (F.4) and (F.7), we can note the following remark. Within the above theoretical description of measurement, the error indicators (for both expected value and standard deviation) are much smaller in the case dealing with higher accuracy characteristics comparatively with the one regarding flawed features.

G: Illustrations for subsection 5.4

In order to illustrate the model discussed in Subsection 5.4, in connection with the description of QMS, let us present here an exercise taken by abbreviation from our article [20] (more computational details can be found in the respective article).

We will refer to a micro-particle of mass m having an one-dimensional motion along the x -axis. Its *in*-wave-function Ψ_{in} is taken of the form $\Psi_{in}(x) = |\Psi_{in}(x)| \cdot \exp \{ i\Phi_{in}(x) \}$ where

$$|\Psi_{in}(x)| \propto \exp \left\{ -\frac{(x-x_0)^2}{4\sigma^2} \right\}, \quad \Phi_{in}(x) = kx. \quad (G.1)$$

Here as well as below in other relations from this Appendix the explicit notations of normalization constants are omitted (they can be added easy by the interested readers). According to the wave function (G.1) the intrinsic features of the considered microparticle are described by the parameters x_0 , σ and k .

Through expressions (G.1), by means of formulas (38), it is simple to find the analytical expressions for probability density ρ_{in} and current j_{in} . As doubly stochastic kernels suggested in (40) we propose here the next two formulas

$$\Gamma(x, x') \propto \exp \left\{ -\frac{(x-x')^2}{2\gamma^2} \right\}, \quad (G.2)$$

$$\Lambda(x, x') \propto \exp \left\{ -\frac{(x-x')^2}{2\lambda^2} \right\}. \quad (G.3)$$

Here parameters γ and λ depict the characteristics of measuring devices/procedures. The values of the respective parameters are associated with an ideal measurement (when both γ and λ tend toward zero), respectively with a nonideal measurement (in cases when at least one of the two parameters is not-null).

Then, by using the procedures presented within Subsection 5.4, it is easy to find the *out*-entities ρ_{out} , j_{out} and Ψ_{out} . By using the respective entities together with the functions from (G.1) one can evaluate the *out* and *in* versions of mean (expected) values and standard deviations for observables of interest. The respective evaluations ensure estimations of the corresponding error indicators. So, for $\hat{x} = x =$ coordinate and $\hat{p} = -i\hbar\nabla_x =$ momentum as operators (observables) of interest, one obtains [20] the following error indicators

$$\mathcal{E} \{ \langle x \rangle \} = 0, \quad \mathcal{E} \{ \Delta x \} = \sqrt{\sigma^2 + \gamma^2} - \sigma, \quad (G.4)$$

$$\mathcal{E} \{ \langle p \rangle \} = 0,$$

$$\mathcal{E} \{ \Delta p \} = \hbar \left| \left[\frac{k^2(\sigma^2 + \gamma^2)}{\sqrt{(\sigma^2 + \lambda^2)(\sigma^2 + 2\gamma^2 - \lambda^2)}} - k^2 + \frac{1}{4(\sigma^2 + \gamma^2)} \right]^{\frac{1}{2}} - k \right|. \quad (G.5)$$

Let us now restrict in the wave function (G.1) to the situation when $x_0 = 0$ $k = 0$ and $\sigma = \sqrt{\frac{\hbar}{2m\omega}}$. Then (G.1) describe the ground state of a harmonic oscillator with $m =$ mass and $\omega =$ angular frequency. As observable of interest of such an oscillator we consider the energy described by the Hamiltonian

$\hat{H} = -\frac{\hbar^2}{2m} \frac{d^2}{dx^2} + \frac{m\omega^2}{2} x^2$. For the respective observable one finds

$$\langle H \rangle_{in} = \frac{\hbar\omega}{2}, \quad \Delta_{in} H = 0, \quad (G.6)$$

$$\langle H \rangle_{out} = \frac{\omega \left[\hbar^2 + (\hbar + 2m\omega\gamma^2)^2 \right]}{4(\hbar + 2m\omega\gamma^2)}, \quad (G.7)$$

$$\Delta_{out} H = \frac{\sqrt{2} m \omega^2 \gamma^2 (\hbar + m\omega\gamma^2)}{(\hbar + 2m\omega\gamma^2)}, \quad (G.8)$$

$$\mathcal{E}\{\langle H \rangle\} = \frac{m^2 \omega^3 \gamma^4}{\hbar + 2m\omega\gamma^2}, \quad (G.9)$$

$$\mathcal{E}\{\Delta H\} = \Delta_{out} H = \frac{\sqrt{2} m \omega^2 \gamma^2 (\hbar + m\omega\gamma^2)}{(\hbar + 2m\omega\gamma^2)}. \quad (G.10)$$

H: A more comprehensive description of measuring errors for random observables

In Subsections 5.2 and 5.4 or Appendices E, F and G, we have discussed the measuring errors for random observables of quantum respectively macroscopic nature. For description of that errors, were used as indicators only the lower order probabilistic parameters (moments and correlations). But those indicators give only first sequences, of limited value, for a global picture of the considered errors. A more comprehensive such a picture can be done in terms of informational entropies. Shortly, for the above discussed observables and errors, the suggested depiction can be illustrated as follows.

Firstly let us refer to the case of a macroscopic random observable \mathcal{A} whose measurements are outlined in Appendix E. The intrinsic characteristics (fluctuations) of \mathcal{A} are considered as being described by the probability distribution $W_{in} = W_{in}(\mathcal{A})$ regarded as carrier of input-information for measurements. The results of measurements are depicted by the distribution $W_{out} = W_{out}(\mathcal{A})$ associated with the out-information of measurements. The informational entropies \mathcal{H}_η ($\eta = in, out$) connected with the above noted distributions are defined through the formulas

$$\mathcal{H}_\eta(\mathcal{A}) = - \int_{-\infty}^{+\infty} W_\eta(\mathcal{A}) \cdot \ln [W_\eta(\mathcal{A})] \cdot d\mathcal{A}. \quad (H.1)$$

By taking into account the transformation (E.1), the main properties of the doubly stochastic kernel $K(\mathcal{A}, \mathcal{A}')$, as well

the formula $\ln(X) \leq X - 1$ one can write

$$\begin{aligned} & \mathcal{H}_{out}(\mathcal{A}) - \mathcal{H}_{in}(\mathcal{A}) \\ &= - \int_{-\infty}^{+\infty} \int_{-\infty}^{+\infty} d\mathcal{A} \cdot d\mathcal{A}' \cdot K(\mathcal{A}, \mathcal{A}') \cdot W_{in}(\mathcal{A}') \\ & \quad \cdot \ln \left[\frac{W_{out}(\mathcal{A})}{W_{in}(\mathcal{A}')} \right] \\ & \geq - \int_{-\infty}^{+\infty} \int_{-\infty}^{+\infty} d\mathcal{A} \cdot d\mathcal{A}' \cdot K(\mathcal{A}, \mathcal{A}') \cdot W_{in}(\mathcal{A}') \\ & \quad \cdot \left[\frac{W_{out}(\mathcal{A})}{W_{in}(\mathcal{A}')} - 1 \right] \\ &= 0. \end{aligned} \quad (H.2)$$

Therefore the errors specific of measurements for \mathcal{A} in its wholeness can be described through the comprehensive error indicator

$$\mathcal{E}\{\mathcal{H}(\mathcal{A})\} = \mathcal{H}_{out}(\mathcal{A}) - \mathcal{H}_{in}(\mathcal{A}) \geq 0. \quad (H.3)$$

This relationship shows that the measuring process can be described by a non-negative change in the informational entropy associated with the investigated observable. The situation when the respective change is null corresponds to the case of an ideal measurement (free of errors), mentioned otherwise in connection with the relationship (E.1).

Mostly, the macroscopic fluctuations described by the here used observable \mathcal{A} are investigated in the so-called Gaussian approximations. Then the entities $W_{in}(\mathcal{A})$ and $K(\mathcal{A}, \mathcal{A}')$ which appear in (E.1) are given by the following formulas

$$\begin{aligned} W_{in}(\mathcal{A}) &\propto \exp \left\{ -\frac{\mathcal{A}^2}{2a^2} \right\}, \\ K(\mathcal{A}, \mathcal{A}') &\propto \exp \left\{ -\frac{(\mathcal{A} - \mathcal{A}')^2}{2b^2} \right\}, \end{aligned} \quad (H.4)$$

where the explicit indication of normalization constants are omitted (the omission can be filled easily by interested readers). In the first formula from (H.4) a denotes the standard deviation of intrinsic fluctuations within the measured system. The symbol b in the second expression from (H.4) depicts the precision parameter of measuring device. Of course, for a scientifically acceptable measuring process, it must be considered that $b \ll a$.

In the alluded cases with Gaussian approximations the output distribution $W_{out}(\mathcal{A})$ has the form

$$W_{out}(\mathcal{A}) \propto \exp \left\{ -\frac{\mathcal{A}^2}{2(a^2 + b^2)} \right\}.$$

Then the comprehensive error indicator (H.3) becomes

$$\mathcal{E}\{\mathcal{H}(\mathcal{A})\} = \frac{1}{2} \ln \left(1 + \frac{b^2}{a^2} \right) \approx \frac{1}{2} \cdot \frac{b^2}{a^2}. \quad (H.5)$$

Now let us refer to the comprehensive informational depiction for measuring errors in cases of random quantum observables. We start the announced reference by discussing the case presented in Subsection 5.2, regarding the measurement of a quantum observable endowed with a discrete spectrum of eigenvalues. In the respective case the input and output data characterizing the measurement are depicted by the following corresponding probabilities

$$\mathcal{P}_{in}^j = |\alpha_j|^2, \quad \mathcal{P}_{out}^j = |\beta_j|^2, \quad (j = 1, 2, \dots, n). \quad (H.6)$$

These probabilities can be associated with the next information entropies

$$\mathcal{H}(\mathcal{P}_\eta) = - \sum_{j=1}^n P_\eta^j \cdot \ln(\mathcal{P}_\eta^j), \quad (\eta = in, out). \quad (H.7)$$

Consequently, for an extensive description of measuring errors for the specified quantum observable, can be used the below comprehensive indicator

$$\mathcal{E}\{\mathcal{H}(\mathcal{P})\} = \mathcal{H}(\mathcal{P}_{out}) - \mathcal{H}(\mathcal{P}_{in}). \quad (H.8)$$

By taking into account the transformation (27), the basic properties of doubly stochastic matrix M_{jk} , plus the evident formula $\ln(X) \leq X - 1$, through some simple calculations (similar to those appealed in (H.2) and (H.3), one finds:

$$\mathcal{E}\{\mathcal{H}(\mathcal{P})\} \geq 0. \quad (H.9)$$

This formula corresponds to ideal or non-ideal measurements, in cases of equality respectively of inequality.

Note that, in cases of examples presented in Appendix F related with Subsection 5.2, the relation (H.8) takes the expressions

$$\begin{aligned} \mathcal{E}\{\mathcal{H}(\mathcal{P})_{FL}\} &= \mathcal{H}(|\beta_k|^2_{FL}) - \mathcal{H}(|\alpha_j|^2) \\ &= 0.131, \end{aligned} \quad (H.10)$$

$$\begin{aligned} \mathcal{E}\{\mathcal{H}(\mathcal{P})_{ACC}\} &= \mathcal{H}(|\beta_k|^2_{ACC}) - \mathcal{H}(|\alpha_j|^2) \\ &= 0.018. \end{aligned}$$

The above expressions correspond to measurements with characteristics of flawed respectively accurate types. The same expressions show that, even in informational-entropic approach, the measuring errors are higher in cases with flawed characteristics comparatively with the ones having accurate features.

Now let us note some things about the comprehensive description of measuring errors in cases approached in Subsection 5.4 and in Appendix G, regarding of quantum observables with continuous spectra. The corresponding measurements, depicted through the transformations (40), can be associated with the following informational entropies

$$\mathcal{H}_\eta(\rho) = - \int_{-\infty}^{+\infty} \rho_\eta(x) \cdot \ln(\rho_\eta(x)) \cdot dx, \quad (H.11)$$

$$\mathcal{H}_\eta(|j\rangle) = - \int_{-\infty}^{+\infty} |j_\eta(x)| \cdot \ln(|j_\eta(x)|) \cdot dx,$$

where $\eta = in, out$. Related with the above entropies can be introduced the next comprehensive error indicators

$$\mathcal{E}\{\mathcal{H}(\rho)\} = \mathcal{H}_{out}(\rho) - \mathcal{H}_{in}(\rho), \quad (H.12)$$

$$\mathcal{E}\{\mathcal{H}(|j\rangle)\} = \mathcal{H}_{out}(|j\rangle) - \mathcal{H}_{in}(|j\rangle).$$

Through some simple calculations (completely similar to the ones used in (H.2) and (H.3)) one finds that the error indicators (H.11) satisfy the relations

$$\mathcal{E}\{\mathcal{H}(\rho)\} \geq 0, \quad \mathcal{E}\{\mathcal{H}(|j\rangle)\} \geq 0 \quad (H.13)$$

These relations with equalities or inequalities refer to the cases of ideal respectively non-ideal measurements.

In particular case of measurement illustrated in Appendix G, associated with the doubly stochastic kernels (G.2) and (G.3), the error indicators (H.12) become

$$\mathcal{E}\{\mathcal{H}(\rho)\} = \ln \sqrt{\frac{\sigma^2 + \gamma^2}{\sigma^2}} \approx \frac{1}{2} \left(\frac{\gamma}{\sigma}\right)^2, \quad (H.14)$$

$$\mathcal{E}\{\mathcal{H}(|j\rangle)\} = \ln \sqrt{\frac{\sigma^2 + \lambda^2}{\sigma^2}} \approx \frac{1}{2} \left(\frac{\lambda}{\sigma}\right)^2.$$

The last expressions of these indicators imply the approximations $\gamma \ll \sigma$ and $\lambda \ll \sigma$, specific to the supposition that measuring devices have high accuracies. Of course that the cases with $\gamma = 0$ and $\lambda = 0$ depict the ideal measurements.

In the case of a harmonic oscillator, mentioned in the end of Appendix G, the first error indicator from (H.12) get the expression

$$\mathcal{E}\{\mathcal{H}(\rho)\} = \ln \sqrt{\frac{\hbar + 2m\omega\gamma^2}{\hbar}} \approx \frac{m\omega}{\hbar} \gamma^2. \quad (H.15)$$

Submitted on November 26, 2020

I: A private letter from the late scientist J. S. Bell to the present author**CERN**1985 Jan 29

Dear Dr Dumitru, thank you for your paper. I agree with what you say about the uncertainty principle: it has to do with the uncertainty in predictions rather than the accuracy of 'measurement'. I think in fact that the word 'measurement' has been so abused in quantum mechanics that it would be good to avoid it altogether.

I will send some papers, including (if I can find copies) those you request.

with best wishes

John Bell

References

1. De Witt B.S., Graham N. Resource letter IQM-1 – on the interpretation of quantum mechanics. *Am. J. Phys.*, 1971, v.39, 724–738 .
2. Nilson D.R. Bibliography on the history and philosophy of Quantum Mechanics. In: Suppes P. (ed.) Logic and probability in quantum mechanics, D. Reidel, Dordrecht, 1976.
3. Balentine L.E. Resource letter IQM-2 — Foundations of quantum mechanics since the Bell inequalities. *Am. J. Phys.*, 1987, v.55, 785–792.
4. Dodonov V.V., Man'ko V.I. Generalization of uncertainty relations in quantum mechanics. *Proc. Lebedev Phys. Institute*, 1987, v.183, 5–70. English version, in: Markov M.A. (ed.) Invariants and evolution of non stationary quantum systems. Nova Science, New York, 1989, 3–101.
5. Auletta G. Foundations and interpretation of quantum mechanics. World Scientific, Singapore, 2000.
6. Cabello A. Bibliographic guide to the foundations of quantum mechanics and quantum information. arXiv: quant-ph/0012089v12.
7. Busch P., Heinonen T., Lahti P. Heisenberg's uncertainty principle. *Physics Reports*, 2007, v.452, 155–176.
8. Sen D., The uncertainty relations in quantum mechanics. *Current Science*, 2014, v.10, 203–218.
9. Li J.-L., Qiao C.-F. Reformulating the quantum uncertainty relation. *Sci. Rep.*, 2015 v.5, 12708.
10. Hilgevoord J., Uffink J. The uncertainty principle. In: Zalta E.N. (ed.) The Stanford Encyclopedia of Philosophy, Winter 2016 Edition.
11. Jijnasu V. The uncertainty principle — a simplified review of the four versions. *Studies in History and Philosophy of Modern Physics*, 2016, v.55, 62–71.
12. Werner R.F., Farrelly T. Uncertainty from Heisenberg to Today. arXiv: 1904.06139v1.
13. Martens H. Uncertainty Principle (PhD thesis). Eindhoven, Technical University, 1991.
14. Bunge M. The interpretation of Heisenberg inequalities. In: Pfeuffer H. (ed.) Denken und Umdenken-zu Werk und Wirkung von Werner Heisenberg, R. Piper, Munchen, 1977.
15. Philosophy. Cambridge Dictionary.
16. Kupczynski M. Invited Comment: Quantum mechanics and modelling of physical reality. *Phys. Scr.*, 2018, v.93, 123001, arXiv: 1804.02288v2.
17. Dumitru S. Uncertainty relations or correlation relations? *Epistemological Letters*, 1977, v.15, 1–78.
18. Dumitru S. Fluctuations but not uncertainties — deconspiracy of some confusions. In: Datta B., Dutta M. (eds.) Recent Advances in Statistical Physics (Proc. Int. Bose Symposium on Statistical Physics, Dec. 28–31, 1984, Calcutta, India), World Scientific, Singapore, 1987, 122–151.
19. Dumitru S. L_z - φ uncertainty relation versus torsion pendulum example and the failure of a vision. *Rev. Roum. Phys.*, 1988, v.33, 11–45.
20. Dumitru S. Reconsideration of the uncertainty relations and quantum measurements. *Progress in Physics*, 2008, v.4, issue 2, 50–68; arXiv: 1205.3892v1.
21. Dumitru S. Do the uncertainty relations really have crucial significances for physics? *Progress in Physics*, 2010, v.6, issue 4, 25–29; arXiv: 1005.0381.
22. Occam's razor. Encyclopedia Britannica.
23. Dirac P.A.M. The evolution of the physicist's picture of Nature. *Scientific American*, 1963, v.208, 45–53.
24. Precept. The Free Dictionary.
25. Heisenberg W. Über den anschaulichen Inhalt der quantentheoretischen Kinematik und Mechanik. *Z. Phys.*, 1927, v.43, 172–198; English translations: (i) Heisenberg W. The physical content of quantum kinematics and mechanics. In: Wheeler J.A., Zurek W.H. (eds.) Quantum Theory and Measurements. Princeton University Press, Princeton, 1983, 62–86, or (ii) Heisenberg W. The Actual content Of quantum theoretical kinematics and mechanics. Nasa Technical Memorandum, NASA TM 77379.
26. Heisenberg W. The physical principles of quantum theory. First German Edition, Leipzig, 1930; English version, Dover Publ., New York, 1949.
27. Robertson H.P. The uncertainty principle. *Phys. Rev.*, 1929, v.34, 163–164.
28. Schrödinger E. About Heisenberg uncertainty relation. *Proceedings of the Prussian Academy of Sciences, Physics-Mathematical Section*, 1930, v.19, 296–303; English versions In: (i) *Bulg. J. Phys.*, 1999, v.26, issue 5/6, 193–203; (ii) arXiv: quantph/9903100 (annotation by A. Angelow and M.-C. Batoni).
29. Bransden B.H., Joachain C.J. Quantum Mechanics. 2nd edition, Pearson Educational Limited, Essex (England), 2000.
30. Griffiths D.J. Introduction to Quantum Mechanics. Second Edition, Pearson Education Inc., 2005.
31. Schwabl F. Quantum Mechanics. Fourth Edition, Springer-Verlag, Berlin, 2007.
32. Dumitru S. Quantum Mechanics — Consistent Probabilistic Formulation. Matrix Rom, Bucharest, 2006 (in Romanian).
33. Born M., Wolf T. Principles of Optics. Pergamon Press, Oxford, 1986.
34. Ryachodhuri C. Heisenberg's microscope a misleading illustration. *Found. Phys.*, 1978, v.8, 845–849 .
35. Scheer J. et al. A possible evidence for a violation of Heisenberg's position-momentum uncertainty relation. *Found. Phys. Lett.*, 1989, v.2, 71–79.
36. Super-resolution microscopy. Wikipedia.
37. Hemmer P., Ben-Benjamin J.S. Invited Comment: The quest for ultimate super resolution. *Phys. Scr.*, 2016, v.91, 093003.
38. Zhou S., Jiang L. A modern description of Rayleigh's criterion. arXiv: 1801.02917v2.
39. Hofer W.A. Heisenberg uncertainty and the scanning tunneling microscope. *Frontiers of Physics*, 2012, v.7, 218–222; arXiv: 1105.3914v3.
40. Rozema L.A., Darabi A., Mahler D.H., Hayat A., Soudagar Y., Steinberg A.M. Violation of Heisenberg's measurement-disturbance relationship by weak measurements. *Phys. Rev. Lett.*, 2012, v.109, 100404; arXiv: 1208.0034v2.
41. Popper K. Quantum mechanics without the “observer”. In: Bunge M. (ed.) Quantum Theory and Reality, Springer, Berlin, 1967, 7–44.
42. Judge D. On the uncertainty relation for L_z and φ . *Phys. Lett.*, 1963, v.5, 189.
43. Carruthers P., Nieto M.M. Phase and angle variables in quantum mechanics. *Rev. Mod. Phys.*, 1968, v.40, 411–440.
44. Roy C.L., Sannigrahi A.B. Uncertainty relation between angular momentum and angle variable. *Am. J. Phys.*, 1979, v.47, 965.
45. Galitski V., Karnakov B., Kogan V.. Problemes de mecanique quantique. Mir, Moscou, 1985.
46. Barnett S.M., Pegg D.T. Quantum theory of rotation angles. *Phys. Rev. A.*, 1990, v.41, issue 7, 3427–3435.
47. Dumitru S. Compatibility versus commutativity — the intriguing case of angular momentum — azimuthal angle. In: Dodonov V.V., Man'ko V.I., (eds.) *Proc. Lebedev Phys. Inst. Acad. Sci. USSR*, v.187; Quantum field theory, quantum mechanics and quantum optics. Pt.1. Symmetries and algebraic structures in physics. Nova Sci. Pub., New York, 1991, 243–246.
48. Nieto M.M. Quantum phase and quantum phase operators: some physics and some history. *Phys. Scr.*, 1993, v.T48, 5–12; arXiv: hep-th/9304036.

49. Lynch R. The quantum phase problem — a critical review. *Physics Reports*, 1995, v.256, 367–436.
50. Kovalski K., Rebielinski J. On the uncertainty relations and squeezed states for the quantum mechanics on a circle. *J. Phys. A: Math. Gen.*, 2002, v.35, 1405–1414.
51. Trifonov D.A. On the position uncertainty measure on the circle. *J. Phys. A: Math. Gen.*, 2003, v.36, 11873–11879.
52. Franke-Arnold S., Barnett S.M., Yao E., Leach J., Courtial J., Padgett M. *New Journal of Physics*, 2004, v.6, issue 103, 1–8.
53. Pegg D.T., Barnett S.M., Zambrini R., Franke-Arnold S., Padgett M. Minimum uncertainty states of angular momentum and angular position. *New Journal of Physics*, 2005, v.7, issue 62, 1–20.
54. Kastrop H.A. Quantization of the canonically conjugate pair angle and orbital angular momentum. *Phys. Rev. A*, 2006, v.73, 052104; arXiv: quant-ph/0510234.
55. Dumitru S. A possible general approach regarding the conformability of angular observables with mathematical rules of quantum mechanics. *Progress in Physics*, 2008, v.4, issue 1, 25–30; arXiv: quant-ph/0602147.
56. Doubrovine B., Novikov S., Fomenko A., *Geometrie contemporaine*. Premier Partie, Mir, Moscou, 1982.
57. Molecular vibration. Wikipedia.
58. Busch P., Lahti P.J. The complementarity of quantum observables: theory and experiments. *Rivista del Nuovo Cimento*, 1995, v.18, issue 4, 1–27; arXiv: quant-ph/0406132.
59. Sharatchandra H. S. Phase of the quantum oscillator. arXiv: quant-ph/9710020.
60. Busch P., Lahti P., Pellonpää J.-P., Ylinen K. Are number and phase complementary observables? *Journal of Physics A: Math. Gen.*, 2001, v.34, 5923–5935; arXiv: quant-ph/0105036.
61. Kitajima S., Shingu-Yano M., Shibata F. Number-phase uncertainty relation. *J. Phys. Soc. Japan*, 2003, v.72, 2133–2136.
62. Bauer M., Mello P.A. The time-energy uncertainty relation. *Ann. Phys.*, 1978, v.111, 38–60.
63. Bush P. The time energy — uncertainty relation. In: Muga J.G., Sala M.R., Egusquiza I.L. (eds.) *Time in Quantum Mechanics*, Springer, Berlin, 2002, 69–98.
64. Urbanowski K. Remarks on the time — energy uncertainty relation. arXiv: 1810.11462v1.
65. Angular resolution. Wikipedia.
66. Folland G.B., Sitaram A. The uncertainty principle: a mathematical survey. *The Journal of Fourier Analysis and Applications*, 1997, v.3, issue 3, 207–238.
67. Hall M. What is the Gabor uncertainty principle? <https://agilescientific.com/blog/2014/1/15/what-is-the-gabor-uncertainty-principle.html>
68. Münster A. *Statistical Thermodynamics*. Springer, Berlin, 1965.
69. Landau L., Lifchitz E. *Physique Statistique*. Première partie, Mir, Moscou 1984.
70. Dumitru S. Fluctuations and thermodynamic inequalities. *Phys. Scr.*, 1974, v.10, 101–103.
71. Dumitru S., Boer A. Fluctuations in the presence of fields — phenomenological Gaussian approximation and a class of thermodynamic inequalities. *Phys. Rev. E*, 2001, v.64, 021108; arXiv: cond-mat/0011444v1.
72. Boer A., Dumitru S. Higher-order correlations for fluctuations in the presence of fields. *Phys. Rev. E*, 2002, v.66, 046116; arXiv: cond-mat/0201171v2.
73. Dumitru S. The Planck and Boltzmann constants as similar generic indicators of stochasticity — some conceptual implications of quantum-nonquantum analogies. *Physics Essays*, 1993, v.6, 5–20; CERN Central Library PRE 32387 rev.; This article was awarded in 1995 with the Dragomir Hurmuzescu prize of the Romanian Academy.
74. Jancel R. *Foundations of Classical and Quantum Statistical Mechanics*. Pergamon Press, New York, 1973.
75. Density matrix. Wikipedia.
76. Zubarev D. N. *Nonequilibrium statistical thermodynamics*. Nauka, Moscow, 1974 (*in Russian*); English version: Consultants Bureau, New York, 1974.
77. De Groot S.R., Mazur P. *Nonequilibrium Thermodynamics*. North-Holland, Amsterdam, 1962.
78. Uffink J., Van Lith J. Thermodynamic uncertainty relations. *Found. Phys.*, 1999, v.29, 655–692; arXiv: cond-mat/9806102v1.
79. Artamonov A.A., Plotnikov E.V. Thermodynamic uncertainty relation as a fundamental aspect of quantum thermodynamics. *Bulletin of the Tomsk Polytechnic University — Resource-Efficient Technologies*, 2018 v.1, 17–29.
80. Tyablikov S.V. *Methods of Quantum Theory of Magnetism*. Nauka, Moscow, 1975 (*in Russian*).
81. Schwabl F. *Statistical Mechanics*. Springer, Berlin, 2002.
82. Observer effect (physics). Wikipedia.
83. Bell J.S. A private letter from the late scientist J. S. Bell to the present author (dated January 29, 1985). See a copy in Appendix I; also in: arxiv:quant-ph/0004013v1.
84. Bell J.S. Against “measurement”. *Physics World*, 1990, v.3, 33–40. Article reprinted also in some books containing Bell’s writings.
85. Category: Principles. Wikipedia.
86. Busch P., Lahti P., Mittelstaedt P. *The Quantum Theory of Measurement*. Second Edition, Springer, Berlin, 1996.
87. Svensson B.E.Y. Pedagogical review of quantum measurement theory with an emphasis on weak measurements. *Quanta*, 2013, v.2, issue 1, 18–49.
88. Wayne M. Philosophical issues in quantum theory. In: Zalta E.N. (ed.) *The Stanford Encyclopedia of Philosophy*, Spring 2017 Edition.
89. Hossenfelder S. At the frontier of knowledge. arXiv: 1001.3538v1.
90. Dumitru S., Verriest E.I. Behaviour patterns of observables in quantum-classical limit. *Int. J. Theor. Physics*, 1995, v.34, issue 8, 1785–1790.
91. Dumitru S., Boer A. On the measurements regarding random observables. *Rom. Journal. Phys.*, 2008, v.53, issue 9/10, 1111–1116.
92. Dumitru S. Routes of quantum mechanics theories. *Progress in Physics*, 2012, v.8, issue 3, L1.
93. Dumitru S. Caducity of idea about wave function collapse as well new views on Schrödinger’s cat and quantum measurements. *Progress in Physics*, 2013, v.9, issue 1, 63–68; arXiv: 1210.4121v3.
94. Dumitru S. Views about the “Oxford questions”, wave function collapse and Schrödinger’s cat — are they real scientific topics or plain fictions? *Progress in Physics*, 2014, v.10, issue 2, 111–113; arXiv: 1311.2581.
95. Klyshko D.N., Lipkine A.I. About the “reduction of wave function”, quantum theory of measurement, and “incomprehension” of quantum mechanics. *Electronic Journal “Investigated in Russia”*, 2000, 703–735.
96. Albertson J. Quantum-mechanical measurement operator. *Phys. Rev.*, 1963, v.129, 940–943.
97. Communication channel. Wikipedia.
98. Doubly stochastic matrix. Wikipedia.
99. Stamatescu I.-O. Wave function collapse. In: Greenberger D., Hentschel K., Weinert F. (eds.) *Compendium of Quantum Physics, Concepts, Experiments, History and Philosophy*. Springer, Dordrecht, 2009, 813–822.
100. Omnes R. Decoherence and wave function collapse. *Found. Phys.*, 2011, v.41, 1857–1880.
101. Weinberg S. Collapse of the state vector. *Phys. Rev. A*, 2012, v.85, 062116; arXiv: 1109.6462.

102. Bassi A., Lochan K., Satin S., Singh T.P., Ulbricht H. Models of wave-function collapse, underlying theories, and experimental tests. *Rev. Mod. Phys.*, 2013, v.85, 471–527; arXiv: 1204.4325.
103. Ghirardi G. Collapse theories. In: Zalta E.N. (ed.) *The Stanford Encyclopedia of Philosophy*, Spring 2016 Edition.
104. Schrödinger E. The present situation in quantum mechanics: A translation of Schrödinger's "cat paradox paper" (1935), Translator: Trimmer J.D. *Proc. Am. Philos. Soc.*, 1980, v.124, 323–338.
105. Hobson A. Review and suggested resolution of the problem of Schrödinger's cat. *Contemporary Physics*, 2018, v.59, issue 1, 16–30; arXiv: 1711.11082v1.
106. Schrödinger's cat. Wikipedia.
107. Dumitru S. Phenomenological theory of recorded fluctuations. *Phys. Lett. A.*, 1974, v.48, 109–110.
108. Boyarsky A., Gora P. *Laws of chaos — invariant measures and dynamical systems in one dimension*. Springer Science — Business Media, 2012, 240.
109. Circular error probable. Wikipedia.
110. The Schrödinger's cat thought experiment. http://www.markstokoe.ca/files/Dfp_Mono_v6_5.pdf
111. Dumitru S. Are the higher order correlations resistant against additional noises? *Optik*, 1999, v.110, 110–112.
112. Einstein A., Podolsky B., Rosen N. Can quantum-mechanical description of physical reality be considered complete? *Phys. Rev.*, 1935, v.47, 777–780.
113. Cantrell C.D., Scully M. The EPR paradox revisited. *Physics Reports*, 1978, v.43, issue 13, 499–508.
114. Schlosshauer M. *Prologue to: Elegance and Enigma — The Quantum Interviews*. Springer, Berlin, 2011, 19.
115. Ozawa M. Heisenberg's uncertainty relation — violation and reformulation, *Journal of Physics: Conference Series*, 2014, v.504, 012024.
116. Okamura K., Ozawa M. Universally valid uncertainty relations in general quantum systems. arXiv: 1808.10615v2.
117. Huang X., Zhang T., Jing N. On uncertainty relations in the product form. arXiv: quant-ph/2003.10696v1.
118. Song Q.-C. et al. A stronger multi-observable uncertainty relation. *Sci. Rep.*, 2017, v.7, 44764.
119. Homayouni S. *Some Generalizations of the Heisenberg Uncertainty Principle* (PhD thesis). Ottawa, Ontario, Canada, Carleton University, 2011.
120. Nguyen Q.H., Bui Q.T. Mathematical uncertainty relations and their generalization for multiple incompatible observables. *VNU Journal of Science: Mathematics Physics*, 2017, v.33, 29–34.
121. Madelung E. *Die Mathematischen Hilfsmittel der Physiker*. Springer Verlag, Berlin, 1957; Russian version: Gosizdat, Moscow, 1961.

Laser Action in the Stellar Atmospheres of Wolf-Rayet Stars and Quasi-Stellar Objects (QSOs)

Pierre A. Millette

E-mail: pierre.millette@uottawa.ca, Ottawa, Canada

In this paper, we reconsider the little-known but critically important physical process of laser action occurring in the stellar atmospheres of Wolf-Rayet stars and, by extension, of QSOs, also known as quasars in the cosmological context. We review the use of the Collisional-Radiative (non-LTE) model for hydrogenic and lithium-like ions to calculate the energy level populations and the existing results for He I, He II, C III and C IV, and for N V and O VI. We review the details of laser action in Wolf-Rayet stars, as well as in QSOs. We note that taking QSOs to be local stellar objects eliminates the problems associated with their cosmological interpretation. We propose that the terminology *quasar* be used to refer to the cosmological interpretation and *QSO* to refer to the stellar interpretation of Quasi-Stellar Objects. We introduce a new star type Q for QSOs, similar to the star type W for Wolf-Rayet stars. We expand the Hertzsprung-Russell diagram to include more massive and hotter stars of type Q and W beyond the stars of type O B. The main sequence thus starts with stars of type Q W O B, followed by the rest of the main sequence. Finally, we note the effort that will be required to understand the classification and evolution of stars of type Q, as has been achieved for Wolf-Rayet stars.

1 Introduction

In this paper, we reconsider a little-known but critically important physical process occurring in the stellar atmospheres of Wolf-Rayet stars and, by extension, of Quasi-Stellar Objects (QSOs), also known as quasars in the cosmological context. Wolf-Rayet stars are known to have an expanding envelope of hot ionized gases, as the stellar atmosphere of the star expands, resulting in mass loss.

If the speed of expansion is low, the expansion will be closer to being isothermal, but as the speed of expansion increases, the expansion will become adiabatic. Under those conditions, as the plasma cools, population inversions will occur in the ionic energy levels due to free electron-ion recombination in higher ionic excited states. Some ionic energy level transitions will undergo laser action [1] resulting in spectra dominated by a small number of strong broad emission lines, which becomes even more evident in QSOs.

2 Wolf-Rayet stars

Wolf-Rayet stars [2] are a type of stars that, like the supergiants, have extended atmospheres whose thickness is an appreciable fraction of their stellar radius [3, p. 243]. Characteristic features in the visible spectra of many O and early B stars, particularly supergiants, and WR stars provide evidence that these objects have extensive envelopes, and that the material generating the lines is flowing outward from the stellar photosphere.

The number of WR stars in our galaxy is small: the 2001 VIIth catalog of galactic WR stars gave the number at 227 stars, comprised of 127 WN stars, 87 WC stars, 10 WN/WC stars and 3 WO stars [4]. The subtypes are covered in the

spectra discussion later in this section. A 2006 update added another 72 WR stars, including 45 WN stars, 26 WC stars and one WO star [5]. The latest number from the August 2020 Galactic Wolf Rayet Catalogue v1.25 is 667 WR stars [6].

The existence of large-scale, rapid, and sometimes violent expansions of stellar atmospheres is well-established observationally [3, p. 471]. Beals [7, 8] first recognized that the great breadths of lines in WR spectra, indicating velocities of the order of 3 000 km/s, could be interpreted in terms of rapid outflow of material. His suggestion that the flow was driven by radiation pressure is supported by current dynamical models. Further evidence for mass loss is provided by infrared and radio continuum observations of several OB and WR stars, which are most readily interpreted in terms of free-free emission from an extended, optically-thick envelope having a density profile consistent with steady outflow of the stellar atmosphere [3, p. 550–551].

We know today, from a variety of observational evidence from spacecraft and ground-based observatories, that in the WR and Of stars and in many early-type supergiants, there are massive trans-sonic stellar winds, that have very small outward velocities in the deeper layers of the stars, but a large outward acceleration producing very large velocities ($v/c \approx 0.01$) at great distances from the stars [3, pp. 471–472, 550]. These flows are driven by radiation pressure acting on the stellar atmosphere [3, p. 523].

Mass loss in stellar winds, particularly in the early-type OB supergiants and WR stars, is well established [3, pp. 266, 523]. The analysis of line profiles and infrared emissions imply estimated mass loss rates \dot{M} of order 10^{-6} to $10^{-5} M_{\odot}/\text{year}$ for O stars and perhaps up to $10^{-4} M_{\odot}/\text{year}$ for

WR stars [9, p. 628]. For comparison, mass loss rates for the solar wind is about $10^{-14} M_{\odot}/\text{year}$. The flow velocities rise from close to zero in the stellar photosphere to highly supersonic values within one stellar radius from the surface. The 3 000 km/s flow is thought to be driven by momentum input to the ionized gas from the intense radiation force exerted by the strong spectrum lines of these extremely luminous stars.

Series of extremely strong emission lines can be observed in the spectra of WR stars. The spectra fall into two broad classes: WN, which have prominent lines of nitrogen N and helium He ions, with a very strong He II Pickering series ($n = 4 \rightarrow n'$), and essentially no lines of carbon C; and WC, where the lines of carbon C and oxygen O are prominent along with the helium He ions, while those of nitrogen N seem to be practically absent [3, p. 485]. An additional subtype WO with strong O VI lines has also recently been added as a separate subtype. The spectra are characterized by the dominance of emission lines, notable for the almost total absence of hydrogen H lines [10].

3 Laser action in stellar atmospheres

In initial modelling calculations, Castor [11] used the escape probability method of basic Sobolev theory to treat the transfer of line radiation in a stellar envelope to provide a coarse analysis of the spectral line formation in Wolf-Rayet stars for a line formed in a two-level atom [3, p. 471–472]. He then used this analysis to calculate the populations of the first thirty levels of hydrogen-like He II ions under statistical equilibrium with all radiative and collisional transitions included [12]. He also applied this analysis to 14 terms and all allowed transitions of helium-like C III ions; no case of laser action was found in the calculations as the existing atomic processes used did not provide sufficient pumping of the excited levels to maintain population inversion [13].

Mihalas [3, p. 485–490] carries out a complete multilevel analysis of the spectrum of an ion using statistical equilibrium equations that consider the radiative and collisional processes contributing to the population of each ionic level under consideration. Typically, the only free parameters in this analysis are T_e , the temperature of the free electrons corresponding to the envelope temperature, n_e , the free electron number density and n_{atom} , the total number density of the species (element) under consideration. The analysis is done under Local Thermodynamic Equilibrium (LTE) conditions, that is under conditions in which each volume element of the plasma fulfills all thermodynamic equilibrium laws derived for plasmas in complete thermodynamic equilibrium (CTE) except for Planck's radiation law [40, p. 12–13].

3.1 Plasma lasers

The possibility of using a recombining plasma as an amplifying medium of electromagnetic radiation was first suggested by Gudzenko and Shelepin [14]. Calculations performed on

a hydrogen plasma [15, 17] subsequently confirmed this suggestion. Such plasmas are called plasma lasers [18].

We consider the basic principles of operation of a plasma laser. The mean time between electron collisions determines the rate of establishment of the electron temperature within a plasma. The smallness of the time between elastic collisions in a dense plasma thus makes it possible, in principle, to rapidly reduce the electron temperature of such a plasma. For example, in plasma densities of order $n_i \sim n_e \sim 10^{15} - 10^{16} \text{ cm}^{-3}$, a single distribution of the electrons is established in a time of order $\tau \sim 10^{-11} - 10^{-10} \text{ s}$ [14], where n_i is the ion number density.

Rapid cooling of a strongly ionized plasma results in rapid recombination of the electrons and the ions into highly excited ionic states. The subsequent relaxation of the electrons to the ground state by spontaneous and non-radiative transitions occurs in a time which, for the estimated values of the plasma parameters used in this work, is larger than 10^{-7} s . At those densities, electron-ion recombination occurs by three-body recombination in a time shorter than 10^{-7} s such that a rapid filling-up of the upper excited levels of the ions occurs. Furthermore, since recombination into highly excited states occurs much more rapidly than into lower states, the establishment of large population inversions is favored.

When large population inversions have been established in the excited levels, the plasma is said to be in a stationary drainage state. It is still substantially ionized. As an example of the time involved, Gudzenko et al. [15] find that for a dense low temperature plasma ($T_e \sim 1000 - 6000 \text{ K}$ and n_e -bound and free states $\sim 10^{13} - 10^{16} \text{ cm}^{-3}$), cooled by a factor of twenty, stationary drainage of the excited discrete levels is established in a time $\sim 10^{-8} - 10^{-7} \text{ s}$. Stationary drainage is maintained for a time $\sim 10^{-5} \text{ s}$, and is followed by a stage in which the plasma is weakly ionized and the population densities of its levels return to normal. Gudzenko et al. [17] find that the above conditions can be significantly relaxed; for example, the cooling can be done more slowly or by stages [40, p. 42–43].

3.2 Adiabatic cooling of a plasma

Various mechanisms of free electron cooling can be used. The method of interest to us, rapid cooling of a plasma by adiabatic expansion, was first investigated by Gudzenko et al. [16] both for magnetized and unmagnetized plasmas.

An example of this cooling mechanism is the adiabatic expansion of a plasma jet in a vacuum. The advantage of this method is that continuous amplification, and thus continuous operation of a laser is possible due to the fact that the different stages of the recombining plasma decay at different times. Thus, as the plasma expands, the stages of the recombination process outlined in the previous Section §3.1 are spread over space and the de-excited medium is thus removed from the active lasing zone. Experimental evidence

of laser action due to the adiabatic expansion of highly ionized hydrogen or hydrogenic plasmas has been given by, for example, [19] and [20].

Under adiabatic expansion conditions, the density n and the temperature T of a gas are related by [17]

$$T n^{1-\gamma} = \text{constant} \quad (1)$$

where

$$\gamma = c_P/c_V \quad (2)$$

is the ratio of the specific heat at constant pressure c_P and the specific heat at constant volume c_V . For a monatomic gas and for a fully ionized plasma of hydrogen, we use [17]

$$\gamma = 5/3. \quad (3)$$

However, it should be noted that the actual value of γ for a plasma is slightly smaller than $5/3$. Denoting the initial density and temperature of the plasma by n_0 and T_0 respectively, and the final density and temperature by n and T respectively, we characterize the expansion by the factor

$$f_E = \frac{n_0}{n} > 1 \quad (4)$$

and the ensuing cooling of the plasma by the factor

$$f_C = \frac{T_0}{T} > 1. \quad (5)$$

Then from (1), we have the relation

$$f_C = f_E^{\gamma-1} \quad (6)$$

under adiabatic expansion conditions. In this work, we use $f_C = 5$; then from (6) and (3), $f_E = 11.2$ [40, p. 43–44].

4 The Collisional-Radiative (non-LTE) model

To calculate the non-equilibrium population of the ionic energy levels, we need to use a model that applies to non-LTE plasmas. The Collisional-Radiative (CR) non-LTE model was first proposed and applied to hydrogenic ions by Bates et al. [21,22] and subsequently used by Bates and Kingston [23] and McWhirter and Hearn [24]. It was first applied to helium by Drawin and Emard [25], to lithium by Gordiets et al. [26], and to cesium by Norcross and Stone [27].

The population densities of the energy levels of ions in non-LTE plasmas must be obtained from the rate coefficients of the individual collisional and radiative processes occurring within the plasma, as summarized in Fig. 1. The physical processes included in the CR model include:

- Collisional ionization by electron impact
Rate coefficient: $S_p(T) \text{ cm}^3 \text{ s}^{-1}$
Number of processes: $n_p n_e S_p(T) \text{ cm}^{-3} \text{ s}^{-1}$
- Three-body recombination
Rate coefficient: $\alpha_p(T) \text{ cm}^6 \text{ s}^{-1}$
Number of processes: $n_e^2 n_i \alpha_p(T) \text{ cm}^{-3} \text{ s}^{-1}$

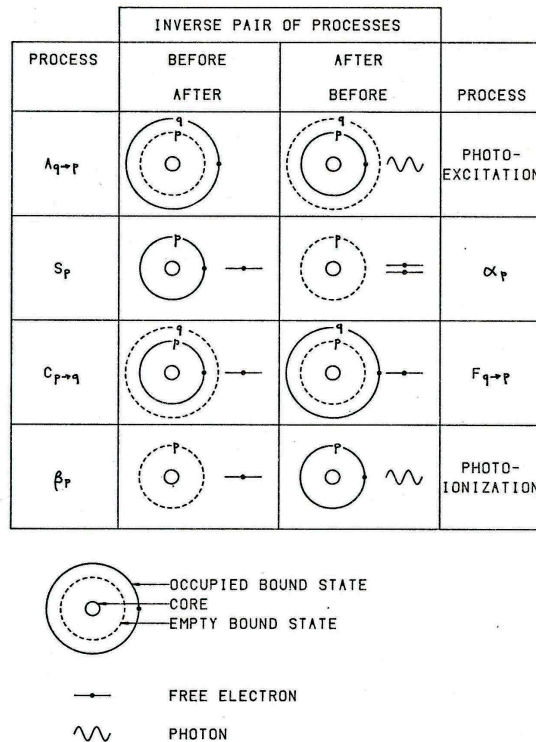


FIGURE 1.2 - PHYSICAL PROCESSES OCCURRING IN A PLASMA.

Fig. 1: This figure provides a summary of the collisional and radiative processes occurring within the plasma, where p and q are ionic energy state labels; $p \geq q$ [40, p. 21].

- Radiative recombination
Rate coefficient: $\beta_p(T) \text{ cm}^3 \text{ s}^{-1}$
Number of processes: $n_e n_i \beta_p(T) \text{ cm}^{-3} \text{ s}^{-1}$
- Collisional excitation by electron impact ($p < q$)
Rate coefficient: $C_{p \rightarrow q}(T) \text{ cm}^3 \text{ s}^{-1}$
Number of processes: $n_p n_e C_{p \rightarrow q}(T) \text{ cm}^{-3} \text{ s}^{-1}$
- Collisional de-excitation by electron impact ($p < q$)
Rate coefficient: $F_{q \rightarrow p}(T) \text{ cm}^3 \text{ s}^{-1}$
Number of processes: $n_q n_e F_{q \rightarrow p}(T) \text{ cm}^{-3} \text{ s}^{-1}$
- Spontaneous transition ($p < q$)
Rate coefficient: $A_{q \rightarrow p} \text{ s}^{-1}$
Number of processes: $n_q A_{q \rightarrow p} \text{ cm}^{-3} \text{ s}^{-1}$

The plasma is assumed to be optically thin such that all radiation emitted within the plasma escapes without being absorbed. The following physical processes are thus neglected:

- Photoexcitation ($p < q$),
- Photoionization.

The differential equation describing the time variation of the population density of a given ionic level p is then given

by

$$\frac{dn_p}{dt} = (\text{electrons entering level } p) - (\text{electrons leaving level } p) . \quad (7)$$

The terms of (7) in parentheses include contributions from all levels $q < p$, $q > p$, and continuum states. Substituting for the collisional and radiative processes considered above, we obtain the differential equation

$$\begin{aligned} \dot{n}_p = & \sum_{q=1}^{p-1} C_{q \rightarrow p} n_e n_q - \\ & - \left[\left(\sum_{q=1}^{p-1} F_{p \rightarrow q} + S_p + \sum_{q=p+1}^{\infty} C_{p \rightarrow q} \right) n_e + \sum_{q=1}^{p-1} A_{p \rightarrow q} \right] n_p + \\ & + \sum_{q=p+1}^{\infty} (F_{q \rightarrow p} n_e + A_{q \rightarrow p}) n_q + \\ & + (\alpha_p n_e + \beta_p) n_e n_i \end{aligned} \quad (8)$$

where the dot over n_p represents differentiation with respect to time. There is such an equation for each and every level $p = 1, 2, \dots, \infty$ of the ion. We thus obtain an infinite number of coupled first order differential equations in the population densities of the discrete levels of the ion.

The population density of level p , n_p , is normalized with the Saha equilibrium population density of level p , n_p^E , [28, p. 154] [29, p. 135]

$$\rho_p = \frac{n_p}{n_p^E}, \quad (9)$$

with n_p^E given by

$$n_p^E = Z_p(T) n_i n_e, \quad (10)$$

where

$$Z_p(T) = \frac{\omega_p}{u_i} \frac{h^3}{2(2\pi m k T)^{3/2}} e^{I_p/kT}, \quad (11)$$

ω_p is the statistical weight of level p , u_i is the ionic partition function, and I_p is the ionization potential of state p . For hydrogenic ions, u_i is the partition function of the bare nucleus and is given by $u_i \simeq 1$. The same holds for lithium-like ions since u_i is then the partition function of a closed shell ion.

The relative population densities of various stages of ionization n_i of a monatomic non-LTE plasma under statistical equilibrium are calculated approximately with the model of House [30]. Even though the calculations are highly simplified, the model provides a first approximation to the ionization equilibrium of monatomic plasmas of hydrogen to iron and a general method of obtaining a consistent set of relative population densities for the ionization stages of these elements.

Given that there exists a high-lying quantum state r above which the discrete levels are in LTE, the normalization (9)

allows us to set the population density of these levels to be given by $\rho_{p>r} = 1$. The infinite set of equations (8) thus becomes a finite set of r coupled equations which can be solved for ρ_p , $p = 1, 2, \dots, r$. The infinite sums appearing in (8) can be cut off at a sufficiently high-lying level $s > r$ above which the rate coefficients involving these states contribute little to the infinite sums of (8). For levels in LTE, detailed balancing between the collisional excitation and de-excitation processes holds and then we can use

$$n_q^E F_{q \rightarrow p} = n_p^E C_{p \rightarrow q}. \quad (12)$$

The set of equations (8) then becomes

$$\begin{aligned} \dot{\rho}_p = & \sum_{q=1}^{p-1} F_{p \rightarrow q} n_e \rho_q - \\ & - \left[\left(\sum_{q=1}^{p-1} F_{p \rightarrow q} + S_p + \sum_{q=p+1}^s C_{p \rightarrow q} \right) n_e + \sum_{q=1}^{p-1} A_{p \rightarrow q} \right] \rho_p + \\ & + \sum_{q=p+1}^r \left(C_{p \rightarrow q} n_e + \frac{Z_q}{Z_p} A_{q \rightarrow p} \right) \rho_q + \frac{1}{Z_p} (\alpha_p n_e + \beta_p) + \\ & + \sum_{q=r+1}^s \left(C_{p \rightarrow q} n_e + \frac{Z_q}{Z_p} A_{q \rightarrow p} \right); p = 1, 2, \dots, r. \end{aligned} \quad (13)$$

4.1 Solution of the system of coupled differential equations

The exact solution of the system of couple differential equations (13) gives the time evolution of the population densities of the ionic levels $\rho_p(t)$, $p = 1, 2, \dots, r$. This solution if of limited use. A simpler solution, known as the quasi-steady state (QSS) approximation, holds for a large class of plasmas and is used extensively in the literature (see [21, 22] and subsequent papers mentioned previously in §4). The steady state (SS) solution is obtained by putting

$$\dot{\rho}_p^{SS}(t) = 0; p = 1, 2, \dots, r. \quad (14)$$

This time-independent solution holds when the rate at which the electrons enter level p equals the rate at which they leave level p . Once the steady state solution is established, a perturbation of the population density of level p will be followed by a return to its steady state value in a time of order

$$\tau_p \sim \left\{ \left[\sum_{q=1}^{p-1} F_{p \rightarrow q} + S_p + \sum_{q=p+1}^s C_{p \rightarrow q} \right] n_e + \sum_{q=1}^{p-1} A_{p \rightarrow q} \right\}^{-1} \quad (15)$$

where τ_p is the relaxation time of level p .

McWhirter and Hearn [24] have calculated τ_p for a wide range of plasma parameters. They conclude that the relaxation time of the ground state is always much greater than that of any of the excited states, even if the plasma is not

near its steady state. This is due to two main reasons: a) the electron collision rate coefficients between excited states are much greater than those involving the ground state; b) the ground state cannot decay by spontaneous radiative transition. Consequently, the population densities of the excited ionic levels come into equilibrium with particular values of the population densities of the ground state, of the free electrons, and of the ions in a time which is very short as compared to the ground state relaxation time. This is the basis of the QSS solution.

4.2 The population coefficients

We thus express the population densities of the excited states as a function of the ground state population density:

$$\rho_p = r_p^{(0)} + r_p^{(1)} \rho_1 ; p = 2, 3, \dots, r. \quad (16)$$

$r_p^{(0)}$ and $r_p^{(1)}$ are called the population coefficients of level p . Furthermore, since the population densities of the excited states are in equilibrium with that of the ground state, we solve the system of coupled equations (13) by putting $\dot{\rho}_{p \geq 2} = 0$ and $\dot{\rho}_1 \neq 0$ since, in general, the ground state is not in equilibrium. In our calculations, we also assume that the free electron and ionic densities, n_e and n_i respectively, do not change substantially during the time of establishment of the QSS.

Substituting the trial solution (16) in the system of equations (13), we obtain a set of equations of the form

$$a_p + b_p \rho_1 = 0 ; p = 2, 3, \dots, r. \quad (17)$$

The general solution of (17), for an arbitrary value of ρ_1 , is $a_p = 0$ and $b_p = 0$. Before proceeding with the solution, certain limiting conditions must be imposed on the population coefficients $r_p^{(0)}$ and $r_p^{(1)}$ corresponding to the cases when $p = 1$ and $p > r$. Substituting $p = 1$ in (16), we obtain the condition $r_1^{(0)} = 0$ and $r_1^{(1)} = 1$. The other condition, which is obtained by putting $p > r$ in (16), has already been imposed on the set of equations, namely $r_{p>r}^{(0)} = 1$ and $r_{p>r}^{(1)} = 0$.

Using these conditions, we obtain the following two sets of $r - 1$ equations in the population coefficients $r_p^{(0)}$ and $r_p^{(1)}$ respectively:

$$\begin{aligned} & \sum_{q=2}^{p-1} F_{p \rightarrow q} n_e r_q^{(0)} - \\ & - \left[\left(\sum_{q=2}^{p-1} F_{p \rightarrow q} + S_p + \sum_{q=p+1}^s C_{p \rightarrow q} \right) n_e + \sum_{q=1}^{p-1} A_{p \rightarrow q} \right] r_p^{(0)} + \\ & + \sum_{q=p+1}^r \left(C_{p \rightarrow q} n_e + \frac{Z_q}{Z_p} A_{q \rightarrow p} \right) r_q^{(0)} = -\frac{1}{Z_p} (\alpha_p n_e + \beta_p) - \\ & - \sum_{q=r+1}^s \left(C_{p \rightarrow q} n_e + \frac{Z_q}{Z_p} A_{q \rightarrow p} \right); \end{aligned} \quad (18)$$

$$\begin{aligned} & \sum_{q=2}^{p-1} F_{p \rightarrow q} n_e r_q^{(1)} - \\ & - \left[\left(\sum_{q=1}^{p-1} F_{p \rightarrow q} + S_p + \sum_{q=p+1}^s C_{p \rightarrow q} \right) n_e + \sum_{q=1}^{p-1} A_{p \rightarrow q} \right] r_p^{(1)} + \\ & + \sum_{q=p+1}^r \left(C_{p \rightarrow q} n_e + \frac{Z_q}{Z_p} A_{q \rightarrow p} \right) r_q^{(1)} = \\ & = -F_{p \rightarrow 1} n_e ; p = 2, 3, \dots, r. \end{aligned} \quad (19)$$

4.3 The population densities

Once the population coefficients $r_p^{(0)}$ and $r_p^{(1)}$ have been obtained from the sets of equations (18) and (19) respectively, they are substituted in (16). For any value of ρ_1 , the population densities ρ_p can then be calculated. From (9) and (10),

$$\rho_p = \frac{n_p}{Z_p n_i n_e}; \quad (20)$$

substituting (20) in (16), we obtain

$$n_p = Z_p n_i n_e r_p^{(0)} + \frac{Z_p}{Z_1} n_1 r_p^{(1)} ; p = 2, 3, \dots, r. \quad (21)$$

As required by the QSS approximation, the population density of the excited state p depends on the value of the ground state population density n_1 , the free electron density n_e , and the ionic density n_i . The population density per unit statistical weight is given by $y_p = n_p / \omega_p$, where ω_p is the statistical weight of level p . The population density per unit statistical weight must be used when the population densities of different states are compared.

4.4 The collisional-radiative rate coefficients

The time evolution of the population density of the ground state can be studied with (13) when $p = 1$. Substituting for ρ_p from (16), and using the previously calculated population coefficients and (9), we obtain the differential equation

$$\dot{n}_1 = -S_{CR} n_e n_1 + \alpha_{CR} n_e n_i. \quad (22)$$

S_{CR} and α_{CR} are called the collisional-radiative ionization and recombination rate coefficients respectively. They are the effective ionization and recombination rate coefficients of the plasma. They are related to the individual atomic rate coefficients by the following expressions:

$$S_{CR} = S_1 + \sum_{q=2}^s C_{1 \rightarrow q} - \frac{1}{Z_1 n_e} \sum_{q=2}^s Z_q (F_{q \rightarrow 1} n_e + A_{q \rightarrow 1}) r_q^{(1)} ; \quad (23)$$

$$\alpha_{CR} = \alpha_1 n_e + \beta_1 + \sum_{q=2}^s Z_q (F_{q \rightarrow 1} n_e + A_{q \rightarrow 1}) r_q^{(0)}. \quad (24)$$

The solution of (22) can easily be shown to be given by

$$n_1(t) = \frac{\alpha_{CR}}{S_{CR}} n_i + \left(n_1(t=0) - \frac{\alpha_{CR}}{S_{CR}} n_i \right) e^{-S_{CR} n_e t}. \quad (25)$$

The steady state population density of the ground state is obtained in the limit $t \rightarrow \infty$:

$$n_1^{SS} = \frac{\alpha_{CR}}{S_{CR}} n_i. \quad (26)$$

4.5 Modifications for lithium-like ions

The CR model must be modified to account for the difference in structure of lithium-like and hydrogenic ions considered previously. The same system of state labelling is used: the ground state ($2s$) is labelled 1, the first excited state ($2p$) is labelled 2, the second excited state ($3s$) is labelled 3, and so on in order of increasing level energy. The derivation of the equations of the CR plasma model for lithium-like ions then parallels that given previously for hydrogenic ions.

The time evolution of the population density of level p in an optically thin plasma is given by (13) as before. The steady state (SS) solution to the set of coupled first order differential equations (13) is obtained as before from (14). However, the quasi-steady state (QSS) solution must be modified to account for the small energy separation of the ground and the first excited states as compared to that of the first and the second excited states, as this is particularly significant for ions with large values of Z such as C IV, N V, and O VI. As a result of this, the population density of the first excited state (level 2) is very much larger than that of the other excited states, and it may even be comparable to that of the ground state.

Consequently, the QSS solution is modified by using a method similar to the one developed by Bates et al. [22] to describe hydrogenic plasmas optically thick toward the lines of the Lyman series. The normalized population density of level p is expressed as a function of the ground and the first excited state population densities:

$$\rho_p = r_p^{(0)} + r_p^{(1)} \rho_1 + r_p^{(2)} \rho_2 \quad (27)$$

where $3 \leq p \leq r$ and $r_p^{(0)}$, $r_p^{(1)}$ and $r_p^{(2)}$ are the population coefficients of level p . The QSS solution is obtained when the population densities of the second and higher excited states are in equilibrium with the population densities of the ground and the first excited states which, in general, are not in equilibrium. We then have $\dot{\rho}_1(t) \neq 0$, $\dot{\rho}_2(t) \neq 0$, and $\dot{\rho}_{p \geq 3}(t) = 0$.

Substituting the solution (27) in the system of equations (13), and using the last condition above, we obtain a set of equations of the form

$$a_p + b_p \rho_1 + c_p \rho_2 = 0; p = 3, 4, \dots, r. \quad (28)$$

For arbitrary values of ρ_1 and ρ_2 , the general solution of (28) is given by $a_p = 0$, $b_p = 0$, and $c_p = 0$. We must also

impose the limiting conditions corresponding to the values of $p = 1, 2$ and $p > r$ on the population coefficients $r_p^{(0)}$, $r_p^{(1)}$ and $r_p^{(2)}$: $r_1^{(0)} = 0$, $r_1^{(1)} = 1$, $r_1^{(2)} = 0$; $r_2^{(0)} = 0$, $r_2^{(1)} = 0$, $r_2^{(2)} = 1$; $r_{p>r}^{(0)} = 1$, $r_{p>r}^{(1)} = 0$, $r_{p>r}^{(2)} = 0$. This last condition has already been applied to derive the system of equations (13).

Using these conditions, we obtain three sets of $r-2$ equations which are solved for the population coefficients $r_p^{(0)}$, $r_p^{(1)}$ and $r_p^{(2)}$ respectively:

$$\sum_{q=3}^{p-1} \mathcal{A}_{pq} r_q^{(0)} - \mathcal{B}_p r_p^{(0)} + \sum_{q=p+1}^r C_{pq} r_q^{(0)} = -\frac{1}{Z_p} (\alpha_p n_e + \beta_p) - \sum_{q=r+1}^s \left(C_{p \rightarrow q} n_e + \frac{Z_q}{Z_p} A_{q \rightarrow p} \right); \quad (29)$$

$$\sum_{q=3}^{p-1} \mathcal{A}_{pq} r_q^{(1)} - \mathcal{B}_p r_p^{(1)} + \sum_{q=p+1}^r C_{pq} r_q^{(1)} = -F_{p \rightarrow 1} n_e; \quad (30)$$

$$\sum_{q=3}^{p-1} \mathcal{A}_{pq} r_q^{(2)} - \mathcal{B}_p r_p^{(2)} + \sum_{q=p+1}^r C_{pq} r_q^{(2)} = -F_{p \rightarrow 2} n_e \quad (31)$$

where

$$\mathcal{A}_{pq} = F_{p \rightarrow q} n_e; \quad (32)$$

$$\mathcal{B}_p = \left(\sum_{q=1}^{p-1} F_{p \rightarrow q} + S_p + \sum_{q=p+1}^s C_{p \rightarrow q} \right) n_e + \sum_{q=1}^{p-1} A_{p \rightarrow q}; \quad (33)$$

$$C_{pq} = C_{p \rightarrow q} n_e + \frac{Z_q}{Z_p} A_{q \rightarrow p}; p = 3, 4, \dots, r. \quad (34)$$

From the population coefficients $r_p^{(0)}$, $r_p^{(1)}$ and $r_p^{(2)}$, the population densities n_p can be calculated for any value of n_1 and n_2 from

$$n_p = Z_p n_i n_e r_p^{(0)} + \frac{Z_p}{Z_1} n_1 r_p^{(1)} + \frac{Z_p}{Z_2} n_2 r_p^{(2)}; \quad (35)$$

$$p = 3, 4, \dots, r$$

where n_i is the ionic density. The time evolution of the population densities of the ground state and the first excited state, n_1 and n_2 respectively, can be obtained by substituting (27) and the population coefficients $r_p^{(0)}$, $r_p^{(1)}$ and $r_p^{(2)}$ into (13) with $p = 1$ and $p = 2$. We then get the two coupled first order differential equations

$$\dot{n}_1 = -S_1^{CR} n_e n_1 + M_{21}^{CR} n_e n_2 + \alpha_1^{CR} n_e n_i \quad (36)$$

$$\dot{n}_2 = -S_2^{CR} n_e n_2 + M_{12}^{CR} n_e n_1 + \alpha_2^{CR} n_e n_i$$

where

$$S_1^{CR} = S_1 + \sum_{q=2}^s C_{1 \rightarrow q} - \frac{1}{n_e Z_1} \sum_{q=3}^s (F_{q \rightarrow 1} n_e + A_{q \rightarrow 1}) Z_q r_q^{(1)}; \quad (37)$$

$$S_2^{CR} = S_2 + F_{2 \rightarrow 1} + \frac{1}{n_e} A_{2 \rightarrow 1} + \sum_{q=3}^s C_{2 \rightarrow q} - \frac{1}{n_e Z_2} \sum_{q=3}^s (F_{q \rightarrow 2} n_e + A_{q \rightarrow 2}) Z_q r_q^{(2)}; \quad (38)$$

$$\alpha_1^{CR} = \alpha_1 n_e + \beta_1 + \sum_{q=3}^s (F_{q \rightarrow 1} n_e + A_{q \rightarrow 1}) Z_q r_q^{(0)}; \quad (39)$$

$$\alpha_2^{CR} = \alpha_2 n_e + \beta_2 + \sum_{q=3}^s (F_{q \rightarrow 2} n_e + A_{q \rightarrow 2}) Z_q r_q^{(0)}; \quad (40)$$

$$M_{21}^{CR} = F_{2 \rightarrow 1} + \frac{1}{n_e} A_{2 \rightarrow 1} + \frac{1}{n_e Z_2} \sum_{q=3}^s (F_{q \rightarrow 1} n_e + A_{q \rightarrow 1}) Z_q r_q^{(2)}; \quad (41)$$

$$M_{12}^{CR} = C_{1 \rightarrow 2} + \frac{1}{n_e Z_1} \sum_{q=3}^s (F_{q \rightarrow 2} n_e + A_{q \rightarrow 2}) Z_q r_q^{(1)}. \quad (42)$$

The coefficients S_1^{CR} , S_2^{CR} and α_1^{CR} , α_2^{CR} are similar to the hydrogenic collisional-radiative ionization rate coefficient S_{CR} (23) and recombination rate coefficient α_{CR} (24) respectively. The coefficients M_{21}^{CR} and M_{12}^{CR} have no hydrogenic counterparts. The collisional-radiative rate coefficient M_{21}^{CR} expresses the recombination which occurs in the ground state due to the neighbouring first excited state and vice versa for the collisional-radiative rate coefficient M_{12}^{CR} .

The general solution of the coupled system of equations (36) can be written as

$$n_j(t) = n_j^{SS} + n_j^{(+)} e^{-\lambda^{(+)} t} - n_j^{(-)} e^{-\lambda^{(-)} t} \quad (43)$$

where $j = 1$ or 2 ,

$$\lambda^{(\pm)} = \frac{n_e}{2} \left(S_1^{CR} + S_2^{CR} \pm \sqrt{(S_1^{CR} - S_2^{CR})^2 + 4 M_{12}^{CR} M_{21}^{CR}} \right), \quad (44)$$

$$n_j^{SS} = \frac{K_j^{SS}}{\lambda^{(+)} \lambda^{(-)}}, \quad (45)$$

$$n_j^{(\pm)} = \frac{n_j(t=0) \lambda^{(\pm)^2} - K_j \lambda^{(\pm)} + K_j^{SS}}{\lambda^{(\pm)} (\lambda^{(+)} - \lambda^{(-)})}, \quad (46)$$

$$K_1^{SS} = n_e^2 n_i (\alpha_1^{CR} S_2^{CR} + \alpha_2^{CR} M_{21}^{CR}), \quad (47)$$

$$K_2^{SS} = n_e^2 n_i (\alpha_2^{CR} S_1^{CR} + \alpha_1^{CR} M_{12}^{CR}), \quad (48)$$

$$K_1 = n_e (\alpha_1^{CR} n_i + S_2^{CR} n_1(t=0) + M_{21}^{CR} n_2(t=0)), \quad (49)$$

$$K_2 = n_e (\alpha_2^{CR} n_i + S_1^{CR} n_2(t=0) + M_{12}^{CR} n_1(t=0)). \quad (50)$$

The steady state population densities, which are obtained in the limit as $t \rightarrow \infty$, are explicitly given by

$$n_1^{SS} = \frac{\alpha_1^{CR} S_2^{CR} + \alpha_2^{CR} M_{21}^{CR}}{S_1^{CR} S_2^{CR} - M_{12}^{CR} M_{21}^{CR}} n_i; \quad (51)$$

$$n_2^{SS} = \frac{S_1^{CR} \alpha_2^{CR} + \alpha_1^{CR} M_{12}^{CR}}{S_1^{CR} S_2^{CR} - M_{12}^{CR} M_{21}^{CR}} n_i. \quad (52)$$

4.6 Calculation of collisional and radiative rate coefficients

The results of the modelling calculations depend to a large extent on the accuracy of the collisional and radiative rate coefficients used in the CR model. The collisional rate coefficients R_n are obtained by integrating the cross-sections σ_n of the collisional processes over the free electron velocity distribution, $f(v)$:

$$R_n(T) = \int_v \sigma_n(v) v f(v) dv. \quad (53)$$

For a Maxwellian velocity distribution of the free electrons, we have

$$f(v) dv = \frac{4}{\sqrt{\pi}} \left(\frac{m}{2kT} \right)^{3/2} v^2 \exp(-mv^2/2kT) dv. \quad (54)$$

The cross-section values are obtained from experimental data, where available, and from various model and theoretical calculations that are usually fitted to semi-empirical expressions. We briefly review the expressions that have been found to be useful in CR model calculations [40].

The spontaneous transition probabilities from an upper state n to a lower state n' are given, within the electric dipole approximation, by the Einstein probability coefficient [31]

$$A_{n \rightarrow n'} = \frac{8\pi^2 e^2}{mc^3} \nu_{nn'}^2 \frac{\omega_{n'}}{\omega_n} f_{n' \rightarrow n} \quad (55)$$

where ω_n and $\omega_{n'}$ are the statistical weights of levels n and n' respectively, $\nu_{nn'}$ is the frequency of the photon emitted as a result of the transition and $f_{n' \rightarrow n}$ is the absorption oscillator strength for the $n' \rightarrow n$ transition. The oscillator strengths can be evaluated exactly for hydrogenic ions using hypergeometric functions. Average lifetime of hydrogenic levels can be calculated from the asymptotic expression given by Millette [32]. For other elements, oscillator strengths for allowed and forbidden transitions can be evaluated using various approximate theoretical methods.

The cross-section for collisional excitation of the optically allowed transition $n' \rightarrow n$ by electron impact is given by [40]

$$\sigma_{n' \rightarrow n}(u) = 4\pi a_0^2 \frac{f_{n' \rightarrow n}}{E_{n'n}^2} \alpha_{n'n} \frac{u - \phi_{n'n}}{u^2} \ln(1.25 \beta_{n'n} u) \quad (56)$$

where $E_{n'n}$ is the threshold energy for the excitation of the $n' \rightarrow n$ transition in Rydbergs, $u = E/E_{n'n}$ is the energy of the impacting electron E in threshold units, $f_{n' \rightarrow n}$ is the absorption oscillator strength for the $n' \rightarrow n$ transition, a_0 is the Bohr radius and $\alpha_{n'n}$, $\beta_{n'n}$ and $\phi_{n'n} \leq 1$ (equal to 1 for atoms) are fit parameters depending on the transition.

The cross-section for collisional excitation of the optically forbidden transition $n' \rightarrow n$ by electron impact is given by [40]

$$\sigma_{n' \rightarrow n}(u) = 4\pi a_0^2 \left(\frac{n'}{n}\right)^3 \frac{\alpha_{n'n}}{E_{n'n}^2} \frac{u - \phi_{n'n}}{u^2} \quad (57)$$

where $E_{n'n}$ is the threshold energy for the excitation of the $n' \rightarrow n$ transition in Rydbergs, $u = E/E_{n'n}$ is the energy of the impacting electron E in threshold units, a_0 is the Bohr radius and $\alpha_{n'n}$ and $\phi_{n'n}$ are fit parameters depending on the transition.

The collisional de-excitation rate coefficients are obtained from the collisional excitation rate coefficients by the principle of detailed balancing as given by (12).

The collisional ionization cross-section from state n by electron impact is given by [33, 40]

$$\sigma_n(u) = 2.66 \pi a_0^2 \left(\frac{I_1^H}{I_n}\right)^2 \xi_n \frac{u-1}{u^2} \ln(1.25 \beta_n u) \quad (58)$$

where $I_1^H = E_1^H$ is the ionization energy of the hydrogen atom in its ground state, $I_n = E_n$ is the ionization energy of the atom or ion in state n , $u = E/I_n$ is the kinetic energy of the incident electron in units of the threshold energy for ionization from state n , ξ_n is the number of equivalent electrons in state n and β_n is a correction (fit) factor of order unity. To obtain the correct threshold law, β_n must be larger than 0.8.

The three-body recombination rate coefficients are obtained from the collisional ionization rate coefficients by the principle of detailed balancing.

The radiative recombination rate coefficients can be obtained from the photo-ionization rate coefficients by the principle of detailed balancing. The available experimental and calculated photo-ionization data are fitted to a semi-empirical function of the form [40]

$$a(u) = \frac{C}{u^p} \left[1 + \frac{b_1}{u} + \frac{b_2}{u^2} + \dots + \frac{b_m}{u^m} \right] \quad (59)$$

where u is the energy of the incident photon in threshold energy units, and C and b_k , $k = 1, \dots, m$ are fit parameters. The parameters p and m are restricted to the range of values $0 \leq p \leq 5$ and $1 \leq m \leq 9$, and p is assigned half-integral values to simplify and facilitate the evaluation of the rate coefficient integrals.

5 Laser action in Wolf-Rayet stars

The strength of an inversely populated transition $q \rightarrow p$ ($p < q$) can be characterized by the fractional gain per unit dis-

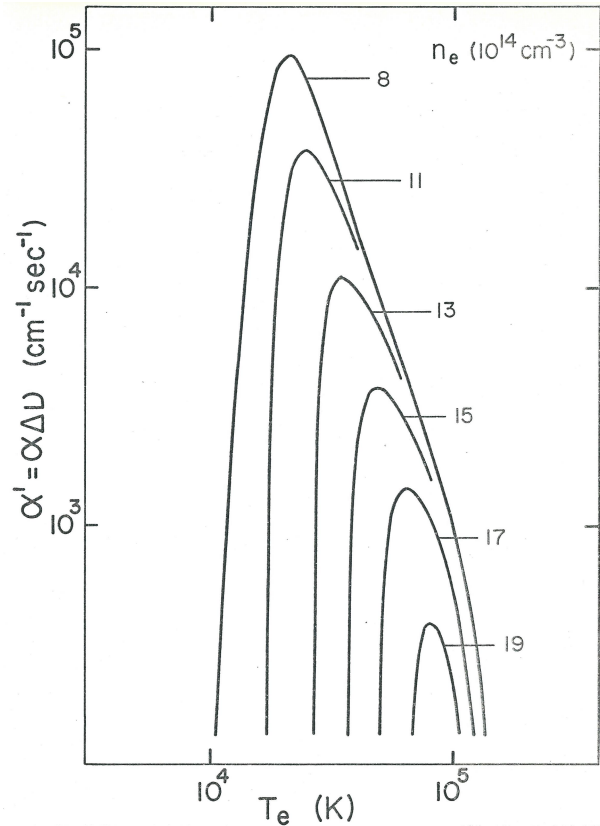


Fig. 2: Typical α' versus T_e plot for the $6f \rightarrow 5d$ transition of C IV [40, p. 249].

tance, α . At the centre of a Doppler-broadened line, it is given by the following expression [34, p. 23]:

$$\alpha = \sqrt{\frac{\ln 2}{\pi}} \left(\frac{\omega_q A_{q \rightarrow p}}{4\pi} \right) \frac{P \lambda_0^2}{\Delta\nu} \quad (60)$$

where λ_0 is the centre wavelength of the transition, $\Delta\nu$ is the linewidth, ω_q is the statistical weight of level q , $A_{q \rightarrow p}$ is the Einstein probability coefficient for spontaneous transition from level q to p , and [35]

$$P = \frac{n_q}{\omega_q} - \frac{n_p}{\omega_p} \quad (61)$$

P is a measure of the population inversion and, for laser action to be operative, $P > 0$. α is related to the intensity of a plane wave at λ_0 by the equation

$$I = I_0 e^{\alpha L} \quad (62)$$

where L is the length over which gain occurs. To be able to compare various transitions without needing to specify the linewidth $\Delta\nu$, we define a quantity α' given by

$$\alpha' = \alpha \Delta\nu \quad (63)$$

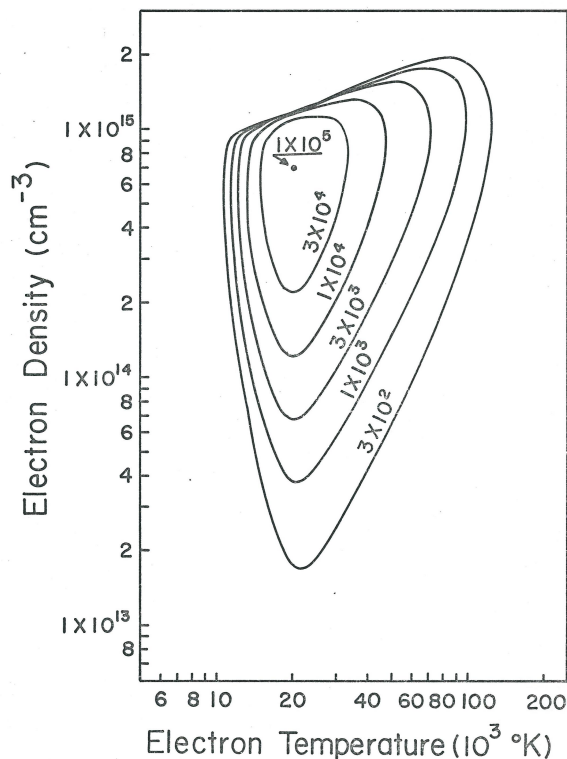


Figure 9.13 - $n_e - T_e$ diagram for the $6f \rightarrow 5d$ transition of C IV ($\lambda 4646$).

Fig. 3: Typical $n_e - T_e$ diagram showing laser gain equi- α' contours in $\text{cm}^{-1} \text{s}^{-1}$ for the $6f \rightarrow 5d$ transition of CIV [40, p. 257].

where α is given by (60).

Model calculations starting from an initial element number density of 10^{14} cm^{-3} are performed for a grid of n_e and T_e values. The inversion is displayed on n_e, T_e plots ($n_e - T_e$ diagrams) showing contours of equal P or α' (equi- α' contours). Fig. 2 shows a typical variation of α' versus T_e for inversely populated transition $6f \rightarrow 5d$ of CIV. Fig. 3 shows a typical $n_e - T_e$ diagram with equi- α' contours for inversely populated transition $6f \rightarrow 5d$ of CIV.

On a three-dimensional plot with α' as the third axis perpendicular to both the n_e and T_e axes, the diagram would appear as a triangular pyramidal-shaped mountain with a very steep slope on the high- n_e side, a steep slope on the low- T_e side, and a gradual slope on the low- n_e , high- T_e side. Strong population inversion thus occurs only within a narrow range of values of n_e and T_e , and each transition has its own region of strong population inversion. This provides a means to classify Wolf-Rayet star parameters from their spectra.

Calculations of population inversions in astronomical plasmas cooled by adiabatic expansion have been performed on ions observed in WR stars by the following investigators. Varshni and Lam [37–39] investigated population inversions in the hydrogen-like He II ion for line $\lambda 4686$ resulting from the transition $4 \rightarrow 3$ in He II.

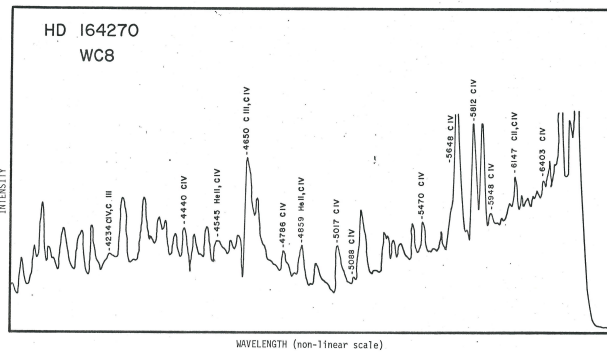


Fig. 4: Spectrum of the WC8 star HD 164270 from [36].

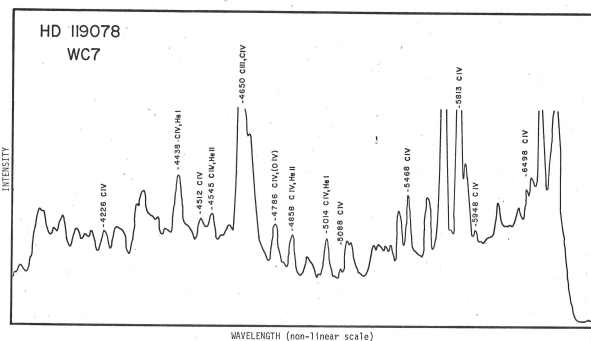


Fig. 5: Spectrum of the WC7 star HD 119078 from [36].

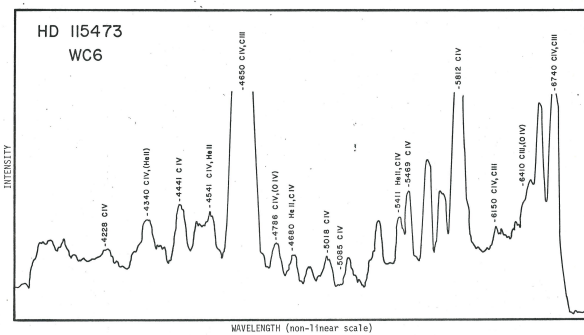


Fig. 6: Spectrum of the WC6 star HD 115473 from [36].

Millette [40] analyzed population inversions in the lithium-like ions C IV, N V and O VI. Population inversions were found to occur in many of the transitions. CIV transitions giving rise to emission lines in the visible region of the spectrum, specifically line $\lambda 4650$ resulting from transitions between levels $6 \rightarrow 5$ in CIV, were investigated. The CIV $\lambda 4646, 4658$ lines arising from the $6f \rightarrow 5d$ and $6g \rightarrow 5f$ transitions respectively, were found to be strongly inverted allowing laser action in plasmas cooled by adiabatic expansion.

The model calculations provide an understanding of the unusual strength of the CIV $\lambda 4650$ emission line in the WC

category of Wolf-Rayet stars, as seen in Fig. 4, Fig. 5 and Fig. 6, which shows the $\lambda 4650$ line becoming more and more prominent in going from a category WC8 to a WC6 Wolf-Rayet star. The lines in WC8 WR stars are relatively sharp, becoming wider and brighter in WC7 WR stars, and even wider and brighter in WC6 WR stars, indicating increasing speed of ejection and increasing laser action.

Varshni and Nasser [41,42] investigated population inversions in He I and in helium-like C III. Four transitions were investigated in the visible region of He I, $\lambda 7281 3^1S \rightarrow 2^1P$, $\lambda 6678 3^1D \rightarrow 2^1P$, $\lambda 5047 4^1S \rightarrow 2^1P$ and $\lambda 4922 4^1D \rightarrow 2^1P$, of which observational evidence is available for $\lambda 7281$ and $\lambda 6678$ in WR stars. Two transitions showed appreciable population inversion in the visible region of C III: $\lambda 4650 2s3p^3S \rightarrow 2p3p^3S$ and $\lambda 5263 2p3p^3S \rightarrow 2p3s^3P^0$.

Millette [40] provides a detailed roadmap to calculate population inversions in hydrogenic and in the lithium-like ions N V and O VI, in addition to C IV.

6 Laser action in Quasi-Stellar Objects

The physical process of population inversions in expanding stellar atmospheres led Varshni to formulate his Plasma Laser Star (PLS) model as an explanation of the spectra of Wolf-Rayet stars and Quasi-Stellar Objects [43–48]. Radio astronomy first detected QSOs in the 1950s as anomalous objects with unexplained properties. QSO 3C 273 was the first radio source quasar for which an optical counterpart was identified in 1963. Its spectrum consisted of one strong emission line and one medium to weak strength line ($\lambda 5637, \lambda 7588$).

QSOs were named quasi-stellar because they look like stars, if not typical stars. In particular QSO spectra are dominated by a small number of very intense and wide lines that could not be readily identified with common elements. In particular, there was a lack of the expected hydrogen Lyman lines, a typical marker in most spectra. This likely provided the impetus for Schmidt [49] to assume that the observed lines in 3C 273 were the $H\alpha$ and $H\beta$ lines, red-shifted to their observed wavelength in the spectrum. This quickly became the standard approach, and ever since, astronomy and cosmology have been transformed, with everything looking like red-shifted objects, even if those red-shifts are superluminal.

Luckily, this possibility did not exist when Wolf-Rayet stars were first discovered in 1867 by astronomers Charles Wolf and George Rayet at the Paris Observatory, otherwise we would be facing an even more confusing puzzle, as hydrogen emission lines are not present in WR spectra either. As chance would have it, WR stars were investigated as stellar objects, which allowed us to eventually determine the presence of laser action in WR stellar atmospheres, which is the same process that is operating in QSO stellar atmospheres.

Banerji and Bhar [50–52] have compared the (unshifted) spectral lines of 633 QSOs discovered till August 1976, assuming they are generated by a population inversion process

similar to that operating in WR stars instead of red shifts, with the laser transitions observed in laboratories till April 1976 [53]. They found that 88% of the QSO lines agreed to within 10 \AA with the laser lines and 94% agreed to within 20 \AA . Their assumption that QSOs are early-type stars with temperatures in the range 104–105 K implied spectral lines with asymmetric shapes and large broadening leading to errors in measurement of up to 20 \AA . They pointed out the similarities between the spectra of QSOs and those of Wolf-Rayet stars, with both deficient in hydrogen. They proposed that the absorption lines of QSOs are produced in the expanding stellar atmosphere, so that they are violet-shifted as in WR stars. Under this model, they showed that 54 of 55 narrow absorption lines in QSO Q 1246-057 can be explained by assuming an average velocity of absorbing ions of 500 km/s.

Taking Quasi-Stellar Objects to be local stellar objects instead of distant galactic objects eliminates the problems associated with their currently accepted cosmological interpretation: energy source, superluminal velocities, optical variability, quasar proper motions [54, 55], quasar binary systems [56, 57], naked (no nebulosity) quasars, *etc.* The properties of QSOs are similar to those of WR stars and, as stars, those are easily explainable in terms of commonly known physical processes.

7 A new star type Q and the Hertzsprung-Russell diagram

We consider the implications of Quasi-Stellar Objects as stellar objects. We need to first be more specific about the terminology used: we use the term *quasar* to refer specifically to the cosmological interpretation of Quasi-Stellar Objects, while we use the term *QSO* to refer to the stellar interpretation of Quasi-Stellar Objects. We introduce a new star type to denote QSOs: stars of type Q, similar to the Wolf-Rayet stars which are denoted as stars of type W.

The Hertzsprung-Russell diagram is extended beyond the stars of type O B towards more massive and hotter stars of type Q and W. The main sequence starts with Q W O B, followed by the standard A F G K M types of the rest of the sequence. As one moves towards star type Q, the stars become increasingly more massive, of higher temperature, with higher speeds of stellar atmosphere ejection and population inversions, with their emission spectra increasingly dominated by the lasing emission lines.

Significant work has been performed on the analysis of WR stars to understand their classification and evolution. WR stars are known to be hot, luminous objects, representative of the late stage of evolution of massive O stars. The details have been worked out over the last forty years [2, 10, 58–65] with the analysis of Wolf-Rayet stars in the Magellanic Clouds dwarf satellite galaxies of the Milky Way providing valuable information. A similar effort is required to understand the classification and evolution of stars of type Q, with the iden-

tification of unrecognized representatives in our galaxy and in the Magellanic Clouds an important step [55, 66].

8 Discussion and conclusion

In this paper, we have reconsidered the little-known but critically important physical process of laser action occurring in the stellar atmospheres of Wolf-Rayet stars and, by extension, of QSOs. We have reviewed the model used for hydrogenic and lithium-like ions in the Collisional-Radiative (non-LTE) model used to calculate the ionic energy level populations, and the existing results for He I, He II, C III and C IV. We have noted the availability of a detailed roadmap in [40] to carry out similar calculations for the lithium-like ions of interest N V and O VI.

We have reviewed the details of laser action in Wolf-Rayet stars. We have considered the historical bifurcation that resulted in the red-shift model of quasar spectra and its cosmological roots. We have also considered the evidence for the presence of laser action in QSOs as in Wolf-Rayet stars, and how taking QSOs to be local stellar objects instead of distant galactic objects eliminates the problems associated with the currently accepted cosmological interpretation.

We have introduced the terminology *quasar* to refer specifically to the cosmological interpretation of Quasi-Stellar Objects and *QSO* to refer to the stellar interpretation of Quasi-Stellar Objects. We have introduced a new star type Q for QSOs, similar to the star type W for Wolf-Rayet stars. We have expanded the Hertzsprung-Russell diagram to include more massive and hotter stars of type Q and W beyond the stars of type O B. The main sequence thus starts with stars of type Q W O B, followed by the standard types A F G K M of the rest of the sequence. Finally, we have noted the effort that will be required to understand the classification and evolution of stars of type Q, as has been achieved for Wolf-Rayet stars.

Received on December 27, 2020

References

1. Menzel D.H. Laser Action in non-LTE Atmospheres. International Astronomical Union Colloquium, Volume 2: Spectrum Formation in Stars With Steady-State Extended Atmospheres, 1970, 134–137.
2. Crowther P.A. Physical Properties of Wolf-Rayet Stars. *Annu. Rev. Astron. Astrophys.*, 2007, v. 45, 177–219. arXiv: astro-ph/0610356v2.
3. Mihalas D. Stellar Atmospheres, 2nd ed. W.H. Freeman and Co., San Francisco, 1978.
4. van der Hucht K.A. The VIIth catalogue of galactic Wolf-Rayet stars. *New Astronomy Reviews*, 2001, v. 45, 135–232.
5. van der Hucht K.A. New Galactic Wolf-Rayet stars, and candidates (Research Note), An Annex to The VIIth Catalogue of Galactic Wolf-Rayet Stars. *Astronomy and Astrophysics*, 2006, v. 458, 453–459.
6. Galactic Wolf Rayet Catalogue. V1.25, www.pacrowther.staff.shef.ac.uk/WRcat/, Aug. 2020.
7. Beals C.S. On the Nature of Wolf-Rayet Emission. *Mon. Not. Royal Ast. Soc.*, 1929, v. 90, 202–212.
8. Beals C.S. The Contours of Emission Bands in Novae and Wolf-Rayet Stars. *Mon. Not. Royal Ast. Soc.*, 1931, v. 91, 966.
9. Mihalas D. and Weibel-Mihalas B. Foundations of Radiation Hydrodynamics, corr. ed. Dover Publications, New York, 1999, pp. 627–645.
10. Abbott D.C. and Conti P.S. Wolf-Rayet Stars. *Ann. Rev. Astron. Astrophys.*, 1987, v. 25, 113–150.
11. Castor J.I. Spectral Line Formation in Wolf-Rayet Envelopes. *Mon. Not. R. Astr. Soc.*, 1970, v. 149, 111–127.
12. Castor J.I. and Van Blerkom D. Excitation of He II in Wolf-Rayet Envelopes. *Astrophys. J.*, 1970, v. 161, 485–502.
13. Castor J.I. and Nussbaumer H. On the Excitation of C III in Wolf-Rayet Envelopes. *Mon. Not. R. Astr. Soc.*, 1972, v. 155, 293–304.
14. Gudzenko L.L., Shelepin L.A. Negative Absorption in a Nonequilibrium Hydrogen Plasma. *Zh. Eksp. Teor. Fiz.*, 1963, v. 45, 1445–1449. *Sov. Phys. JETP*, 1964, v. 18, 998–1000.
15. Gudzenko L.L., Shelepin L.A. Amplification in Recombination Plasma. *Dokl. Akad. Nauk. SSSR*, 1965, v. 160, 1296–1299. *Sov. Phys. - Dokl.*, 1965, v. 10, 147.
16. Gudzenko L.L., Filippov S.S., Shelepin L.A. Rapid Recombination of Plasma Jets. *Zh. Eksp. Teor. Fiz.*, 1966, v. 51, 1115–1119. *Sov. Phys. JETP*, 1967, v. 24, 745–748.
17. Gudzenko L.L., Mamachun A.T., and Shelepin L.A. *Zh. Tekh. Fiz.*, 1967, v. 37, 833. *Sov. Phys. - Tech. Phys.*, 1967, v. 12, 598.
18. Gudzenko L.L., Shelepin L.A., Yakovlenko S.I. Amplification in recombining plasmas (plasma lasers). *Usp. Fiz. Nauk*, 1974, v. 114, 457. *Sov. Phys. - Usp.*, 1975, v. 17, 848.
19. Gol'dfarb V.M., Il'ina E.V., Kostygova I.E., Luk'yanov G.A. and Silant'ev, V.A. *Opt. Spektrosk.*, 1966, v. 20, 1085. *Optics and Spectrosc.*, 1969, v. 20, 602.
20. Gol'dfarb V.M., Il'ina E.V., Kostygova I.E. and Luk'yanov G.A. *Opt. Spektrosk.*, 1969, v. 27, 204. *Optics and Spectrosc.*, 1969, v. 27, 108.
21. Bates D.R., Kingston A.E. and McWhirter R.W.P. *Proc. Roy. Soc.*, 1962, v. A267, 297.
22. Bates D.R., Kingston A.E. and McWhirter R.W.P. *Proc. Roy. Soc.*, 1962, v. A270, 155.
23. Bates D.R. and Kingston A.E. *Planet. Space Sci.*, 1963, v. 11, 1.
24. McWhirter R.W.P. and Hearn A.G. *Proc. Phys. Soc.*, 1963, v. 82, 641.
25. Drawin H.W. and Emard F. Instantaneous Population Densities of the Excited Levels of Hydrogen Atoms, Hydrogen-like Ions, and Helium Atoms in Optically Thin and Thick Non-LTE Plasmas. Euratom-C.E.A. Report No. EUR-CEA-FC-534, 1970.
26. Gordiets B.F., Gudzenko L.I. and Shelepin L.A. Relaxation processes and amplification of radiation in a dense plasma. *Zh. Eksp. Teor. Fiz.*, 1968, v. 55, 942. *Sov. Phys. - JETP*, 1969, v. 28, 489.
27. Norcross D.W. and Stone P.M. *J. Quant. Spectrosc. Radiat. Transfer*, 1968, v. 8, 655.
28. Unsöld A. The New Cosmos, 2nd edition. Springer-Verlag, Berlin, 1977.
29. Griem H.R. Plasma Spectroscopy. McGraw-Hill, New York, 1964.
30. House L.L. *Astrophys. J. Suppl.*, 1964, v. 8, 307.
31. Menzel D.H. and Pekeris C.L. *Mon. Not. Roy. Astron. Soc.*, 1935, v. 96, 77.
32. Millette P.A. and Varshni Y.P. New Asymptotic Expression for the Average Lifetime of Hydrogenic Levels. *Can. J. Phys.*, 1979, v. 57 (3), 334–335.
33. Drawin H.W. Collision and Transport Cross-Sections. Euratom-C.E.A. Report No. EUR-CEA-FC-383, 1966.
34. Willett C.S. Gas Lasers: Population Inversion Mechanisms. Pergamon Press, New York, 1974.

35. Lengyel B. A. Introduction to Laser Physics. John Wiley, New York, 1966.
36. Smith H.J. Ph.D. Thesis, Dept. of Astronomy, Harvard University, Cambridge, 1955.
37. Varshni Y.P., Lam C. S. Emission Line 4686 in the Quasi-Stellar Objects. *J. Roy. Astron. Soc. Canada*, 1974, v. 68, 264.
38. Varshni Y.P., Lam C. S. Laser Action in Stellar Envelopes. *Bull. Amer. Astron. Soc.*, 1975, v. 7, 551.
39. Varshni Y.P., Lam C. S. Laser Action in Stellar Envelopes. *Astrophys. Space Sci.*, 1976, v. 45, 87.
40. Millette P. A. Laser Action in CIV, NV, and OVI Plasmas Cooled by Adiabatic Expansion. University of Ottawa, Ottawa, ON, 1980. LaTeX typeset, researchgate.net/publication/283014713, 2015.
41. Nasser R.M. Population Inversion in He I and C III in Recombining Plasmas. University of Ottawa, Ottawa, ON, 1986.
42. Varshni, Y.P., Nasser R. M. Laser Action in Stellar Envelopes II. He I. *Astrophys. Space Sci.*, 1986, v. 125, 341.
43. Varshni Y.P. Laser Action in Quasi-Stellar Objects? *Bull. Amer. Phys. Soc.*, 1973, v. 18, 1384.
44. Varshni Y.P. No Redshift in Quasi-Stellar Objects. *Bull. Amer. Astron. Soc.*, 1974, v. 6, 213.
45. Varshni Y.P. The Redshift Hypothesis and the Plasma Laser Star Model for Quasi-Stellar Objects. *Bull. Amer. Astron. Soc.*, 1974, v. 6, 308.
46. Varshni Y.P. Alternative Explanation for the Spectral Lines Observed in Quasars. *Astrophys. Space Sci.*, 1975, v. 37, L1.
47. Varshni Y.P. Electron Density in the Emission-Line Region of Wolf-Rayet Stars. *Astrophys. Space Sci.*, 1978, v. 56, 385.
48. Varshni Y.P. The Physics of Quasars. *Phys. Canada*, 1979, v. 35, 11.
49. Schmidt M. 3C 273: A Star-Like Object with Large Red-Shift. *Nature*, 1963, v. 197, 1040.
50. Banerji S. and Bhar G.C. Plasma laser star model of QSOs. *Astrophysics and Space Science*, 1978, v. 56, 443–451.
51. Banerji S. and Bhar G.C. Analysis of the plasma laser star model of QSOs. *Astrophysics and Space Science*, 1979, v. 61, 337–347.
52. Banerji S., Bhar G.C. and Mukherji P.K. Are QSOs local objects? I. A new interpretation of the emission and absorption spectra of a few QSOs. *Astrophysics and Space Science*, 1982, v. 87, 217–236.
53. Willett, C. S. Laser Lines in Atomic Species. In: Progress in Quantum Electronics, Vol. 1, Part 5, Pergamon, 1971.
54. Luyten W.J. A Search for Faint Blue Stars. Paper 50, University of Minnesota Observatory, Minneapolis, 1969.
55. Varshni Y.P. Proper Motions and Distances of Quasars. *Speculations in Science and Technology*, 1982, v. 5 (5), 521–532.
56. Mortlock D. J., Webster R. L. and Francis P.J. Binary Quasars. *Mon. Not. R. Astron. Soc.*, 1999, v. 309, 836–846.
57. Hennawi J.F., et al. Binary Quasars in the Sloan Digital Sky Survey: Evidence for Excess Clustering on Small Scales. *Astronomical Journal*, 2006, v. 131, 1–23.
58. Conti P. S. and Garmany C. D., De Loore C. and Vanbeveren D. The Evolution of Massive Stars: The Numbers and Distribution of O Stars and Wolf-Rayet Stars. *Astrophys. J.*, 1983, v. 274, 302–312.
59. Humphreys R. M. and Nichols M., Massey P. On the Initial Masses and Evolutionary Origins of Wolf-Rayet Stars. *Astron. J.*, 1985, v. 90, 101–108.
60. Conti P. S. and Vacca W.D. The Distribution of Massive Stars in the Galaxy: I. Wolf-Rayet Stars. *Astron. J.*, 1990, v. 100, 431–444.
61. Langer N., Hamann W.-R., Lennon M., Najarro F., Pauldrach A.W. A. and Puls J. Towards an understanding of very massive stars. A new evolutionary scenario relating O stars, LBVs [Luminous Blue Variables] and Wolf-Rayet stars. *Astron. Astrophys.*, 1994, v. 290, 819–833.
62. Crowther P. A., Smith L. J., Hillier D. J. and Schmutz W. Fundamental parameters of Wolf-Rayet stars. III. The evolutionary status of WNL [WN7 to WN9] stars. *Astron. Astrophys.*, 1995, v. 293, 427–445.
63. Hainich R., Rühling U., Todt H., Oskinova L. M., Liermann A., Gräfener G., Foellmi C., Schnurr O. and Hamann W.-R. The Wolf-Rayet stars in the Large Magellanic Cloud. A comprehensive analysis of the WN class. *Astronomy & Astrophysics*, 2014, v. 565, A27, 1–62.
64. Koesterke L. and Hamann W.-R. Spectral analyses of 25 Galactic Wolf-Rayet stars of the carbon sequence. *Astron. Astrophys.*, 1995, v. 299, 503–519.
65. Barlow M. J. and Hummer D. J. The WO Wolf-Rayet stars. *Symposium – International Astronomical Union*, 1982, v. 99, 387–392.
66. Varshni Y.P. O VI and He II Emission Lines in the Spectra of Quasars. *Astrophys. Space Sci.*, 1977, v. 46, 443.

Physics of Transcendental Numbers Meets Gravitation

Hartmut Müller

E-mail: hm@interscalar.com

Transcendental ratios of physical quantities can provide stability in complex dynamic systems because they inhibit the occurrence of destabilizing resonance. This approach leads to a fractal scalar field that affects any type of physical interaction and allows reformulating and resolving some unsolved tasks in celestial mechanics and astrophysics. We verify the model claims on the gravitational constants and the periods of orbital and rotational motion of the planets, planetoids and large moons of the solar system as well as the orbital periods of exoplanets and the gravitational constants of their stars.

Introduction

Despite the abundance of theoretical approaches engaged to explain the origin of gravitational interaction dealing with superstrings, chameleons or entropic forces [1], the community of physicists still expects compatibility for centuries: any modern theory must allow deriving Newton's law of universal gravitation as classic approximation. In the normal case of weak gravity and low velocities, also Einstein's field equations obey the correspondence principle.

Besides of nostalgia, what could be the reason of this condition? Newton's law of gravitation cannot be verified in the scale of the solar system, because the mass of a planet cannot be measured, and Kepler's laws of planetary motion do not compellingly require Newton's law of gravitation for their derivation. Moreover, Newton's theory of gravitation leads to inconsistencies already in the case of three interacting bodies.

It is a common belief that John Couch Adams and Urbain Le Verrier applying Newton's law of gravitation could predict the orbit and correct position of Neptune based on motions of Uranus. However, this is not exactly what they did.

Adopting the Titius-Bode law [2], Adams assumed the semi-major axis of Neptune being 37.25 AU; Le Verrier estimated 36.15 AU. The deviation from the correct value 30.07 AU is more than 20%. Adopting Pontécoulant's *Théorie Analytique* to his perturbation approach, Adams calculated an eccentricity of 0.1206; Le Verrier got 0.1076. The right value is 0.0086, a deviation of more than 1100%. Adams calculated the longitude of the perihelion being at 299°; Le Verrier arrived at 284° while the correct is 44°. Finally, applying Newton's law of gravitation, Adams estimated Neptune's mass with 1/6666 solar mass; Le Verrier calculated 1/9300. Actually, the ratio is 1/19300. Again, a deviation of > 200%. It is a miracle how with all these errors Le Verrier could guess the right longitude 326° of the current position of Neptune. Obviously, he was very lucky [3].

Kepler's laws of planetary motion cannot explain why the solar system has established the orbital periods 90560 days (Pluto), 60182 (Neptune), 30689 (Uranus), 10759 (Saturn), 4333 (Jupiter), 1682 (Ceres), 687 (Mars), 365 (Earth), 225 (Venus) and 88 days (Mercury), because there are infinitely

many pairs of orbital periods and distances that fulfill Kepler's laws. Einstein's field equations do not reduce the theoretical variety of possible orbits, but increases it even more.

But now, after the discovery of thousands of exoplanetary systems, we can recognize that the current distribution of the planetary and lunar orbits in our solar system is not accidental. Many planets in the extrasolar systems like Trappist 1 or Kepler 20 have nearly the same orbital periods as the large moons of Jupiter, Saturn, Uranus and Neptune [4]. That's amazing, because Trappist 1 is 40 light years away from our solar system and Kepler 20 nearly 1000 light years [5, 6].

The question is, why they prefer similar orbital periods if there are infinite possibilities? Obviously, there are orbital periods preferred anywhere in the galaxy. Why these orbital periods are preferred? What makes them attractive?

Despite perturbation models and parametric optimization, the reality of planetary systems is still a theoretical problem. The notoriously high failure rate of interplanetary missions, flyby anomalies [7] and unexpected accelerations of spacecraft indicate a profound lack of understanding gravity.

In spiral galaxies, the orbiting of stars around their centers seems to strongly disobey both Newton's law of universal gravitation and general relativity. Recently, an 85% dark matter universe is required for saving the conventional paradigm.

Perhaps the concept of gravitation itself requires a revision. Obviously, it is not about details, but an important part of the hole is missing. For finding the missing part, let us go back to the roots of the idea of gravitation ...

The empirical universality of free fall led ancient philosophers to the idea that weight could be a universal property of matter. For a long time, this observation underpinned the geocentric worldview powered by Aristoteles; he believed that heavier objects experience a higher gravitational acceleration.

Centuries later, in his famous book '*De revolutionibus orbium coelestium*', Nicolaus Copernicus (1543) interpreted weight as divine phenomenon by which all things, including stars, planets and moons, are brought toward one another. In the '*Astronomia nova*', Johannes Kepler (1609) compared weight with magnetism and hypothesized that any two stones attract each other in a way that is proportional to their masses. In the meantime, Galileo Galilei (1590) discovered that the

acceleration of free falling test bodies at a given location does not depend on their masses, physical state or chemical composition. Modern measurements [8] confirm Galilei's discovery with a precision of a trillionth. In a vacuum, indeed, a one gram light feather and a one kilogram heavy lead ball experience the same acceleration of free fall. Long time before Friedrich Bessel (1832) and Lorand Eötvös (1908), Galileo Galilei's discovery was experimentally confirmed by Isaac Newton (1680) comparing the periods of pendulums of different masses but identical length. Nevertheless, in his universal law of gravitation, Newton (1687) postulated that gravity depends on the masses of the involved bodies. Though, he was deeply uncomfortable with this idea. 26 years after the first publication of his "Principia", in the age of 71, Newton wrote: "I have not yet been able to discover the cause of these properties of gravity from phenomena and I feign no hypotheses." Newton recognized the importance of not confusing gravity acceleration with the force that gravity can cause [9]. Actually, the question is not, does the force caused by gravity depend on the masses of the moving bodies. The question is rather, does mass *cause* the acceleration of free fall.

Analyzing the astronomical observations of Tycho Brahe, Johannes Kepler (1619) discovered that for every planet, the ratio of the cube of the semi-major axis R of the orbit and the square of the orbital period T is constant for a given orbital system. In the case of the Earth, this ratio defines the geocentric gravitational constant μ . Kepler's discovery is confirmed by high accuracy radar and laser ranging of the motion of artificial satellites. Thanks to Kepler's discovery, Earth's surface gravity acceleration can be derived from the orbital elements of any satellite, also from Moon's orbit:

$$g = \frac{\mu}{r^2} = \frac{\mu}{(6378000 \text{ m})^2} = 9.81 \text{ m/s}^2,$$

$$\mu = 4\pi^2 \frac{R^3}{T^2} = 3.9860044 \cdot 10^{14} \text{ m}^3/\text{s}^2,$$

where R is the semi-major axis of Moon's orbit, T is the orbital period of the Moon and r is the equatorial radius of the Earth. No data about the masses or the chemical composition of the Earth or the Moon is needed.

Here it is important to underline that R and T are measured, but the identity $\mu = GM$ being the core of Newton's law of universal gravitation, is a theoretical presumption that provides mass as a source of gravity and the universality of the coefficient G as "gravitational constant".

One of the basic principles of scientific research is the falsifiability of a theory. Obviously, any theory that postulates gravitation of mass as forming factor of the solar system is not falsifiable, because there is no method to *measure* the mass of a planet. Actually, no mass of any planet, planetoid or moon is measured, but only calculated based on the theoretical presumption $\mu = GM$.

Naturally, G is estimated in laboratory scale where masses can be measured. However, not only the correctness of the

original experimental setup performed by Henry Cavendish (1798) is still under discussion, but also the correctness of more recent variants. There are large uncertainties not only in the obtained values of G , but even regarding the suitability of the applied methods of measuring gravity.

It is believed that gravitation cannot be screened. Because of this, it is virtually impossible to isolate the gravitational interaction between two masses from the presumed perturbative effects created by surrounding mass distributions. Invented by John Michell (1783), the instrument of choice for measuring G , the torsion pendulum, is subject to a variety of parasitic couplings and systematic effects which ultimately limit its suitability as a gravity transducer. George Gillies [10] listed about 350 papers almost all of which referred to work carried out with a torsion balance. Other sensitive mechanical devices are also pressed to the limits of their performance capabilities when employed for this purpose.

Besides of all the difficulties to measure G in laboratory, isn't there any other way to evidence the dependency of gravity on mass? For example, the Earth's surface masses are not uniformly distributed. There are huge mountains with a rock density of about three tons per cubic meter. There are oceans in which the density of water is only one ton per cubic meter - even at a depth of 10 kilometers. According to the logic of Newton's law of universal gravitation, these mass distribution inhomogeneities should act on sensitive gravimetric instruments. However, they do not [11].

In order to explain the absence of gravimetric evidence, the idea of isostasy [12] was invented. According to this hypothesis, the deeper the ocean, the more powerful the dense compensating deposits under its bottom; the higher the mountains, the looser is their foundation. Isostasy allegedly forms over huge periods of time, comparable to geological eras.

However, there are cases when very strong redistribution of surface masses occurs in a time period that is negligible by geological standards. For example, this happens during the eruption of an underwater volcano, when a seamount or even a new island builds up in a few days [13]. In these cases, there is no time to establish isostasy, and gravimetric instruments should react to these changes. Obviously, they do not react as expected, and for making gravity calculations more realistic, ground deformation data and numerical modelling is applied.

Gravimetric practice evidences that it is nearly impossible separating variations in gravity acceleration from low frequency seismic activity. Actually, gravimeters *are* long-period seismometers [14]. This is why the distribution of gravitational anomalies on gravity maps is indistinguishable from the zones of earthquakes and seismic activity.

Customarily, gravimetric data are recalculated with special corrections that providently consider the alleged effect of surface mass inhomogeneities. The corrections depend on the adopted model of the distribution of surface masses mainly based on seismic exploration. The idea to apply those corrections was proposed by Pierre Bouguer (1749). Now the dif-

ference between the really measured values of gravity and the theoretically calculated for an assumed mass density, is traditionally called a Bouguer-anomaly. Fluctuations in altitude of orbiting satellites indicating gravity variations are interpreted as caused by mass inhomogeneities [15]. In this way, gravimetric maps of planets and asteroids are being compiled.

In the case of mass as source of gravity, in accordance with Newton’s shell theorem, a solid body with a spherically symmetric mass distribution should attract particles outside it as if its total mass were concentrated at its center. In contrast, the attraction exerted on a particle should decrease as the particle goes deeper into the body and it should become zero at the body’s center.

The Preliminary Reference Earth Model [16] affirms the decrease of the gravity acceleration with the depth. However, this hypothesis is still under discussion. In 1981, Stacey, Tuck, Holding, Maher and Morris [17, 18] reported anomalous measures (larger values than expected) of the gravity acceleration in deep mines and boreholes. In [19] Frank Stacey writes that “geophysical measurements indicate a 1% difference between values at 10 cm and 1 km (depth); if confirmed, this observation will open up a new range of physics.”

Furthermore, measurements of G are notoriously unreliable, so the constant is in permanent flux and the official value is an average. If G is changing, then G could depend on a new field. But this could also evidence that gravity itself may be changing. As mentioned Terry Quinn [20] of the Bureau International des Poids et Mesures (BIPM), the discrepant results may demonstrate that we do not understand the metrology of measuring weak force or signify some new physics.

Introduced with the postulated equation $\mu = GM$ as coefficient compensating the dimension of mass, G has no known confirmed dependence on any other fundamental constant. Suppose G would be estimated to be two times larger than the currently recommended value, this would simply mean that the masses of celestial bodies would be estimated to be two times smaller. However, this change would not have any impact on calculations depending on μ . In this case, the hypothesis that mass *causes* gravity, could turn out to be a dispensable assumption.

In view of this situation, it is understandable to intensify the search of possible derivations of G from theory. As mentioned Gillies [10], some recent approaches seek the ad hoc introduction of a new field or effect to create a situation in which a value for G can be built from ratios of other fundamental constants and numerical factors. However, most of the attempts come from a general relativistic starting point to examine the outcome of some scenario in which G arises from the calculations. For instance, Yanpeng Li [21] derives

$$G = \frac{1}{16 \pi \cdot c \cdot \eta} = 6.636 \cdot 10^{-11} \text{ m}^3 \text{ kg}^{-1} \text{ s}^{-2}$$

from general relativity by introducing the “eigen-modulus of a tensor” as measure of its converging ability. According to

Li, the eigen-modulus of the Einstein tensor equals $1/16 \text{ m/s}^3$, the mass density $\eta = 1 \text{ kg/m}^3$ comes from the eigen-modulus of the energy-momentum tensor, c is the speed of light. Despite the numerical fit of the derived G value with the wide spectrum of data achieved in laboratory, the generality of this derivation and the physical sense of a mass density that equals 1 kg/m^3 may be questioned.

Introducing his geometric theory of gravitation, a century ago Einstein supposed that gravity is indistinguishable from, and in fact the same thing as, acceleration. Identifying gravity with acceleration $g = c \cdot f$, the gradient of a conservative gravitational field can be expressed in terms of frequency shifts:

$$\frac{\Delta f}{f} = g \frac{\Delta h}{c^2}.$$

Already in 1959, Robert Pound and Glen Rebka [22] verified this equation in their famous gravitational experiment. Sending gamma rays over a vertical distance of $\Delta h = 22.56 \text{ m}$, they measured a blueshift of $\Delta f/f = 2.46 \cdot 10^{-15}$ that corresponds precisely with Earth’s surface gravity 9.81 m/s^2 .

Actually, also Kepler’s 3rd law is of geometric origin and can be derived from Gauss’s flux theorem in 3D-space within basic scale considerations. It applies to all conservative fields which decrease with the square of the distance, similar to the geometric dilution of the intensity of light into 3D-space.

The theoretical reduction of gravity to an acceleration enables the orbital motion to be identified with free fall. Orbital and rotational motions are periodic. So is free fall. Only the aggregate state of the planet prevents the free fall from becoming a damped oscillation. Considering gravity acting with the speed of light c , we can express gravity in units of time. For instance, Earth’s surface gravity $g_{\text{Earth}} = 9.81 \text{ m/s}^2$ corresponds with an oscillation period of 355 days that is quite close to Earth’s orbital period:

$$T_{\text{Earth}} = \frac{c}{g_{\text{Earth}}} = \frac{299792458 \text{ m/s}}{9.81 \text{ m/s}^2} = 355 \text{ d}.$$

At an altitude of 100 km above sea level, Earth’s gravity reduces down to 9.51 m/s^2 that corresponds with the orbital period of 365.25 days. In a series of experiments we demonstrated [23] that inside of finite spatial configurations which boundaries coincide with equipotential surfaces of the Fundamental Field (fig. 2), gravity acceleration reduces locally by $0.3 g$ down to 9.51 m/s^2 .

The surface gravity $g_{\text{Sun}} = 274 \text{ m/s}^2$ of the Sun corresponds with an oscillation period of 12.7 days that is the first harmonic of its equatorial period 25.4 days of rotation. Similar coincidences are valid for the surface gravities of Mercury, Venus, Mars and even for Saturn and Jupiter. Although the definition of a planet’s surface is conventional (especially in the case of gas giants), all these coincidences suggest the existence of an underlying connection of the gravity of a celestial body with its *own* orbital and rotational motions. Despite the rich history of crucial discoveries in astronomy and

astrophysics and the development of sophisticated theories of gravitation, the distribution of stable orbits in the solar system remains to be little understood. In this context, the discovery of Johann Daniel Titius (1766) is even more remarkable. He found that the sequence of the planetary semi-major axes can be approximated by the exponential term:

$$a_n = 0.4 + 0.3 \cdot 2^n,$$

where the index n is $-\infty$ for Mercury, 0 for Venus, 1 for the Earth, 2 for Mars etc. Based on this idea, Johann Elert Bode, in 1772, first suggested that an undiscovered planet could exist between the orbits of Mars and Jupiter. William Herschel's discovery of Uranus in 1781 near the predicted distance 19.6 AU for the next body beyond Saturn increased faith in the law of Titius and Bode. In 1801, near the predicted for $n = 3$ distance 2.8 AU from Sun, Giuseppe Piazzi discovered the planetoid Ceres and the Franz Xaver von Zach group found further large asteroids.

In 1968, Stanley Dermott [24] found a similar progression for the major satellites of Jupiter, Saturn and Uranus. Nevertheless, at last, the hypothesis of Titius and Bode was discarded after it failed as a predictor of Neptune's orbit.

Surprisingly, recent astronomical research [25] suggests that exoplanetary systems follow Titius-Bode-like laws. Raw statistics from exoplanetary orbits indicate the exponential increase of semi-major axes as function of planetary index. It has been shown [2] that many exoplanetary systems follow an exponential progression of the form

$$a_n = a_0 + e^{bn}$$

with $n = 0, 1, 2, \dots$; a_0 and b are constants to be determined for each system. Since its formulation, the Titius-Bode law has proved to be highly predictive, although its physical origin remains largely unclear.

Not only the distribution of stable orbits, but also the origin of the configuration of gravity fields in the solar system remains disputed. Furthermore, there is no known law concerning the rotation of celestial bodies besides conservation of the angular momentum [26] that they retain from the protoplanetary disks, so that the final distribution of the rotational periods appears as to be accidental.

In this article we demonstrate that the rotational and orbital periods of the planets, planetoids and large moons of the solar system as well as their gravitational constants approximate numeric attractors corresponding with the transcendental frequency ratios of scale-invariant eigenstates in chain systems of oscillating protons and electrons. The claims of our model we verify also on orbital periods of exoplanets and the gravitational constants of their stars.

Methods

In [27] we have shown that the difference between rational, irrational algebraic and transcendental numbers is not only a

mathematical task, but it is also an essential aspect of stability in complex dynamic systems. For instance, integer frequency ratios provide resonance interaction that can destabilize a system [28]. Actually, it is transcendental numbers that define the preferred ratios of quantities which avoid destabilizing resonance interaction [29]. In this way, transcendental ratios of quantities sustain the lasting stability of periodic processes in complex dynamic systems. With reference to the evolution of a planetary system and its stability, we may therefore expect that the ratio of any two orbital periods should finally approximate a transcendental number.

Among all transcendental numbers, Euler's number $e = 2.71828\dots$ is unique, because its real power function e^x coincides with its own derivatives. In the consequence, Euler's number allows inhibiting resonance interaction regarding any interacting periodic processes and their derivatives. Because of this unique property of Euler's number, complex dynamic systems tend to establish relations of quantities that coincide with values of the natural exponential function e^x for integer and rational exponents x .

Therefore, we expect that periodic processes in real systems prefer frequency ratios close to Euler's number and its rational powers. Consequently, the logarithms of their frequency ratios should be close to integer $0, \pm 1, \pm 2, \dots$ or rational values $\pm 1/2, \pm 1/3, \pm 1/4, \dots$. In [30] we exemplified our hypothesis in particle physics, astrophysics, cosmology, geophysics, biophysics and engineering.

Based on this hypothesis, we introduced a fractal model of matter [31] as a chain system of harmonic quantum oscillators and could show the evidence of this model for all known hadrons, mesons, leptons and bosons as well. In [32] we have shown that the set of stable eigenstates in such systems is fractal and can be described by finite continued fractions:

$$\mathcal{F}_{jk} = \ln(\omega_{jk}/\omega_{00}) = \langle n_{j0}; n_{j1}, n_{j2}, \dots, n_{jk} \rangle, \quad (1)$$

where ω_{jk} is the set of angular eigenfrequencies and ω_{00} is the fundamental frequency of the set. The denominators are integer: $n_{j0}, n_{j1}, n_{j2}, \dots, n_{jk} \in \mathbb{Z}$. The cardinality $j \in \mathbb{N}$ of the set and the number $k \in \mathbb{N}$ of layers are finite. In the canonical form, all numerators equal 1. We use angle brackets for continued fractions.

Any finite continued fraction represents a rational number [33]. Therefore, the ratios ω_{jk}/ω_{00} of eigenfrequencies are always irrational, because for rational exponents the natural exponential function is transcendental [34]. This circumstance provides for lasting stability of those eigenstates of a chain system of harmonic oscillators because it prevents resonance interaction [35] between the elements of the system.

The distribution density of stable eigenstates reaches local maxima near reciprocal integers $\pm 1/2, \pm 1/3, \pm 1/4, \dots$ that are attractor points (fig. 1) in the fractal set \mathcal{F}_{jk} of natural logarithms. Integer logarithms $0, \pm 1, \pm 2, \dots$ represent the most stable eigenstates (main attractors).

In the case of harmonic quantum oscillators, the continued fractions \mathcal{F}_{jk} define not only fractal sets of natural angular frequencies ω_{jk} , angular accelerations $a_{jk} = c \cdot \omega_{jk}$, oscillation periods $\tau_{jk} = 1/\omega_{jk}$ and wavelengths $\lambda_{jk} = c/\omega_{jk}$ of the chain system, but also fractal sets of energies $E_{jk} = \hbar \cdot \omega_{jk}$ and masses $m_{jk} = E_{jk}/c^2$ which correspond with the eigenstates of the system. For this reason, we call the continued fraction \mathcal{F}_{jk} the *Fundamental Fractal* of stable eigenstates in chain systems of harmonic quantum oscillators.



Fig. 1: The distribution of stable eigenvalues of \mathcal{F}_{jk} for $k = 1$ (above) and for $k = 2$ (below) in the range $-1 \leq \mathcal{F}_{jk} \leq 1$.

The spatio-temporal projection of the Fundamental Fractal \mathcal{F}_{jk} of stable eigenstates is a fractal scalar field of transcendental attractors, the *Fundamental Field* [36].

The connection between the spatial and temporal projections of the Fundamental Fractal is given by the speed of light $c = 299792458$ m/s. The constancy of c makes both projections isomorphic, so that there is no arithmetic or geometric difference. Only the units of measurement are different.

Figure 2 shows the linear 2D-projection $\exp(\mathcal{F}_{jk})$ of the first layer of the Fundamental Field

$$\mathcal{F}_{j1} = \langle n_{j0}; n_{j1} \rangle = n_{j0} + \frac{1}{n_{j1}}$$

in the interval $-1 < \mathcal{F}_{j1} < 1$. The upper part of figure 1 shows the same interval in the logarithmic representation. The Fundamental Field is topologically 3-dimensional, a fractal set of embedded spheric equipotential surfaces. The logarithmic potential difference defines a gradient directed to the center of the field that causes a central force of attraction. Because of the fractal logarithmic hyperbolic metric of the field, every equipotential surface is an attractor. The scalar potential difference $\Delta\mathcal{F}$ of sequent equipotential surfaces at a given layer k is defined by the difference of continued fractions (1):

$$\begin{aligned} \Delta\mathcal{F} &= \mathcal{F}(j,k) - \mathcal{F}(j+1,k) = \\ &= \langle n_{j0}; n_{j1}, n_{j2}, \dots, n_{jk} \rangle - \langle n_{j0}; n_{j1}, n_{j2}, \dots, n_{j+1,k} \rangle. \end{aligned}$$

For instance, at the first layer $k=1$, the potential differences have the form:

$$\Delta\mathcal{F} = \frac{1}{n_{j1}} - \frac{1}{n_{j1} + 1} = \frac{1}{n_{j1}^2 + n_{j1}}.$$

Therefore, the potential difference between sequent equipotential surfaces at any given layer $k + 1$ decreases parabolically, approximating zero near an equipotential surface of the layer k . This is why any equipotential surface is an attractor where potential differences decrease and processes can gain stability. Main attractors at the layer $k = 0$ correspond with

integer logarithms, subattractors at deeper layers $k > 0$ correspond with rational logarithms.

The Fundamental Field is of pure arithmetical origin, and there is no particular physical mechanism required as field source. It is all about transcendental ratios of frequencies [29] that inhibit destabilizing resonance. In this way, the Fundamental Field concerns all repetitive processes which share at least one characteristic — the frequency. Therefore, we postulate the universality of the Fundamental Field that affects any type of physical interaction, regardless of its complexity.

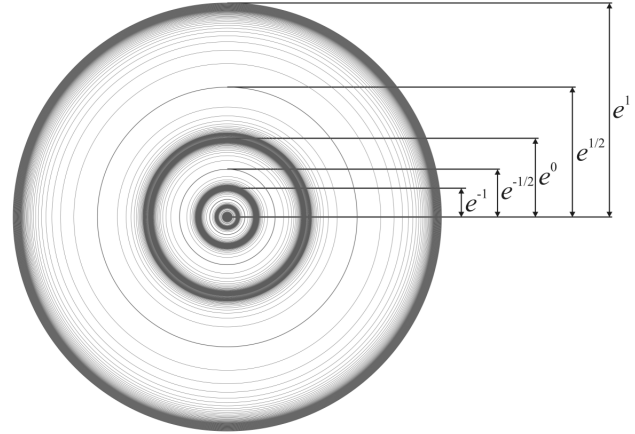


Fig. 2: The equipotential surfaces of the Fundamental Field in the linear 2D-projection for $k = 1$.

In fact, scale relations in particle physics [31, 37, 38], nuclear physics [39, 40] and astrophysics [4] obey the same Fundamental Fractal (1), without any additional or particular settings. The proton-to-electron rest energy ratio approximates the first layer of the Fundamental Fractal that could explain their exceptional stability [30]. The life-spans of the proton and electron top everything that is measurable, exceeding 10^{29} years [41].

PROPERTY	ELECTRON	PROTON
$E = mc^2$	0.5109989461(31) MeV	938.2720813(58) MeV
$\omega = E/\hbar$	$7.76344 \cdot 10^{20}$ Hz	$1.42549 \cdot 10^{24}$ Hz
$\tau = 1/\omega$	$1.28809 \cdot 10^{-21}$ s	$7.01515 \cdot 10^{-25}$ s
$\lambda = c/\omega$	$3.86159 \cdot 10^{-13}$ m	$2.10309 \cdot 10^{-16}$ m

Table 1: The basic set of the physical properties of the electron and proton. Data from Particle Data Group [41]. Frequencies, oscillation periods and wavelengths are calculated.

These unique properties of the electron and proton predestinate their physical characteristics as fundamental units. Table 1 shows the basic set of electron and proton units that can be considered as a fundamental metrology (c is the speed of light in a vacuum, \hbar is the Planck constant). In [32] was

shown that the fundamental metrology (tab. 1) is completely compatible with Planck units [42]. Originally proposed in 1899 by Max Planck, these units are also known as natural units, because the origin of their definition comes only from properties of nature and not from any human construct. Max Planck wrote [43] that these units, “regardless of any particular bodies or substances, retain their importance for all times and for all cultures, including alien and non-human, and can therefore be called natural units of measurement”. Planck units reflect the characteristics of space-time.

We hypothesize that scale invariance according the Fundamental Fractal (1) calibrated on the physical properties of the proton and electron is a universal characteristic of organized matter and criterion of stability. This hypothesis we have called *Global Scaling* [30].

On this background, atoms and molecules emerge as stable eigenstates in fractal chain systems of harmonically oscillating protons and electrons. Andreas Ries [38] demonstrated that this model allows for the prediction of the most abundant isotope of a given chemical element.

In [44] we applied the Fundamental Fractal (1) to macroscopic scales interpreting gravity as attractor effect of its stable eigenstates. Indeed, the orbital and rotational periods of planets, planetoids and large moons of the solar system correspond with attractors of electron and proton stability [32]. This is valid also for the planets [30] of the systems Trappist 1 and Kepler 20. Planetary and lunar orbits [4] correspond with equipotential surfaces of the Fundamental Field, as well as the metric characteristics of stratification layers in planetary atmospheres [45]. In [36] we demonstrated that the Fundamental Field (fig. 2) in the interval of the main attractors $\langle 49 \rangle \leq \mathcal{F} \leq \langle 52 \rangle$ of proton stability reproduces the 2D profile of the Earth’s interior confirmed by seismic exploration.

Results

We will show now that the orbital and rotational periods of planets, planetoids and moons as well as their gravity accelerations approximate stable eigenstates of our model of matter as fractal chain system of oscillating protons and electrons, described by the Fundamental Fractal.

In accordance with the equation (1), we calculate the natural logarithm of the ratio of the measured value to the corresponding electron or proton unit taken from table 1. For instance, the orbital period of Jupiter T_O (Jupiter) = 4332.59 days = $3.7434 \cdot 10^8$ seconds [46] matches the main attractor $\mathcal{F}\langle 66 \rangle$ of *electron* stability:

$$\ln\left(\frac{T_O(\text{Jupiter})}{2\pi \cdot \tau_e}\right) = \ln\left(\frac{3.7434 \cdot 10^8 \text{ s}}{2\pi \cdot 1.28809 \cdot 10^{-21} \text{ s}}\right) = 66.00.$$

In contrast to orbital motion, rotation is an angular motion, so that the proton or electron angular oscillation periods are applied as units. The rotation period $T_R(\text{Ceres}) = 9$ hours = 32400 seconds of Ceres, the largest body of the main asteroid

belt, matches the main attractor $\mathcal{F}\langle 66 \rangle$ of *proton* stability:

$$\ln\left(\frac{T_R(\text{Ceres})}{\tau_p}\right) = \ln\left(\frac{32400 \text{ s}}{7.01515 \cdot 10^{-25} \text{ s}}\right) = 66.00.$$

Table 3 gives an overview of the orbital and rotational periods as well as the gravitational constants of the planets including the planetoid Ceres and large moons.

Within our model, the approximation level of an attractor of stability indicates evolutionary trends. For instance, Venus’ OE2 = 63.04 indicates that the orbital period of the Morning star must slightly decrease for reaching the center of the main attractor $\mathcal{F}\langle 63 \rangle$. On the contrary, Moon’s OE2 = 60.94 indicates that its orbital period must still increase for reaching the center of the main attractor $\mathcal{F}\langle 61 \rangle$. Actually, exactly this is observed [47]. As well, Uranus’ OE2 = 67.96 let us expect an increase of its orbital period in order to reach the main attractor $\mathcal{F}\langle 68 \rangle$. Mercury’s OE1 = 63.94 indicates that in future it could overcome the current tidal 3/2 locking by reaching the main attractor $\mathcal{F}\langle 64 \rangle$ of electron stability. Mercury’s RP1 = 71.05 indicates that its rotation must speed up slightly [26] in order to reach the attractor $\mathcal{F}\langle 71 \rangle$ of proton stability. Earth’s RP1 = 66.98 indicates that our planet must slow its rotation by 24 minutes per turn in order to reach the main attractor $\mathcal{F}\langle 67 \rangle$.

Despite conservation of angular momentum [26], there is no known law concerning the rotation of celestial bodies. The more remarkable is the correspondence of the rotation periods of planets, planetoids and large moons with attractors of the Fundamental Fractal (1) as shown in table 3.

For instance, Mars, Ceres and Jupiter have reached the main attractor $\mathcal{F}\langle 66 \rangle$ in quite different way. In the case of Mars and Jupiter, the attractor $\mathcal{F}\langle 66 \rangle$ stabilizes the orbital period T_O . In the case of the planetoid Ceres, the same attractor $\mathcal{F}\langle 66 \rangle$ stabilizes the period of rotation T_R . Actually, the difference lays in the reference units. In the case of Jupiter’s orbital period, the reference unit is the oscillation period of the electron $2\pi\tau_e$; in the case of Mars, it is the angular oscillation period of the electron τ_e , and in the case of the rotational period of Ceres, it is the angular oscillation period of the proton τ_p . Now we can write down the following relations:

$$T_O(\text{Jupiter}) = 2\pi \cdot T_O(\text{Mars}),$$

$$T_O(\text{Mars}) = \frac{\tau_e}{\tau_p} \cdot T_R(\text{Ceres}).$$

The complete (polar) rotational period of the Sun approximates the main attractor $\mathcal{F}\langle 63 \rangle$ of electron stability:

$$\ln\left(\frac{T_R(\text{Sun})}{\tau_e}\right) = 63.01.$$

The orbital period of Venus approximates the same attractor $\mathcal{F}\langle 63 \rangle$, as table 3 shows. Consequently, the scaling factor 2π

connects the orbital period of Venus with the rotational period of the Sun:

$$T_O(\text{Venus}) = 2\pi \cdot T_R(\text{Sun}).$$

Archimedes' number $\pi = 3.14159\dots$ is transcendental and therefore, it does not violate the principle of avoiding destabilizing resonance. Needless to say that these relations cannot be derived from Kepler's laws or Newton's law of gravitation. The proton-to-electron ratio (tab. 1) approximates the seventh power of Euler's number and its square root:

$$\ln\left(\frac{\omega_p}{\omega_e}\right) = \ln\left(\frac{1.42549 \cdot 10^{24} \text{ Hz}}{7.76344 \cdot 10^{20} \text{ Hz}}\right) \approx 7 + \frac{1}{2} = \langle 7; 2 \rangle.$$

In the consequence of this potential difference of the proton relative to the electron, the scaling factor $\sqrt{e} = 1.64872\dots$ connects attractors of proton stability with similar attractors of electron stability in alternating sequence. The following Diophantine equation describes the correspondence of proton calibrated attractors n_p with electron calibrated attractors n_e . Non considering the signature, only three pairs (n_p, n_e) of integers are solutions to this equation: (3, 6), (4, 4), (6, 3).

$$\frac{1}{n_p} + \frac{1}{n_e} = \frac{1}{2}.$$

Figure 3 demonstrates this situation on the first layer of the Fundamental Fractal (1). Both, the attractors of proton and electron stability are represented at the first layer, so we can see clearly that among the integer or half, only the attractors $\pm 1/3, \pm 1/4$ and $\pm 1/6$ are common. In these attractors, proton stability is supported by electron stability and vice versa, so we expect that they are preferred in real systems.

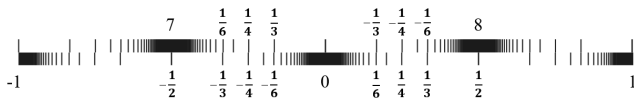


Fig. 3: The distribution of the attractors of proton (bottom) stability in the range $-1 < \mathcal{F} < 1$ of the attractors of electron (top) stability. Natural logarithmic representation.

Figure 4 shows the distribution of the number of exoplanets with orbital periods in the range $5 \text{ d} < T_O < 24 \text{ d}$ that corresponds with the range of logarithms $59.2 < \ln(T_O/2\pi\tau_e) < 60.8$ on the horizontal axis. According with table 1, τ_e is the electron angular oscillation period. The histogram contains data of 1430 exoplanets and shows clearly the maximum corresponding with the main attractor $\mathcal{F}\langle 60 \rangle$. Other maxima correspond with the attractors $\mathcal{F}\langle 59; 2 \rangle$ and $\mathcal{F}\langle 60; 2 \rangle$; even the subattractors $\mathcal{F}\langle 60; -4 \rangle$ and $\mathcal{F}\langle 60; 4 \rangle$ can be distinguished.

The histogram evidences that the majority of the analyzed 1430 exoplanets [48] prefer orbital periods close to 10–11 days corresponding with the main attractor $\mathcal{F}\langle 60 \rangle$, as well as periods close to 6–7 days or close to 17–18 days corresponding with the attractors $\mathcal{F}\langle 59; 2 \rangle$ and $\mathcal{F}\langle 60; 2 \rangle$. Because of the logarithm $7+1/2$ of the proton-to-electron ratio, the attractors

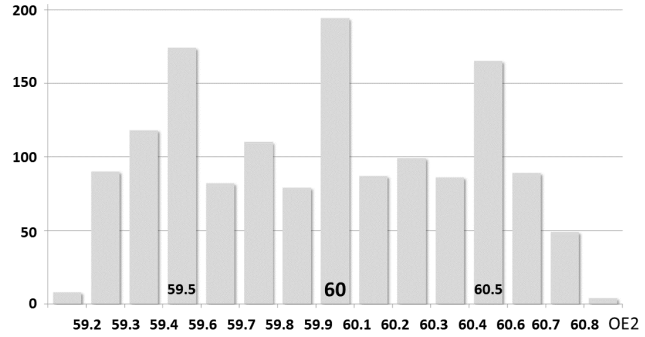


Fig. 4: The histogram shows the distribution of the number of exoplanets with orbital periods in the range $5 \text{ d} < T_O < 24 \text{ d}$. The logarithms $\text{OE2} = \ln(T_O/2\pi\tau_e)$ are on the horizontal axis. Corresponding with table 1, τ_e is the electron angular oscillation period. Data of 1430 exoplanets taken from [48].

$\mathcal{F}\langle 59; 2 \rangle$ and $\mathcal{F}\langle 60; 2 \rangle$ of electron stability are actually the main attractors $\mathcal{F}\langle 67 \rangle$ and $\mathcal{F}\langle 68 \rangle$ of proton stability.

Now we can also explain the origin of the Titius-Bode law. The OE2 column in tab. 3 shows that the orbital periods of Ceres, Jupiter, Saturn and Uranus approximate the sequence of the main attractors $\mathcal{F} = \langle 65 \rangle, \langle 66 \rangle, \langle 67 \rangle$ and $\langle 68 \rangle$ of electron stability. The ratio of main attractors equals Euler's number $e = 2.71828\dots$. Considering Kepler's third law, from this directly follows that the ratio of the semi-major axes of Ceres, Jupiter, Saturn and Uranus approximates the cube root of the square of Euler's number $e^{2/3} = 1.9477\dots$. This is why the Titius-Bode law approximates the exponential function 2^n . However, not all orbital periods approximate main attractors. The Earth-Venus orbital period ratio approximates the square root of Euler's number. Consequently, the ratio of their semi-major axes approximates the cube root of Euler's number $e^{1/3} = 1.3956\dots$. The same is valid for Umbriel and Ariel, the moons of Uranus. The Neptune-Uranus orbital period ratio approximates $e^{2/3}$. Consequently, the ratio of their semi-major axes approximates $e^{4/9} = 1.5596\dots$

The eigenvalues of \mathcal{F} are transcendental, and their distribution (1) is logarithmically fractal. This is why Titius-Bode-like equations cannot deliver a general and complete model of an orbital system.

Among the orbital and rotational periods, tab. 3 shows that also the gravitational constants μ obey the Fundamental Fractal (1) approximating main attractors and the preferred subattractors as shown in fig. 3.

In accordance with [46], surface gravities g are given for a distance from the center of the celestial body that coincides with the radius of the solid or liquid surface, without consideration of the centrifugal effects of rotation. For gas giants such as Jupiter, Saturn, Uranus, and Neptune, where the surfaces are deep in the atmosphere and the radius is not known, the surface gravity is given at the 1 bar pressure level in the atmosphere. In this way, any surface gravity is given for an individual distance from the local center of gravitation.

Earth’s surface gravity corresponds to the equatorial radius at sea level 6378 km, and the surface gravity of Uranus corresponds to its equatorial radius of 25559 km where the atmospheric pressure equals 1 bar. Although the surface gravities on Venus and Uranus are identical equal 8.87 m/s^2 , this does not mean that they indicate comparable gravitational fields. Therefore, we cannot use the surface gravity accelerations for comparison, but only the gravitational constants μ .

STAR	$\mu, \text{ m}^3/\text{s}^2$	MP	\mathcal{F}	MP - \mathcal{F}
Trappist 1	$1.1976 \cdot 10^{19}$	40.99	$\langle 41 \rangle$	-0.01
Proxima Cent	$1.5725 \cdot 10^{19}$	41.26	$\langle 41; 4 \rangle$	0.01
Gliese 1061	$1.6966 \cdot 10^{19}$	41.34	$\langle 41; 3 \rangle$	0.01
Barnard’s star	$2.6154 \cdot 10^{19}$	41.77	$\langle 42; -4 \rangle$	0.02
Struve 2398 B	$3.7765 \cdot 10^{19}$	42.14	$\langle 42; 6 \rangle$	-0.02
Gliese 876	$4.2851 \cdot 10^{19}$	42.27	$\langle 42; 4 \rangle$	0.02
Lacaille 9352	$6.4378 \cdot 10^{19}$	42.67	$\langle 43; -3 \rangle$	0.00
Tau Ceti	$1.0414 \cdot 10^{20}$	43.15	$\langle 43; 6 \rangle$	-0.01
HD 69830	$1.1402 \cdot 10^{20}$	43.24	$\langle 43; 4 \rangle$	-0.01
55 Cancri	$1.2480 \cdot 10^{20}$	43.33	$\langle 43; 3 \rangle$	0.00
Upsilon Andro	$1.7598 \cdot 10^{20}$	43.68	$\langle 44; -3 \rangle$	0.01

Table 2: The gravitational constants μ of some stars calculated from data [48] of orbital periods and semi-major axes of their planets. $MP = \ln(\mu/\lambda_p^3\omega_p^2)$. Corresponding with tab. 1, λ_p is the proton angular wavelength and ω_p is the proton angular frequency. Continued fractions (1) of the Fundamental Fractal \mathcal{F} are given in angle brackets.

Table 3 shows that the gravitational constants μ of Pluto, Neptune, Jupiter, Mars and Venus approximate main attractors $\mathcal{F}=\langle n_0 \rangle$ of electron stability. The gravitational constants of the other planets and planetoids of the solar system approximate the rational subattractors $\mathcal{F}=\langle n_0 \pm 1/2 \rangle$, $\langle n_0 \pm 1/3 \rangle$, $\langle n_0 \pm 1/4 \rangle$ or $\langle n_0 \pm 1/6 \rangle$. As well, the gravitational constants of the large moons of Jupiter, Saturn, Uranus and Neptune approximate main attractors of electron and proton stability and the same rational subattractors. This is valid also for exoplanetary systems. Table 2 shows the gravitational constants μ of some near stars calculated from data [48] of the orbital periods and semi-major axes of their planets.

Conclusion

Perhaps, the conventional paradigm of physical interaction should be completed by the principle of avoiding those interactions that potentially can destabilize a system.

Admittedly, the principle of minimum action is an essential part of theoretical physics at least since Pierre de Fermat (1662) and Pierre Louis Moreau de Maupertuis (1741),

Joseph-Louis Lagrange (1788) and William Rowan Hamilton (1834) applied in the Euler – Lagrange equations of motion.

The novelty of our solution we see in the purely numerical approach that rediscovers Euler’s number, its integer powers and roots as attractors of transcendental numbers. Approximating transcendental ratios of quantities defined by integer and rational natural logarithms, complex dynamic systems can avoid destabilizing resonance interactions between their elements and gain lasting stability. As we have shown in this paper, planetary systems make extensive use of this solution.

Finally, we can explain why Jupiter’s orbital period equals 4332.59 days: With this orbital period, Jupiter occupies the main equipotential surface $\mathcal{F}=\langle 66 \rangle$ of the Fundamental Field of transcendental attractors and in this way, Jupiter avoids destabilizing resonance interactions with the orbital motions of other planets and gains lasting stability of its own orbital motion. In other words, there is a fractal scalar field of transcendental temporal attractors corresponding with integer and rational powers of Euler’s number. One of these attractors is $\mathcal{F}=\langle 66 \rangle$, and it has materialized as a stable orbital period in the solar system among the attractors $\mathcal{F} = \langle 62 \rangle, \langle 63 \rangle, \langle 64 \rangle, \langle 65 \rangle, \langle 67 \rangle, \langle 68 \rangle, \langle 69 \rangle$ and their subattractors. Smaller attractors $\mathcal{F} = \langle 58 \rangle, \langle 59 \rangle, \langle 60 \rangle$ and $\langle 61 \rangle$ and their subattractors define stable orbital periods in moon systems and in the majority of the discovered so far exoplanetary systems.

Naturally, the Fundamental Field \mathcal{F} of transcendental attractors does not materialize in the scale of planetary systems only. At subatomic scale, it defines the proton-to-electron ratio and in this way, allows the formation of stable atoms and complex matter. At planetary scale, now we can distinguish attractors of electron stability and attractors of proton stability. While the attractors of electron stability define stable orbital periods, the attractors of proton stability define stable rotational periods. For instance, the attractor $\mathcal{F}=\langle 66 \rangle$ of *electron* stability defines the orbital period of Jupiter, and the same attractor $\mathcal{F}=\langle 66 \rangle$ of *proton* stability defines the rotational period of Mars. In this way, the law behind the distribution of stable orbital and rotational periods is the same Fundamental Field of transcendental attractors.

Interpreting gravity in terms of frequency, we did demonstrate that the distribution of gravity in the solar system is not accidental, but obeys the same Fundamental Field \mathcal{F} . As well, the gravitational constants μ of extrasolar systems obey the logarithmically fractal metric (1) of \mathcal{F} . This circumstance let us suppose that even entire planetary systems prefer avoiding destabilizing resonance interactions between them.

Acknowledgements

The author is grateful to Simon Shnoll, Viktor Panchelyuga, Valery Kolombet, Oleg Kalinin, Viktor Bart, Andreas Ries, Michael Kauderer, Ulrike Granögger and Leili Khosravi for valuable discussions.

Submitted on January 7, 2021

Body	T_O , d	OE1	\mathcal{F}	OE2	\mathcal{F}	T_R , h	RP1	\mathcal{F}	RP2	\mathcal{F}	μ , m^3/s^2	ME	\mathcal{F}
Eris	204199.00	71.69	(72; -3)	69.86	(70; -6)	349.44	69.66	(70; -3)	67.82	(68; -6)	$1.10800 \cdot 10^{12}$	17.28	(17; 4)
Pluto	90560.09	70.88	(71; -6)	69.04	(69)	153.29	68.84	(69; -6)	67.00	(67)	$8.62000 \cdot 10^{11}$	17.03	(17)
Neptune	60193.20	70.47	(70; 2)	68.64	(69; -3)	16.11	66.58	(66; 2)	64.75	(65; -4)	$6.83653 \cdot 10^{15}$	26.01	(26)
Uranus	30688.49	69.80	(70; -6)	67.96	(68)	17.24	66.65	(67; -3)	64.81	(65; -6)	$5.79394 \cdot 10^{15}$	25.84	(26; -6)
Saturn	10759.21	68.75	(69; -4)	66.91	(67)	10.56	66.16	(66; 6)	64.32	(64; 3)	$3.79312 \cdot 10^{16}$	27.72	(28; -4)
Jupiter	4332.60	67.84	(68; -6)	66.00	(66)	9.93	66.10	(66; 6)	64.26	(64; 3)	$1.26687 \cdot 10^{17}$	28.93	(29)
Ceres	1683.80	66.90	(67; -6)	65.06	(65)	9.00	66.00	(66)	64.16	(64; 6)	$6.26274 \cdot 10^{10}$	14.41	(14; 2)
Mars	686.97	66.00	(66)	64.16	(64; 6)	24.62	67.01	(67)	65.17	(65; 6)	$4.28284 \cdot 10^{13}$	20.93	(21)
Earth	365.25	65.37	(65; 3)	63.53	(63; 2)	24.00	66.98	(67)	65.15	(65; 6)	$3.98600 \cdot 10^{14}$	23.16	(23; 6)
Venus	224.70	64.88	(65; -6)	63.04	(63)	243.03	72.48	(72; 2)	70.64	(71; -3)	$3.24859 \cdot 10^{14}$	22.96	(23)
Mercury	87.97	63.94	(64)	62.11	(62; 6)	58.65	71.05	(71)	69.22	(69; 6)	$2.20320 \cdot 10^{13}$	20.27	(20; 4)
Moon	27.32	62.78	(63; -6)	60.94	(61)	sync	70.29	(70; 3)	68.45	(68; 2)	$4.90487 \cdot 10^{12}$	18.77	(19; -4)
Callisto	16.69	62.28	(62; 3)	60.44	(60; 2)	sync	69.80	(70; -6)	67.96	(68)	$7.17929 \cdot 10^{12}$	19.15	(19; 6)
Ganymede	7.15	61.44	(61; 2)	59.60	(60; -3)	sync	68.95	(69)	67.11	(67; 6)	$9.88783 \cdot 10^{12}$	19.47	(19; 2)
Europa	3.55	60.74	(61; -4)	58.90	(59)	sync	68.25	(68; 4)	66.41	(66; 2)	$3.20274 \cdot 10^{12}$	18.34	(18; 3)
Io	1.77	60.04	(60)	58.20	(58; 6)	sync	67.55	(67; 2)	65.72	(66; -3)	$5.95992 \cdot 10^{12}$	18.96	(19)
Iapetus	79.32	63.84	(64; -6)	62.00	(62)	sync	71.36	(71; 3)	69.52	(69; 2)	$1.20500 \cdot 10^{11}$	15.06	(15)
Titan	15.95	62.24	(62; 4)	60.40	(60; 2)	sync	69.75	(70; -4)	67.91	(68)	$8.96273 \cdot 10^{12}$	19.37	(19; 3)
Rhea	4.52	60.98	(61)	59.14	(59; 6)	sync	68.49	(69; 2)	66.65	(67; -3)	$1.54000 \cdot 10^{11}$	15.31	(15; 3)
Dione	2.74	60.47	(60; 2)	58.64	(59; -3)	sync	67.99	(68)	66.15	(66; 6)	$7.10000 \cdot 10^{10}$	14.53	(14; 2)
Tethys	1.89	60.10	(60; 6)	58.27	(58; 3)	sync	67.62	(68; -3)	65.78	(66; -6)	$4.12000 \cdot 10^{10}$	13.99	(14)
Enceladus	1.37	59.78	(60; -6)	57.94	(58)	sync	67.30	(67; 3)	65.46	(65; 2)	$7.20000 \cdot 10^9$	12.24	(12; 4)
Mimas	0.94	59.41	(59; 3)	57.57	(57; 2)	sync	66.92	(67)	65.09	(65)	$2.50000 \cdot 10^9$	11.18	(11; 6)
Oberon	13.46	62.07	(62)	60.23	(60; 6)	sync	69.58	(69; 2)	67.75	(68; -4)	$1.93000 \cdot 10^{11}$	15.53	(15; 2)
Titania	8.71	61.63	(62; -3)	59.79	(60; -6)	sync	69.15	(69; 6)	67.31	(67; 3)	$2.20000 \cdot 10^{11}$	15.66	(16; -3)
Umbriel	4.14	60.89	(61; -6)	59.05	(59)	sync	68.40	(68; 3)	66.57	(66; 2)	$8.95000 \cdot 10^{10}$	14.76	(15; -4)
Ariel	2.52	60.39	(60; 3)	58.55	(58; 2)	sync	67.91	(68; -6)	66.07	(66)	$7.88000 \cdot 10^{10}$	14.64	(15; -3)
Miranda	1.41	59.81	(60; -6)	57.98	(58)	sync	67.33	(67; 3)	65.49	(65; 2)	$4.00000 \cdot 10^9$	11.65	(12; -3)
Triton	5.88	61.24	(61; 4)	59.40	(59; 2)	sync	68.75	(69; -4)	66.92	(67)	$1.42689 \cdot 10^{12}$	17.53	(17; 2)

Table 3: The sidereal orbital periods T_O , rotational periods T_R and gravitational constants μ of the planets, planetoids and large moons of the solar system. OE1 = $\ln(T_O/\tau_e)$, OE2 = $\ln(T_O/2\pi\tau_e)$, RP1 = $\ln(T_R/\tau_p)$, RP2 = $\ln(T_R/2\pi\tau_p)$, ME = $\ln(\mu/\lambda_e^3\omega_e^2)$. Corresponding with tab. 1, τ_e is the *electron* angular oscillation period, τ_p is the *proton* angular oscillation period, λ_e is the *electron* angular wavelength and ω_e is the *electron* angular frequency. The continued fractions (1) of the Fundamental Fractal \mathcal{F} are given in angle brackets. Although some data is shown with two decimals only, for calculating the logarithms, high precision data [46, 49–51] were used.

References

1. Verlinde E. On the origin of gravity and the laws of Newton. *arXiv:1001.0785v1* [hep-th] 6 Jan 2010.
2. Lara P., Cordero-Tercero G., Allen Ch. The reliability of the Titius-Bode relation and its implications for the search for exoplanets. *arXiv:2003.05121v1* [astro-ph.EP] 11 Mar 2020.
3. Brookes C. J. On the prediction of Neptune. Provided by the NASA Astrophysics Data System. *Kluwer Academic Publishers*, (1970).
4. Müller H. Global Scaling of Planetary Systems. *Progress in Physics*, 2018, v. 14, 99–105.
5. Gillon M. et al. Seven temperate terrestrial planets around the nearby ultracool dwarf star TRAPPIST-1. *Nature*, 21360, 2017.
6. Hand E. Kepler discovers first Earth-sized exoplanets. *Nature*, 9688, 2011.
7. Turyshev S. G., Toth V. T. The Puzzle of the Flyby Anomaly. *arXiv:0907.4184v1* [gr-qc] 23 Jul 2009.
8. Schlamminger S. et al. Test of the Equivalence Principle Using a Rotating Torsion Balance. *arXiv:0712.0607v1* [gr-qc] 4 Dec 2007.
9. Janiak A. Newton and the Reality of Force. *Journal of the History of Philosophy*, vol. 45, Nr. 1 (2007) 127–147.
10. Gillies G. T. The Newtonian gravitational constant: recent measurements and related studies. *Rep. Prog. Phys.*, vol. 60, 151–225, (1997).
11. Stacey F. D., Tuck G. J. Geophysical evidence for non-newtonian gravity. *Nature*, v. 292, pp. 230–232, (1981).
12. Miller A. H. Gravity and Isostasy. *Journal of the Royal Astronomical Society of Canada*, vol. 20, p. 327, (1926).
13. Battaglia M., Gottsmann J., Carbone D., Fernández J. 4D volcano gravimetry. *Geophysics*, vol.73, Nr. 6, (2008).
14. Van Camp M. Measuring seismic normal modes with the GWR C021 superconducting gravimeter. *Physics of the Earth and Planetary Interiors*, vol. 116, pp. 81–92, (1999).
15. Heki K., Matsuo K. Coseismic gravity changes of the 2010 earthquake in central Chile from satellite gravimetry. *Geophysical Research Letters*, vol. 37, L24306, (2010).
16. Dziewonski A. M., Anderson D. L. Preliminary reference Earth model. *Physics of the Earth and Planetary Interiors*, vol. 25, 297–356, (1981).
17. Stacey F. D. et al. Constraint on the planetary scale value of the Newtonian gravitational constant from the gravity profile within a mine. *Phys. Rev. D* 23, 1683, (1981).
18. Holding S. C., Stacey F. D., Tuck G. J. Gravity in mines. An investigation of Newton's law. *Phys. Rev.*, D 33, 3487 (1986).
19. Stacey F. D. Gravity. *Science Progress*, vol. 69, No. 273, pp. 1–17, (1984).
20. Quinn T., Speake C. The Newtonian constant of gravitation – a constant too difficult to measure? An introduction. *Phil. Trans. Royal Society A* 372, 20140253.
21. Yanpeng Li. A Possible Exact Solution for the Newtonian Constant of Gravity. *British Journal of Mathematics and Computer Science*, vol. 19(3), 1–25, (2016).
22. Pound R. V., Rebka Jr. G. A. Gravitational Red-Shift in Nuclear Resonance. *Physical Review Letters*, 3 (9): 439–441, (1959).
23. Müller On the Acceleration of Free Fall inside Polyhedral Structures. *Progress in Physics*, 2018, vol. 14, 220–225.
24. Dermott S. F. On the origin of commensurabilities in the solar system - II: The orbital period relation. *Mon. Not. R. Astron. Soc.*, 141 (3): 363–376, (1968)
25. Lovis C. et al. The HARPS search for southern extra-solar planets. *Astronomy and Astrophysics*, manuscript Nr. HD10180, ESO, (2010)
26. Colombo G. Rotational Period of the Planet Mercury. *Letters to Nature*, Nr. 5010, p. 575, (1965)
27. Müller H. On the Cosmological Significance of Euler's Number. *Progress in Physics*, 2019, v. 15, 17–21.
28. Dombrowski K. Rational Numbers Distribution and Resonance. *Progress in Physics*, 2005, v. 1, no. 1, 65–67.
29. Müller H. The Physics of Transcendental Numbers. *Progress in Physics*, 2019, vol. 15, 148–155.
30. Müller H. Global Scaling. The Fundamentals of Interscalar Cosmology. *New Heritage Publishers*, Brooklyn, New York, USA, ISBN 978-0-9981894-0-6, (2018).
31. Müller H. Fractal Scaling Models of Natural Oscillations in Chain Systems and the Mass Distribution of Particles. *Progress in Physics*, 2010, v. 6, 61–66.
32. Müller H. Scale-Invariant Models of Natural Oscillations in Chain Systems and their Cosmological Significance. *Progress in Physics*, 2017, v. 13, 187–197.
33. Khintchine A.Ya. Continued fractions. University of Chicago Press, Chicago, (1964).
34. Hilbert D. Über die Transcendenz der Zahlen e und π . *Mathematische Annalen*, 43, 216–219, (1893).
35. Panchelyuga V.A., Panchelyuga M. S. Resonance and Fractals on the Real Numbers Set. *Progress in Physics*, 2012, v. 8, no. 4, 48–53.
36. Müller H. Quantum Gravity Aspects of Global Scaling and the Seismic Profile of the Earth. *Progress in Physics*, 2018, vol. 14, 41–45.
37. Müller H. Emergence of Particle Masses in Fractal Scaling Models of Matter. *Progress in Physics*, 2012, v. 8, 44–47.
38. Ries A. Bipolar Model of Oscillations in a Chain System for Elementary Particle Masses. *Progress in Physics*, 2012, vol. 4, 20–28.
39. Ries A. Qualitative Prediction of Isotope Abundances with the Bipolar Model of Oscillations in a Chain System. *Progress in Physics*, 2015, vol. 11, 183–186.
40. Ries A., Fook M. Fractal Structure of Nature's Preferred Masses: Application of the Model of Oscillations in a Chain System. *Progress in Physics*, 2010, vol. 4, 82–89.
41. Tanabashi M. et al. (Particle Data Group), *Phys. Rev. D* 98, 030001 (2018), www.pdg.lbl.gov
42. Astrophysical constants. Particle Data Group, pdg.lbl.gov
43. Planck M. Über Irreversible Strahlungsvorgänge. *Sitzungsbericht der Königlich Preußischen Akademie der Wissenschaften*, 1899, v.1, 479–480.
44. Müller H. Gravity as Attractor Effect of Stability Nodes in Chain Systems of Harmonic Quantum Oscillators. *Progress in Physics*, 2018, vol. 14, 19–23.
45. Müller H. Global Scaling of Planetary Atmospheres. *Progress in Physics*, 2018, v. 14, 66–70.
46. NASA Planetary Fact Sheet - Metric (2019).
47. Bills B. G., Ray R. D. Lunar Orbital Evolution: A Synthesis of Recent Results. *Geophysical Research Letters*, v. 26, Nr. 19, pp. 3045–3048, (1999).
48. Catalog of Exoplanets. Observatoire de Paris, <http://exoplanet.eu/catalog/>
49. Jacobson R. A. et al. The gravity field of the saturnian system from satellite observations and spacecraft tracking data. *The Astronomical Journal*, vol. 132, 2520–2526, (2006).
50. Jacobson R. A. The orbits of the uranian satellites and rings, the gravity field of the uranian system. *The Astronomical Journal*, vol. 148, 76–88, (2014).
51. Petropoulos A. E. Problem Description for the 6'h Global Trajectory Optimisation Competition. *Jet Propulsion Laboratory*, California Institute of Technology, (2012).

The Role Played by Plasma Waves in Stabilizing Solar Nuclear Fusion

Tianxi Zhang

Department of Physics, Chemistry, and Mathematics, Alabama A & M University, Normal, Alabama 35762, USA.

E-mail: tianxi.zhang@aamu.edu

Since the wave function of two-scattering protons has been used for that of diproton or helium-2 in the conventional analysis with Fermi theory, the probability for a diproton to form a deuteron via a β^+ -decay has been extremely under calculated. This implies that the rareness of β^+ -decay in diprotons is not rare enough to inhibit the solar nuclear fusion. To meet the observed rate of solar nuclear fusion, the core of the Sun must involve another significant physical effect to inhibit solar nuclear fusion. This study finds that plasma waves can play this role, because they significantly reduce the electric permittivity of the core plasma and thus extremely raise the Coulomb barrier or shift the Gamow peak to a higher energy of particles. It is shown that, if the frequency of plasma waves that are globally generated in the core plasma of turbulences is about 1.28 times the plasma frequency, the Sun can have the actual fusion rate or shine on at the currently observed luminosity. Therefore, in addition to the quantum tunneling effect and rareness of β^+ -decay, plasma waves can also play an essential role in the solar nuclear fusion and power emission. The result of this study may also give implications to supernova explosion, missing solar neutrino, and plasma nuclear fusion in laboratory.

1 Introduction

The Sun is a giant natural fusion reactor [1]. It smashes about 3.6×10^{38} hydrogen nuclei or protons per second to produce helium nuclei or α -particles, while releasing nuclear power of 3.85×10^{26} W. This nuclear fusion process occurring in the core of the Sun has been comprehensively investigated for many decades based on the well-developed stellar nucleosynthesis and quantum physics. It is well known that, in the dense and hot core of the Sun with ~ 1.5 keV (or $\sim 1.67 \times 10^7$ K) temperature and Boltzmann-Maxwell's distribution of the core's total 1.2×10^{56} protons, there should not be any proton able to overcome the 820 keV (or 9.5×10^9 K) Coulomb barrier to make the fusion reactions occur.

According to Gamow's quantum tunneling probability [2] however, the energy region where nuclear reactions are most likely to occur (i.e. the Gamow peak) is around 10^8 K. This allows one part per million of the core's total 1.2×10^{56} protons to penetrate the Coulomb barrier. With this probability of barrier tunneling or penetration, the high ion-collision frequency of 20 terahertz means that the core of the Sun fuses all its protons within the order of only microseconds (i.e. a rate of 10^{63} s^{-1} , 25 orders of magnitude higher than the actual reaction rate) and thus would instantaneously explode. It is generally believed that the major reasons why the Sun does not instantaneously blow up are (1) the difficulty of double proton (also called diproton) formation (estimated to be lowered only by $\sim 10^{-6}$ according to the Gamow tunneling probability), (2) the rareness of β^+ -decay from diprotons (needed to be lowered by $\sim 10^{-25}$ according to the Sun's actual luminosity) and (3) the squeezing of the Sun's strong gravity.

However, in the conventional analysis and calculation of the Fermi theory of the β^+ -decay, the significant wave func-

tion of two-scattering protons was usually used for the inefficient wave function of the diproton outside the potential energy well [3]. This is not physical and greatly weakens the wave function of the diproton inside the potential energy well, so that leads to the probability for a diproton to form a deuteron via a β^+ -decay to be extremely under calculated [4]. In other words, the rareness of β^+ -decay in diprotons may not be rare enough to inhibit the solar nuclear fusion or lower the fusion rate by 25 orders of magnitude, in order to stop the Sun's instantaneous explosion and have the currently observed luminosity. The quantum tunneling effect allows many diprotons formed in the Sun's core, but the probability for a diproton to form a deuteron via a β^+ -decay may not be lower than that for a diproton to separate back to two protons by 25 orders of magnitude. Observations have only given an upper bound that a diproton (or helium-2 nucleus) gets β^+ -decay by less than one per ten thousands, i.e. $< 0.01\%$ [5].

In this paper, we propose a new mechanism of inhibition that can significantly reduce the fusion reaction rate and thus effectively prevent the Sun from an instantaneous explosion. We suggest that the core of the Sun involves a significant physical effect or inhibitor called plasma oscillation or wave, which significantly reduces the electric permittivity of the core plasma. A significantly reduced electric permittivity will greatly raise the Coulomb barrier as well as efficiently lower the Gamow tunneling probability. These changes lead to greatly shift the Gamow peak to the region of higher energies of particles. Quantitative study in this paper indicates that if the frequency ω of plasma oscillations or waves that are globally generated in the core plasma of turbulences is about 1.28 times the plasma frequency ω_p , the Sun can have the actual fusion rate or shine on at the currently observed luminosity.

Therefore, in addition to the quantum tunneling effect, the plasma oscillations may play also an essential role in the Sun's nuclear fusion and power emission. The quantum tunneling effect makes the fusion to occur, while the plasma oscillations in association with the weak β^+ -decay of diprotons guarantees that the Sun will not explode. We also suggest that a supernova explosion occurs when plasma oscillations in the core of a star at the end of its life are significantly weakened in intensity or changed in frequency, that causes the heavy ion fusion to be significantly speeded up and the huge amount of energies and neutrinos to be instantaneously emitted. The result of this study also gives important implications to plasma nuclear fusion in laboratory and the solar neutrino missing problem.

2 Coulomb barrier and solar nuclear power emission

The measurement of power emission indicates that the luminosity of the Sun at present is about 3.85×10^{26} W, which can be calculated from

$$L_{\odot} = 4\pi R^2 \sigma T^4, \quad (1)$$

where $R = 7 \times 10^8$ m is the radius of the Sun, $\sigma = 5.67 \times 10^{-8}$ W/(m²K⁴) is the Stefan-Boltzmann constant, and $T = 5778$ K is the surface temperature of the Sun. At this luminosity, the Sun's gravitational energy, determined by

$$U = \frac{3GM^2}{5R} \approx 2.3 \times 10^{41} \text{ J}, \quad (2)$$

can only let it shine about $U/L_{\odot} \sim 19$ million years, which is the thermal or Kelvin-Helmholtz timescale determined by K/L_{\odot} and is much shorter than the actual Sun's lifetime. Here $G = 6.67 \times 10^{-11}$ N m²/kg² is the gravitational constant, $M = 1.99 \times 10^{30}$ kg is the mass of the Sun, K is the internal energy or the total kinetic energy of particles in the Sun, determined by

$$K = \frac{3}{2} k_B N T_{\text{core}} \approx 4.1 \times 10^{41} \text{ J}, \quad (3)$$

with $k_B = 1.38 \times 10^{-23}$ the Boltzmann constant, $N = M/m_p$ the total number of protons within the Sun, $m_p = 1.67 \times 10^{-27}$ kg the mass of the proton, and $T_{\text{core}} = 1.67 \times 10^7$ K the temperature of the core of the Sun. It should be noted here that the hot core of the Sun is about 1/3 of its diameter or 1/10 of its mass, which means that the internal energy of the Sun should be several times less than that given by (3).

The total number of protons in the core of the Sun is given by

$$N_0 = \frac{1}{10} \frac{M}{m_p} \sim 1.2 \times 10^{56}, \quad (4)$$

or number density to be $n_0 \sim 2.2 \times 10^{30}$ m⁻³. It is the number or number density of protons available for fusion and the Sun should be mainly powered by nuclear fusion. According to nuclear physics, every time four protons are fused to form one

helium, the reactions produce two neutrinos, two positrons, and two photons, and release in total a net energy of $E_{4p} \sim 27$ MeV from the deficit of $\sim 3\%$ masses of four protons. The energy from the fusion of all protons in the core of the Sun, calculated by

$$E = \frac{1}{10} \frac{M}{4m_p} E_{4p} \approx 1.3 \times 10^{44} \text{ J}, \quad (5)$$

can run the Sun at the present rate of emission for about 10 billion years. On the other hand, to have the present energy emitting rate, the Sun needs to fuse its protons at a rate of about

$$\frac{dN_0}{dt} = \frac{4L_{Sun}}{E_{4p}} \approx 3.6 \times 10^{38} \text{ s}^{-1} \quad (6)$$

protons in one second.

In order to fuse protons, the extremely high Coulomb barrier between them, determined by

$$U_C = \frac{q_p^2}{4\pi\epsilon_0 d_p} \approx 8.2 \times 10^2 \text{ keV or } 9.5 \times 10^9 \text{ K}, \quad (7)$$

must be overcome [6]. Here $q_p = 1.6 \times 10^{-19}$ C is the proton's electric charge (equal to the fundamental unit of charge e), $\epsilon_0 = 8.85 \times 10^{-12}$ C²/(m²N) is the electric permittivity constant in free space, and $d_p = 1.76 \times 10^{-15}$ m is the diameter of a proton. Since the average kinetic energy of protons in the Sun's core with temperature 1.67×10^7 K, $K = (3/2)k_B T_{\text{core}} = 2.16$ keV, is about 383 times lower than the Coulomb barrier between protons, and it must be very hard to have protons to be able to climb over the Coulomb barrier. According to the Boltzmann-Maxwellian distribution function [7, 8], we have the number of protons with velocity in the range $v - v+dv$ to be given by

$$dN = N_0 \left(\frac{m}{2\pi k_B T} \right)^{3/2} 4\pi v^2 \exp\left(-\frac{mv^2}{2k_B T}\right) dv, \quad (8)$$

or with energy in the range of $E - E+dE$ to be given by,

$$dN = N_0 \frac{2\pi}{(\pi k_B T)^{3/2}} \sqrt{E} \exp\left(-\frac{E}{k_B T}\right) dE. \quad (9)$$

Here N_0 is the total number of all particles. Then, the number of protons with energy above the Coulomb barrier U_C can be found by integrating the function (9) with respect to the energy (E) in the range from U_C to infinity as

$$\begin{aligned} N_C &= N_0 \int_{U_C}^{\infty} \frac{2\pi}{(\pi k_B T)^{3/2}} \sqrt{E} \exp\left(-\frac{E}{k_B T}\right) dE \\ &= \frac{2N_0}{\sqrt{\pi}} \sqrt{\frac{U_C}{k_B T}} \exp\left(-\frac{U_C}{k_B T}\right) + N_0 \operatorname{erfc}\left(\sqrt{\frac{U_C}{k_B T}}\right). \end{aligned} \quad (10)$$

Considering the ion collision frequency in the hot core of the Sun to be calculated by

$$\nu_i = 4.8 \times 10^{-8} Z_i^4 \mu^{-1/2} n_i \ln \Lambda T_i^{-3/2} \text{ s}^{-1}, \quad (11)$$

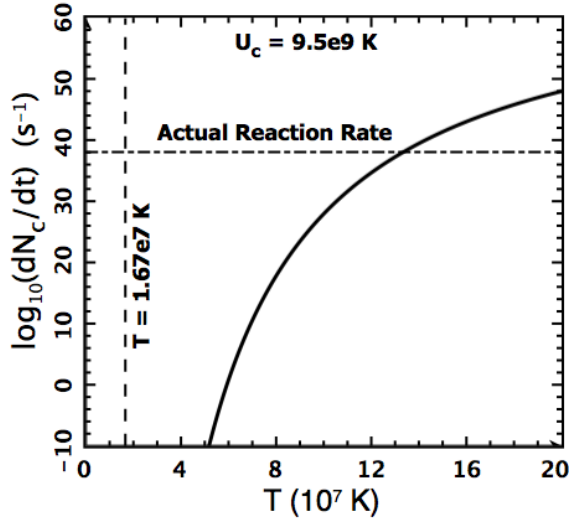


Fig. 1: The reaction rate of protons is plotted as a function of the Sun's core temperature in the case of without considering the quantum tunneling effect. The result indicates that no nuclear fusion can actually occur.

where Z_i is the ion charge state, μ is the ion-proton mass ratio, n_i is the number of ions per cubic centimeter, $\ln \Lambda$ is the Coulomb logarithm with a convenient choice to be 10, and T_i is the ion temperature in units of eV. For protons in the Sun's core, the collision frequency can be $\nu_p \sim 2 \times 10^{13}$ Hz. The reaction rate of protons that can climb over the Coulomb barrier can then be estimated by

$$\frac{dN_c}{dt} = N_c \nu_p s^{-1}. \quad (12)$$

Fig. 1 plots this reaction rate of protons as a function of the core temperature. It is seen that the reaction rate of the protons is about zero (many orders of magnitude less than $10^{-10} s^{-1}$), so that no nuclear fusion occurs in the core of the Sun if the core temperature is equal to the conventional value $T_{core} = 1.67 \times 10^7$ K. For the reaction rate of protons to be the actually observed rate of 3.6×10^{38} protons per second, the Sun's core temperature must be about 1.3×10^8 K or above. Therefore from classical physics, solar nuclear fusion will hardly occur.

3 Quantum tunneling effect on solar nuclear reaction

Quantum tunneling effect plays an essential role in solar nuclear fusion. According to the Gamow tunneling probability [2], given by

$$P_g = \exp\left(-\sqrt{\frac{E_g}{E}}\right), \quad (13)$$

one can determine the number of protons with energy between E and $E+dE$ that can tunnel through or penetrate the

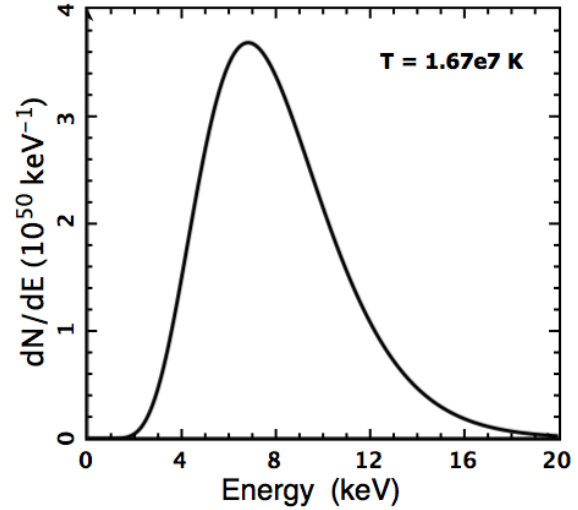


Fig. 2: Energy spectrum of protons that can penetrate the Coulomb barrier for fusion. The number of tunneling protons per unit energy in the core of the Sun is plotted as a function of the energy. The maximum is usually called the Gamow peak, which is located near the energy of about 7 keV.

Coulomb barrier as

$$dN_g = P_g dN$$

$$= N_0 \frac{2\pi}{(\pi k_B T)^{3/2}} \sqrt{E} \exp\left(-\frac{E}{k_B T} - \sqrt{\frac{E_g}{E}}\right) dE, \quad (14)$$

where E_g is the Gamow energy determined by

$$E_g = 2m_r c^2 (\pi \alpha Z_a Z_b)^2. \quad (15)$$

Here m_r is the reduced mass of the nuclei, c is the speed of light, Z_a and Z_b are the ionization states of the nuclei, and $\alpha = e^2/(2\epsilon_0 h c)$ is the fine-structure constant.

The distribution (14) for the number of tunneling protons with respect to the energy exhibits a maximum called the Gamow peak that has energy to be significant (about 120 times) less than the Coulomb barrier, so that the quantum tunneling effect greatly enhances the reaction rate in the core of the Sun. To see in more details the increase of the tunneling probability, we plot in Fig. 2 the Gamow peak for the Sun's core with temperature 1.67×10^7 K. The energy of the peak is around 7 keV and the height of the peak is around 3.7×10^{50} protons per keV.

Both the height and energy of the Gamow peak depend on the temperature of the Sun's core. Evaluating the extreme value of (14), we can obtain the energy of Gamow peak as a function of the core's temperature and other parameters or constants as the following implicit equation

$$1 - \frac{2E_p}{k_B T} + \sqrt{\frac{E_g}{E_p}} = 0. \quad (16)$$

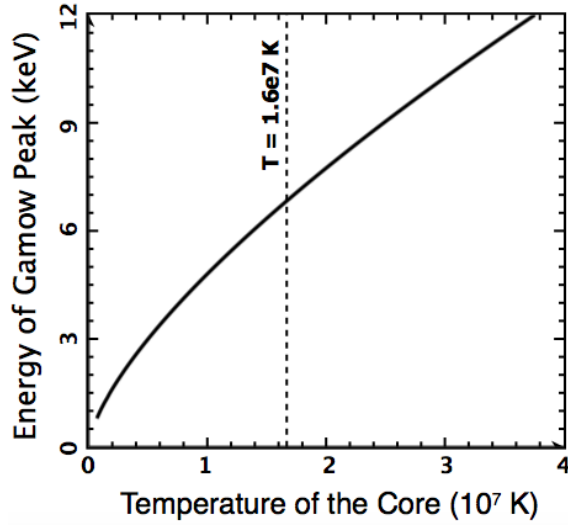


Fig. 3: The energy of the Gamow peak is plotted as a function of the temperature of the core.

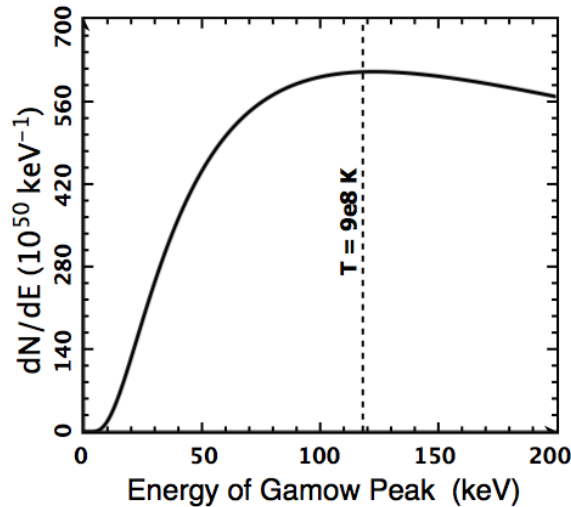


Fig. 4: The number of protons per unit energy is plotted as a function of the energy of the Gamow peak, which increases with the temperature core.

Substituting the energy of the Gamow peak (E_p) back into (14), we can determine the height of the Gamow peak as a function of the core's temperature and other parameters or constants. Fig. 3 plots the energy of the Gamow peak as a function of the temperature of the core. It is seen that the energy of the Gamow peak increases as the temperature of the core increases. The Gamow peak is at about 7 keV if the core temperature is 1.67×10^7 K and increases to 10 keV when the core temperature increases to 3×10^7 K. Fig. 4 plots the number of tunneling protons per unit energy (i.e. per keV) as a

function of the energy of the Gamow peak, which increases as the temperature of the core increases as shown in Fig. 3. This further shows that the number of tunneling protons per unit energy reaches a maximum ($\sim 6 \times 10^{52}$ keV $^{-1}$) when the energy of the Gamow peak is about 120 keV (or the temperature of the core is about 0.9 billion Kelvins). In the Sun's core temperature of 1.67×10^7 K, the energy of the Gamow peak is only 7 keV and the maximum number of tunneling protons is about 3.6×10^{50} keV $^{-1}$. Based on this peak of the maximum number of tunneling nuclei, we can find the maximum reaction rate as a function of the energy of the Gamow peak or the temperature of the core. This result may be important to optimize plasma fusion in the laboratory.

Then, the number of protons that can penetrate or tunnel through the Coulomb barrier can be found by integrating the function (14) with respect to the energy (E) in the range from zero to infinity as

$$N_g = \int_0^{\infty} P_g dN$$

$$= \lim_{E_2 \rightarrow \infty} \int_0^{E_2} \frac{2\pi \sqrt{E}}{(\pi k_B T)^{3/2}} \exp\left(-\frac{E}{k_B T} - \sqrt{\frac{E_g}{E}}\right) dE. \quad (17)$$

Multiplying N_g with the collision frequency, we obtain the reaction rate of nuclear fusion with the quantum tunneling effect as

$$\frac{dN_g}{dt} = N_g \nu_p. \quad (18)$$

To see the reaction rate quantitatively, we plot in Fig. 5 the reaction rate (18) as a function of the upper energy of the integration (E_2), which should approach infinity (or a value that is big enough, e.g. 30 keV). For the core of the Sun, the reaction rate saturates at $\sim 2 \times 10^{63}$ protons per second when the upper energy of the integration is $E_2 \gtrsim 30$ keV. This reaction rate is an order of magnitude 25 times higher than the actual reaction rate. Without a significant inhibitor to greatly slow down the reactions, the Sun should have instantaneously exploded.

4 Plasma oscillation effect on solar nuclear fusion

Plasma oscillations or waves can be considered as a great inhibitor for the solar nuclear reaction, because the dielectric constant of plasma with plasma oscillations or waves is given by [9]

$$\epsilon_r = 1 - \frac{\omega_p^2}{\omega^2}, \quad (19)$$

where ω_p is the plasma frequency defined by

$$\omega_p = \sqrt{\frac{n_e e^2}{\epsilon_0 m_e}}, \quad (20)$$

and ω is the frequency of plasma waves generated in the core by the oscillations of free electrons. Eq. (19) indicates that

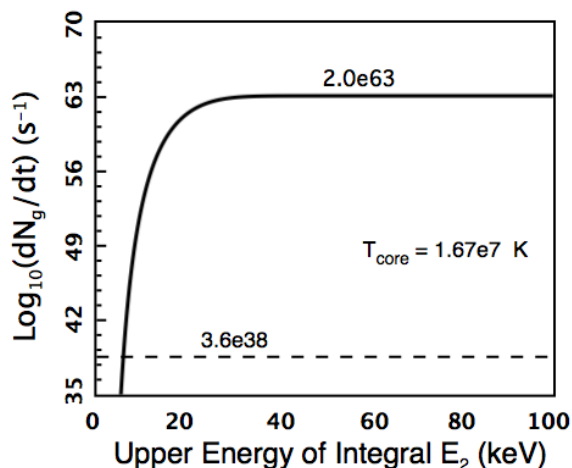


Fig. 5: The reaction rate of protons in the core of the Sun. The number of adequate collisions per second between protons is plotted as a function of the upper energy of the integration.

plasma oscillations or waves can make the dielectric constant to be less than unity and hence raises the Coulomb barrier and increases Gamow energy or reduces quantum tunneling probability. Increases of both the Coulomb barrier and the Gamow energy can greatly reduce the fusion reaction rate.

There are several types of plasma waves that can be initiated by electron oscillations [10] such as electrostatic Langmuir waves [11] with the dispersion relation given by

$$\omega^2 = \omega_p^2 + 3k^2 v_{Te}^2, \quad (21)$$

where v_{Te} is the thermal velocity of electrons and k is the wavenumber. Fig. 6 shows the dispersion relation of the Langmuir waves by plotting the wave frequency as a function of the wavenumber. It is seen that the frequency is about 1.28 times the plasma frequency when the wavenumber is about $k \sim 10^{9.4} \sim 2.5 \times 10^9 \text{ m}^{-1}$. It is about half of the wavenumber of blackbody radiation at the peak, $k_{bb} = T_{core}/(2.9 \times 10^{-3}) \sim 5.8 \times 10^9 \text{ m}^{-1} \sim 2.3k$ and also half of the Debye wavenumber, $k_d = [n_e e^2 / (\epsilon_0 k_B T_{core})]^{1/2} \sim 5.0 \times 10^9 \text{ m}^{-1} \sim 2k$. In the core of the Sun, we have $\omega_p \sim 3.6 \times 10^{18} \text{ Hz}$, i.e. in the X-ray frequency range.

To see the plasma oscillation effect on the solar nuclear fusion, we plot in Fig. 7 the reaction rate (18) as a function of the upper energy of the integration in three cases with the frequencies of plasma oscillations or waves given by $\omega/\omega_p = 1.25, 1.28, 1.32$, respectively. For the core of the Sun with $\omega/\omega_p \sim 1.28$, the reaction rate saturates at $\sim 3.6 \times 10^{38}$ protons per second when the upper energy of the integration is $E_2 \geq 80 \text{ keV}$. This reaction rate is in magnitude about the order of the actual reaction rate. Slightly varying the frequency, we have a reaction rate quite different. In general, the higher

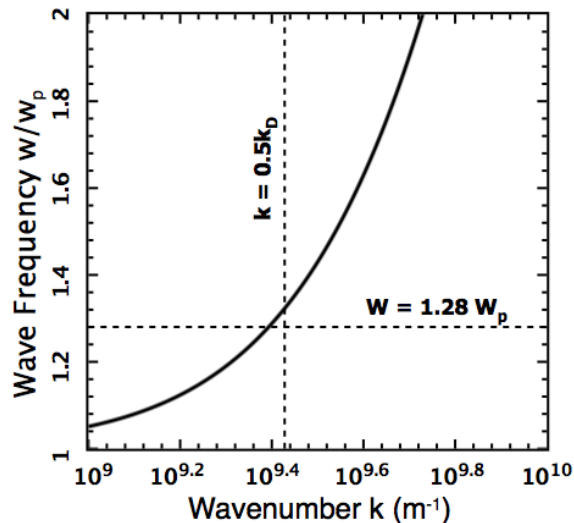


Fig. 6: The dispersion relation of the plasma Langmuir waves. The frequency of the waves is plotted as a function of the wavenumber. It is seen when the wavenumber is about half of the Debye wavenumber or wavelength is about the diameter or twice the radius of the Debye sphere.

the frequency of the plasma waves, the weaker the effect of plasma oscillations on the nuclear fusion is. It is an extremely efficient inhibitor of the solar nuclear fusion.

5 Discussions and conclusions

At the end of its life, a star runs out proton-proton fusion and thus varies the plasma oscillations, which causes this efficient inhibitor to be ineffective. With this reason, we suggest that supernova explosions may occur when plasma oscillations in the core of a star at the end of its life are significantly weakened in intensity or changed in frequency that cause the heavy ion fusion to be significantly speeded up and out of control and the huge amount of energies and neutrinos to be instantaneously emitted. This study of the role of plasma oscillation played in solar nuclear fusion provides us an alternative mechanism for supernova explosions, in addition to the previously proposed and developed models of supernova explosions driven by magnetohydrodynamic (MHD) rotation [12], acoustic waves [13], neutrinos [14], and gravitational field shielding [15].

The plasma oscillations or waves with frequency about 1.28 times the plasma frequency can reduce the electric permittivity or the dielectric constant by a factor of one third in comparison with free space. The effective refractive index of plasma is given by $n = \sqrt{\epsilon_r} \sim 0.6$. Postulating the mass energy conversion in plasma by $E = mc^2/n^2$ leads to the deficit of 3% proton masses in fusion that can produce three times the nuclear energy. Then, having the same luminosity, the Sun only needs to fuse one third of the early suggested num-

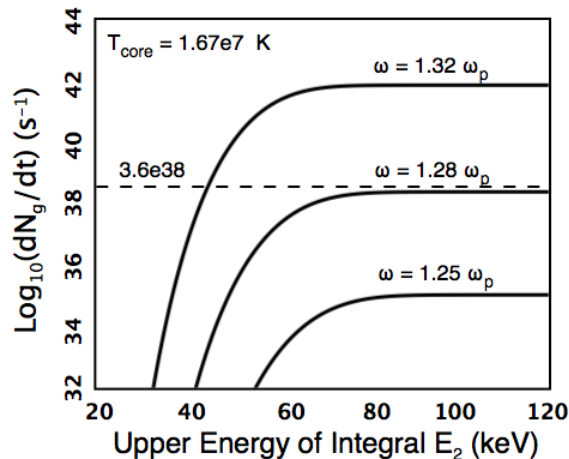


Fig. 7: The reaction rate of protons in the core of the Sun. The number of adequate collisions per second between protons is plotted as a function of the upper energy of the integration. Here the plasma oscillation effect on the reaction rate is included.

ber of protons, i.e. $\sim 1.2 \times 10^{38}$ protons per second. This result provides us an alternative of quantitatively explaining the missing two thirds of the solar neutrinos [16]. The Sun's lifetime is thus tripled, to be over thirty billion years.

Plasma oscillations with appropriate frequency of disturbances may also affect the nuclear reactions of plasma fusion in the laboratory. Above the plasma frequency ($\omega > \omega_p$), plasma oscillations would reduce the reaction rates and hence make the fusion hard to occur. Below the plasma frequency ($\omega < \omega_p$), however, plasma oscillations can lead to a negative dielectric constant, which switches the Coulomb interaction between nuclei to be an attractive force from a repulsive one. In this case, the Coulomb barrier disappears and nuclei fuse freely. Therefore, the result of this study also gives an important implication to plasma nuclear fusion in the laboratory. Regarding plasma fusion in the laboratory, the author has recently developed two new mechanisms: (1) plasma fusion at some keV with extremely heated ^3He ions or tritons [17–19]; (2) plasma fusion with Coulomb barrier lowered by scalar field [20].

As a consequence of this study, except for the conventional inhibitor of unlikely β^+ -decay from diprotons, we find that plasma oscillations or waves can be an efficient inhibitor for the solar nuclear fusion, as it significantly reduces the electric permittivity of the core plasma and thus extremely raises the Coulomb barrier or shifts the Gamow peak to a higher energy of particles. When the frequency of plasma oscillations or Langmuir waves that are globally generated in the core plasma of turbulences is about 1.28 times the plasma frequency, the Sun can have the actual fusion rate or shine on at the currently observed luminosity. Therefore, in addition to the quantum tunneling effect, the weak β^+ -decay, the plasma

oscillations play also an essential role in the Sun's nuclear fusion and power emission.

Acknowledgements

The author acknowledges Bing Li for support and also thanks reviewers and editors for improving the manuscript quality.

Received on February 2, 2020

References

- Zirin H. *Astrophysics of the Sun*. Cambridge Univ. Press, Cambridge, 1988.
- Gamow G. Zur Quantentheorie des Atomkernes. *Z. Physik*, 1928, v. 51, 204–212.
- Bethe H.T. The Formation of Deuterons by Proton Combination. *Physical Review*, 1938, v. 54, 248-254
- Zhang T.X. A Critical Issue on Solar Nuclear Fusion. 2021, to be submitted
- en.wikipedia.org/wiki/Isotopes_of_helium.
- Coulomb P.M. *Histoire de l'Académie Royale des Sciences*. 1875, 569–577.
- Maxwell J.C. On the Motions and Collisions of Perfectly Elastic Spheres. *Philosophical Magazine and Journal of Science*, 1860, v. 19, 19–32.
- Boltzmann L. Weitere Studien über das Wärmegleichgewicht unter Gasmolekülen. *Sitzungsber. Kais. Akad. Wiss.*, 1872, v. 66, 275–370.
- Fitzpatrick R. *Classical Electromagnetism*. <http://farside.ph.utexas.edu/teaching>, 2006.
- Stix T.H. *Waves in Plasmas*. Springer, AIP Press, 1992.
- Langmuir I. The Interaction of Electron and Positive Ion Space Charges in Cathode Sheaths. *Physical Review*, 1929, v. 33, 954
- Meier D.L., Epstein R.I., Arnett D., Schramm D.N. Magnetohydrodynamic Phenomena in Collapsing Stellar Cores. 1976, *Astrophysical Journal*, 1976, v. 204, 869–878.
- Burrows A., Livne E., Dessart L., Ott C.D., Murphy J. Features of the Acoustic Mechanism of Core-Collapse Supernova Explosions. *Astrophysical Journal*, 2007, v. 655, 416–433.
- Colgate S.A., White R.H. The Hydrodynamic Behavior of Supernovae. *Astrophysical Journal*, 1966, v. 143, 626–681.
- Zhang T.X. Gravitational Field Shielding and Supernova Explosions. *Astrophysical Journal Letters*, 2010, v. 725, L117–L121.
- Davis R.Jr., Harmer D.S., Hoffman K.C. Search for Neutrinos from the Sun. *Physical Review Letters*, 1968, v. 20, 1205–1209.
- Zhang T.X. Two-Stage Heating Mechanism for Plasma Fusion at 10 MK. *Proceedings of IEEE 25th Symposium on Fusion Engineering (SOFE)*, 2013, 978-1-4799-0171-5/13.
- Zhang T.X., Ye M.Y. Plasma fusion at 10 MK with Extremely Heated ^3He Ions. *IEEE Transactions on Plasma Science*, 2014, v.42, 1430–1437.
- Zhang T.X. Plasma fusion of Deuterons at Kiloelectron Volts with Extremely Heated Tritons. *IEEE Transactions of Plasma Science*, 2020, v. 48, 2884–2891.
- Zhang T.X. Nuclear Fusion with Coulomb Barrier Lowered by Scalar Field. *Progress in Physics*, 2019, v. 15, 191–196.

Antarctic Circumpolar Current: Driven by Gravitational Forces?

Franklin Potter

Sciencegems, 8642 Marvale Drive, Huntington Beach, CA 92646 USA.

E-mail: frank11hb@yahoo.com

ORCID: 0000-0002-9440-2291

The Antarctic Circumpolar Current (ACC) is the largest ocean current, one that travels west to east at a velocity of about 2 m/s greater than the Earth's rotation velocity at latitudes from 40°S to about 60°S. Simple models of the winds driving this current consider a linear relationship between the wind strength and the water transport. However, the behavior is much more complex. The ultimate energy source driving the winds and this current remains to be identified. I investigate whether a gravitational force dictated by Quantum Celestial Dynamics (QCM) is the true energy source that maintains the ACC.

1 Introduction

The Antarctic Circumpolar Current (ACC), the largest ocean current on Earth, flows west to east at about 2 m/s faster than the Earth's rotation at its latitude of about 40°S to about 60°S near the Antarctic continent [1, 2], as shown in Figure 1. Its mean transport is estimated to be about 134 sverdrup, i.e., $134 \times 10^6 \text{ m}^3/\text{s}$. There are two different atmospheric winds to consider: the winds along the ACC and the winds along the contours of Antarctica, with variations in both able to cause robust changes in ACC transport. They are considered to be the major driving force of this enormous water current.

But the ACC current extends to the ocean floor, with a strong current velocity of about 2 cm/s at a depth of 3000 meters [3,4]. So this approach becomes quite complicated by involving thermodynamic mixing vertically and horizontally, various wind strength and direction changes, Coriolis force effects, eddies, etc.

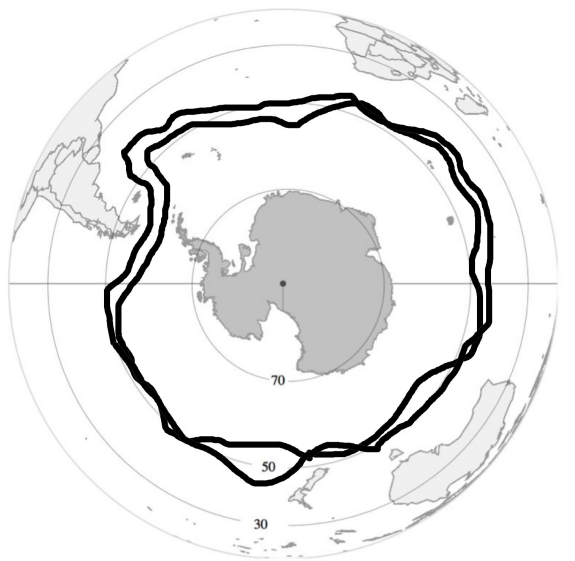


Fig. 1: Antarctic Circumpolar Current moving west to east faster than the Earth's rotation, showing its deviations from a circular path with many latitude variations.

Ultimately, one might expect to identify a powerful and consistent energy source that would be capable of forcing such a large water transport at all depths as well as help drive the winds in the atmosphere.

Herein I apply Quantum Celestial Mechanics (QCM) to the binary system of the rotating Earth and the orbiting Moon, both objects providing the total system vector angular momentum required by QCM [5] to determine its gravitational stationary energy states exhibiting the quantization of angular momentum per unit mass. I can use the familiar general relativistic Schwarzschild metric because the QCM equilibrium radii r_{eq} are much larger than the 9 millimeter Schwarzschild radius r_g of the Earth. These QCM states at specific equilibrium radii in the plane of the Equator are assumed to define rotational cylinders co-axial to the Earth's rotation axis that intersect the Earth's surface. In particular, I am interested in determining whether the QCM angular momentum quantization per unit mass approach can be the source of the driving force responsible for the Antarctic Circumpolar Current.

2 QCM brief history review

In 2003 Howard G. Preston and I introduced [5] Quantum Celestial Mechanics (QCM) to explain the spacings of planetary orbits in the Solar System and in all known exoplanetary systems. In the Schwarzschild metric, the quantization of the total angular momentum per unit mass in a gravitationally bound system constrains the possible orbital radii to specific allowed values determined by quantization integers.

At that time, we were not successful in finding a system that could be a definitive test of QCM. Unfortunately, there existed no gravitationally bound system with three or more celestial objects for which the angular momentum was known to within 10%, not for the Solar System nor for the Jovian planets and their satellites. Therefore, we proposed several laboratory experiments to test for a repulsive gravitational QCM force, including the response of two pendulums in a microwave vacuum chamber and of the response of one LIGO interferometer to the slow one rotation per hour spin of a 10 kg mass several meters distant. Neither tests were

approved.

However, the 2015 New Horizons flyby of Pluto and its 5 moons did provide the data [6] for the definitive test of QCM, with the predicted QCM orbital constraint relation verified to within 2.4%.

The QCM gravitational wave equation derived from the general relativistic Hamilton-Jacobi equation is

$$g^{\alpha\beta} \frac{\partial^2 \Psi}{\partial x^\alpha \partial x^\beta} + \frac{\Psi}{H} = 0 \quad (1)$$

in which the scalar $\Psi = \exp[iS'/H]$, for $S' = S/\mu_i c$, with S the classical action, μ_i the mass of the particle acted upon, and c the speed of light in vacuum. The system scaling length is defined as $H = L_T/M_T c$, with L_T the total vector angular momentum for the system of total mass M_T .

This QCM gravitational wave equation is not quantum gravity. However, there is a relationship to the Schrödinger equation in quantum mechanics that was derived from the normal Hamilton-Jacobi equation using the transformation $\Psi = \exp[iS/h]$, with the classical action S and the universal Planck's constant h . Our H is not a universal constant.

The inherent generality and power of this gravitational wave equation arises from its dependence upon only two important physical parameters that characterize the gravitationally bound system: the total mass M_T and the total vector angular momentum L_T , both quantities defining H . In planetary systems, for example, the larger the value of H , the larger the spacings will be between the allowed QCM orbital equilibrium radii.

Successful applications of QCM have included the prediction of a Solar System total angular momentum of 1.86×10^{45} kg-m²/s, most of which is contributed by the Oort Cloud at about 40,000 AU, a value about 50 times the listed angular momentum of the Sun plus the 8 planets [7]. Compared to all the known exoplanetary systems, our Solar System is unique because no other system exhibits such large planetary spacings that require this large total system angular momentum value.

Successful applications to galaxies and clusters of galaxies describe how QCM can fit their almost constant rotational velocities without invoking dark matter. Also, QCM was shown to be able to derive the MOND relation, which fits the galaxy rotational data extremely well and is considered a viable competitor to dark matter approaches [8].

A new interpretation [9] of the redshifts of light from distance sources in the Universe was introduced by applying the interior metric in a static Universe, thereby revealing a possible negative QCM gravitational potential that becomes more negative non-linearly from the observer, meaning that the light source is in a deeper negative gravitational potential for all observers. As such, the clocks at the light source tick slower than at the observer and the observed redshifts are purely gravitational redshifts. No dark energy is required to

agree with the measured SNe Ia redshifts that have been interpreted as a recently accelerating Universe, and the Hubble value becomes distance dependent.

3 QCM Schwarzschild metric radial equation

Applying the general relativistic Schwarzschild metric to the QCM wave equation for radius values beyond r_g , dropping very small terms, and then evaluating the angular equations in spherical polar coordinates, leaves the radial r equation [5]

$$\frac{d^2 \Psi}{dr^2} + \frac{2}{r} \frac{d\Psi}{dr} + \left[\frac{E}{\mu} + \frac{r_g c^2}{2r} - \frac{\ell(\ell+1)H^2 c^2}{2r^2} \right] \Psi \approx 0, \quad (2)$$

with ℓ the angular momentum integer from the θ and ϕ coordinates.

From the energy expression in the square bracket, the effective potential

$$V_{eff} = -\frac{r_g c^2}{2r} + \frac{\ell(\ell+1)H^2 c^2}{2r^2}, \quad (3)$$

and the equilibrium radius for the QCM state ℓ is

$$r_{eq} = \ell(\ell+1) \frac{2H^2}{r_g}. \quad (4)$$

If one decides to use the Schwarzschild metric in cylindrical coordinates instead, then the product $\ell(\ell+1)$ usually becomes replaced by m^2 , with m the integer for the ϕ direction quantization.

I will take this r_{eq} to be at the plane of the Equator for defining a cylinder co-axial with the Earth's rotation axis that extends in both directions to intersect the Earth's surface in North and South latitudes. Thus, by knowing the H and r_g values to calculate r_{eq} , one can predict the equilibrium radii of all the QCM states.

4 Results

4.1 Earth spin only

The total vector angular momentum of the Earth-Moon system is required by QCM. However, a preliminary simple calculation that considers just the rotation of the Earth about its axis is instructive.

The pertinent physical parameters of the Earth-Moon system are listed in Table 1, including the Earth's moment of inertia factor $\alpha = 0.827$ and the average angle factor $\beta = \text{Cos}(23.4^\circ)$ between the Earth's equatorial plane and the plane of the Moon's orbit. If only the Earth's spin angular momentum is considered, $H = 3.26$ meters, so

$$r_{eq} = \ell(\ell+1) 2.36 \times 10^3 \text{ m}. \quad (5)$$

Beginning with the $\ell = 1$ state, all the r_{eq} values will be too small for any important relationship to the ACC around Antarctica.

Table 1: Earth–Moon QCM parameters.

Parameter	Spin only	Earth–Moon
Mass (10^{24} kg)	5.972	6.045
Radius (10^6 m)	6.37	385.0
Period (10^6 s)	0.08614	2.3605
α	0.827	—
β	—	0.918
L_T (10^{33} kg-m ² /s)	5.847	32.5
H (m)	3.26	17.94

4.2 Earth–Moon total angular momentum

The QCM wave equation requires the total vector angular momentum of the gravitationally bound system in its applications. The orbital vector angular momentum value for the Moon is the much larger contributor in the Earth–Moon system but varies considerably, repeating every 18.6 years, because the angle between the Moon’s orbital plane and the Earth’s equatorial plane reaches a maximum difference angle of $28^{\circ}36'$ and a minimum of $18^{\circ}20'$.

Without accounting for this variation in the difference angle, the Moon’s orbital motion would contribute about 2.91×10^{34} kg-m²/s. Assuming an average difference angle of about 23.4° with respect to the Earth’s equatorial plane, with cosine $23.4^{\circ} = 0.918$, the Moon’s average vector orbital angular momentum contribution is about 2.67×10^{34} kg-m²/s.

Therefore, the Earth-Moon H = 17.94 meters and

$$r_{eq} = \ell(\ell + 1) 71.52 \times 10^3 \text{ m.} \tag{6}$$

The r_{eq} calculated values and their surface intersection latitudes for $\ell = 1$ to 9 are listed in Table 2.

The two QCM equilibrium radii r_{eq} for $\ell = 6$ and $\ell = 7$ intersect the surface at North and South latitudes of 61.9° and 51.0° , but only their South latitudes have a path that allows water to transport completely around the surface of the Earth

Table 2: Earth–Moon QCM equilibrium states.

ℓ	r_{eq} ($\times 10^6$ m)	Latitude
1	0.143	88.7°
2	0.429	86.1°
3	0.858	82.3°
4	1.430	77.0°
5	2.146	70.3°
6	3.004	61.9°
7	4.005	51.0°
8	5.149	36.1°
9	6.437	—

just north of Antarctica .

Note that the $\ell = 1$ to 4 states have equilibrium radii that may be applicable in the Arctic Ocean at the North Pole. The remainder intersect land masses on the surface. All these QCM rotating cylinders could be creating mass currents underneath the crust in the mantle and within interior parts of the Earth, even supporting the generation of the magnetic field and the recent magnetic north pole’s rapid movement past the rotational North Pole toward Russia.

Qualitative radial probability distributions for the QCM cylinders that could be affecting the ACC are shown in Figure 2. The vertical line at 6.37×10^6 m, is the approximate Earth radius. Their wide radial distributions within the Earth adds to the complexity of interpreting their actions.

As determined below, all displacements from the equilibrium radius will experience a QCM driving force back toward r_{eq} , here interpreted as the distance from the Earth’s rotation axis for simplified discussion purposes only. This radial force keeps the ACC roughly localized in the r coordinate, although the qualitative probability distributions shown in Figure 2 reveal a large spread in the radial direction underneath the surface. Moreover, displacements in latitude along the surface are also displacements in the r coordinate, resulting in a complex dynamics to consider in any detailed analysis.

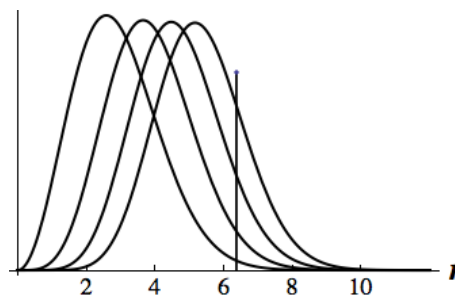


Fig. 2: Representation of the probability distributions for the $\ell = 6, 7, 8, 9$, QCM states with the Earth radius line at 6.37×10^6 m.

A fluid dynamics computer simulation would be needed to better understand the actual behavior of the ACC when QCM forces, winds, Coriolis effects, water density, and water viscosity are accounted for. The atmosphere above the ocean water would also be subject to the QCM forces in both the r direction and the ϕ direction. A rough estimate of the dynamics is considered below.

4.3 Estimates of QCM forces

In the following simplified analysis of the Earth–Moon system, winds and Coriolis forces are ignored. In the ϕ -direction, the QCM angular momentum per unit mass L/μ for a free particle at the equilibrium radius r_{eq} is given by the QCM constraint,

$$\frac{L}{\mu} = mcH, \quad (7)$$

with $|m| = \ell$ at the Equator, assuming a co-axial cylinder. Thus, substituting $L = \mu v_\phi r$ for the angular momentum produces the ϕ velocity

$$v_\phi = \frac{mcH}{r}. \quad (8)$$

QCM predicts for the $m = 6$ state a velocity $v_\phi \sim 1.1 \times 10^4$ m/s, and at the $m = 7$ state a $v_\phi \sim 1.26 \times 10^4$ m/s, values which can be compared to the actual average ACC velocity of about 212 m/s with respect to the stars. A large reduction in these predicted ϕ -velocities would be required of viscosity effects in the water and impedance effects of the land interruption at the ocean bottom and at the edges of the continents.

The torque τ required to keep the volume flow $V \sim 4 \times 10^{26}$ m³/s of ACC moving at approximately 2 m/s faster than the Earth's rotational velocity can be estimated, using the viscosity $\eta = 1.6$ cP for water at about 2°C, to be

$$\tau = 2\pi\eta V \approx 10^{14} \text{ Nm}, \quad (9)$$

which translates to a force of about 10^{-12} N to keep a kilogram of water moving at 2 m/s faster than the Earth's velocity.

Depending upon just where vertically and horizontally one calculates the driving torque pushing the water, QCM force values up to only about 10^{-9} N are estimated to be required. Any vertical water movement at the ACC latitude introduces displacement components in both the radial direction from the rotation axis and in the latitudinal direction. For simplicity, any latitudinal direction movement is assumed to be included within the r direction movement for the spherical geometry of the Earth's surface.

A small displacement from r_{eq} in the radial direction results in an acceleration, calculated by taking the negative gradient of V_{eff} , to get

$$a_r = -\frac{r_g c^2}{2r^2} + \frac{m^2 H^2 c^2}{r^3}. \quad (10)$$

So, if the water is at $r > r_{eq}$ or at $r < r_{eq}$, this QCM acceleration tries to move the water back to r_{eq} .

Water temperature differences are important. The surface water may be at a different temperature than the water below, so their density differences produce vertical mixing. Therefore, any water at the QCM equilibrium radius may move to a different radius value, with the radial velocity v_r resulting in a force in the ϕ direction. From Eq. 8, the ϕ acceleration

$$a_\phi = -\frac{mcH}{r^2} v_r. \quad (11)$$

Using the $m = 6$ and $m = 7$ parameters at the ACC, the expression becomes approximately

$$a_\phi = -0.003 v_r. \quad (12)$$

So both the sinking water and the rising water will experience a ϕ direction acceleration due to the QCM angular momentum per unit mass constraint, the accelerations depending upon the radial velocity directions and magnitudes.

These QCM forces and accelerations, when considered along with Coriolis forces and other influences, could be simulated on computer to determine their relative importance to the transport of the ACC.

Therefore, the estimated results of these QCM derivations suggest force and acceleration values strong enough to keep the ACC transport moving around the Antarctic continent, meaning that the ACC may be in a gravitational energy state dictated by the QCM quantization of angular momentum per unit mass constraint.

5 Conclusion

I have applied the QCM gravitational wave equation to the rotation of the Earth by utilizing both the total vector angular momentum of the Earth's spin plus the larger value of the average angular momentum of the Moon in orbit. The QCM $\ell = 6$ state at $r_{eq} = 3.0 \times 10^6$ m intersects the Earth's surface at 61.9°S latitude, and the $\ell = 7$ state at $r_{eq} = 4.0 \times 10^6$ m intersects the Earth's surface at 51.0°S latitude. Both QCM cylinders intersect the surface in the wide latitude region where the ACC flows faster than the Earth's rotation velocity by about 2 m/s.

The enormous QCM predicted velocity of about 1.1×10^4 m/s with respect to the stars is much larger than the actual ACC velocity of about 212 m/s. Viscosity effects on the water transport at all depths would need to be a significant opposing force to be able to reduce this QCM velocity to its actual velocity. Rough estimates of the pertinent forces suggest values on the order of 10^{-12} N to 10^{-9} N per kilogram are required.

Temperature differences produce mixing, which moves water away from the equilibrium radius measured from the rotation axis, resulting in an acceleration in both the r direction and the ϕ direction. The QCM forces combined with the Coriolis force and other effects make for a complex transport of the ACC. However, a computer simulation that includes the QCM force driving the ACC would be necessary in order to evaluate the atmosphere and ocean behaviors in more detail.

Therefore, the QCM wave equation applied in the familiar Schwarzschild metric suggests that the true energy source for the ACC could be gravitational.

Acknowledgements

The author thanks Sciencegems.com for continuing encouragement and support.

Submitted on February 23, 2021

References

1. Zika J. D. et al. Acceleration of the Antarctic Circumpolar Current by Wind Stress along the Coast of Antarctica. *Journal of Physical Oceanography*, 2013, v. 43 (12), 2772–2784.
2. Whitworth III T. The Antarctic Circumpolar Current. *Oceanus*, 1988, v. 32, 53–58.
3. Thompson A. F. and Garabato, A. C. N. Equilibration of the Antarctic Circumpolar Current by Standing Meanders. *Journal of Physical Oceanography*, 2014, v. 44 (7), 1811–1828.
4. Marynets K. On the modeling of the flow of the Antarctic Circumpolar Current. *Monatshefte für Mathematik*, 2019, v. 188, 561–565.
5. Preston H. G. and Potter F. Exploring Large-scale Gravitational Quantization without \hbar in Planetary Systems, Galaxies, and the Universe. arXiv: gr-qc/0303112.
6. Potter F. Update on Pluto and Its 5 Moons Obeying the Quantization of Angular Momentum per Unit Mass Constraint of Quantum Celestial Mechanics. *Progress in Physics*, v. 12 (1), 2016, 56–58. Online: <http://www.ptep-online.com/2016/PP-44-10.PDF>.
7. Potter F. Multi-planet Exosystems all obey Orbital Angular Momentum Quantization per Unit Mass predicted by Quantum Celestial Mechanics (QCM). *Progress in Physics*, v. 9 (3), 2013, 60–61. Online: <http://www.ptep-online.com/2013/PP-34-17.PDF>.
8. Potter F. and Preston H. G.. Quantum Celestial Mechanics: large-scale gravitational quantization states in galaxies and the Universe. *1st Crisis in Cosmology Conference: CCC-I*, Lerner E. J. and Almeida J. B. eds., AIP CP822, 2006, 239–252. .
9. Potter F. and Preston H. G. Cosmological Redshift Interpreted as Gravitational Redshift. *Progress in Physics*, v. 3 (2), 2007, 31–33. Online: <http://www.ptep-online.com/2007/PP-09-06.PDF>.

Stellar Evolution of High Mass-Loss Stars

Pierre A. Millette

E-mail: pierre.millette@uottawa.ca, Ottawa, Canada

In this paper, we investigate the 37 strongest QSO emission lines of stars of type Q in the catalog of Hewitt & Burbidge [22], as determined by Varshni *et al* [21]. We identify the candidate lines from atomic spectra lines data and determine the estimated T_e range down to the 50% ionic element density for the identified candidate emission lines. This information assists in the classification of Q stars from the 37 QSO dominant emission lines. We use the Hertzsprung-Russell diagram to analyze and determine the role of mass loss in the evolution of stars. We review the nucleosynthesis process that leads from massive O stars to WN and then WC Wolf-Rayet stars as a result of mass loss, and then consider the nucleosynthesis of oxygen in massive stars, showing that ^{16}O oxygen has a significant presence in massive stars beyond the WC stage, until the generation of ^{28}Si , where it disappears. This leads us to postulate more than one population of stars of type Q. One group identified by Varshni [27] with O VI and He II emission lines in their spectra implying much higher temperatures and positioning those QSO stars above the WR region in the HRD. The other group with emission lines dominated by temperatures in the O II and O III range, indicating a lower temperature range of QSO stars with a significant number of ionized oxygen lines and some Si emission lines, in addition to the nitrogen WN and carbon WC lines. We postulate that these QSO spectra correspond to unrecognized Wolf-Rayet stars, in particular WO stars and WSi pre-supernova stars, extending into lower temperatures. In that scenario, Q stars would be the end-state of the Wolf-Rayet evolution process, prior to moving to the supernova state.

1 Introduction

In a recent paper [1], we reviewed the physical process of laser action that is occurring in the stellar atmospheres of stars of type W (Wolf-Rayet) and stars of type Q (QSOs), due to the rapid adiabatic expansion of the stellar atmosphere of these stars, resulting in population inversions in the ionic energy levels due to free electron-ion recombination in the cooling plasma. Laser action in non-LTE stellar atmospheres was first proposed by Menzel in [2] and plasma lasers by Gudzenko in [3]. This results in the extremely strong broad emission lines observed in the spectra of these stars.

Significant work has been performed over the last forty years on the analysis of the emission line spectra of WR stars to understand their classification and evolution [4–15] and is still an ongoing area of research. Previously [1], we noted that a similar effort will be required to understand the classification and evolution of stars of type Q, as has been achieved for Wolf-Rayet stars. In this paper, we take an initial stab at this problem.

In addition, we examine the stellar evolution of high-mass-loss stars, characterized by WR and QSO stars, and refine our proposal to enhance the Hertzsprung-Russell Diagram (HRD) by including stars of type W and stars of type Q in the HRD [1]. This allows us to postulate that QSO stars can be identified as unrecognized Wolf-Rayet stars, in particular WO stars and WSi pre-supernova stars, to position them on the HRD, and provide a better understanding of the evolution of high mass-loss stars as displayed in the Hertzsprung-Russell Diagram.

2 Spectra of stars of type W

The emission line spectra of Wolf-Rayet stars are dominated by lines of helium He, carbon C, nitrogen N and oxygen O. The spectra fall into two broad classes: WN stars, which have prominent lines of nitrogen N and helium He ions, with a very strong He II Pickering series ($n = 4 \rightarrow n'$), and essentially no lines of carbon C; and WC stars, where the lines of carbon C and oxygen O are prominent along with the helium He ions, while those of nitrogen N seem to be practically absent [19, p. 485]. An additional subtype WO with strong O VI lines has also recently been added as a separate subtype. The spectra are characterized by the dominance of emission lines, notable for the almost total absence of hydrogen H lines [4].

The number of WR stars in our galaxy is small: the 2001 VIIth catalog of galactic WR stars gave the number at 227 stars, comprised of 127 WN stars, 87 WC stars, 10 WN/WC stars and 3 WO stars [16]. A 2006 update added another 72 WR stars, including 45 WN stars, 26 WC stars and one WO star [17]. The latest number from the August 2020 Galactic Wolf-Rayet Catalogue v1.25 is 667 WR stars [18].

Wolf-Rayet stars have extended atmospheres whose thickness is an appreciable fraction of their stellar radius [19, p. 243]. The material generating the lines is flowing outward from the stellar photosphere. These flows are driven by radiation pressure acting on the stellar atmosphere. Mass loss in stellar winds, particularly in WR stars, is well established [19, pp. 266, 523]. Mass loss rates \dot{M} for WR stars are estimated to be of order 10^{-5} up to perhaps $10^{-4} M_{\odot}/\text{year}$ [20, p. 628] — for comparison, the mass loss rate for the solar

wind is about $10^{-14} M_{\odot}/\text{year}$. The massive trans-sonic stellar winds flow velocities in WR stars rise from close to zero in the stellar photosphere to highly supersonic values of order 3 000 km/s within one stellar radius from the surface. Rapid cooling of the strongly ionized plasma results in rapid recombination of the free electrons and the ions into highly excited ionic states, resulting in population inversions and laser action.

3 Spectra of stars of type Q

Similar physical processes are expected to predominate in QSO stars due to the physical similarity of WR and QSO spectra, including the almost total absence of hydrogen H lines. However, while the number of identified WR stars is relatively small, the number of identified QSO stars is larger as we will see later.

Varshni *et al* [21] studied the distribution of QSO spectral emission lines (in the observed frame, i.e. unshifted) of 7 315 QSOs from the catalog of Hewitt & Burbidge [22], of which 5 176 have emission lines. This resulted in a total of 14 277 emission lines in the range $\lambda 1271$ to $\lambda 17993$, with the vast majority in the visual range $\lambda 3200$ to $\lambda 5600^*$.

A number of very strong peaks were found in a histogram of the statistical frequency of the emission lines against wavelength using 4 Å bins. The emission line distribution was expressed in units of standard deviation above a random average, to ensure the lines are statistically significant. The 37 strongest QSO emission lines in the catalog were more than four standard deviations above the random average, of which 13 peaks were above 5σ , of which 3 peaks were above 6σ , of which one peak was above 8σ . These lines are given in Table 1 including the number of standard deviations above a random average.

The 37 QSO emission lines were compared with Wolf-Rayet emission lines in [21], and 27 were found to also occur in WR star spectra, 7 in novae-like star spectra, and two in novae spectra. These are also included in Table 1, along with corresponding candidate element emission lines identification. The lines have been compared against existing sources of data such as Willett's [23] and Bennett's [24] lists of laser transitions observed in laboratories and the *NIST Atomic Spectra Database Lines Data* [25].

In Table 2, we have added the estimated T_e range down to the 50% ionic element density obtained from House [26] for the identified candidate element emission lines. In Tables 3 and 4, we determine the best known line identification and estimated T_e range down to the 50% ionic element density from House [26] respectively, for the 37 QSO emission lines identified in [21]. This provides information to assist in the classification of Q stars from the 37 QSO dominant emission lines.

*The notation λ indicates wavelengths measured in Å.

Varshni [27] also investigated O VI and He II emission lines in the spectra of QSOs, planetary nebulae and Sanduleak stars (WO stars characterized by a strong O VI emission line at $\lambda 3811.34$ — one example, blue supergiant star Sk -69 202, was identified as the progenitor of supernova 1987A). O VI emission lines imply much higher temperatures ($180\,000\text{ K} < \text{O VI} < 230\,000\text{ K}$) than those of Table 4, which are dominated by temperatures in the O II and O III range ($16\,000\text{ K} < \text{O II} < 46\,000\text{ K}$ and $46\,000\text{ K} < \text{O III} < 73\,000\text{ K}$ respectively).

4 Comparative numbers of O, W and Q stars

The comparative numbers of O, W and Q stars provide hints on their relative classification with respect to their evolution and the Hertzsprung-Russell diagram. O stars are known to be massive hot blue-white stars with surface temperatures in excess of 30 000 K. Wolf-Rayet stars have typical masses in the range of 10 – $25 M_{\odot}$, extending up to $80 M_{\odot}$ for hydrogen-rich WN stars [5], and surface temperatures ranging from 30 000 K to around 210 000 K.

Conti *et al* [6] measured the actual numbers and distributions of O stars and Wolf-Rayet stars in a volume-limited sample of stars within 2.5 kpc of the Sun. They found the observed WR/O star number ratio to be given by

$$\frac{\text{WR}}{\text{O} (M \geq 40 \pm 5 M_{\odot})} = 0.36 \pm 0.15. \quad (1)$$

The distribution of WR stars matches that of massive O stars, primarily close to the galactic plane, predominantly in spiral arms Population I stars, which is seen to indicate that WR stars are descendant from the most luminous and massive O stars, likely due to mass loss.

From the latest number of 667 WR stars seen previously in §2, we obtain an estimated number of O stars of

$$1\,850^{+1\,350}_{-550},$$

that is between 1 300 and 3 200, from (1). These results are in the same ballpark as available catalogues of O stars, which are still very much a work in progress [28–33]. This number is similar to that of planetary nebulae with about 2 700 known in 2008 (MASH catalogue) [34, 35]. These distributions and numbers of O stars and Wolf-Rayet stars agree with the changes to the Hertzsprung-Russell diagram suggested in [1] to include more massive and hotter stars of type W beyond the stars of type O B.

For the number of stars of type Q, we saw previously in §3 that the Hewitt & Burbidge catalog of 1993 [22] included 7 315 QSOs, of which 5 176 have emission lines, which represents 11 times the current number of known WR stars. However, the latest edition of the *Sloan Digital Sky Survey Quasar Catalog DR16Q* [36] to August 2018, includes a total of 750 414 quasars (100 times the 1993 Hewitt & Burbidge catalog number). This represents 1 125 times the number of WR

QSO λ (Å)	σ	WR λ (Å)	NL λ (Å)	Nova λ (Å)	Emitter λ candidates	Emitter λ candidates	Emitter λ candidates
3356	4.0	3358.6			N III λ 3355	O III λ 3355.9	C III λ 3358
3489	4.1	3493			O IV λ 3489.83	O II λ 3488.258	O II λ 3494.04
3526	6.7				C V λ 3526.665	O II λ 3525.567	
3549	4.3				O II λ 3549.091	Si III λ 3549.42	
3610	4.6	<3609.5)			C III λ 3609.6	He I λ 3613.6	N II λ 3609.097
3648	5.4	3645.4			O II λ 3646.56	O IV λ 3647.53	O IV λ 3642
3683	4.4	3687	3685.10		O II λ 3683.326	O III λ 3682.383/6.393	N IV λ 3689.94
3719	4.7	<3721.0)			O III λ 3721	O V λ 3717.31	
3770	4.7	<3769.5)			N III λ 3770.36/1.05	Si III λ 3770.585	O III λ 3774.026
3781	5.3	3784.8			He II λ 3781.68	O II λ 3784.98	N III λ 3779
3831	5.1	3829.9			He II λ 3833.80	C II λ 3831.726	O II λ 3830.29
3842	4.7				O IV λ 3841.07	N II λ 3842.187/.449	O II λ 3842.815
3855	5.0	3856.6			N II λ 3855.096/.374	O II λ 3856.134	He II λ 3858.07
3890	8.4	<3889.0)			He I λ 3888.64	C III λ 3889.18/.670	O III λ 3891.759
3903	5.6		3903.0		O III λ 3903.044		
3952	4.4	<3954.2)			O II λ 3954.3619	Si III λ 3952.23/3.071	
4012	6.0	<4008.4)			N III λ 4007.88	N III λ 4013.00	Si III λ 4010.236
4135	4.8	?			N III λ 4134.91/6.07	O V λ 4134.11	N II λ 4133.673
4276	5.9	?	4276.6	4275.5	O II λ 4275.5	O II λ 4275.994	O II λ 4276.620
4524	4.7	<4520.4)			N III λ 4523.56/7.9	O III λ 4524.2/7.3	O V λ 4522.66
4647	4.0	4650.8			C III λ 4647.40/51.35	O II λ 4647.803/9.1348	O III λ 4649.973
4693	4.7	?	4697.0		O II λ 4693.195	N II λ 4694.274/7.638	O III λ 4696.225
4771	4.1	?	4772.1		N IV λ 4769.86	O IV λ 4772.6	O II λ 4773.782
4801	4.3	<4799.6)			O IV λ 4800.74	Si III λ 4800.43	
4817	4.4	4814.6	4814.4		O IV λ 4813.15	Si III λ 4813.33/9.72	N II λ 4815.617
4910	4.9	4909.2			N III λ 4904.78	Si III λ 4912.310	
4925	4.5	<4924.6)			O II λ 4924.531	He I λ 4921.9	
4956	7.0	4958		4959.0	O II λ 4955.705	O III λ 4958.911	
5018	5.6	<5018.3)			He I λ 5015.67	C IV λ 5015.9/7.7	N II λ 5016.39
5035	4.2				N III λ 5038.31		
5049	5.5	5049.9			He I λ 5047.7	C III λ 5048.95	O III λ 5049.870
5096	5.5	5092.9			N III λ 5097.24	O III λ 5091.880	O II λ 5090.920
5111	4.8		5111.5		O II λ 5110.300/1.913	Si III λ 5111.1	O III λ 5112.18
5173	4.6	5171.1			N II λ 5171.266/2.344	N II λ 5173.385	O III λ 5171.29
5266	5.3	5266.3			O III λ 5268.301		
5345	4.1	5343.3			O II λ 5344.104	C III λ 5345.881	
5466	4.0	<5469.9)			Si II λ 5466.43/9.21	O V λ 5471.12	Si III λ 5473.05

Table 1: QSO emission lines in the range λ 3200 to λ 5600 from Varshni *et al* [21] (NL: novae-like star).

QSO λ (\AA)	σ	WR λ (\AA)	NL λ (\AA)	Nova λ (\AA)	Emitter T_e (K) candidates	Emitter T_e (K) candidates	Emitter T_e (K) candidates
3356	4.0	3358.6			33k < N III < 65k	46k < O III < 73k	29k < C III < 58k
3489	4.1	3493			73k < O IV < 130k	16k < O II < 46k	16k < O II < 46k
3526	6.7				92k < C V < 730k	16k < O II < 46k	
3549	4.3				16k < O II < 46k	18k < Si III < 46k	
3610	4.6	<3609.5>			29k < C III < 58k	He I < 26k	18k < N II < 33k
3648	5.4	3645.4			16k < O II < 46k	73k < O IV < 130k	73k < O IV < 130k
3683	4.4	3687	3685.10		16k < O II < 46k	46k < O III < 73k	65k < N IV < 103k
3719	4.7	<3721.0>			46k < O III < 73k	146k < O V < 184k	
3770	4.7	<3769.5>			33k < N III < 65k	18k < Si III < 46k	46k < O III < 73k
3781	5.3	3784.8			26k < He II < 73k	16k < O II < 46k	33k < N III < 65k
3831	5.1	3829.9			26k < He II < 73k	15k < C II < 29k	16k < O II < 46k
3842	4.7				73k < O IV < 130k	18k < N II < 33k	16k < O II < 46k
3855	5.0	3856.6			18k < N II < 33k	16k < O II < 46k	26k < He II < 73k
3890	8.4	<3889.0>			He I < 26k	29k < C III < 58k	46k < O III < 73k
3903	5.6		3903.0		46k < O III < 73k		
3952	4.4	<3954.2>			16k < O II < 46k	18k < Si III < 46k	
4012	6.0	<4008.4>			33k < N III < 65k	18k < Si III < 46k	
4135	4.8	?			33k < N III < 65k	146k < O V < 184k	18k < N II < 33k
4276	5.9	?	4276.6	4275.5	16k < O II < 46k		
4524	4.7	<4520.4>			33k < N III < 65k	46k < O III < 73k	146k < O V < 184k
4647	4.0	4650.8			29k < C III < 58k	16k < O II < 46k	46k < O III < 73k
4693	4.7	?	4697.0		16k < O II < 46k	18k < N II < 33k	46k < O III < 73k
4771	4.1	?	4772.1		65k < N IV < 103k	73k < O IV < 130k	16k < O II < 46k
4801	4.3	<4799.6>			73k < O IV < 130k	18k < Si III < 46k	
4817	4.4	4814.6	4814.4		73k < O IV < 130k	18k < Si III < 46k	18k < N II < 33k
4910	4.9	4909.2			33k < N III < 65k	18k < Si III < 46k	
4925	4.5	<4924.6>			16k < O II < 46k	He I < 26k	
4956	7.0	4958		4959.0	16k < O II < 46k	46k < O III < 73k	
5018	5.6	<5018.3>			He I < 26k	65k < C IV < 92k	18k < N II < 33k
5035	4.2				33k < N III < 65k		
5049	5.5	5049.9			He I < 26k	29k < C III < 58k	46k < O III < 73k
5096	5.5	5092.9			33k < N III < 65k	46k < O III < 73k	16k < O II < 46k
5111	4.8		5111.5		16k < O II < 46k	18k < Si III < 46k	46k < O III < 73k
5173	4.6	5171.1			18k < N II < 33k	46k < O III < 73k	
5266	5.3	5266.3			46k < O III < 73k		
5345	4.1	5343.3			16k < O II < 46k	29k < C III < 58k	
5466	4.0	<5469.9>			8.2k < Si II < 18k	146k < O V < 184k	18k < Si III < 46k

Table 2: QSO emission lines in the range $\lambda 3200$ to $\lambda 5600$ with estimated T_e range down to the 50% ionic element density from House [26].

QSO λ (\AA)	WR λ (\AA)	NL λ (\AA)	Nova λ (\AA)	Emitter QSO λ	Emitter WR λ	Emitter NL λ	Emitter Nova λ
3356	3358.6			O III λ 3355.9	C III λ 3358		
3489	3493			O II λ 3488.258	O II λ 3494.04		
3526				O II λ 3525.567			
3549				O II λ 3549.091			
3610	(3609.5)			C III λ 3609.6			
3648	3645.4			O IV λ 3647.53	O II λ 3646.56		
3683	3687	3685.10		O II λ 3683.326	O III λ 3686.393	O III λ 3686.393	
3719	(3721.0)			O III λ 3721	O III λ 3721		
3770	(3769.5)			N III λ 3770.36	N III λ 3770.36		
3781	3784.8			He II λ 3781.68	O II λ 3784.98		
3831	3829.9			C II λ 3831.726	O II λ 3830.29		
3842				N II λ 3842.187			
3855	3856.6			N II λ 3855.096	O II λ 3856.134		
3890	(3889.0)			C III λ 3889.670	C III λ 3889.18		
3903		3903.0		O III λ 3903.044		O III λ 3903.044	
3952	(3954.2)			Si III λ 3952.23	O II λ 3954.3619		
4012	(4008.4)			N III λ 4013.00	N III λ 4007.88		
4135	?			N III λ 4134.91			
4276	?	4276.6	4275.5	O II λ 4275.994		O II λ 4276.620	O II λ 4275.5
4524	(4520.4)			O III λ 4524.2	O V λ 4522.66		
4647	4650.8			C III λ 4647.40	C III λ 4651.35		
4693	?	4697.0		O II λ 4693.195		O III λ 4696.225	
4771	?	4772.1		N IV λ 4769.86		O IV λ 4772.6	
4801	(4799.6)			O IV λ 4800.74	O IV λ 4800.74		
4817	4814.6	4814.4		N II λ 4815.617	Si III λ 4813.33	O IV λ 4813.15	
4910	4909.2			Si III λ 4912.310	Si III λ 4912.310		
4925	(4924.6)			O II λ 4924.531	O II λ 4924.531		
4956	4958		4959.0	O II λ 4955.705	O III λ 4958.911		O III λ 4958.911
5018	(5018.3)			C IV λ 5017.7	C IV λ 5017.7		
5035				N III λ 5038.31?			
5049	5049.9			C III λ 5048.95	O III λ 5049.870		
5096	5092.9			N III λ 5097.24	O III λ 5091.880		
5111		5111.5		Si III λ 5111.1		O II λ 5111.913	
5173	5171.1			N II λ 5173.385	N II λ 5171.266		
5266	5266.3			O III λ 5268.301?	O III λ 5268.301?		
5345	5343.3			O II λ 5344.104	O II λ 5344.104		
5466	(5469.9)			Si II λ 5466.43	Si II λ 5469.21		

Table 3: QSO emission lines in the range λ 3200 to λ 5600 with best known line identification.

QSO λ (\AA)	WR λ (\AA)	NL λ (\AA)	Nova λ (\AA)	Emitter QSO T_e	Emitter WR T_e	Emitter NL T_e	Emitter Nova T_e
3356	3358.6			46k<O III<73k	29k<C III<58k		
3489	3493			16k<O II<46k	16k<O II<46k		
3526				16k<O II<46k			
3549				16k<O II<46k			
3610	<3609.5)			29k<C III<58k			
3648	3645.4			73k<O IV<130k	16k<O II<46k		
3683	3687	3685.10		16k<O II<46k	46k<O III<73k	46k<O III<73k	
3719	<3721.0)			46k<O III<73k	46k<O III<73k		
3770	<3769.5)			33k<N III<65k	33k<N III<65k		
3781	3784.8			26k<He II<73k	16k<O II<46k		
3831	3829.9			15k<C II<29k	16k<O II<46k		
3842				18k<N II<33k			
3855	3856.6			18k<N II<33k	16k<O II<46k		
3890	<3889.0)			29k<C III<58k	29k<C III<58k		
3903		3903.0		46k<O III<73k		46k<O III<73k	
3952	<3954.2)			18k<Si III<46k	16k<O II<46k		
4012	<4008.4)			33k<N III<65k	33k<N III<65k		
4135	?			33k<N III<65k			
4276	?	4276.6	4275.5	16k<O II<46k		16k<O II<46k	16k<O II<46k
4524	<4520.4)			46k<O III<73k	146k<O V<184k		
4647	4650.8			29k<C III<58k	29k<C III<58k		
4693	?	4697.0		16k<O II<46k		46k<O III<73k	
4771	?	4772.1		65k<N IV<103k		73k<O IV<130k	
4801	<4799.6)			73k<O IV<130k	73k<O IV<130k		
4817	4814.6	4814.4		18k<N II<33k	18k<Si III<46k	73k<O IV<130k	
4910	4909.2			18k<Si III<46k	18k<Si III<46k		
4925	<4924.6)			16k<O II<46k	16k<O II<46k		
4956	4958		4959.0	16k<O II<46k	46k<O III<73k		46k<O III<73k
5018	<5018.3)			65k<C IV<92k	65k<C IV<92k		
5035				33k<N III<65k			
5049	5049.9			29k<C III<58k	46k<O III<73k		
5096	5092.9			33k<N III<65k	46k<O III<73k		
5111		5111.5		18k<Si III<46k		16k<O II<46k	
5173	5171.1			18k<N II<33k	18k<N II<33k		
5266	5266.3			46k<O III<73k	46k<O III<73k		
5345	5343.3			16k<O II<46k	16k<O II<46k		
5466	<5469.9)			8.2k<Si II<18k	8.2k<Si II<18k		

Table 4: QSO emission lines in the range $\lambda 3200$ to $\lambda 5600$ with best known line identification and with estimated T_e range down to the 50% ionic element density from House [26].

stars — quite obviously, we are dealing with a phenomenon that is not as rare as O stars, WR stars or planetary nebulae.

There is a total of between 100 billion and 400 billion stars estimated in the Milky Way galaxy. The number of QSOs just represents about 2×10^{-6} times the estimated number of stars in the Milky Way galaxy, thus a fairly rare phenomenon, even if it is about 10^3 times more numerous than Wolf-Rayet stars. This requires further analysis in terms of understanding and positioning stars of type Q on the Hertzsprung-Russell diagram, with some of the QSOs with strong O VI lines [27] likely lying beyond the stars of type W O B as suggested in [1] and some having temperatures in the WR star range. The estimated number of quasars may be inflated due to the tendency in modern astronomy to identify redshifts as a predominant causative factor, but even if it is off by a factor of ten, the QSO phenomenon is much more common than Wolf-Rayet stars, in spite of their similarity.

We take a brief look at novae and novae-like stars [37], given their presence in Tables 1 to 4. These are part of what are known as *cataclysmic variables* (CVs), which are binary star systems consisting of a white dwarf and a normal star companion. Matter transfer to the white dwarf from the companion star results in the formation of an accretion disk around the white dwarf, which produces occasional cataclysmic outbursts of matter.

A main sequence star in a binary system evolves into a white dwarf for a mass below the Chandrasekhar limit (white dwarf maximum mass limit of about $1.4 M_{\odot}$). Novae are CV white dwarfs that undergo an eruption that can change by 10–12 magnitudes in a few hours. They are subdivided into classical novae (single observed eruption with a spectroscopically detected shell of ejected matter), recurrent novae (multiple observed outbursts with detected shell of matter), and dwarf nova (multiple observed eruptions with no shell of detected matter).

Nova-like (NL) variables include all “non-eruptive” cataclysmic variables. These systems have spectra, mostly emission spectra, indicating that they are possibly novae that have not been observed. A catalogue of cataclysmic variables to 2006 contains 1 600 CVs [38].

5 The Hertzsprung-Russell diagram and the role of mass loss in the evolution of stars

The Hertzsprung-Russell diagram is a powerful tool to analyze and represent stellar evolution and understand the characteristics and properties of stars. Most HR diagrams cover the temperature range 40 000 K and below, thus ignoring hotter and more massive stars of interest in this work.

From an idealized perspective, the main sequence is a vaguely diagonal curve running from the upper left to the lower central part of the diagram; from it, vaguely horizontal branches tend to the right of the diagram. The main sequence is known as the Zero-Age Main Sequence (ZAMS) which a

star enters when it starts core hydrogen burning; massive stars (O,B) rapidly burn the hydrogen in $\sim 3 \times 10^6$ years, while low mass stars (M) burn the hydrogen more slowly in $\sim 2 \times 10^{11}$ years.

As the core hydrogen becomes depleted, the star moves towards the horizontal portion of the diagram, and once core hydrogen burning terminates, it moves towards the right on the horizontal branch, becoming a red giant for cooler less massive stars (G) or a red supergiant for hot massive stars (O). Interestingly enough, in a recent study of stars of types O and early-B in the Wing of the Small Magellanic Cloud (SMC) satellite galaxy, Ramachandra *et al* [39] have found that the above scenario applies to O stars with initial mass below $\sim 30 M_{\odot}$, while O stars with initial mass above $\sim 30 M_{\odot}$ appear to always stay hot.

Once a star has exhausted its core hydrogen (and hydrogen shell), it enters its core helium burning phase. In Fig. 1, we reproduce the very important Hertzsprung-Russell diagram of [39] for the stars of types O and early-B of the SMC Wing: it covers the temperature range up to 200 000 K, shows the Helium Zero-Age Main Sequence (He-ZAMS) and also exceptionally includes the Wolf-Rayet (WR) stars. As we saw previously, the red giant and supergiant scenario, where the hydrogen-depleted stars veer off the ZAMS to the right, applies to O stars with initial mass below $\sim 30 M_{\odot}$ (shaded portion in Fig. 1). However, as we see in Fig. 1, for O stars with initial mass above $\sim 30 M_{\odot}$, the hydrogen-depleted stars veer off the ZAMS to the left to become WR stars, which are known to be hydrogen-deficient. Of the main factors affecting massive star evolution, focusing on rotation, binarity and mass-loss rate, we believe this dichotomy in behaviour is because of the massive mass loss in WR stars as seen in §2 driving laser action in their stellar atmospheres, while [39] believes it is due to the rapid rotation of the stars, leading to efficient mixing of the stellar interior and quasi-chemically homogeneous evolution (QCHE).

The work of Ramachandra *et al* [39] is an excellent example of using one of the better tools at our disposal to understand stellar astrophysical problems by performing analysis on the observed data in neighbouring galaxies, as mentioned in [1]. Along those lines, Hainich *et al* [40] has performed an analysis of single WN Wolf-Rayet stars in the Small Magellanic Cloud. Fig. 2 is a reproduction of the Hertzsprung-Russell diagram for the WN stars of the Small Magellanic Cloud (SMC) from Hainich *et al* [40], which also includes the WN stars of the Large Magellanic Cloud (LMC) and the Milky Way (MW). It corresponds to the upper left portion of Ramachandra’s HRD for log luminosity > 5.2 and temperatures $> 25 000$ K (in the WR region), and provides details for the WNE and WNL populations of the SMC, LMC and Milky Way galaxy. WNE is a subtype for early-type WN stars (WN2–WN5), while WNL is for late-type WN stars (WN6–WN11).

This HRD provides more details on WN star properties:

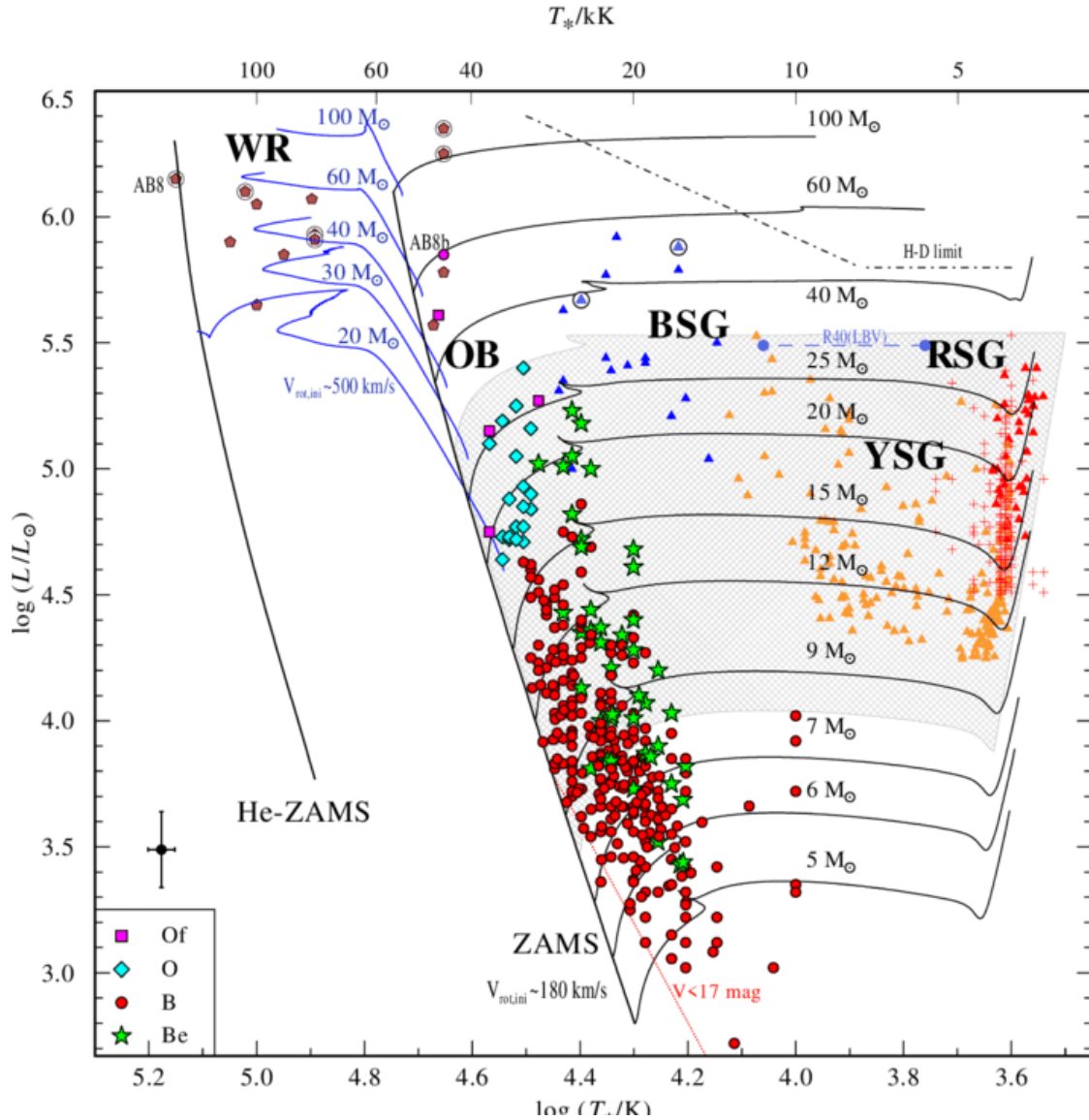


Fig. 1: Hertzsprung Russell diagram for massive stars in the Wing of the SMC reproduced from Ramachandra *et al* [39]. Typical error bar shown at bottom left corner. The brown pentagons represent WR stars (encircled if in a binary system), yellow symbols represent yellow supergiant (YSG) stars, blue triangles for BSGs (blue supergiant), and red triangles for RSGs (red supergiant). Black tracks show standard stellar evolutionary paths, while the blue tracks show the paths of quasi-chemically homogeneously evolving (QCHE) WR stars.

most WNE stars are on the left of the ZAMS line, but to the right of the He-ZAMS line; while most WNL stars are on the right of the ZAMS line, but close to it in the hydrogen depletion region of the stellar evolution curve, above log luminosity > 5.5 corresponding to stellar masses where the stars do not evolve into colder supergiants, as mentioned by Ramachandra *et al* [39]. See also Figures 7 and 8 of [11] for WN stars in the Large Magellanic Cloud. Thus, the calculated WR star evolution curves that extend to the right into lower temperature supergiant stars, usually seen in published HR diagrams, are likely incorrect, especially considering their high mass-loss rates driving laser action in their stellar atmo-

spheres. The Luminous Blue Variable (LBV) stars included in such stellar evolution curves are more than likely variable Wolf-Rayet stars.

Metallicity is a measure of the abundance of elements heavier than hydrogen or helium in an astronomical object. Hence stars and nebulae with relatively high carbon, nitrogen, oxygen, neon, *etc* abundance have high metallicity values z (the metallicity of the Sun is $z = 0.0134$). The degree of wind mass-loss of WR stars depends on their initial metallicity. Metallicity thus has an effect on the evolution of massive stars and of WR stars in particular. The Small Magellanic Cloud is a low-metallicity environment, lower than the metal-

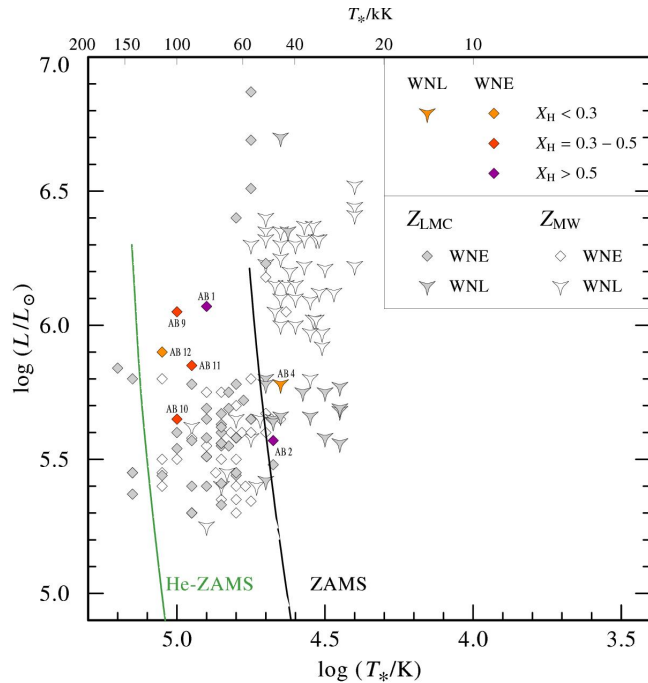


Fig. 2: Hertzsprung-Russell diagram for WN stars in the Small Magellanic Cloud (SMC) reproduced from Hainich *et al* [40]. Includes the Large Magellanic Cloud (LMC gray-filled symbols) and Milky Way (MW open symbols) WN stars.

deficient Large Magellanic Cloud itself lower in comparison to the Milky Way. SMC WN stars thus have on average lower mass-loss rates and weaker winds than their counterparts in the LMC and the Milky Way [40]. A reduction in the mass-loss rate at lower metallicity results in weaker emission line spectra in WR stars, a clear indication that the strong emission lines are due to the mass-loss rate which results in lasing transitions as seen in [1].

The process that leads from massive O stars to WR stars as a result of mass loss is believed to be well understood [41]. As a massive star evolves and loses mass, it eventually exposes He and N (the products of CNO burning) at the surface and is then spectroscopically identified as a WN star. As the star continues losing mass, it eventually exposes C and O (the products of He burning) at the surface and is then identified as a WC star. The mass loss rates depend on the metallicity of the environment which results in different WC/WN ratios as observed in Local Group galaxies. This is reflected in lower WC/WN ratios in lower metallicity environments: $(WC/WN)_{SMC} = 0$, $(WC/WN)_{LMC} = 0.25$ and $(WC/WN)_{MW} = 1$ [40].

Meyer *et al* [42] have analyzed the nucleosynthesis of oxygen in massive stars (see also [43]). In their model calculations, they find that in the WC stars, the oxygen in the C/O zone is dominated by the ^{16}O isotope. This matter which is part of the helium burning core, does not partake in the

carbon shell burning. This is followed by the O/Ne zone where the star experiences convective shell carbon burning and where there is a slight ^{16}O depletion, but where ^{16}O still strongly dominates the oxygen abundances. This is followed by the O/Si zone where the star experiences shell neon burning which increases the ^{16}O slightly. Finally, the star burns its ^{16}O into ^{28}Si and heavier isotopes both in pre-supernova and supernova nucleosynthesis, devoid of any oxygen.

Thus they find that oxygen has a significant presence in massive stars beyond the WC stage, until the generation of ^{28}Si , where it disappears. Considering Table 3, this behavior is interesting due to the presence of, in addition to the ionized nitrogen and carbon lines, a significant number of ionized oxygen lines, and the presence of some standalone silicon lines.

6 The evolution of stars of type Q

Given all of these considerations, how does the evolution of stars of type Q fit in the Hertzsprung-Russell diagram? We know that they are undergoing high mass-loss due to the broad high intensity spectral lines indicative of laser action in their stellar atmosphere. As seen in Table 3, their emission spectra are dominated by lines of ionized He, C, N, O and Si, with many lines in common with WR stars and novae-like stars.

There may be more than one population of stars of type Q. One group identified by Varshni [27] with O VI and He II emission lines in their spectra, in common with planetary nebulae and Sanduleak stars, implies much higher temperatures in the range $180\,000\text{ K} < \text{O VI} < 230\,000\text{ K}$, positioning those QSO stars above the WR region in the HRD of Ramachandra *et al* [39] given in Fig. 1. However, there are emission lines as given in Table 3, which are dominated by temperatures in the O II and O III range ($16\,000\text{ K} < \text{O II} < 46\,000\text{ K}$ and $46\,000\text{ K} < \text{O III} < 73\,000\text{ K}$ respectively), indicating a lower temperature range of QSO stars.

Indeed, as seen previously, these QSO emission line spectra have a significant number of ionized oxygen lines. WN and WC Wolf-Rayet stars predominate, with WN stars having the upper hand in low metallicity environments. However, the recently recognized WO lines are rare — could the QSO spectra with a significant number of ionized O emission lines and some Si emission lines, correspond to unrecognized much more numerous WO Wolf-Rayet stars extending into lower temperatures? They would in effect fill up the Hertzsprung-Russell diagram of Ramachandra *et al* [39] given in Fig. 1 in the range $16\,000\text{ K} < T_e < 73\,000\text{ K}$ for stellar masses above $\sim 30 M_{\odot}$.

For example, if we look at QSO 3C 273, the first radio source quasar for which an optical counterpart was identified in 1963, its spectrum consisted of one strong emission line and one medium to weak strength line ($\lambda 5637$, $\lambda 7588$). Comparing these lines against existing sources of data [23–25], the following identifications are obtained from the *NIST*

Atomic Spectra Database Lines Data and the corresponding estimated T_e range down to the 50% ionic element density obtained from House [26] for the identified candidate element emission lines (see Table 5). Based on this information, we would be inclined to conclude that the broad observed emission lines correspond to C II $\lambda 5640.55$ and O II $\lambda 7593$, with an estimated stellar temperature in the range $16\,000\text{ K} < T_e < 29\,000\text{ K}$.

QSO λ (Å)	strength	Emitter λ	Emitter T_e
5637	S	C II $\lambda 5640.55$	$15\text{k} < \text{C II} < 29\text{k}$
		Si II $\lambda 5633/41$	$8.2\text{k} < \text{Si II} < 18\text{k}$
7588	M-W	O II $\lambda 7593$	$16\text{k} < \text{O II} < 46\text{k}$
		C III $\lambda 7586.41$	$29\text{k} < \text{C III} < 58\text{k}$
		O IV $\lambda 7585.74$	$73\text{k} < \text{O IV} < 130\text{k}$

Table 5: QSO 3C 273 observed emission lines, identification and estimated T_e range down to the 50% ionic element density obtained from House [26].

7 Laser action in WR and QSO stars

The details of the process of laser action in the stellar atmospheres of Wolf-Rayet stars and Quasi-Stellar Object stars are given in [1]. The physical process of population inversions in expanding stellar atmospheres led Varshni to formulate his Plasma Laser Star (PLS) model as an explanation of the spectra of Wolf-Rayet stars and Quasi-Stellar Objects [47–52]. Model calculations starting from an initial element number density of 10^{14} cm^{-3} are performed for a grid of free electron number density n_e and temperature T_e values. The population inversion is displayed on $n_e - T_e$ diagrams showing contours of equal P or α' , where [44]

$$P = \frac{n_q}{\omega_q} - \frac{n_p}{\omega_p}, \quad (2)$$

where n_q is the population density and ω_q is the statistical weight of level q , and [45, p, 23]

$$\alpha = \sqrt{\frac{\ln 2}{\pi}} \left(\frac{\omega_q A_{q \rightarrow p}}{4\pi} \right) \frac{P \lambda_0^2}{\Delta\nu}, \quad (3)$$

where λ_0 is the centre wavelength of the transition, $\Delta\nu$ is the linewidth, $A_{q \rightarrow p}$ is the Einstein probability coefficient for spontaneous transition from level q to p , and $\alpha' = \alpha \Delta\nu$. Fig. 3 shows a typical $n_e - T_e$ diagram with equi- α' contours for inversely populated transition $6f \rightarrow 5d$ of C IV.

Taking Quasi-Stellar Objects to be local stellar objects instead of distant galactic objects eliminates the problems associated with their currently accepted cosmological interpre-

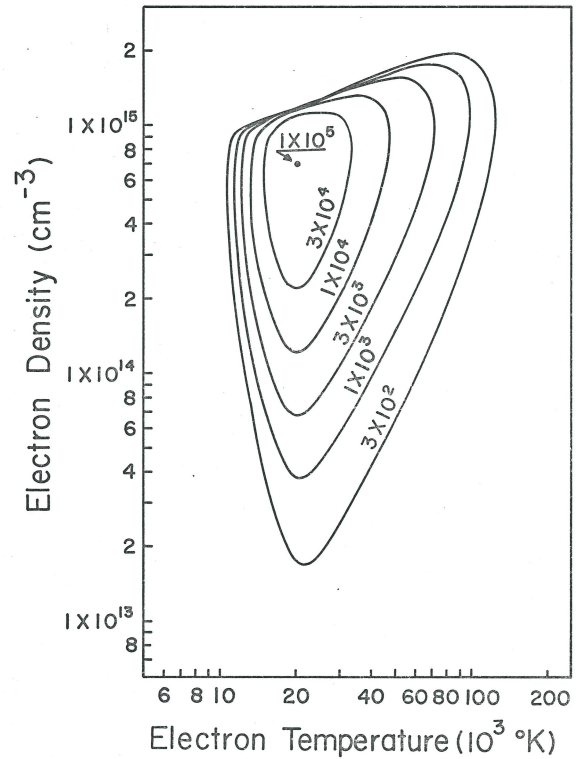


Figure 9.13 - $n_e - T_e$ diagram for the $6f \rightarrow 5d$ transition of C IV ($\lambda 4646$).

Fig. 3: Typical $n_e - T_e$ diagram showing laser gain equi- α' contours in $\text{cm}^{-1}\text{ s}^{-1}$ for the $6f \rightarrow 5d$ transition of C IV [46, p. 257].

tation: energy source, superluminal velocities, optical variability, quasar proper motions [53, 54], quasar binary systems [55, 56], naked (no nebulosity) quasars, *etc.* The properties of QSOs are similar to those of WR stars and, as stars, those are easily explainable in terms of commonly known physical processes. QSO stars could very well be unrecognized Wolf-Rayet stars, in particular WO stars and WSi pre-supernova stars. In that case, Q stars would be the end-state of the Wolf-Rayet evolution process and would account for their number larger than WN and WC W stars (about 10^3 times), prior to moving to the supernova state.

8 Discussion and conclusion

In this paper, we have investigated the 37 strongest QSO emission lines of stars of type Q in the catalog of Hewitt & Burbidge [22], investigated by Varshni *et al* [21]. We have used Willett's [23] and Bennett's [24] lists of laser transitions observed in laboratories and the *NIST Atomic Spectra Database Lines Data* [25] to identify candidate lines. In addition, we have determined the estimated T_e range down to the 50% ionic element density obtained from House [26] for the identified candidate element emission lines. This information assists in the classification of Q stars from the 37 QSO dominant

emission lines.

We have summarized the comparative numbers of O, W, and Q stars, novae and planetary nebulae to provide hints on their relative classification with respect to their evolution and the Hertzsprung-Russell diagram. The Hertzsprung-Russell diagram is a powerful tool to analyze and represent stellar evolution and has been used to determine the role of mass loss in the evolution of stars. In particular, we have considered the very important HR diagram of Ramachandra *et al* [39] for the stars of types O and early-B of the SMC Wing as it covers the temperature range up to 200 000 K, shows the Helium Zero-Age Main Sequence (He-ZAMS) and also exceptionally includes the Wolf-Rayet (WR) stars. In addition, their determination that hydrogen-depleted O stars with initial mass below $\sim 30 M_{\odot}$ evolve off the ZAMS to the right into colder red giants and supergiants, while hydrogen-depleted O stars with initial mass above $\sim 30 M_{\odot}$ appear to always stay hot and veer off the ZAMS to the left to become Wolf-Rayet stars, beyond the O stars, is indicative of laser action in their stellar atmosphere.

We have reviewed the nucleosynthesis process that leads from massive O stars to WN and then WC Wolf-Rayet stars as a result of mass loss. We then considered the nucleosynthesis of oxygen in massive stars and found that ^{16}O oxygen has a significant presence in massive stars beyond the WC stage, until the generation of ^{28}Si , where it disappears. This has lead us to postulate more than one population of stars of type Q. One group identified by Varshni [27] with O VI and He II emission lines in their spectra implying much higher temperatures and positioning those QSO stars above the WR region in the HRD of Ramachandra *et al* [39].

The other group with emission lines dominated by temperatures in the O II and O III range, indicating a lower temperature range of QSO stars with a significant number of ionized oxygen lines, in addition to the nitrogen WN and carbon WC lines. We postulate that these QSO spectra, with a significant number of ionized O emission lines and some Si emission lines, correspond to unrecognized Wolf-Rayet stars, in particular WO stars and WSi pre-supernova stars, extending into lower temperatures. They in effect fill up the HRD of Ramachandra *et al* [39] in the range $16\,000\text{ K} < T_e < 73\,000\text{ K}$ for stellar masses above $\sim 30 M_{\odot}$. In that scenario, Q stars would be the end-state of the Wolf-Rayet evolution process and would account for their number larger than WN and WC W stars, prior to moving to the supernova state.

Received on February 15, 2021

References

1. Millette P.A. Laser Action in the Stellar Atmospheres of Wolf-Rayet Stars and Quasi-Stellar Objects (QSOs). *Prog. Phys.*, 2021, v. 17 (1), 71–82.
2. Menzel D.H. Laser Action in non-LTE Atmospheres. International Astronomical Union Colloquium, Volume 2: Spectrum Formation in Stars With Steady-State Extended Atmospheres, 1970, 134–137.
3. Gudzenko L. L., Shelepin L. A., Yakovlenko S. I. Amplification in recombining plasmas (plasma lasers). *Usp. Fiz. Nauk*, 1974, v. 114, 457. *Sov. Phys. - Usp.*, 1975, v. 17, 848.
4. Abbott D. C. and Conti P. S. Wolf-Rayet Stars. *Ann. Rev. Astron. Astrophys.*, 1987, v. 25, 113–150.
5. Crowther P. A. Physical Properties of Wolf-Rayet Stars. *Annu. Rev. Astron. Astrophys.*, 2007, v. 45, 177–219. arXiv: astro-ph/0610356v2.
6. Conti P. S. and Garmany C. D., De Loore C. and Vanbeveren D. The Evolution of Massive Stars: The Numbers and Distribution of O Stars and Wolf-Rayet Stars. *Astrophys. J.*, 1983, v. 274, 302–312.
7. Humphreys R. M. and Nichols M., Massey P. On the Initial Masses and Evolutionary Origins of Wolf-Rayet Stars. *Astron. J.*, 1985, v. 90, 101–108.
8. Conti P. S. and Vacca W. D. The Distribution of Massive Stars in the Galaxy: I. Wolf-Rayet Stars. *Astron. J.*, 1990, v. 100, 431–444.
9. Langer N., Hamann W.-R., Lennon M., Najarro F., Pauldrach A. W. A. and Puls J. Towards an understanding of very massive stars. A new evolutionary scenario relating O stars, LBVs [Luminous Blue Variables] and Wolf-Rayet stars. *Astron. Astrophys.*, 1994, v. 290, 819–833.
10. Crowther P. A., Smith L. J., Hillier D. J. and Schmutz W. Fundamental parameters of Wolf-Rayet stars. III. The evolutionary status of WNL [WN7 to WN9] stars. *Astron. Astrophys.*, 1995, v. 293, 427–445.
11. Hainich R., Rühling U., Todt H., Oskinova L. M., Liermann A., Gräfener G., Foellmi C., Schnurr O. and Hamann W.-R. The Wolf-Rayet stars in the Large Magellanic Cloud. A comprehensive analysis of the WN class. *Astronomy and Astrophysics*, 2014, v. 565, A27 (62 pp.).
12. Torres A. V. and Conti P. S. Spectroscopic Studies of Wolf-Rayet Stars. III. The WC Subclass. *Astrophys. J.*, 1986, v. 300, 379–395.
13. Koesterke L. and Hamann W.-R. Spectral analyses of 25 Galactic Wolf-Rayet stars of the carbon sequence. *Astron. Astrophys.*, 1995, v. 299, 503–519.
14. Barlow M. J. and Hummer D. J. The WO Wolf-Rayet stars. *Symposium – International Astronomical Union*, 1982, v. 99, 387–392.
15. Kingsburgh R. L., Barlow M. J. and Storey P. J. Properties of the WO Wolf-Rayet stars. *Astron. Astrophys.*, 1994, v. 295, 75–100.
16. van der Hucht K. A. The VIIIth catalogue of galactic Wolf-Rayet stars. *New Astronomy Reviews*, 2001, v. 45, 135–232.
17. van der Hucht K. A. New Galactic Wolf-Rayet stars, and candidates (Research Note), An Annex to The VIIIth Catalogue of Galactic Wolf-Rayet Stars. *Astronomy and Astrophysics*, 2006, v. 458, 453–459.
18. Galactic Wolf Rayet Catalogue. V1.25, www.pacrowther.staff.shef.ac.uk/WRcat/, Aug. 2020.
19. Mihalas D. *Stellar Atmospheres*, 2nd ed. W. H. Freeman and Co., San Francisco, 1978.
20. Mihalas D. and Weibel-Mihalas B. *Foundations of Radiation Hydrodynamics*, corr. ed. Dover Publications, New York, 1999, pp. 627–645.
21. Varshni Y. P., Talbot J., Ma Z. Peaks in Emission Lines in the Spectra of Quasars. In: Lerner E. J. and Almeida J. B., eds. 1st Crisis in Cosmology Conference, CCC-I. American Institute of Physics Conference Proceedings, v. 822, 2006.
22. Hewitt A., Burbidge G. A Revised and Updated Catalog of Quasi-stellar Objects. *Astrophys. J. Supp.*, 1993, v. 87, 451.
23. Willett C. S. Laser Lines in Atomic Species. In: *Progress in Quantum Electronics*, Vol. 1, Part 5, Pergamon, 1971.
24. Bennett W. R. Jr. *Atomic Gas Laser Transition Data: A Critical Evaluation*.IFI/Plenum, New York, NY, 1979.
25. Kramida A., Ralchenko Y., Reader J., and NIST ASD Team. NIST Atomic Spectra Database (ver. 5.8). National Institute of Standards and Technology, Gaithersburg, MD, 2020. //physics.nist.gov/asd, accessed 14 January 2021.

26. House L. L. Ionization Equilibrium of the Elements from H to Fe. *Astrophys. J. Suppl.*, 1964, v. 8, 307–328.
27. Varshni Y. P. O VI and He II Emission Lines in the Spectra of Quasars. *Astrophys. Space Sci.*, 1977, v. 46, 443.
28. Maíz-Apellániz J. and Walborn N. R. A Galactic O Star Catalog. *Astrophys. J. Suppl.*, 2004, v. 151, 103–148.
29. Sota A., Maíz-Apellániz J., Walborn N. R., and Shida R. Y. The Galactic O Star Catalog V.2.0. arXiv: astro-ph/0703005.
30. Sota A., Maíz-Apellániz J., Walborn N. R., Alfaro E. J., Barrá R. H., Morrell N. I., Gamen R. C. and Arias J. L. The Galactic O-Star Spectroscopic Survey. I. Classification System and Bright Northern Stars in the Blue-Violet at R~2500. *Astrophys. J. Suppl.*, 2011, v. 193, 24–73.
31. Maíz Apellániz J., Pellerin A., Barbá R. H., Simón-Díaz S., Alfaro E. J., Morrell N. I., Sota A., Penatés Ordaz M. and Gallego Calvente A. T. The Galactic O-Star Spectroscopic (GOSSS) and Northern Massive Dim Stars (NoMaDS) Surveys, the Galactic O-Star Catalog (GOSC), and Marxist Ghost Buster (MGB). arXiv: astro-ph/1109.1492.
32. Sota A., Maíz-Apellániz J., Morrell N. I., Barrá R. H., Walborn N. R., Gamen R. C., Arias J. L., and Alfaro E. J. The Galactic O-Star Spectroscopic Survey (GOSSS). II. Bright Southern Stars. *Astrophys. J. Suppl.*, 2014, v. 211, 10–93.
33. Maíz-Apellániz J., Moragón A. Á., de Zárata Alcarazo L. O. and the GOSSS team. The Galactic O-Star Catalog (GOSC) and the Galactic O-Star Spectroscopic Survey (GOSSS): current status. arXiv: astro-ph/1610.03320.
34. Parker Q. A., Acker A., Frew D. J., Hartley M., Peyaud A. E. J., Ochsenbein F., Phillipps S., Russell D., Beaulieu S. F., Cohen M., Köppen J., Miszalski B., Morgan D. H., Morris R. A. H., Pierce M. J. and Vaughan A. E. The Macquarie/AAO/Strasbourg H α Planetary Nebula Catalogue: MASH. *Mon. Not. R. Astron. Soc.*, 2006, v. 373, 79–94.
35. Miszalski B., Parker Q. A., Acker A., Birkby J. L., Frew D. J. and Kovacevic A. MASH II: more planetary nebulae from the AAO/UKST H α survey. *Mon. Not. R. Astron. Soc.*, 2008, v. 374, 525–534.
36. The Sloan Digital Sky Survey Quasar Catalog: sixteenth data release (DR16Q). www.sdss.org/dr16/algorithms/qso_catalog/, Aug. 2018.
37. scienceworld.wolfram.com/astronomy. accessed 24 Jan 2021.
38. Downes R. A., Webbink R. F., Shara M. M., Ritter H., Kolb U. and Duerbeck H. W. A Catalog and Atlas of Cataclysmic Variables: The Final Edition. *The Journal of Astronomical Data*, 2005, v. 11, 2.
39. Ramachandran V., Hamann W.-R., Oskinova L. M., Gallagher J. S., Hainich R., Shenar T., Sander A. A. C., Todt H. and Fulmer L. Testing massive star evolution, star formation history, and feedback at low metallicity. Spectroscopic analysis of OB stars in the SMC Wing. *Astronomy and Astrophysics*, 2019, v. 625, A104 (20 pp.). arXiv: astro-ph/1903.01762v2.
40. Hainich R., Pasemann D., Todt H., Shenar T., Sander A. and Hamann W.-R. Wolf-Rayet stars in the Small Magellanic Cloud. I. Analysis of the single WN stars. *Astronomy and Astrophysics*, 2015, v. 581, A21 (30 pp.).
41. Massey P. A Census of Massive Stars Across the Hertzsprung-Russell Diagram of Nearby Galaxies: What We Know and What We Don't. arXiv: astro-ph/0903.0155v2.
42. Meyer B. S., Nittler L. R., Nguyen A. N. and Messenger S. Nucleosynthesis and Chemical Evolution of Oxygen. *Review in Mineralogy & Geochemistry*, 2008, v. 68, 31–53. semanticscholar.org/paper/Nucleosynthesis-and-Chemical-Evolution-of-Oxygen-Meyer-Nittler.
43. Wallerstein G., Iben I. Jr., Parker P., Boesgaard A. M., Hale G. M., Champagne A. E., Barnes C. A., Käppeler F., Smith V. V., Hoffman R. D., Timmes F. X., Sneden C., Boyd R. N., Meyer B. S. and Lambert D. L. Synthesis of the elements in stars: forty years of progress. *Reviews of Modern Physics*, 1997, v. 69 (4), 995–1084.
44. Lengyel B. A. Introduction to Laser Physics. John Wiley, New York, 1966.
45. Willett C. S. Gas Lasers: Population Inversion Mechanisms. Pergamon Press, New York, 1974.
46. Millette P. A. Laser Action in CIV, NV, and O VI Plasmas Cooled by Adiabatic Expansion. University of Ottawa, Ottawa, ON, 1980. LaTeX typeset: researchgate.net/publication/283014713, 2015.
47. Varshni Y. P. Laser Action in Quasi-Stellar Objects? *Bull. Amer. Phys. Soc.*, 1973, v. 18, 1384.
48. Varshni Y. P. No Redshift in Quasi-Stellar Objects. *Bull. Amer. Astron. Soc.*, 1974, v. 6, 213.
49. Varshni Y. P. The Redshift Hypothesis and the Plasma Laser Star Model for Quasi-Stellar Objects. *Bull. Amer. Astron. Soc.*, 1974, v. 6, 308.
50. Varshni Y. P. Alternative Explanation for the Spectral Lines Observed in Quasars. *Astrophys. Space Sci.*, 1975, v. 37, L1.
51. Varshni Y. P. Electron Density in the Emission-Line Region of Wolf-Rayet Stars. *Astrophys. Space Sci.*, 1978, v. 56, 385.
52. Varshni Y. P. The Physics of Quasars. *Phys. Canada*, 1979, v. 35, 11.
53. Luyten W. J. A Search for Faint Blue Stars. Paper 50, University of Minnesota Observatory, Minneapolis, 1969.
54. Varshni Y. P. Proper Motions and Distances of Quasars. *Speculations in Science and Technology*, 1982, v. 5 (5), 521–532.
55. Mortlock D. J., Webster R. L. and Francis P. J. Binary Quasars. *Mon. Not. R. Astron. Soc.*, 1999, v. 309, 836–846.
56. Hennawi J. F., et al. Binary Quasars in the Sloan Digital Sky Survey: Evidence for Excess Clustering on Small Scales. *Astronomical Journal*, 2006, v. 131, 1–23.

Physics of Numbers as Model of Telepathic Entanglement

Hartmut Müller, Renata Angeli, Roberta Baccara, Rose Line Hofmann,
Simona Muratori, Olga Nastasi, Giuliana Papa, Francesca Santoni,
Claudio Venegoni, Francesco Zanellati, Leili Khosravi

E-mail: hm@interscalar.com

The physics of transcendental numbers leads to a fractal scalar field that causes numeric entanglements affecting any type of interaction. In this paper, we apply this our approach to the analysis of telepathic communication in both aspects, the theoretical and experimental.

Introduction

The history of science is replete with confident proclamations about all sorts of impossible things like flying machines heavier than air, and most of those proclamations have proven to be hilariously or poignantly wrong. So the current paradigm declares also telepathy to be impossible [1].

The term ‘telepathy’ comes from the Greek ‘tele’ meaning ‘distant’ and ‘pathos’ meaning ‘feeling, perception, experience’ and can be defined [2] as the transmission of information from one person to another without using any known human sensory channel or physical interaction.

Introduced by the British scholar Frederic W. H. Myers in 1882, ‘telepathy’ substituted the earlier term ‘thought transference’ in psychology. The concept of telepathy was originally more an attempt to objectify and detach the concept of thought transference from its connection with spiritism, media and belief in ghosts.

Telepathy challenges the scientific understanding of experience, that David Chalmers [3] has termed the ‘hard problem’ of consciousness. Indeed, centuries of philosophical disputes did not explain the nature of consciousness. Aside from recognizing that consciousness differs from matter in many ways, there is no scientific consensus.

However, the dominant view in recent time is more materialistic than ever before: consciousness is thought to emerge from highly complex biological processes, which in turn are based ultimately on interactions between subatomic particles.

Roger Penrose and Stuart Hameroff [4] hypothesize that consciousness originates from quantum processing in neuron dendritic spine microtubules.

Shan Gao [5] analyzes the role of consciousness during quantum measurement process and supposes quantum nonlocality as model of telepathic communication. Huping Hu and Maoxin Wu [6, 7] hypothesize that consciousness is intrinsically connected to quantum spin in the sense that nuclear and electron spin is the ‘mind-pixel’ and the unity of mind is presumably achieved by entanglement of these mind-pixels. They assume [8] that spin is the primordial process in non-spatial and non-temporal pre-spacetime being the manifestation of quantum entanglement, implying instantaneous interconnectedness of all matters in the universe through gravity

and consciousness. As well, George Williams [9] supposes the existence of a non-local proto-conscious field that underlies both matter and consciousness. Within the Global Consciousness Project of the Princeton Engineering Anomalies Research Laboratory at the Princeton University, the Rodger Nelson group [10] demonstrated that human consciousness interacts with physical random event generators [11], causing them to produce nonrandom patterns associated with special states of group consciousness.

In our research we focus on the physics of numbers as approach to study the physical consequences of arithmetic properties of numbers being ratios of measured quantities. In [12] we have shown that this approach leads to a fractal scalar field that causes numeric entanglements affecting any type of interaction including gravitation [13]. In this paper, we apply our approach to the analysis of telepathic communication in both aspects, the theoretical and experimental.

Theoretical Approach

Measurement is the source of scientific data that allow for developing and proving theoretical models of the reality. The result of a measurement is the ratio of two quantities where one of them is the reference quantity called unit of measurement. All that can be measured – space, time, energy, mass – is quantity. Numbers are symbols of quantity. Despite their non-materiality, numbers represent a reality that has unlimited power and produces physical effects. These effects are a subject of study in the physics of numbers.

On the one hand, numbers appear as created by intellect, on the other, our intellect cannot manipulate them, for example, avoid the appearance of primes when counting, or design a cube and a sphere both of the same volume. Indeed, measuring, counting and calculating are inherent abilities of all things. Even atoms have to configure the number of electrons on each energy level. Thus, the universality of the numbers suggests that they are not anthropogenic, but cosmogenic.

Distances, durations, angles, velocities – when measured, first they are real numbers, and only when applied to models they can become vectors. Real numbers are scalars, and scaling is the process that creates them. Indeed, when we observe something from a far scale, we cannot distinguish

details. Different objects appear as identical and we cannot anymore individuate them. The abundance of properties of the objects reduces to their number that follows the laws of arithmetic or the laws of statistics.

Extreme scaling is the process that creates numbers and can possibly even release objects from their materiality. The scale of electrons is in the range of picometer. Protons and electrons appear to be elementary just because the difference between the observer’s macroscale and the subatomic scale is huge. This is why they behave like numbers and their properties appear quantized following the laws of quantum statistics.

Numbers are omnipresent and therefore, non-local. This non-locality of the numbers might be the true cause of the quantum physical entanglement that Albert Einstein called ‘spooky action at a distance’. In this context, all electrons and protons are identical because there is probably only one electron and only one proton that can materialize everywhere. In the same meaning there is only one number $e=2.71828\dots$ and only one number $\pi=3.14159\dots$ that can materialize any-time and anywhere.

Max Planck’s discovery that the energy $E=\hbar\omega$ of a photon depends only on a *number* that is its frequency ω , is a key event in the history of physics. From this discovery, quantum physics was born. As the energy of a quantum oscillator increases with its frequency, every additional increase of the frequency requires more and more energy. Probably, this process leads to the emergence of a resistance that appears as inertia. Indeed, the frequency $7.8 \cdot 10^{20}$ Hz defines the threshold where electrons can form. Surpassing the threshold of $1.4 \cdot 10^{24}$ Hz, protons can form. In [14] we introduced scaling as mechanism of particle mass generation, alternative to the Higgs model. In [15] we have demonstrated that it is the transcendence of Euler’s number that stabilizes the thresholds of materialization including the proton-to-electron ratio.

In the framework of the physics of numbers, all structures and processes in the universe are materializations of numeric relationships. Within this our approach, we significantly extend the meaning of quantum entanglement in the sense of an instantaneous connectivity that originates from the divisibility of numbers. The meaning of this connectivity is that, for example, the n^{th} cycle of a given process has something in common with the n^{th} cycle of any other process, independently of its nature, duration or location.

This kind of ‘numeric entanglement’ is a consequence of the divisibility of the number n being the index of the n^{th} cycle of a periodical process. It has nothing to do with resonance or simultaneity, but with scaling; it is a connectivity that does not depend on temporal coincidences or spatial distances.

Let us imagine two periodic processes, one occurs on Earth and another occurs on Kepler 452b that is 1400 light years away in the Cygnus constellation of the Milky Way. Because of the huge spatial and temporal distance, they cannot be synchronized by the speed of light. By the way, that’s exactly why probably nobody in the Galaxy uses radio signals

or other forms of light for interstellar communication. Nevertheless, both periodic processes are numerically connected, and this circumstance allows for communication.

In [12] we have demonstrated that the physics of transcendental numbers leads to a fractal scalar field that affects any type of physical interaction including gravitation. In this paper, we hypothesize that this field causes numeric entanglements making possible connectivity associated with telepathy or other forms of extrasensory perception. But first, now we are going to derive this fractal scalar field from the physics of transcendental numbers.

In physics of numbers [16], the difference between rational, irrational algebraic and transcendental numbers is not only a mathematical task, but it is also an essential aspect of stability in complex dynamic systems. While integer frequency ratios provide parametric resonance interaction that can destabilize a system [17, 18], it is transcendental numbers that define the preferred ratios of quantities which avoid destabilizing resonance interaction [15]. In this way, transcendental ratios of quantities can sustain the stability of periodic processes in complex dynamic systems.

Among all transcendental numbers, Euler’s number $e = 2.71828\dots$ is unique, because its real power function e^x coincides with its own derivatives. In the consequence, Euler’s number allows inhibiting resonance interaction regarding any interacting periodic processes and their derivatives.

Alexandr Khinchin [19] demonstrated that any real number has a biunique representation as a continued fraction. Applying this to the real argument x of the natural exponential function e^x , we get:

$$x = \langle n_0; n_1, n_2, \dots, n_k \rangle. \tag{1}$$

We use angle brackets for continued fractions. All denominators n_1, n_2, \dots, n_k including the free link n_0 are integer. The numerators equal 1. The length of the continued fraction is given by the number k of layers.

The canonical form (all numerators equal 1) does not limit our conclusions, because every continued fraction with partial numerators different from 1 can be transformed into a canonical continued fraction using the Euler equivalent transformation [20]. With the help of the Lagrange [21] transformation, every continued fraction with integer denominators can be represented as a continued fraction with natural denominators that is always convergent [22].

Naturally, the rational eigenvalues of the finite continued fractions (1) have a fractal distribution. The first layer is given by the truncated after n_1 continued fraction:

$$x = \langle n_0; n_1 \rangle = n_0 + \frac{1}{n_1}.$$

The denominator n_1 follows the sequence of integer numbers $\pm 1, \pm 2, \pm 3$ etc. The second layer is given by the truncated

after n_2 continued fraction:

$$x = \langle n_0; n_1, n_2 \rangle = n_0 + \frac{1}{n_1 + \frac{1}{n_2}}$$

Figure 1 shows the first and the second layer in comparison. As we can see, reciprocal integers $\pm 1/2, \pm 1/3, \pm 1/4, \dots$ are the attractor points of the distribution. In these attractors, the distribution density always reaches a local maximum. Integers $0, \pm 1, \dots$ are the main attractors of the distribution.

Now let's remember that we are observing the fractal distribution of rational values $x = \langle n_0; n_1, n_2, \dots, n_k \rangle$ of the real argument x of the natural exponential function e^x . What we see is the fractal distribution of transcendental numbers of the type $\exp(\langle n_0; n_1, n_2, \dots, n_k \rangle)$ on the natural logarithmic scale. Near integer exponents, the distribution density of these transcendental numbers is maximum. Consequently, for integer and rational exponents x , the natural exponential function e^x defines attractor points of transcendental numbers and create islands of stability.

Figure 1 shows that these islands are not points, but ranges of stability. Integer exponents $0, \pm 1, \pm 2, \pm 3, \dots$ are attractors which form the widest ranges of stability. Half exponents $\pm 1/2$ form smaller islands, one third exponents $\pm 1/3$ form the next smaller islands and one fourth exponents $\pm 1/4$ form even smaller islands of stability etc.

For rational exponents, the natural exponential function is always transcendental [23]. Increasing the length k of the continued fraction (1), the density of the distribution of transcendental numbers of the type $\exp(\langle n_0; n_1, n_2, \dots, n_k \rangle)$ is increasing as well. Nevertheless, their distribution is not homogeneous, but fractal. Applying continued fractions and truncating them, we can represent the real exponents x of the natural exponential function e^x as rational numbers and make visible their fractal distribution.

The application of continued fractions doesn't limit the universality of our conclusions, because continued fractions deliver biunique representations of all real numbers including transcendental. Therefore, the fractal distribution of transcendental eigenvalues of the natural exponential function e^x of the real argument x , represented as continued fraction, is an inherent characteristic of the number continuum. This characteristic we call the *Fundamental Fractal* [24].

In physical applications, the natural exponential function e^x of the real argument x is the ratio of two physical quanti-



Fig. 1: The Fundamental Fractal – the fractal distribution of transcendental numbers of the type e^x with $x = \langle n_0; n_1, n_2, \dots, n_k \rangle$ on the natural logarithmic scale for $k = 1$ (first layer above) and for $k = 2$ (second layer below) in the range $-1 \leq x \leq 1$.

ties where one of them is the reference quantity called unit of measurement. Therefore, we can rewrite the equation (1):

$$\ln(X/Y) = \langle n_0; n_1, n_2, \dots, n_k \rangle \tag{2}$$

where X is the measured physical quantity and Y the unit of measurement. In this way, the natural exponential function e^x of the rational argument $x = \langle n_0; n_1, n_2, \dots, n_k \rangle$ generates the set of preferred ratios X/Y of quantities which avoid destabilizing resonance and provide the lasting stability of real systems regardless of their complexity.

Therefore, we expect that periodic processes in real systems prefer frequency ratios close to Euler's number and its rational powers. Consequently, the logarithms of their frequency ratios should be close to integer $0, \pm 1, \pm 2, \dots$ or rational values $\pm 1/2, \pm 1/3, \pm 1/4, \dots$

In [12] we verified the model claims on the gravitational constants and the periods of orbital and rotational motion of the planets, planetoids and large moons of the solar system as well as the orbital periods of exoplanets and the gravitational constants of their stars.

Naturally, the Fundamental Fractal (2) of transcendental stability attractors does not materialize in the scale of planetary systems only. At subatomic scale, it stabilizes the proton-to-electron ratio and in this way, allows the formation of stable atoms and complex matter.

Scale relations in particle physics [14] obey the same Fundamental Fractal (2), without any additional or particular settings. The proton-to-electron frequency ratio approximates the Fundamental Fractal at the first layer that could explain their exceptional stability [25]:

$$\ln\left(\frac{\omega_p}{\omega_e}\right) = \ln\left(\frac{1.42549 \cdot 10^{24} \text{ Hz}}{7.76344 \cdot 10^{20} \text{ Hz}}\right) \approx 7 + \frac{1}{2} = \langle 7; 2 \rangle.$$

ω_p and ω_e are the proton and electron angular frequencies. In the consequence of the ratio $\exp(7 + 1/2)$, the scaling factor $\sqrt{e} = 1.64872\dots$ connects attractors of proton stability with similar attractors of electron stability in alternating sequence. Figure 2 demonstrates this situation on the first layer of the Fundamental Fractal (1), and one can see clearly that among the integer or half, only the attractors $\pm 1/3, \pm 1/4$ and $\pm 1/6$ are common. In these attractors, proton stability is supported by electron stability and vice versa, so we expect that they are preferred in real systems. As we have shown in our paper [12], planetary systems make extensive use of these common attractors.

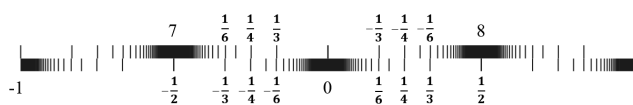


Fig. 2: The distribution of the attractors of proton (bottom) stability in the range $-1 < x < 1$ of the attractors of electron (top) stability. Natural logarithmic representation.

PROPERTY	ELECTRON	PROTON
$E = mc^2$	0.5109989461(31) MeV	938.2720813(58) MeV
$\omega = E/\hbar$	$7.76344 \cdot 10^{20}$ Hz	$1.42549 \cdot 10^{24}$ Hz
$\tau = 1/\omega$	$1.28809 \cdot 10^{-21}$ s	$7.01515 \cdot 10^{-25}$ s
$\lambda = c/\omega$	$3.86159 \cdot 10^{-13}$ m	$2.10309 \cdot 10^{-16}$ m

Table 1: The basic set of the physical properties of the electron and proton. Data from Particle Data Group [29]. Frequencies, oscillation periods and wavelengths are calculated.

The spatio-temporal projection of the Fundamental Fractal (2) is a fractal scalar field of transcendental attractors, the *Fundamental Field* [26]. The connection between the spatial and temporal projections of the Fundamental Fractal is given by the speed of light $c = 299792458$ m/s. The constancy of c makes both projections isomorphic, so that there is no arithmetic or geometric difference. Only the units of measurement are different. In [27] we have shown that the constancy of the speed of light is a consequence of the stabilizing function of Euler’s number.

The exceptional stability of the electron and proton predestinate their physical characteristics as fundamental units. Table 1 shows the basic set of electron and proton units that we consider as a fundamental metrology (c is the speed of light in a vacuum, \hbar is the Planck constant). In [24] was shown that the fundamental metrology (tab. 1) is completely compatible with Planck units [28].

The Fundamental Field is topologically 3-dimensional, it is a fractal set of embedded spherical equipotential surfaces. Figure 3 shows the linear 2D-projection $\exp(1/n_1)$ of the first layer of the Fundamental Field with both proton and electron attractors of stability. Figure 2 shows the same interval in the logarithmic representation.

In [30] we have shown that the frequency boundaries of the brain activity ranges Delta, Theta, Alpha, Beta and Gamma do not appear as to be accidental, but correspond with attractors of proton and electron stability of the Fundamental Fractal (2). In this way, Euler’s number determines temporal scales of stability of the central nervous system. Indeed, mammals including human have electrical brain activity [31] of the Theta type in the frequency range between 3 and 7 Hz, of Alpha type between 8 and 13 Hz and Beta type between 14 and 37 Hz. Below 3 Hz the brain activity is of the Delta type, and above 37 Hz the brain activity changes to Gamma. The frequencies 3.0 Hz, 8.2 Hz, 13.5 Hz and 36.7 Hz define the boundaries. The logarithms of their ratios are close to integer and half values:

$$\ln\left(\frac{8.2}{3.0}\right) = 1.00; \quad \ln\left(\frac{13.5}{8.2}\right) = 0.50; \quad \ln\left(\frac{36.7}{13.5}\right) = 1.00.$$

The correspondence of the boundary frequency ratios with

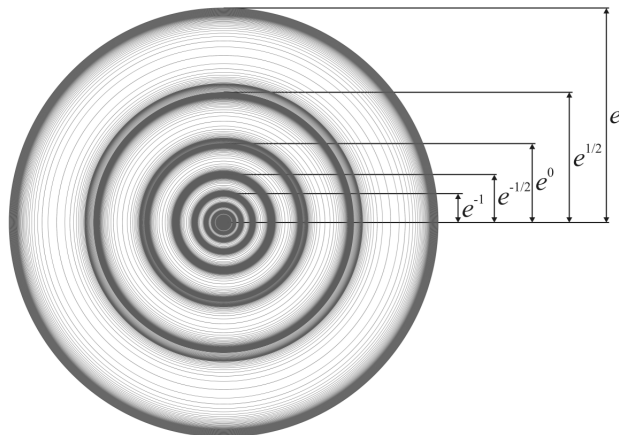


Fig. 3: The Fundamental Field with equipotential surfaces of both proton and electron attractors of stability in the linear 2D-projection for $k = 1$ in the range $-1 < x < 1$.

integer and half powers of Euler’s number evidences that the stability of the frequency boundaries is essential for brain activity. In fact, Theta-Alpha or Alpha-Beta violence can cause speech and comprehension difficulties, depression and anxiety disorders. Figure 6 shows how precisely the frequency boundaries of all subranges of brain activity correspond with main attractors of proton and electron stability.

Furthermore, similar boundary frequencies we find in the Earth’s electromagnetic field spectrum, for example the fundamental Schumann mode 7.8 Hz. Solar X-ray bursts can cause variations of the Schumann resonances [32]. In this case, the fundamental increases up to 8.2 Hz reaching exactly the stable Theta-Alpha boundary. The second Schumann mode 13.5 Hz coincides precisely with the Alpha-Beta boundary. It is remarkable that solar activity affects this mode much less or does not affect it at all because of its Euler stability. The third Schumann mode 20.3 Hz must increase up to 22.2 Hz for reaching the next island of electron stability. By the way, such an increase is observed recently. Schumann resonances occur up to 60 Hz in order to reach the subsequent island of electron stability.

The coincidence of the boundary frequencies of brain activity with Schumann resonances demonstrates how precisely the electrical activity of biological systems is embedded in the electromagnetic activity of the Earth. Important to know that Euler’s number and its roots make possible this embedding, because they are attractors of transcendental numbers and form islands of stability. They allow for exchanging information between systems of very different scales – the biophysical and the geophysical.

Here and in the following we use the letter E for attractors of electron stability, and the letter P for attractors of proton stability. For instance, the attractor E(-48) dominates the Delta activity range while E(-45) dominates the Beta activity

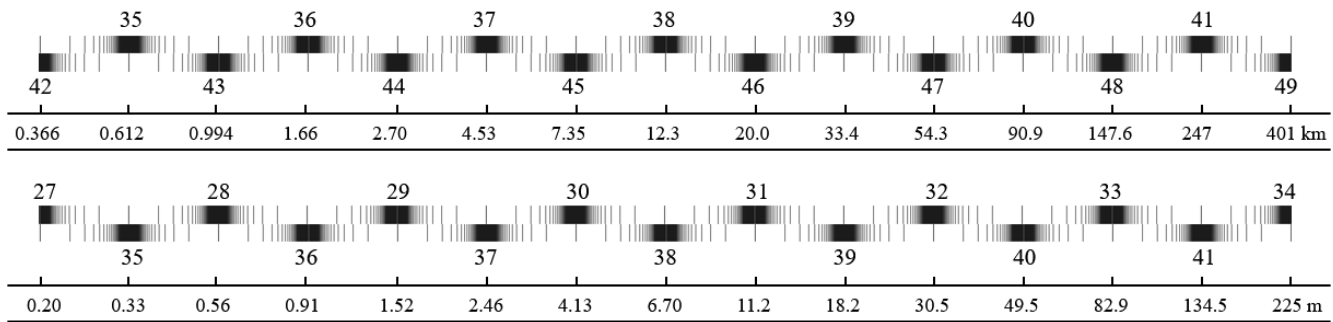


Fig. 4: Radii of equipotential surfaces of the Fundamental Field (Fig. 3) and the corresponding attractors of electron and proton stability in the natural logarithmic representation.

range. The Theta and Gamma activity ranges are dominated by the attractors P(-54) and P(-51) of proton stability. These logarithms are multiples of 3. Low Delta, High Delta, Alpha and Low Gamma are transition ranges, which boundaries are defined by both, attractors of electron and proton stability. For instance, dividing the Theta – Alpha boundary frequency 8.2 Hz by the electron angular frequency, we can see how precisely it matches with the attractor E(-46) of electron stability:

$$\ln\left(\frac{8.2 \text{ Hz}}{7.76344 \cdot 10^{20} \text{ Hz}}\right) = -46.00.$$

The correspondence of the boundary frequencies with attractors of proton and electron stability evidences that quantum physical stability of the frequency boundaries is essential for brain activity. Perhaps, this could also indicate that brain-to-brain entanglements are possible. Probably, the attractor frequencies are the key. To verify this hypothesis, we designed an experimental setup that we describe in the following.

Experimental Setup

The experiments of telepathic communication described in this paper were performed continuously over a period of four years. The participants have decades of experience in meditation, and are married couples respective good friends. They took turns in their roles as sender and receiver. During the first year, a sender usually tried to transmit the information about an arbitrarily chosen object – an apple, stone, ring or painting – that the receiver had to identify and describe in written form and draw.

For reduction of the interference of electrical brain activity by low frequency external electromagnetic fields, a part of the receivers and/or senders applied hypo-electromagnetic constructions made of 1/16 aluminum sheet, similar to the described in [13] polyhedrons, as helmets. Larger constructions of the same material were used to stay inside a hypo-electro-magnetic space where modulated red light was applied as well. For LED modulation, the frequencies 3, 5, 13, 23, 37, 61 or 101 Hz (fig. 6) of electron and proton stability were chosen. The dimensions of the structures coincide

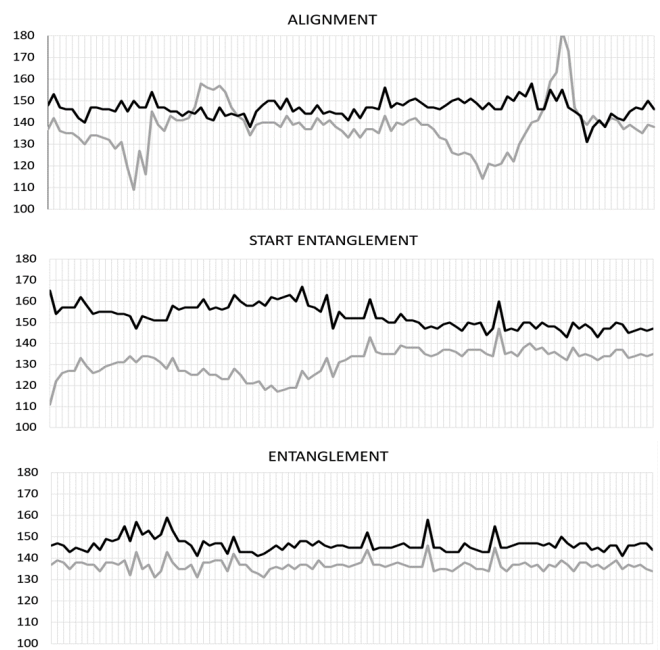


Fig. 5: The electric skin potential of the sender (black curve) and the receiver (grey curve) measured with transient recorders of two DSOs. The resolution is 100 measurements per second. The time-window of each graphic is one second.

with the radii P(35)=0.33 m, E(28)=0.56 m, P(36)=0.91 m, E(29)=1.52 m and P(37)=2.46 m of equipotential surfaces of the Fundamental Field.

The distance between sender and receiver partly was chosen in accordance with radii of main equipotential surfaces of the Fundamental Field. Fig. 4 shows the complete spectrum of sizes and distances that was applied in the experiments.

The durations of the transmission setup stages were chosen in accordance with main temporal attractors of the Fundamental Fractal (fig. 7). In the first generation of the experiments, the long version of the transmission setup stages was chosen taking 15 minutes. Then, in the next generations of

experiments, the short version that takes 5 minutes only was established.

The protocols of these experiments contain information not only about the very object, its origin, meaning and background, but also about the physical and mental state of the sender, colors of dress and other details of the environment, and of course, time and geographic location. Particular attention was paid to the perception of time. During the experiments, the participants usually were at home in Milan, Malnate, Ferrara, Ravenna, Arezzo, Spigno Saturnia, Castel di Fiori or Citta della Pieve, so that the telepathic communication did occur over large distances up to 420 km beeline.

In experiments over short distances up to 7 meters, the electric skin potential of the participants was measured. Two digital storage oscilloscopes were used. During the experiment, the participants were contacting the measurement electrodes of the DSO with a finger.

Figure 5 shows the signals of the sender (black curve) and the receiver (grey curve) measured with the transient recorder of the DSO. The resolution of the transient recorder is 100 measurements per second. The graphic at the top shows one second of the alignment during the second minute after the start of the experiment. The middle graphic shows one second of the initial phase of the entanglement during the third minute, and the graphic at the bottom shows one second of the entanglement during the fourth minute.

The unexpected success and the frequent cases of very detailed description of the objects and even the sender's environment inspired to continue the experiments under more controlled conditions.

Therefore, in the 2nd generation of experiments, the arbitrarily chosen object was substituted by a simple geometric form. The sender chooses one of four easily distinguishable forms – cross, triangle, square or circle – for transmission, and the receiver must identify it.

Furthermore, for controlling the dependence of transmission success on the number of participants, the experiments were carried out with two and more receivers. In the 3^d generation, the geometric forms were substituted by six domino number configurations (fig. 8).

In the 4th generation of experiments, the geometric forms were substituted by Chladni patterns. Fine sand particles accumulate in nodal patterns on the surface of vibrating metal plates, as described by Galileo Galilei (1630), Robert Hook (1680) and Ernst Chladni (1787). The emerging patterns depend only on the geometry of the plate and the vibration frequency of the particles, and do not depend on their mass or chemical composition. This characteristic remembers gravity – as the acceleration of free fall does not depend on the mass of the test body or its chemical composition.

For the experiments, Chladni patterns (fig. 9) emerging on square plates vibrating with the frequencies of 150, 175, 179, 400 and 525 Hz were used. On the Fundamental Fractal, these frequencies are distributed around the main nodes $E\langle-43\rangle$ and

$E\langle-42\rangle$ of electron stability, as fig. 10 shows.

The 5th generation of experiments dealt with 5 kingdoms of nature – human, animal, vegetal, mineral and celestial bodies. The transmission time extended throughout the day without specific mental focus. The sender shall transmit the idea of a concrete representative of one of these 5 kingdoms that the receiver has to identify as detailed as possible. If the kingdom of the transmitted representative was identified correctly (for example, animal), the coefficient of success was counted as 1/5, and if the representative was identified (for example, lion), the transmission was double rated. In the 6th generation of experiments, the sender tried to transmit one of five 'states of soul'. The first set of such states included courage, patience, joy, beauty and kindness, and the second set included enthusiasm, calm, trust, gratitude and benevolence. The qualities have been modified to avoid falling into monotony due to the fact that after about a month the participants felt that the exact perceptions decrease.

Results

A total of 242 experiments were carried out from September 2016 to November 2020, and the unexpected high rate of success let the participants believe in the reality of telepathy. With growing up experience, the receiver felt to be capable observing the world through the eyes of the sender. Obviously, every kind of information can be transmitted and is not limited by emotions or feelings, but can include detailed descriptions of real objects as well as numbers, regular forms and even sophisticated patterns or paintings.

The chance probability that the receiver is able to correctly guess one of five possibilities is $1/5 = 20\%$. However, the combined hit rates in our 114 experiments of that type was 72%. Statistically, this excess would never occur by chance; it corresponds to odds against chance of billions to one. This fact indicates that sender and receiver had shared indeed the same information. Such a high rate of success is not typical for the branch. As reported in [1, 33], good hit rates typically exceed the statistical expectation by 3 – 12%. Therefore, a possible significance of special conditions is obvious. Friendship and love are powerful connectors, and our research would not be necessary for a confirmation. Although these factors of success were always present in our research, they alone cannot explain the exceptionally high hit rates.

Initially, the hit rates did correlate with the distance between sender and receiver depending on the vicinity to a main equipotential surface of the Fundamental Field, but with increasing experience, this factor did lose its significance. As well, hypo-electromagnetic conditions initially did support the occurrence of telepathic entanglements significantly. Also modulated light initially did it, if the modulation frequency did correspond with an attractor of electron or proton stability. Despite this development, the statistics of the experiments evidence the permanent significance of the temporal and spa-

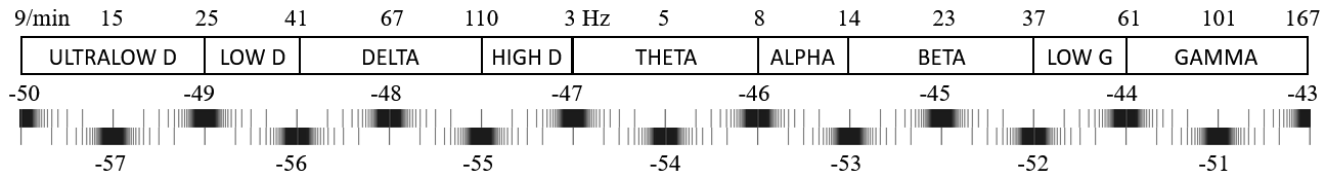


Fig. 6: The frequency boundaries of the brain activity ranges and the corresponding attractors of proton (below) and electron (above) stability of the Fundamental Fractal (2) in the natural logarithmic representation.

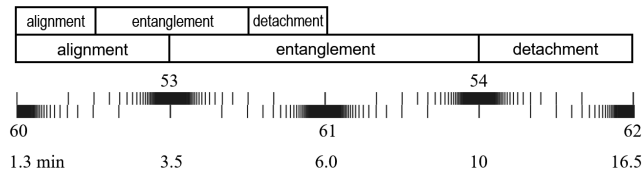


Fig. 7: The duration of transmission setup stages in minutes (below) and the corresponding attractors of proton and electron stability.

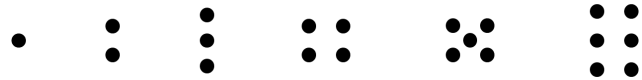


Fig. 8: Domino number configurations applied in the 3th generation.

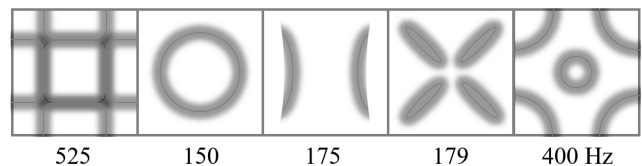


Fig. 9: Chladni patterns emerging on a vibrating square metal plate driven with the frequencies 150, 175, 179, 400 and 525 Hz.

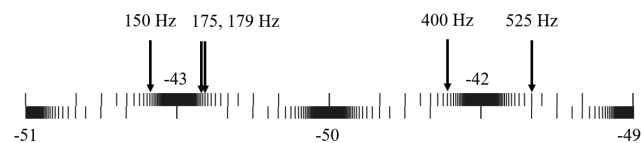


Fig. 10: The applied frequencies 150, 175, 179, 400 and 525 Hz and the corresponding attractors of proton (below) and electron (above) stability of the Fundamental Fractal (2) in the natural logarithmic representation.

tial attractors for the dynamics of the telepathic entanglement. Closer to the end of the four years' experience, indeed, the durations of the transmission setup stages automatically obeyed the Fundamental Fractal in a very natural way.

Starting with the 2nd generation, the experiments were carried out with two and more receivers. This fact in particular enables a more precise model selection and clearly shows that telepathy is not limited by individual entanglement.

Conclusion

Finally, our experiments helped to discard some conventional hypotheses provided to explain telepathy. Considering the empirical fact that electromagnetic isolation supports telepathic entanglement, today we discard the idea that telepathy is based on electromagnetic waves. It would also be a joke to think that gravitational waves could be responsible for telepathy. We suppose that telepathy has nothing to do with signal transmission. In some cases indeed, the receiver got the information *before* the sender decided to share it.

We hypothesize that besides of electromagnetic and gravitational fields, there is another long-range phenomenon – the Fundamental Field – that is of pure numeric origin and non-material, like consciousness. This Fundamental Field could turn out to be a primordial field from which consciousness originates. Being not limited by any physical process, the Fundamental Field causes numeric entanglements affecting any type of interaction.

Within our approach, telepathy is an access to a common quantum physical pool of information. Thanks to the non-locality of this pool, every telepathist can get the required information. Any process, any event updates the quantum physical information pool automatically. No sender is needed. Accessing the pool, the participant A seeks for information that is related to the participant B.

Obviously, special conditions can facilitate this access. In our experiments, those conditions were always related to the Fundamental Field. Therefore, we propose numeric entanglement as model of telepathic sharing of information.

Acknowledgements

The authors are grateful to the Community of Living Ethics for permanent support on all stages of the study.

Submitted on February 27, 2021

References

1. Radin D. Thinking about telepathy. *Think*, March 2003, doi: 10.1017/S1477175600000415.
2. Telepathy. www.britannica.com
3. Chalmers D. Facing up to the problem of consciousness. *Journal of Consciousness Studies*, (1995).
4. Hameroff S., Penrose R. Conscious Events as Orchestrated Space-Time Selections. *NeuroQuantology*, 2003, v. 1, 10–35.

5. Gao Shan. A primary quantum model of telepathy. *SSRN Electronic Journal*, doi: 10.2139/ssrn.3076089, (2002).
6. Hu H. P., Wu M. X. Spin-Mediated Consciousness Theory. *Med. Hypotheses*, 2004, v. 63, 633–646; arXiv: quant-ph/0208068.
7. Hu H. P., Wu M. X. Nonlocal Effects of Chemical Substances on the Brain Produced through Quantum Entanglement. *Progress in Physics*, 2006, v. 3, 20–26.
8. Hu H. P., Wu M. X. Thinking outside the box II: The Origin, Implications and Applications of Gravity and its role in Consciousness. *Neuro-Quantology*, 2006, v. 4, 5–16; Cogprints: ID4581.
9. Williams G. Psi and the Problem of Consciousness. *The Journal of Mind and Behavior*, 2013, v. 34, no 3, 4, 259–284.
10. Nelson R. D. Correlation of Global Events with REG Data. *The Journal of Parapsychology*, 2001, v. 65, 247–271.
11. Nelson R. D., Bradish G. J., Dobyns Y. H. Random Event Generator Qualification, Calibration, and Analysis. Princeton University, PEAR 89001, (1989).
12. Müller H. Physics of Transcendental Numbers Meets Gravitation. *Progress in Physics*, 2021, v. 17, 83–92.
13. Müller H. On the Acceleration of Free Fall inside Polyhedral Structures. *Progress in Physics*, 2018, v. 14, 220–225.
14. Müller H. Emergence of Particle Masses in Fractal Scaling Models of Matter. *Progress in Physics*, 2012, v. 8, 44–47.
15. Müller H. The Physics of Transcendental Numbers. *Progress in Physics*, 2019, v. 15, 148–155.
16. Müller H. On the Cosmological Significance of Euler's Number. *Progress in Physics*, 2019, v. 15, 17–21.
17. Dombrowski K. Rational Numbers Distribution and Resonance. *Progress in Physics*, 2005, v. 1, no. 1, 65–67.
18. Panchelyuga V.A., Panchelyuga M. S. Resonance and Fractals on the Real Numbers Set. *Progress in Physics*, 2012, v. 8, no. 4, 48–53.
19. Khintchine A.Ya. Continued fractions. University of Chicago Press, Chicago, (1964).
20. Skorobogatko V. Ya. The Theory of Branched Continued Fractions and mathematical Applications. Moscow, Nauka, (1983).
21. Lagrange J. L. Additions aux elements d'algebre d'Euler. (1798).
22. Markov A. A. Selected work on the continued fraction theory and theory of functions which are minimum divergent from zero. Moscow–Leningrad, (1948).
23. Hilbert D. Über die Transcendenz der Zahlen e und π . *Mathematische Annalen*, 1893, v. 43, 216–219.
24. Müller H. Scale-Invariant Models of Natural Oscillations in Chain Systems and their Cosmological Significance. *Progress in Physics*, 2017, v. 13, 187–197.
25. Müller H. Global Scaling. The Fundamentals of Interscalar Cosmology. *New Heritage Publishers*, Brooklyn, New York, USA, ISBN 978-0-9981894-0-6, (2018).
26. Müller H. Quantum Gravity Aspects of Global Scaling and the Seismic Profile of the Earth. *Progress in Physics*, 2018, v. 14, 41–45.
27. Müller H. The Cosmological Significance of Superluminality. *Progress in Physics*, 2019, v. 15, 26–30.
28. Astrophysical constants. Particle Data Group, www.pdg.lbl.gov
29. Tanabashi M. et al. (Particle Data Group), *Phys. Rev. D* 98, 030001 (2018), www.pdg.lbl.gov
30. Müller H. Chain Systems of Harmonic Quantum Oscillators as a Fractal Model of Matter and Global Scaling in Biophysics. *Progress in Physics*, 2017, v. 13, 231–233.
31. Tesche C. D., Karhu J. Theta oscillations index human hippocampal activation during a working memory task. *PNAS*, 2000, v. 97, no. 2, 919–924.
32. Roldugin V. C. et al. Schumann resonance frequency increase during solar X-ray bursts. *Journal of Geophysical Research*, 2014, v. 109, A01216.
33. De Peyer J. Telepathic Entanglements: Where are we Today? *Psychoanalytic Dialogues*, 2014, v. 24, 109–121.

Dirac 4×1 Wavefunction Recast into a 4×4 Type Wavefunction

G. G. Nyambuya^{1,2}

¹National University of Science and Technology, Faculty of Applied Sciences – Department of Applied Physics, Fundamental Theoretical and Astrophysics Group, P. O. Box 939, Ascot, Bulawayo, Republic of Zimbabwe.

²The Copperbelt University, School of Mathematics and Natural Sciences – Department of Physics, Fundamental Theoretical and Astrophysics Group, P. O. Box 21692, Jambo Drive – Riverside, Kitwe, Republic of Zambia. E-mail: physicist.ggn@gmail.com

As currently understood, the Dirac theory employs a 4×1 type wavefunction. This 4×1 Dirac wavefunction is acted upon by a 4×4 Dirac Hamiltonian operator, in which process, four independent particle solutions result. Insofar as the real physical meaning and distinction of these four solutions, it is not clear what these solutions really mean. We demonstrate herein that these four independent particle solutions can be brought together under a single roof wherein the Dirac wavefunction takes a new form as a 4×4 wavefunction. In this new formation of the Dirac wavefunction, these four particle solutions precipitate into three distinct and mutuality dependent particles (ψ_L, ψ_N, ψ_R) that are eternally bound in the same region of space. Given that quarks are readily found in a mysterious threesome cohabitation-state eternally bound inside the proton and neutron, we make the suggestion that these Dirac particles (ψ_L, ψ_N, ψ_R) might be quarks. For the avoidance of speculation, we do not herein explore this idea further but merely present it as a very interesting idea worthy of further investigation. We however must say that, in the meantime, we are looking further into this very interesting idea, with the hope of making inroads in the immediate future.

I am among those who think that Science has great beauty.

Marie Skłodowska-Curie (1867-1934)

1 Introduction

As currently understood, the Dirac theory [1, 2] employs a 4×1 type wavefunction, ψ . This 4×1 Dirac wavefunction is acted upon by a 4×4 Dirac Hamiltonian operator, H_D , in which process, four independent particle solutions result, i.e. $\psi[1], \psi[2], \psi[3]$, and $\psi[4]$. To this day, insofar as the real physical meaning and distinction of these four solutions, it remains unclear what these solutions really mean. We demonstrate herein that these four independent particle solutions can be brought together under a single roof wherein the Dirac wavefunction takes a new form as a 4×4 wavefunction. To that end, we shall start by introducing the well-known Dirac equation.

That is to say: for a particle whose rest-mass and wavefunction are m_0 and ψ respectively, the corresponding Dirac equation is given by:

$$i\hbar\gamma^\mu\partial_\mu\psi = m_0c_0\psi, \quad (1)$$

where: $\hbar = 1.054571817 \times 10^{-34}$ J s (CODATA 2018) is the normalized Planck constant, $c_0 = 299792458 \times 10^8$ m s⁻¹ (CODATA 2018) is the speed of light in *vacuo*, $\iota = \sqrt{-1}$, and:

$$\gamma^0 = \begin{pmatrix} \mathcal{I}_2 & \emptyset \\ \emptyset & -\mathcal{I}_2 \end{pmatrix}, \quad \gamma^i = \begin{pmatrix} \emptyset & \sigma^i \\ -\sigma^i & \emptyset \end{pmatrix}, \quad (2)$$

are the 4×4 Dirac γ -matrices where \mathcal{I}_2 and \emptyset are the 2×2 identity and null matrices respectively, and the four component Dirac wave-function, ψ , is defined as follows:

$$\psi = \begin{pmatrix} \psi_0 \\ \psi_1 \\ \psi_2 \\ \psi_3 \end{pmatrix} = \begin{pmatrix} \psi_L \\ \psi_R \end{pmatrix}, \quad (3)$$

is the 4×1 Dirac four component wavefunction and ψ_L and ψ_R are the Dirac [1, 2] bispinors that are defined such that:

$$\psi_L = \begin{pmatrix} \psi_0 \\ \psi_1 \end{pmatrix}, \quad \text{and}, \quad \psi_R = \begin{pmatrix} \psi_2 \\ \psi_3 \end{pmatrix}. \quad (4)$$

Throughout this paper, unless otherwise specified, the Greek indices will be understood to mean ($\mu, \nu, \dots = 0, 1, 2, 3$) and the lower case English alphabet indices ($i, j, k \dots = 1, 2, 3$).

The Dirac equation can be recast into the Schrödinger formalism as follows: $H_D\psi = E\psi$, where $E = -i\hbar\partial/\partial t$ is the usual quantum mechanical energy operator, and:

$$H_D = i\hbar c_0 \gamma^j \frac{\partial}{\partial x^j} - \gamma^0 m_0 c_0^2, \quad (5)$$

is the Dirac Hamiltonian operator. In §4, we shall for the purposes of efficiently making our point regarding the 4×4 wavefunction approach, use the Dirac equation in the Schrödinger formalism.

Now, in closing this introductory section, we shall give the synopsis of the present paper. In §2, we shall for instructive, completeness and self-containment purposes, present the

traditional free particle solutions of the Dirac equation. Thereafter in §3, we shall discuss some of the major shortcomings of the Dirac equation – this we do in order to demonstrate that there still is a lot more about the Dirac equation that still needs to be understood. Then, in §4, we present the main task of the present paper – i.e. the Dirac wavefunction is cast into a 4×4 type wavefunction. Thereafter in §5, we proceed to make our suggestion regarding the new formulation of the Dirac wavefunction. Lastly, in §6 a general discussion is given and no conclusion is made.

2 Free particle solutions of the Dirac equation

The free particle solutions of the Dirac equation are obtained by assuming a free particle wavefunction of the form: $\psi = ue^{ip_\mu x^\mu/\hbar}$, where: u , is a four component object, i.e. $u^T = (u_0 \ u_1 \ u_2 \ u_3)$, where the superscript- T on u is the transpose operator. This u -function is assumed to have no space and time dependence. With this in mind, one will proceed to substituting this free particle solution: $\psi = ue^{ip_\mu x^\mu/\hbar}$, into (1), where-after some elementary algebraic operations – they will be led to the following linear quad-set of simultaneous equations:

$$(E - m_0c_0^2)u_0 - c_0(p_x - ip_y)u_3 - cp_zu_2 = 0, \quad (6a)$$

$$(E - m_0c_0^2)u_1 - c_0(p_x + ip_y)u_2 + cp_zu_3 = 0, \quad (6b)$$

$$(E + m_0c_0^2)u_2 - c_0(p_x - ip_y)u_1 - cp_zu_0 = 0, \quad (6c)$$

$$(E + m_0c_0^2)u_3 - c_0(p_x + ip_y)u_0 + cp_zu_1 = 0. \quad (6d)$$

An important fact to note about the above array or set of simultaneous equations is that the four solutions u_j (where: $j = 0, 1, 2, 3$) are superluminally entangled, that is to say, a change in one of the components affects every other component instantaneously i.e. in zero time interval. What this means is that for linearly dependent solutions of u_j , the Dirac equation – just as it predicts spin as a relativistic quantum phenomenon, it also predicts entanglement as a quantum phenomenon. If they exist as a separate reality in different regions of space, then, the particles, ψ_L , and, ψ_R , are entangled.

Without further ado, we shall now present the four formal solutions of the Dirac equation, these are given by: $\psi[k] = u[k] \exp(ip_\mu x^\mu/\hbar)$, where the $u[k]$'s are such that:

$$u[1] = \begin{pmatrix} 1 \\ 0 \\ \frac{c_0p_z}{E + m_0c_0^2} \\ \frac{c_0(p_x + ip_y)}{E + m_0c_0^2} \end{pmatrix} \quad u[2] = \begin{pmatrix} 0 \\ 1 \\ \frac{c_0(p_x - ip_y)}{E + m_0c_0^2} \\ -\frac{c_0p_z}{E + m_0c_0^2} \end{pmatrix} \quad (7)$$

$$u[3] = \begin{pmatrix} \frac{c_0p_z}{E - m_0c_0^2} \\ \frac{c_0(p_x + ip_y)}{E - m_0c_0^2} \\ 1 \\ 0 \end{pmatrix} \quad u[4] = \begin{pmatrix} \frac{c_0(p_x - ip_y)}{E - m_0c_0^2} \\ -\frac{c_0p_z}{E - m_0c_0^2} \\ 0 \\ 1 \end{pmatrix}$$

These solutions (2) are obtained as follows:

1. From (6), u_0 , and u_1 are fixed so that: $u_0 = 1$, and, $u_1 = 0$, and the resultant set of equations is solved for u_2 , and, u_3 .
2. Similarly, from (6), u_0 , and u_1 are fixed so that: $u_0 = 0$, and, $u_1 = 1$, and the resultant set of equations is solved for u_2 , and, u_3 .
3. Again, from (6), u_2 , and u_3 are fixed so that: $u_2 = 1$, and, $u_3 = 0$, and the resultant set of equations is solved for u_0 , and, u_1 .
4. Similarly, from (6), u_2 , and u_3 are fixed so that: $u_2 = 0$, and, $u_3 = 1$, and the resultant set of equations is solved for u_0 , and, u_1 .

Now, having presented the solutions of the Dirac equation, we shall proceed to present what we feel are some of the important major shortcomings of the Dirac equation.

3 Major shortcomings of the Dirac equation

While the Dirac equation is one of the most successful equations in physics, it is not without its own shortcomings. We here briefly review some of its shortcomings.

3.1 Anomalous gyromagnetic ratios

It is a well-known fact that in its bare and natural form, the Dirac equation predicts a gyromagnetic ratio (g_D) equal to two (i.e. $g_D = 2$) and this prediction is very close to the gyromagnetic ratio of the electron [$g_E = 2 + 0.002319304362(2)$], hence, the Dirac equation is said to give a good description of the electron. On the contrary, the spin-1/2 proton (g_P) and neutron (g_N), which – like the electron – are thought to be fundamental particles and thus are naturally expected to readily submit to a successful description by the Dirac equation – these particles have gyromagnetic ratios that are at variance i.e. ($g_P = 2 + 3.5856947(5)$; $g_N = 2 - 5.8260855(9)$) with the Dirac prediction. The Dirac equation lacks in its nature infrastructure the devices to correctly predict the g-ratio of any arbitrary spin-1/2 particle. This state of affairs and aspect of the Dirac equation is very disappointing. In a future paper, we will propose a solution to this problem. We must say that, in the existing literature, there exists appropriate amendments that have been made to the Dirac theory in order to solve this problem. However, these solutions lack the much needed universal character.

3.2 Negative energy solutions

Further – as is well-known, one of Dirac’s purpose in the formulation of his equation was to eliminate the unwanted negative energy solutions present in the Klein-Gordon equation [3, 4]. However, negative energy solutions are still present in Dirac’s equation, and this led Dirac [5] to accept these solutions as physically realistic and to propose the existence of antimatter. Carl Anderson [6] confirmed Dirac’s hypothesis and latter, Giuseppe Occhialini and Patrick Blackett [7] did the same.

The existence of antimatter is now commonplace in the scientific literature. What is not clear about this antimatter particles (antiparticles) is whether or not they have negative energy and mass. Do antimatter particles fall up or down in a gravitational field? Experiments [8] are not clear and this question still needs to be answered (see *e.g.* [9–12]). For according to Einstein’s [13] mass energy equivalence ($E = mc_0^2$), if the energy of antiparticles is negative, their mass should be negative too. If this is the case, it follows from *Newton’s Law of Gravitation* that in a gravitational field, antiparticles ought to fall up and not down!

3.3 Whereabouts of antimatter

Furthermore – apart from the the question of whether antiparticles fall up or down, there is the yet to be an answer to the question of the whereabouts of this antimatter [14–16]. The Dirac equation not only is symmetric under electric *Charge Conjugation* (C), but, symmetric under all the known discrete symmetries of *Time* (P) and *Parity* (P) reversal including the combination of any of these these discrete symmetries – i.e. CP, CT, PT, and, CPT. This symmetric nature of the Dirac equation leads to the prediction that the Universe must contain equal amounts of matter and antimatter. This is at variance with physical experience. Otherwise, due to the annihilation of matter and antimatter into radiation, the Universe would be a radiation bath, which is clearly not the case.

This prediction of the Dirac equation is ‘*very unfortunate*’ because it is at complete variance with physical and natural as we know and experience it. That is to say, given that matter and antimatter will annihilate to form radiation should they ever come into contact, the exist of equal positions of matter and antimatter in the Universe would mean that if the Dirac prediction on the matter-antimatter census is correct, then, the Universe ought to be no more than a radiation bath. Clearly, this is not what we see around us.

3.4 Lack of a universal character

Additionally – every fermion particle (electron, proton, neutron, neutrinos, quarks *etc*) in particle physics is described by the Dirac equation. This gives the superficial impression that the Dirac equation is a universal equation for all spin-1/2 particles. A closer look will reveal that, while this equation is

used to describe fermion, it needs to be supplemented in order to match-up with experimental data. As already pointed out in §3.1, the g-ratios of every other particle save for that of the electron are not in conformity with the natural Dirac equation. If the Dirac equation were indeed a universal equation for all fermions, it must contain within its natural infrastructure the necessary adjustable parameters that would make it fit with the experimental data of a given particle. These post-experimental adjustments that are made in order that the Dirac equation fits to experimental data are of *ad hoc* nature.

Apart from the inability to explain in a smooth manner the g-ratios of different fermions, we have the issue of the universality of spin. That is to say, the Dirac equation is an equation only capable of explaining spin-1/2 particles, an not any general spin particle. For example, in order to explain spin-3/2, we need to find another equation for this – the Rarita-Schwinger equation [17] in this case. In general, fermions have spin $\pm n/2$ with: $n = 1, 3, 5, 7, \dots, 2r + 1, \text{etc}$. This implies that a new equation is required for every spin particle.

3.5 Fundamental origins of the Dirac equation

Lastly – another very important and yet largely ignored reality is that of the fundamental origins of the Dirac equation. That is to say, despite success, it remains that Dirac guessed his equation – albeit in a very educated manner. All he sought was an equation linear in both the space and time derivatives such that when this equation is “squared” it would yield the Klein-Gordon equation. It can be said that this issue of the origins of the Dirac equation is not unique to the Dirac equation, but all quantum mechanical equations.

The Klein-Gordon equation is derived from the well-known Einstein [18] energy-momentum dispersion relation: $E^2 = p^2 c_0^2 + m_0^2 c_0^4$, via the successful method of canonical quantization that was used by Schrödinger to arrive at his successful equation that describes the atomic world. Dirac’s method of arriving at his equation is not fundamental at all, and to this day, no real progress on this has been made. Where does the Dirac equation really come from? This is yet another question that also needs an answer.

4 4 × 4 Dirac wavefunction

The very fact that the Dirac Hamiltonian, H_D , is a 4×4 component object acting on, ψ , this readily implies that, ψ , can be a $4 \times k$ component object where: $k = 1, 2, 3, 4, 5, \text{etc}$. If: $1 \leq k < 4$, the resulting system of equations is over-determined and will thus have more than one solution, and if: $k > 4$, the resultant system of equations is under-determined and is unable to yield a solution. If: $k = 4$, the system has one and only solution, and this is the case of the 4×4 Dirac wavefunction that we would like to have a look at.

In the event of a 4×4 Dirac wavefunction where as usual:

$\psi = ue^{ip_\mu x^\mu/\hbar}$, the u -function is such that:

$$u = \begin{pmatrix} u_{00} & u_{01} & u_{02} & u_{03} \\ u_{10} & u_{11} & u_{12} & u_{13} \\ u_{20} & u_{21} & u_{22} & u_{23} \\ u_{30} & u_{31} & u_{32} & u_{33} \end{pmatrix} = \begin{pmatrix} u_a & u_b \\ u_c & u_d \end{pmatrix}, \quad (8)$$

where likewise:

$$\begin{aligned} u_a &= \begin{pmatrix} u_{00} & u_{01} \\ u_{10} & u_{11} \end{pmatrix} & u_b &= \begin{pmatrix} u_{02} & u_{03} \\ u_{12} & u_{13} \end{pmatrix} \\ u_c &= \begin{pmatrix} u_{20} & u_{21} \\ u_{30} & u_{31} \end{pmatrix} & u_d &= \begin{pmatrix} u_{22} & u_{23} \\ u_{32} & u_{33} \end{pmatrix} \end{aligned} \quad (9)$$

Of this 4×4 component wavefunction, ψ , we shall require of it to observe the following constraint:

$$\psi^\dagger \psi = \psi \psi^\dagger = \varrho I_4, \quad (10)$$

where: I_4 , is the 4×4 identity matrix, and, $\varrho \in \mathbb{R}$, is a real zero-rank object – it is the quantum mechanical probability density amplitude. This constraint i.e. (10) is required by the unified theory of gravitation and electromagnetism [19] that we are currently working on.

Now, substituting the new 4×4 component wavefunction into the Dirac equation (1), we will have:

$$\begin{pmatrix} (E - m_0 c_0^2) I_2 & -c_0 \vec{\sigma} \cdot \vec{p} \\ c_0 \vec{\sigma} \cdot \vec{p} & -(E + m_0 c_0^2) I_2 \end{pmatrix} \begin{pmatrix} u_a & u_b \\ u_c & u_d \end{pmatrix} = 0. \quad (11)$$

As we proceed, the reader must take note of the fact that the object, $\vec{\sigma} \cdot \vec{p}$, is a 2×2 matrix, i.e.:

$$\vec{\sigma} \cdot \vec{p} = \begin{pmatrix} p_z & p_x - ip_y \\ p_x + ip_y & -p_z \end{pmatrix}. \quad (12)$$

This matrix, $\vec{\sigma} \cdot \vec{p}$, is hermitian.

Now, from (11), four equations will result and these are:

$$u_a = \left(\frac{c_0 \vec{\sigma} \cdot \vec{p}}{E - m_0 c_0^2} \right) u_c, \quad (13a)$$

$$u_b = \left(\frac{c_0 \vec{\sigma} \cdot \vec{p}}{E - m_0 c_0^2} \right) u_d, \quad (13b)$$

$$u_c = \left(\frac{c_0 \vec{\sigma} \cdot \vec{p}}{E + m_0 c_0^2} \right) u_a, \quad (13c)$$

$$u_d = \left(\frac{c_0 \vec{\sigma} \cdot \vec{p}}{E + m_0 c_0^2} \right) u_b. \quad (13d)$$

For a solution to this set of simultaneous equation, we shall set as a constraint the following:

$$u_a = u_d = I_2 \sqrt{\varrho/2}. \quad (14)$$

This naturally leads to the following for, u_b , and, u_c , i.e.:

$$u_b = \sqrt{\varrho/2} \left(\frac{c_0 \vec{\sigma} \cdot \vec{p}}{E - m_0 c_0^2} \right). \quad (15a)$$

$$u_c = \sqrt{\varrho/2} \left(\frac{c_0 \vec{\sigma} \cdot \vec{p}}{E + m_0 c_0^2} \right). \quad (15b)$$

Hence:

$$u = \sqrt{\varrho/2} \begin{pmatrix} I_2 & \frac{c_0 \vec{\sigma} \cdot \vec{p}}{E - m_0 c_0^2} \\ \frac{c_0 \vec{\sigma} \cdot \vec{p}}{E + m_0 c_0^2} & I_2 \end{pmatrix}. \quad (16)$$

Writing this 4×4 matrix (16) in full, it will be as it appears in (17). Immediately, one will be quick to notice that columns (1), (2), (3), and (4) of this matrix (17) are in-fact the traditional solutions ($u[1], u[2], u[3], u[4]$) to the Dirac equation given in (2). What this means is that the 4×4 wavefunction is a grand synthesis of these four traditional solutions into one giant set of mutually dependent quadruplet system of particles.

5 Quarks

Apart from the simplification of bringing four independent particle solutions into a single particle solution, we suggest that this recasting of the Dirac wavefunction into a 4×4 wavefunction provides additional physical simplification in the analysis of the solution. To that end, let us start-off by writing down the full 4×4 Dirac wavefunction: $\psi = ue^{ip_\mu x^\mu/\hbar}$. For the 4×4 Dirac wavefunction, the u -function has been defined in (17) and from that definition, it follows that:

$$\psi = \begin{pmatrix} \psi_N & \psi_R \\ \psi_L & \psi_N \end{pmatrix}, \quad (18)$$

where – accordingly:

$$\psi_N = I_2 \sqrt{\varrho/2} \exp\left(\frac{ip_\mu x^\mu}{\hbar}\right), \quad (19a)$$

$$\psi_R = \sqrt{\varrho/2} \left(\frac{c_0 \vec{\sigma} \cdot \vec{p}}{E - m_0 c_0^2} \right) \exp\left(\frac{ip_\mu x^\mu}{\hbar}\right), \quad (19b)$$

$$\psi_L = \sqrt{\varrho/2} \left(\frac{c_0 \vec{\sigma} \cdot \vec{p}}{E + m_0 c_0^2} \right) \exp\left(\frac{ip_\mu x^\mu}{\hbar}\right). \quad (19c)$$

In-comparison, i.e. between ψ as defined in (3) and the resultant definition of it in (18), we see that the initially four particles: ψ_a, ψ_b, ψ_c , and, ψ_d , have been reduced to three because, ψ_a , and, ψ_d , are identical – i.e. $\psi_a = \psi_d = \psi_N$. In (18), we have according to the parlance of the Dirac formalism identified ψ_b , and, ψ_c , with the right and the left-handed Dirac components. In terms of handedness, we have in the same parlance defined a new form of handedness in the ψ_N -particle,

$$u = \sqrt{Q/2} \begin{pmatrix} 1 & 0 & \frac{c_0 p_z}{E - m_0 c_0^2} & \frac{c_0(p_x - i p_y)}{E - m_0 c_0^2} \\ 0 & 1 & \frac{c_0(p_x + i p_y)}{E - m_0 c_0^2} & -\frac{c_0 p_z}{E - m_0 c_0^2} \\ \frac{c_0 p_z}{E + m_0 c_0^2} & \frac{c_0(p_x - i p_y)}{E + m_0 c_0^2} & 1 & 0 \\ \frac{c_0(p_x + i p_y)}{E + m_0 c_0^2} & -\frac{c_0 p_z}{E + m_0 c_0^2} & 0 & 1 \end{pmatrix} \quad (17)$$

a handedness that we shall call – *neutral-handedness*, hence, ψ_N , is a neutral-handed particle, this particle is neither left nor right-handed, hence our calling it neutral-handed particle and hence the subscript- N in its denotation.

Now, in the set: ψ_N , ψ_R , and, ψ_L , we have a trio of particles that are not only mutually dependent but entangled, and in addition to this, they are confined in the same region of space. Each of these particles do not exist independently of the other, they can never be free of each other far-away from the region defined by the ψ -particle system. The boundary in spacetime of the ψ -particle system is defined by the normalization of conditions of this particle system, i.e. $\langle \psi | \psi \rangle = \mathcal{I}_4$.

Now, given the following there facts:

1. The proton and neutron are each known to contain three quarks living inside them.
2. Further, the quarks strongly appear to be unable to exist independent of each other.
3. Furthermore, these quarks strongly appear to be eternal prisoners inside the proton and neutron. They are unable to exist beyond the radius demarcating the proton and neutron particle systems.

From these facts – i.e. the obvious similarity in the nature of quarks and the trio ψ_N , ψ_R , ψ_L , it is natural to wonder whether or not these three particles ψ_N , ψ_R , ψ_L are the quarks whose origins we have thus far elusively sought to understand? From this viewpoint, the present recasting of the Dirac wavefunction surely opens up a new avenue of thinking regarding the Dirac equation and quarks, hence justifying the need to seriously consider the 4×4 Dirac wavefunction. With that having been said, we must at this very juncture say that – it is not our intention to explore this idea that the set (ψ_N , ψ_R , ψ_L) might explain quarks and the reason for this is simple that we feel it is too early for us to do so, otherwise all that we would do is to speculate.

6 Discussion

As currently accepted and understood, the Dirac theory [1, 2] employs a 4×1 type wavefunction. This 4×1 Dirac wavefunction is acted upon by a 4×4 Dirac Hamiltonian, in which process, four independent particle solutions result and insofar as the real physical meaning and distinction of these four

solutions, it is not clear what these solutions really mean. It is this that this paper has made an endeavour to provoke a thought process where a physical meaning can be attached to these four independent particle solutions of the Dirac equation and this is *via* the recasting of the Dirac wavefunction into a 4×4 type wavefunction.

We first presented this idea of a 4×4 Dirac wavefunction in [20, 21]. Prior to the said presentation [20, 21], we had never seen or heard of it anywhere in the literature. Therein [20], this idea was presented as no more than a *mathematical curiosity*, with no physical meaning attached to it. We had to come back to this idea now because we realised that it is necessary for the theory that we are currently working on [19], that is, a unified field theory of the gravitational and electromagnetic phenomenon.

What we have herein done with Dirac's four independent particle solutions, is to demonstrate that these can be represented as a quadruplet particle system wherein the Dirac wavefunction takes a new form as a 4×4 wavefunction. In this new formation, these four particle solutions precipitate into three distinct and mutually dependent particles (ψ_L , ψ_N , ψ_R) that are permanently bound in the same region of space.

Realizing that the proton and neutron are composite particles each comprising three quarks that are in (color) confinement, we proceeded logically to make the natural suggestion to the effect that these Dirac particles (ψ_L , ψ_N , ψ_R) might be quarks. Whether or not these particles are quarks, this surely is something that further investigations will have to be establish.

Received on March 6, 2021

References

1. Dirac P. A. M. The Quantum Theory of the Electron. *Proc. Roy. Soc. Lon. A: Math. Phys. & Eng. Sci.*, 1928, v. 117 (778), 610–624.
2. Dirac P. A. M. The Quantum Theory of the Electron. Part II. *Proc. Roy. Soc. Lon. A: Math., Phys. & Eng. Sci.*, 1928, v. 118 (779), 351–361.
3. Klein O. Quantentheorie und fünfdimensionale Relativitätstheorie. *Zeitschrift für Physik*, 1926, v. 37 (12), 895–906.
4. Gordon W. Der Comptoneffekt nach der Schrödingerschen Theorie. *Zeitschrift für Physik*, 1926, v. 40 (1), 117–133.
5. Dirac P. A. M. A Theory of Electrons and Protons. *Proc. Roy. Soc. Lon. A: Math., Phys. & Eng. Sci.*, 1930, v. 126 (801), 360–365.

6. Anderson C. A. The Positive Electron. *Phys. Rev.*, 1933, v.43 (6), 491–494.
7. Fitch V. L. Elementary Particle Physics: The Origins. *Rev. Mod. Phys.*, 1999, v. 71 (2), S25–S32.
8. Charman A. E., Amole C., Ashkezari M. D., *et al.* Description and First Application of a New technique to Measure the Gravitational Mass of Antihydrogen. *Nature Comm.*, 2013, v. 4 (1).
9. Schiff L. I. Sign of the Gravitational Mass of a Positron. *Phys. Rev. Lett.*, 1958, v. 1 (7), 254–255.
10. Morrison P. Approximate Nature of Physical Symmetries. *Am. J. Phys.*, 1958, v. 26 (6), 358–368.
11. Nieto M. M. and Goldman T. The Arguments Against Antigravity and the Gravitational Acceleration of Antimatter. *Phys. Rep.*, 1991, v. 205 (5), 221–281.
12. Apostolakis A., Aslanides E., Backenstoss G., *et al.* Tests of the Equivalence Principle with Neutral Kaons. *Phys. Lett. B*, 1999, v. 452 (3–4), 425–433.
13. Einstein A. Ist die Trägheit eines Körpers von seinem Energieinhalt Abhängig? *Ann. der Phys.*, 1905, v. 323 (13), 639–641.
14. Sakhorov A. D. Violation of CP Symmetry, C-Asymmetry and Baryon Asymmetry of the Universe. *Pisma Zh. Eksp. Teor. Fiz.*, 1967, v. 5, 32–35.
15. Weidenspointner G., Skinner G., Jean P., and *et al.* An Asymmetric Distribution of Positrons in the Galactic disk Revealed by γ -Rays. *Nature*, 2008, v. 451 (7175), 159–162.
16. Neri N. and The LHCb collaboration. Measurement of Matter-Antimatter Differences in Beauty Baryon Decays. *Nature Phys.*, 2017, v. 13 (4), 391–396.
17. Rarita W. and Schwinger J. S. On a Theory of Particles with Half-Integral Spin. *Phys. Rev.*, 1941, v. 60 (1), 61–61.
18. Einstein A. Zur Elektrodynamik bewegter Körper (On the Electrodynamics of Moving Bodies). *Ann. der Phys.*, 1905, v. 322 (10), 891–921.
19. Nyambuya G. G. Fundamental Geometrodynamical Justification of Gravitomagnetism (I). *Prog. Phys.*, 2020, v. 16 (2), 73–91.
20. Nyambuya G. G. On the Dirac Wavefunction as a 4×4 Component Function. *Prespacetime Journal*, 2016, v. 7 (8), 1232–1243.
21. Nyambuya G. G. On the Possible Origins of the Dirac Equation. *Prespacetime Journal*, 2016, v. 7 (13), 1818–1826.

Progress in Physics is an American scientific journal on advanced studies in physics, registered with the Library of Congress (DC, USA): ISSN 1555-5534 (print version) and ISSN 1555-5615 (online version). The journal is peer reviewed and listed in the abstracting and indexing coverage of: Mathematical Reviews of the AMS (USA), DOAJ of Lund University (Sweden), Scientific Commons of the University of St.Gallen (Switzerland), Open-J-Gate (India), Referential Journal of VINITI (Russia), etc. Progress in Physics is an open-access journal published and distributed in accordance with the Budapest Open Initiative: this means that the electronic copies of both full-size version of the journal and the individual papers published therein will always be accessed for reading, download, and copying for any user free of charge. The journal is issued quarterly (four volumes per year).

Electronic version of this journal: <http://www.ptep-online.com>

Advisory Board of Founders:

Dmitri Rabounski, Editor-in-Chief
Florentin Smarandache, Assoc. Editor
Larissa Borissova, Assoc. Editor

Editorial Board:

Pierre Millette
Andreas Ries
Gunn Quznetsov
Ebenezer Chifu

Postal address:

Department of Mathematics and Science, University of New Mexico,
705 Gurley Avenue, Gallup, NM 87301, USA
